CHARACTERISTICS OF COUPLED NONGRAY RADIATING GAS FLOWS WITH ABLATION PRODUCT EFFECTS ABOUT BLUNT BODIES DURING PLANETARY ENTRIES

by

KENNETH SUTTON

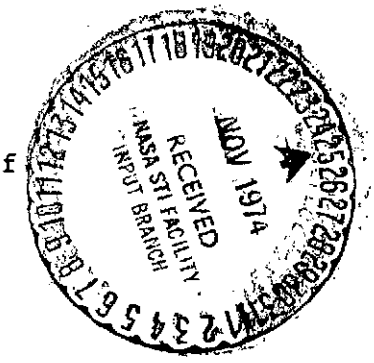

A thesis submitted to the Graduate Faculty of
North Carolina State University at Raleigh
in partial fulfillment of the
requirements for the degree of
Doctor of Philosophy

DEPARTMENT OF MECHANICAL AND AEROSPACE ENGINEERING

RALEIGH

1 9 7 3

APPROVED BY:

Francis J. Hale

Robin F. Barrett

Alonzo F. Coots

Frederick O. Smetana

Chairman of Advisory Committee

ABSTRACT

SUTTON, KENNETH. Characteristics of Coupled Nongray Radiating Gas Flows with Ablation Product Effects about Blunt Bodies during Planetary Entries. (Under the direction of FREDERICK OTTO SMETANA).

A computational method is developed for the fully-coupled solution of nongray, radiating gas flows with ablation product effects about blunt bodies during planetary entries. The treatment of radiation accounts for molecular band, continuum, and atomic line transitions with a detailed frequency dependence of the absorption coefficient. The ablation of the entry body is solved as part of the solution for a steady-state ablation process.

Application of the developed method is shown by results at typical conditions for unmanned, scientific probes during entry to Venus. The radiative heating rates along the downstream region of the body can, under certain conditions, exceed the stagnation point value. The radiative heating to the body is attenuated in the boundary layer at the downstream region of the body as well as at the stagnation point of the body.

Results from a study of the radiating, inviscid flow about spherically-capped, conical bodies during planetary entries are presented and show that the nondimensional, radiative heating distributions are nonsimilar with entry conditions. Therefore, extreme caution should be exercised in attempting to extrapolate results from known distributions to other entry conditions for which solutions have not yet been obtained.

BIOGRAPHY

Kenneth Sutton was [redacted]. He was reared in Jacksonville, Florida and graduated from Andrew Jackson High School in 1957. He attended Jacksonville University for two years before transferring to the University of Florida where he received the degree of Bachelor of Mechanical Engineering in 1962.

After graduating, he accepted a position with the Langley Research Center of the National Aeronautics and Space Administration in Hampton, Virginia. He received his graduate education through the NASA Graduate Study Program. In 1963 he returned to the University of Florida and received the degree of Master of Engineering in 1964. He began night studies in 1964 with the Tidewater Extension Center of George Washington University and received the degree of Master of Science in Governmental Administration in 1967. He entered North Carolina State University at Raleigh in 1968 to begin advanced studies in the Department of Mechanical and Aerospace Engineering. He returned to the Langley Research Center in 1969 where he performed the analysis presented in this thesis.

He is presently assigned to the Advanced Entry Analysis Branch of the Spacecraft Systems Division at the Langley Research Center. He is a member of the American Institute of Aeronautics and Astronautics and the American Society of Mechanical Engineers. He is registered as a Professional Engineer by the State of Florida.

ACKNOWLEDGEMENTS

The author wishes to express his appreciation to the National Aeronautics and Space Administration for its continued support of his graduate studies and for supporting the research presented in the thesis.

The author wishes to thank the members of his advisory committee for their help and cooperation. He is especially grateful to Dr. Frederick O. Smetana for his assistance and patience during the author's studies and research investigation.

Special appreciation is extended to Mr. Gerald D. Walberg of the Langley Research Center for proposing the topic of the research investigation, for his continued support of the investigation, and for his consultation on many technical matters. The author is appreciative of the technical consultation given to him by members of the Langley Research Center: Dr. Walter B. Olstad, Mr. Linwood B. Callis, Dr. Robert E. Boughner, Mr. Ralph A. Falanga, Mr. John T. Suttles, and Dr. G. Louis Smith. Also, the author is grateful for the technical assistance by members of the Aerotherm Corporation: Mr. William E. Nicolet, Dr. Robert M. Kendall, and Mr. Eugene P. Bartlett.

The author is grateful for the pleasant conversation, encouragement, and technical assistance extended to him by his office colleagues, Mr. Randolph A. Graves, Jr., and Mr. E. Vincent Zoby. Special gratitude is expressed to Mr. Bennie W. Cocke, Jr. of the Langley Research Center for his guidance and help in the author's earlier career. Also,

appreciation is extended to Mr. James H. Godwin of Langley Research Center for his assistance and friendship during the many nights the author spent at the computer complex.

The author's graduate study was made easier by the work of Mr. Dick Cole and Mr. John Witherspoon of the Langley Research Center and Miss Eleanor Bridgers of North Carolina State University in efficiently handling the necessary administrative arrangements during his enrollment at North Carolina State University.

The author wishes to express his appreciation to Miss Mary Anne Monaco for her editorial assistance and typing the original draft of the thesis. Gratitude is also expressed to Mr. Charles R. Pruitt of the Langley Research Center for handling the final preparation of the thesis.

TABLE OF CONTENTS

LIST OF TABLES

LIST OF FIGURES

Page

Page

LIST OF SYMBOLS

A	parameter defined by eq. 21
a	sonic velocity, see eq. 49
B	parameter defined by eq. 22
B_ν	Planck function
C	parameter defined by eq. 23
C_1	parameter defined by eq. A4
C_2	parameter defined by eq. A5 or eq. 35
C_3	parameter defined by eq. A6 or eq. 36
c_p	specific heat
$\bar{c}_p$	specific heat parameter defined by eq. 61
D	parameter defined by eq. 24
D_{ij}	binary diffusion coefficient for ith and jth chemical species
$\bar{D}$	self-diffusion coefficient of a reference species
E	parameter defined by eq. 25
E_n	exponential integral of order n
E_3	exponential integral of order 3
F^R	divergence of radiative flux defined by eq. 26
F_i	diffusion factor of ith chemical species in a given chemical system, see eq. 57
f	represents the variables p,u,v, or h in eqs. 37 to 39
f	stream function for boundary-layer equations, defined by eq. 70
g_i	metric coefficient for ith coordinate, used herein as $g_1=\lambda$, $g_2=1$, $g_3=r$ (see eqs. 6 to 8)
H	total enthalpy, $h+u^2/2$, in boundary-layer equations

h	enthalpy
$\bar{h}$	enthalpy parameter defined by eq. 61
h^*	Planck constant
h_a^o	heat of formation of undecomposed ablation material
I_ν	monochromatic radiation intensity
j_i	diffusional mass flux of chemical element i, see eq. 58
K	body curvature parameter defined by eq. 9
$\bar{K}_i$	mass fraction of chemical element i
k	thermal conductivity
ℓ	differential line element in eqs. 6 and 7
M	molecular weight
m_a	ablation rate of the heatshield
P_1	thermodynamic variable defined by eqs. 31 and 48
P_3	thermodynamic variable defined by eqs. 32 and 49
p	pressure
q^C	convective heat flux, see eq. 60
q^R	radiative heat flux
q_{cond}	heat flux conducted into the heatshield
Re_θ	momentum thickness Reynolds number for boundary layer
Rn	nose radius of body at s=0, see Figure 3
r	radial distance from axis of symmetry of body, see Figure 3
r_b	body radius from axis of symmetry, see Figure 3
S	transformed s coordinate for inviscid-layer equations, defined by eq. 15
SF	stream function for inviscid-layer equations, defined by eq. 45

s	coordinate along the body surface, see Figure 3
T	transformed t coordinate defined by eq. 15
$\overline{T}$	temperature
$\overline{T}_\delta$	temperature at $y=\delta$ in inviscid flow field
t	time
t_υ	dummy variable of monochromatic optical depth in eqs. 76 to 78
u	velocity tangent to body surface, see Figure 3
V_∞	free-stream velocity
V_e	entry velocity
v	velocity normal to body surface, see Figure 3
W	weight of entry probe
W/C_dA	ballistic coefficient where the drag coefficient, C_d, is for area, A, of the probe's base
x_i	general coordinates, used herein as $x_1=s$, $x_2=y$, and $x_3=\phi$ (see eqs. 6 and 7)
$\overline{x}_j$	mole fraction of chemical species j
Y	transformed y coordinate, defined by eq. 15
y	coordinate normal to the body surface, see Figure 3
Z_j	quantity for jth chemical species defined by eq. 59
$\overline{Z}_i$	quantity for ith chemical element defined by eq. 59
z	distance along axis of symmetry of body
z	function for the exponential integral of order n, $E_n(z)$
α_{ij}	mass fraction of chemical element i in chemical species j
β	difference between the angle of the shock wave and the angle of the body surface, see Figure 3
γ	angle between a ray and the normal for radiation flux in eq. 71

γ_e	entry angle
δ	shock stand-off distance of inviscid layer
δ^*	boundary-layer displacement thickness defined by eq. 2
δ^t	total thickness of shock layer defined by eq. 1
ϵ_ν	monochromatic emissivity defined by eqs. 76 and 78
ϵ_w	emissivity of the heatshield
η	transformed y coordinate for boundary-layer equations, defined by eq. 69
θ	angle of body surface relative to axis of symmetry of body, see Figure 3
θ_c	cone half angle for a spherically-capped, conical body
λ	curvature parameter defined by eq. 9
λ_δ	value of λ at $y=\delta$
μ	viscosity in boundary-layer equations
μ_1	parameter defined by eq. 59
μ_2	parameter defined by eq. 59
μ_ν	monochromatic linear absorption coefficient corrected for induced emission
$\bar{\mu}_\nu$	μ_ν for molecular band transitions, defined by eq. 81
ν	radiation frequency
ξ	transformed s coordinate for boundary-layer equations, defined by eq. 69
ρ	density
$\rho\epsilon_d$	turbulent eddy diffusivity
$\rho\epsilon_h$	turbulent eddy conductivity
$\rho\epsilon_m$	turbulent eddy viscosity
σ	Stefan-Boltzmann constant

τ_ν monochromatic optical depth defined by eq. 75

τ_w aerodynamic shear at the wall

ϕ azimuth angle, see Figure 3

Ω solid angle

subscripts

a refers to the ablation material

c refers to the char of the decomposed ablation material

e refers to the boundary-layer edge

g refers to the pyrolysis gas of the decomposed ablation material

i,j refers to the ith or jth chemical species or chemical element

o refers to stagnation-point values, s=0

s refers to conditions behind a normal shock wave

w refers to the body wall

∞ refers to free-stream conditions

δ refers to conditions at $y=\delta$ in the inviscid layer

ν refers to radiation frequency

superscripts

C,L refers to continuum transitions, including molecular band transitions, or line transitions in eq. 79

1,2 refers to the first or second step in the two-step numerical method for the radiating, inviscid flow solution

+,- refers to the direction of the radiative flux (+ refers to the radiative flux toward the shock wave and - refers to the radiative flux toward the body)

prime refers to dimensional quantities in the section of Radiating, Inviscid Flow Field Solution

INTRODUCTION

One of the major scientific endeavors of the present day is the exploration of the planets by unmanned and manned spacecraft. The present technique for planetary entry is to use atmospheric friction as a brake to slow the spacecraft from hypersonic speeds. During hypersonic entry the gas around the body in the formed shock layer is heated by the dissipated kinetic energy. In order for the spacecraft to survive, the main body of the spacecraft will be protected from this source of intense heat by the use of an ablative heat shield material. The speeds required for planetary entries will be well in the excess of the parabolic speed in order to reduce trip times for interplanetary travel. The temperatures of the heated gas behind a shock wave associated with these high-speed entries are sufficient for gas radiation to be a major contributor to the heating of the spacecraft. The inclusion of radiative heating in the energy equation of flow field solutions causes a strong coupling between the radiative transport, the inviscid shock layer, the boundary layer, and the ablative heat shield analyses. Computational methods for the solution of this complex flow phenomena are required before heat shields can be designed to survive during planetary entries at speeds in excess of parabolic speed.

At entry speeds less than parabolic speed the radiative heating is negligible and convection through the boundary layer is the dominant mode of heat transport to the body. The neglect of radiative transport uncouples the inviscid flow equations and the boundary layer equations; however, the boundary layer analysis and the heat shield analysis are

still coupled. Extensive analyses for boundary layers with mass injection have been conducted over the years so that the necessary inputs to the heat shield analysis for convective heating and mass diffusion can be determined without a coupled solution of the equations.

At entry speeds in excess of parabolic speed the radiative transport cannot be neglected and the radiative heating can be much more dominant than convective heating. In general, the radiative transport in a gas is governed by integral equations involving the absorption coefficient integrated over both radiation frequency spectrum and three-dimensional space. The absorption coefficient is dependent on the temperature, density, and the number density of the species present in the gas (ref. 1, page 721). Thus, the radiative transport is dependent on the thermodynamic profiles throughout the gas layer between the shock wave and body. The absorption of radiation by the cooler gas in the boundary layer will change the thermodynamic profiles in the boundary layer and affect the convective heating and mass diffusion to the heat shield. In early studies, the incident radiation to the spacecraft was taken as the radiation from the inviscid shock layer. Later studies have shown that the boundary layer, with and without injection of ablation products, can absorb radiation and reduce the incident radiative heating to the spacecraft. For high-speed planetary entry, the solution of the flow field equations and the heat shield analysis is very complex because of the coupling of radiative transport.

The radiative transport to the stagnation region of blunt bodies for entries into air has been the primary interest for most studies of

radiating flow fields with ablation product effects. The interest for entries into air was due to Earth reentry after exploration of the Earth's moon and preliminary studies for Earth reentry after exploration of Mars. There is a need for investigation of the radiating flow field in other gaseous atmospheres because of the increased interest in exploration of other planets (Venus, Jupiter, etc.). The emphasis on the stagnation region was due to a simplification of the solution and because the radiative heating was considered to be greatest in this region. However, the recent results by Olstad (ref. 2) and by Callis (ref. 3) for an inviscid, radiating flow field have shown that the radiative heating to the flank regions of blunted-conical bodies can equal or exceed the radiative heating to the stagnation region. As discussed by Page (ref. 4), most of the heat shield surface and weight is downstream of the stagnation region and valid treatment of fully-coupled solutions is needed downstream of the stagnation region along cone flanks or over spherical noses. Anderson (ref. 5) states the need for additional solutions of the coupled radiative problem with ablation product effects to complement the existing results. These points illustrate the need for a method of calculating the fully-coupled radiating flow field, with ablation product effects, around the entire body and for entries into atmospheres of arbitrary gases.

The purpose of the present study is to investigate and develop a computational method for a fully-coupled solution of the radiating flow field, with ablation products injection, about blunt bodies for entries into arbitrary gas mixtures. Basically, the method is to separate the

radiating flow field into an outer inviscid layer and an inner boundary layer with injected ablation products; then, the two solutions are coupled by the radiative transport through both layers and by the boundary layer displacement thickness for mass injection. The radiative flux is included in the energy equation of both the inviscid solution and the boundary layer solution. As previously stated, the fully-coupled formulation for radiating planetary entry is very complex and all approaches require varying degrees of approximation in order to obtain a solution. By separating the two different layers of flow, a better treatment should be possible for the solution of each layer.

A second-order, time-asymptotic technique is used for the solution of the inviscid shock layer. The set of unsteady governing equations is hyperbolic, thus the technique is valid in both the subsonic and supersonic regions of the inviscid flow about the body. A computer program for a numerical solution of the technique is developed in the study. An equilibrium thermodynamic subroutine and a detailed radiative transport subroutine are included in the computer program so that arbitrary gas mixtures can be considered. Moretti and Abbett (ref. 6) used a time-asymptotic technique for an inviscid flow solution without radiation in a perfect gas and Callis (refs. 3 and 7) used a time-asymptotic technique for a radiating, inviscid flow solution in air.

The solution of the inner gas layer is for a nonsimilar, multicomponent boundary layer with mass injection, unequal diffusion coefficients, and arbitrary chemical species. The numerical, integral matrix method of Barlett and Kendall (ref. 8) is used for the boundary

layer solution and there is an existing computer program called BLIMP. In the computer program, the thermodynamic properties and transport properties (viscosity, etc.) are calculated as part of the solution. The injection rate of ablation products can be either prespecified or calculated during the solution for a steady-state ablation process. The computer program is modified in the present study to account for radiative transport within the boundary layer.

The radiative transport solution for coupling the inviscid layer and the boundary layer is for a nongray gas with molecular band, continuum, and atomic line transitions. The integration over the radiation spectrum uses a detailed frequency dependence of the absorption coefficients and the tangent slab approximation is used for integration over physical space. An existing computer program (RAD/EQUIL) of the numerical method by Nicolet (ref. 9) is used for the solution of the radiative transport. In addition to using this program for coupling the flow fields, an extensive modification of the program is made so that it can be used efficiently as a subroutine in the developed computer program for the inviscid radiating layer.

The application of the present developed method is shown by a study of typical points on an entry trajectory for Venus. To the author's knowledge, there are no published results for a fully-coupled radiating solution with ablation products injection at either the stagnation or downstream regions on a body for Venusian entry. The validity of the method is investigated by a comparison with published results for Earth entry.

REVIEW OF LITERATURE

The review of literature is restricted to prior studies which present the more pertinent results for the radiating flow about blunt bodies with ablation products injection. The fully-coupled solution of radiating flow with ablation analysis is a complex problem and involves many disciplines; therefore, a detailed review of the entire field for the thermal analysis during planetary entry is not presented. A good review and extensive reference list for radiating shock layers is given by Anderson (ref. 5). Similarly, a review of ablative heat shields for planetary entries is given by Walberg and Sullivan (ref. 10). These two articles provide a good review of the present technology of radiative heating and ablation analysis for high-speed planetary entry. For additional discussions of the background information presented in the Introduction on planetary gas dynamics and planetary entry, the reader is referred to references 4 and 11 to 15. Information on trajectory analysis for planetary missions is available in reference 16. A discussion on types of heat shield materials and ablation mechanisms is given in reference 17. A good analysis on the coupling between the boundary layer and a charring ablator is given by Kendall et al., (ref. 18).

The remaining sections of the literature survey present more detailed information which is pertinent to an analysis of the radiating flow about blunt bodies. The first section discusses features of radiation transport modeling. The second section is a discussion on radiating flow field analyses. In addition to flows about blunt bodies, a

discussion is presented on significant and applicable results from stagnation region analyses. Finally, a section is presented on the thermal analyses for Venusian entry.

Radiation Transport Modeling

An atom or molecule in a high-temperature gaseous medium can emit and absorb radiation at a frequency characteristic of some transition from one quantum state to another and each specie has an absorption spectrum which can be expressed in terms of an absorption coefficient. Because of quantum transtions, the absorption coefficient is a function of frequency. Radiation of a given frequency travels in physical space a distance (radiation mean free path) before being absorbed. (The above description is from reference 1, page 721.) Thus, the radiative transport in a gaseous medium is a function of frequency and distance and the equation for the total radiative transport is an integral over both frequency spectrum and physical space.

The solution for a radiating flow field is a set of integro-differential equations and approximations are used to solve this complex system of equations. One of the approximations deals with the spatial aspect of radiative transport. The absorption of radiation at a point in the flow field is a function of the emitted radiation from surrounding fluid elements; and, since radiation travels a distance before being absorbed, the radiative transport is a three-dimensional problem in space. To reduce the complexity of the solution, the "tangent slab approximation"

is usually used for radiating flow fields. This approximation treats the gas layer as a one-dimensional slab in calculation of the radiative transport. The radiative heat flux is neglected except in the direction normal to either the body or shock wave.

Garrett (ref. 19), after a review of the studies of references 20 to 22, states the error introduced by the approximation should be less than 5 percent at the stagnation point. Page (ref. 4), in a discussion of the three-dimensional effects, concludes that the tangent slab approximation is sufficiently accurate for engineering calculations when the shock-layer thickness is small compared to the curvature ($\sim 1/12$). Page's conclusions are based primarily on the studies by Chien (ref. 23) and by Wilson (ref. 24). The study by Wilson was a comparison of the tangent slab approximation with an exact three-dimensional numerical calculation at the stagnation and downstream regions of a blunted, conical body for a typical Earth reentry. The error for the tangent slab approximation was 15 percent at the stagnation region and less error at the conical region. The tangent slab approximation is used in the present study.

In radiation transport modeling, the gas may be treated as transparent, gray, or nongray. A transparent gas is assumed to emit radiation but not absorb radiation. The treatment of a gray or nongray gas allows both emission and absorption. However, the absorption coefficient is assumed constant over the frequency spectrum for a gray gas. A frequency dependence of the absorption coefficient, either approximate or in detail, is included for a nongray gas. Anderson (ref. 5) traces the

historical development of radiating flow fields and shows the progression from transparent, continuum only, uncoupled calculations used by early investigators to the nongray, continuum and line, coupled energy calculations which are current today. As discussed by Anderson, a gray gas analysis is not sufficiently accurate for reentry applications and the gas should be treated as nongray.

The frequency dependence of absorption coefficient for a nongray gas is treated in detail or by a "step-model". In a step model, the frequency dependence is broken into a number of discrete steps (see, for example, references 7 and 25 to 27). The number of steps are generally from two to nine. The calculation of the radiative heat flux involves an integral over frequency and using a step-model will simplify the integration. However, the injection of ablation products into the flow field increases the number of species to be considered and there is a rapid change in chemical composition in the boundary layer. A step-model has to be constructed for the particular gas composition and the addition of ablation products will complicate the construction. Boughner (ref. 25) had difficulty in developing a general step-model for a CO_2-N_2 mixture; and, the developed step-model was only valid over a restricted and narrow range of conditions. The difficulty was due to molecular band radiation.

The radiative heat flux with ablation product effects has been calculated for a nongray gas and the frequency dependence of absorption coefficient was considered in detail (see, for example, references 19, 28, and 29). There are computer programs for calculating the detailed,

nongray radiative transport of which the ones used primarily for reentry application are RATRAP, developed by Wilson (ref. 30); SPECS, developed by Thomas (ref. 31); and RAD/EQUIL, developed by Nicolet (refs. 9 and 32). Suttles (ref. 33) made a comparison of these programs in a recent study and concluded that the RAD/EQUIL program depended on fewer approximations, included more detail, and required less computer time than RATRAP and SPECS. The RAD/EQUIL program is used in the present study.

As discussed by Penner and Olfe (ref. 13), radiation is coupled to the conservation equations by the radiation pressure, radiation energy density, and radiation energy transfer. The radiation pressure and radiation energy density are usually negligible and can be neglected even when the radiation energy transfer is very important. The two terms can be and are neglected in solutions which deal primarily with radiative heating (refs. 13 and 34). Therefore, the coupling between radiation and the conservation equations is due to the divergence of the radiative heat flux in the energy equation.

For additional information on radiation and radiative transport, the interested reader is referred to the numerous available books. Two good books with which the author is most familiar are by Penner (ref. 35) and by Penner and Olfe (ref. 13). Radiative heating is considered in the book on gas dynamics by Vincenti and Kruger (ref. 34). Also, references 36 to 38 present analyses of radiative transport for high-temperature gases.

Radiating Flow Fields

The interest of the present study is the radiating flow field about blunt bodies; therefore, the flow in both the stagnation region and the downstream region has to be considered. Also, the prior studies which included ablation product effects have been for the stagnation region. A discussion and literature survey are presented first on the pertinent results from analyses of stagnation-region flow; then a discussion and literature survey are presented for flow about blunt bodies.

Flow at Stagnation Region

The recent doctoral thesis by Garrett (ref. 19) presents a detailed review of the various methods used for solving the radiating flow field at the stagnation region. Also, the various methods of solution are discussed in the papers by Goulard et al (ref. 39) and by Anderson (ref. 5). The reader is referred to these papers for a description of the solutions. Only the pertinent results will be presented here.

The earlier studies by Howe and Viegas (ref. 40) and by Hoshizaki and Wilson (refs. 41 and 42) have shown there is a coupling between radiative and convective heating and that radiation from the higher-temperature inviscid region can be absorbed by the lower-temperature viscous region. Later studies have shown that the ablation products injected into the flow field from ablative heat shields can significantly reduce the radiative heating to the body (refs. 19, 22, 28, 29, 43, and 44). These studies were for Earth reentry except a limited part of the study by Wilson (ref. 44) was for Jovian entry. Hoshizaki and

Lasher (ref. 22) state that atomic carbon from the ablation products is the principle absorber and Smith et al. (ref. 28) show that carbon monoxide can also significantly absorb the radiation from the radiating shock layer.

The recent thesis by Garrett (ref. 19) presents a comparison of the results at the stagnation region for air injection and ablation product injection. Garrett uses an implicit finite difference method for a solution at the stagnation-point of a blunt body and treats the entire shock layer as viscous. The results of Garrett show that massive injection of ablation products from a carbon phenolic heat shield into air reduced the radiative heating to the body by 40 percent; but, massive injection of air only reduced the radiative heating by 15 percent. A comparison of results presented by Garrett for solutions from various studies showed that ablation products reduce the radiative heating; but, there were significant differences in the magnitude of the reduction.

Smith et al. (ref. 28) used a method for the stagnation region which is similar to the method in the present study. That is, separating the inviscid layer and the boundary layer and then coupling the two by the radiative transport. The study was for Earth reentry with ablation product effects. The derivation of the boundary layer equations included the radiative heat flux in the energy equation and was for moderate and strong blowing. However, the results presented did not include the radiative heat flux in the energy equation for the boundary layer and was only for strong blowing. The solution of the equations was by numerical methods and Dr. Smith has stated there are difficulties in

extending the solution to include radiative heat flux in the boundary-layer energy equation and to include moderate blowing. The problem has not been solved.* The study by Smith et al. did show that the basic method is valid and in the present study the treatment of the boundary-layer solution is much better than the approximate method used by Smith et al.

Hoshizaki and Lasher (ref. 22) treated the entire shock layer as viscous and stated the advantage is that it eliminates the necessity of matching the radiative heat flux at the inviscid-viscid interface. Garrett (ref. 19) treated the entire layer as viscous and there were irregularities in the enthalpy profiles at the inviscid-viscid interface for strong blowing. The enthalpy profiles come from the energy equation and this equation is where the radiative transport is coupled to the flow equations. In the present study, the coupling is not a direct matching of the radiative heat flux at the interface. The radiative heat flux to be coupled in the energy equation of the boundary layer is taken from the solution of the radiative transport over the entire shock layer. The magnitude of the radiative heat flux from the boundary layer toward the inviscid layer is small compared to the flux toward the boundary layer from the inviscid layer (see, for example, ref. 28). Thus, in the present method the solution for the radiating inviscid layer is solved once and an iteration is only required between the boundary layer solution and radiative transport solution.

---

*Personal communication with Dr. G. Louis Smith, Langley Research Center, Hampton, Virginia

Garrett (ref. 19) and Rigdon et al. (ref. 29) state the need for properly calculating the thermodynamic properties of the ablation products. In the present study, the thermodynamic properties are calculated during the solution for both the inviscid region and the boundary layer and arbitrary gases can be considered.

As illustrated by the comparisons presented by Garrett (ref. 19), there are discrepancies for the magnitude of radiative heating reduction due to ablation effects even for the stagnation region. The existing results are primarily for Earth reentry and calculations need to be performed for other planetary entries. Anderson (ref. 5) states that realistic calculations for radiative heating to entry vehicles should definitely account for ablation effects and additional radiative coupled analyses with ablation effects should be made in order to complement the existing results.

Flow about Blunt Bodies

There have been a number of studies and numerical solutions for the radiative heating with ablation effects at the blunt-body stagnation region but solutions for the downstream regions of the flow field are not so advanced. The few studies which have considered the radiating flow about blunt bodies have shown that radiative heating at the flank regions of hemisphere-conical bodies can be a large fraction and even exceed the radiative heating at the stagnation point (refs. 2, 3, 45, and 46). These studies were for Earth reentry, used a step-model for the radiative transport, and did not include ablation product effects.

The study by Olstad (ref. 2) was for an inviscid shock layer with the solution of the flow field by the method developed by Maslen (ref. 47) but modified for radiative transport. The method of Maslen is based on the flow being parallel to the shock wave and uses a von Mises transformation. This method uncouples the y-momentum equation. However, the method is not strictly valid at the stagnation region. The study by Olstad was for the Earth reentry of blunted-conical bodies with cone half angles of 30, 45, and 60 degrees. A step-model was used for the radiative transport. The results showned that the radiative heating along the cone flanks was comparable to the stagnation region values for the larger cone angles. Olstad also presented some preliminary results for air injection into the shock layer. These solutions were performed by using the Maslen method for an inner inviscid layer. The results showed that the air injection was more effective in reducing the radiative heating at the stagnation region than at the downstream region. The enthalpy profiles of the inner inviscid layer give the appearance of a boundary layer but are a result of absorption of the radiant energy emitted by the outer inviscid layer.

Callis (ref. 3) investigated the radiating, inviscid flow about long blunt bodies by using a time-asymptotic technique. A discussion of this technique is given below. The study by Callis was for Earth reentry and a step-model was used for the radiative transport. The body shapes were spherically capped cones. The results showed that for larger cone angles (60 degrees half angle) the inviscid radiative heating rates were in excess of the stagnation values over a large portion of the flank region.

Callis states that this increase in heating rates along the cone flanks could pose a serious thermal protection problem.

Chou (ref. 46) presents an approximate method for the flow about blunt bodies in which the entire layer is considered to be viscous. The solution is based on an approximate method for nonsimilar terms, the specie continuity equation is neglected, the density-viscosity product is constant, and the wall conditions are for constant mass injection and temperature along the body. An equation is developed for the nonsimilarity of the tangential velocity and Chou states that the validity of the equation cannot be defined rigorously and the physcial reason for the successful application is not clear. The application of the method was for Earth reentry and the injected gas was air. However, radiative transport was not considered for the air injection cases. A comparison was made with the method of Olstad (ref. 2) for inviscid radiating flow. The check cases were supplied by Dr. Olstad and Chou states that his method is valid when the results are compared. However, there is some question about the manner in which the results are being compared and the comparison may not be as good as shown by Chou. The disagreement over the comparison of the results has not been resolved.*

Prior solutions for the radiating flow about blunt bodies did not include ablation product effects and were for Earth reentry. The need for a fully-coupled solution with ablation products for arbitrary gases can be illustrated by the studies of Tauber (refs. 48 and 49) and Tauber

---

*Personal communications with Dr. W. B. Olstad, Langley Research Center, Hampton, Virginia

and Wakefield (ref. 50). These studies were for planetary entry into Jupiter, Saturn, Uranus, and Neptune with a nominal atmospheric composition of 85 percent hydrogen and 15 percent helium (mole fraction). The basis for the thermal analysis is presented in the paper by Tauber and Wakefield. These studies had to rely on stagnation-point results for the thermal analysis at the downstream regions. Results from the solutions for Earth reentry and the limited results by Wilson (ref. 44) for H_2-He mixture were used. This recourse had to be used because of the lack of results for flow around bodies with ablation product effects and the lack of results for entry into planets other than Earth. Additional discussion of this problem is given by Page (ref. 4).

There is no method which is generally accepted as being best, even when radiative transport is not included, for the shock layer solution around hypersonic blunt bodies (ref. 39). This point is shown in the paper by Perry and Pasiuk (ref. 51) in which numerous solutions are compared and are compared with experimental data. There is considerable scatter between the different solutions even in the region of subsonic flow. The solution used in the present study for the radiating, inviscid layer is a numerical method of a time-asymptotic technique.

Prior studies have used the time-asymptotic technique for the solution of an inviscid flow field (see, for example, refs. 3, 6, 52 and 53). The time-asymptotic technique retains the time dependent terms in the governing equations of the flow field and permits the time to increase until steady-state conditions are reached. By retaining the time dependent terms, the set of governing equations is hyperbolic and the same

computational method can be used in both the subsonic and supersonic regions of the flow along the body. The development of the technique is due to the studies by Von Neumann and Richtmyer (ref. 54), by Lax (ref. 55), and by Lax and Wendroff (ref. 56). The present method for the solution of the radiating, inviscid flow field is based on the studies of Moretti and Abbett (ref. 6), Callis (ref. 3), and MacCormack (refs. 57 and 58).

Moretti and Abbett (ref. 6) applied the time-asymptotic technique to flow around blunt bodies without radiative transport. The advantages of the method over other methods are discussed briefly by Moretti and Abbett (ref. 6) and more fully by Moretti and Abbett (ref. 59). A comparison of their results with the data presented by Perry and Pasiuk showed the method to be as accurate in matching the experimental data as any other method. Also, it was shown that the shock wave can be treated as a discontinuity and thereby reduce the number of mesh points required in an accurate numerical solution.

Callis (ref. 7), applied the time-asymptotic technique to stagnation-point solutions and Callis (ref. 3), applied the technique for flow about long blunt bodies. The solutions were for radiating, inviscid flow and showed the time-asymptotic technique to be valid for radiating flow fields. Callis stresses the need for treating the shock wave as a discontinuity. In addition to reducing the number of mesh points, the property profiles are more accurately defined for the radiative transport.

In the studies by Callis, and by Moretti and Abbett, a Taylor series expansion with the first three terms retained was used for the advancement of the flow field variables in time. Thus, the solutions are of second-order accuracy in time and require first-order and second-order time derivatives of the flow field variables. A method of second-order accuracy has been developed by MacCormack (refs. 57 and 58) which requires only the first-order time derivatives of the flow field variables. Basically, the method involves a two-step process for the advancement in time with the spatial derivatives of the flow field variables taken in alternate directions. The general method of MacCormack is used in the present study and is described further in the section on Analysis. Anderson (ref. 60) compared the two methods of time advancement in a time-asymptotic technique for the steady-state, nonequilibrium, flow in a nozzle and states the method developed by MacCormack to require fewer computations and 30 percent less computer time for identical results.

The studies by Moretti and Abbett, by Callis, and by MacCormack have shown the numerical methods for the time-asymptotic technique to be convergent, stable, and insensitive to initial guesses. A numerical method of second-order accuracy for the time-asymptotic technique and a discontinuous shock wave is used in the present study for the radiating, inviscid flow field solution.

Thermal Analyses for Venusian Entry

The fully-coupled solution for the radiating flow field with ablation product effects has been investigated in several studies for Earth

reentry (refs. 19, 22, 28, 29, 43, and 44) and Wilson (ref. 44) investigated a solution for Jupiter entry. These solutions were for the stagnation region of the body. At present, there are no published results for a fully-coupled solution with ablation product effects at either the stagnation or downstream regions for Venusian entry. A good review of the present state of technology of thermal analyses and ablation analyses for Venusian entry is given by Walberg and Sullivan (ref. 10).

The primary emphasis at the present time is for unmanned exploration of Venus. A description of the exploration and the scientific experiments is presented in references 61 to 64. Additional information on trajectories, body shapes, and body sizes for unmanned entries is given in references 65 to 69. The entry velocities range from 10 to 15 km/s with the velocities for peak radiative heating being from 7 to 13 km/s. The range of stagnation-point pressure on the body is 1 to 10 atmospheres. The exploration of Venus is a multi-probe, entry mission with one large probe and three small probes. The nominal body for the probes is a spherically capped, conical shape with a .34 meter nose radius and a 60 degree half angle for the large probe and a .14 meter nose radius and a 45 degree half angle for the small probes.

Models of the Venusian atmosphere are given in references 62, 63, and 70. The data for the models are primarily from the flights of Mariner V and Venera 4. Carbon dioxide is the major gas component for the Venusian atmosphere with up to 10 percent by volume of nitrogen.

Reviews of analytical and experimental studies of the radiative heating for Venusian entry and for gas compositions similar to Venusian

atmosphere are presented in references 10, 25, 39, and 71. Therefore, a complete review of the literature will not be given. The results of a recent experimental study in a shock tube for the convective and radiative heating in air and in a .90 CO_2 - .10 N_2 mixture (mole fraction) are presented by Livingston and Williard (ref. 72). A review of the existing studies shows there is a difference in the radiative transport between air and CO_2/N_2 mixtures. The CO_2/N_2 mixtures begin to radiate at a lower temperature than air because of molecular band transitions, primarily CN and CO. At velocities less than 10 km/s the radiative heating can be as much as a factor of 10 greater than air. However, at velocities above 10 km/s the radiative heating is comparable in the two types of gases because of the domination of the atomic processes present.

A detailed study of radiative heating in CO_2/N_2 mixtures is presented in the thesis by Boughner (ref. 25). However, atomic line transitions were neglected and only flight velocities from 8.5 to 10.5 km/s were considered. Most of the study was for a mixture of 50 percent CO_2 and 50 percent N_2 (mole fraction) and the results showed the emission spectrum to be dominated by the CO(4+) band system and the red and violet bands of CN.

Deacon and Rumpel (ref. 71) present results for the radiative heating of a .80 CO_2 - .20 N_2 mixture (by mole fraction) at flight velocities from 5 to 16.5 km/s. The important radiators were found to be CO(4+) band system, continuum from carbon, and atomic transitions of neutral carbon. This study was for a constant property layer. Deacon and Rumpel states that to correct for a nonadiabatic layer the corrections

from air studies would have to be applied due to the lack of data for CO_2/N_2 mixtures.

Spiegel et al. (ref. 69), present results for the thermal protection of a spacecraft during a Venusian entry. This investigation was for a completely uncoupled solution. In the study it was assumed: the shock layer is isothermal, no coupling between radiative and convective heating, no radiation absorption by ablation products, and no radiation cooling. The study was for a spherically capped, conical body with a .15 m nose radius and a 60 degree cone half angle. The heat-shield material was high-density phenolic nylon. The results show the radiative heating at a location on the cone flank to be greater by a factor of two than the stagnation-point value. Also, the ablation rates of the heat-shield material are comparable for the cone flank and the stagnation point. These results need to be verified by a fully-coupled solution.

A recent, but unpublished, analysis has been conducted by the present author and R. A. Falanga for the fully-coupled, radiating, flow field solution with ablation products injection at the stagnation point of a blunt body for Venusian entry.* The method of solution was similar to the present method except the radiating, inviscid, flow field solution was by the method of Falanga and Sullivan (ref. 73) and can only be used in the subsonic region of flow about a blunt body. The results of this recent study were that the boundary layer with ablation products injection will reduce the radiative heating to the body by 35 percent at

---

*Publication pending in Journal of Spacecraft and Rocket.

velocities of 9.86 and 11.18 km/s; but, the reduction was only 14 percent at a velocity of 8.11 km/s. The injection rates were for the steady-state ablation of a high-density, phenolic-nylon, material.

METHOD OF ANALYSIS

The radiating flow field about the entry body is separated into an outer layer where the inviscid flow equations are applicable and an inner viscous layer where the boundary layer equations are applicable. The divergence of the radiative flux is included in the energy equation for the solution of each layer and the boundary layer is coupled to the inviscid shock layer by the radiative transport through both layers and by the boundary layer displacement thickness. This coupling of the boundary layer solution to the inviscid shock layer solution is illustrated by the temperature profile shown in Figure 1. The inviscid flow field is displaced from the wall by the boundary-layer displacement thickness and the boundary-layer profiles are used out to the point where the boundary-layer edge values and their derivatives equal the inviscid layer values. For the boundary-layer solution, the radiative transport is calculated from the mated profiles for the entire layer. The total thickness of the flow field now becomes

$$\delta^t = \delta + \delta^* \tag{1}$$

where δ is the thickness of the inviscid shock layer (shock stand-off distance) and δ^* is the boundary layer displacement thickness calculated from

$$\delta^* = \int_0^{y_e} \left(1 - \frac{\rho u}{\rho_e u_e}\right) dy + \frac{1}{\rho_e u_e r_b} \int_0^s (\rho v)_w r_b \, ds \tag{2}$$

The first term on the RHS of the expression is the usual term for the displacement thickness of a compressible boundary layer without mass injection and is due to the retardation of the flow in the boundary

layer. The second term is the increase in displacement thickness due to mass injection at the wall for around the body.

The methods of solution of the inviscid flow field, the boundary layer, and the radiative transport are presented in sub-sections of the Method of Analysis. The solution for the radiating, inviscid flow field about a blunt body was developed in the present study and the development of the flow field equations and the numerical method is described in detail. A second-order, time-asymptotic technique is used for the solution. The solution of the inner viscous layer is for a nonsimilar, multicomponent boundary layer with mass injection, unequal diffusion coefficients, and arbitrary chemical species. An existing computer program (BLIMP) is used for the boundary layer solution with modifications made in the present study for coupling the radiative transport and mating the solution to the inviscid flow field. The radiative transport solution is for a nongray gas with molecular band, continuum, and line transitions. An existing computer program (RAD/EQUIL) is used for the solution. In addition to using RAD/EQUIL for coupling the radiative transport through the entire layer, an extensive modification of the program was made in the present study so that it could be used effectively as a subroutine in the developed computer program for the radiative, inviscid flow field.

The radiating, inviscid flow field solution is calculated only once for the fully coupled solution; but, an iteration is required to couple the boundary layer solution to the inviscid flow solution because of inclusion of the radiative heat flux in the boundary layer and locating

the boundary layer edge in the inviscid flow field. The boundary layer solution is assumed not to affect the inviscid layer solution through higher order effects such as recalculating the inviscid solution for an "effective" body composed of the original body plus the displacement thickness. Also, the radiative heat flux from the boundary layer toward the inviscid layer is small compared to the flux from the inviscid layer toward the boundary layer. Thus, the inviscid layer solution should be only slightly affected by the boundary layer solution. The boundary conditions for the boundary layer edge are the appropriate values and their derivatives at the match point in the inviscid flow solution and are not the values at the wall condition of the inviscid flow solution.

The calculation procedure for the fully-coupled solution is shown in Figure 2. The steps in the procedure are:

1. An inviscid, radiating solution is calculated from trajectory data.
2. A boundary layer solution with uncoupled radiative transport is calculated using the inviscid wall values for the boundary layer edge conditions. For steady-state ablation, the radiative heating to the wall is taken as the inviscid wall value.
3. The profiles from the inviscid solution and the boundary layer solution are mated and the radiative transport is calculated for the entire layer.
4. A boundary layer solution with coupled radiative transport is calculated using the values at the match point of the two layers for the boundary layer edge values.
5. Steps 3 and 4 are repeated until the radiative transport through the

layer, the match point condition, and the ablation rates (for steady-state ablation) converge.

The inviscid flow field and the boundary layer solutions are for the flow around a body and the coupling of the two layers and the convergence of the final solution is applied at each location around the body.

The solutions of the radiating inviscid flow, the boundary layer, and the radiative transport for the total layer are calculated by separate computer programs which are coupled through the iteration procedure. Approximately nine hours of total computer time are required for a fully coupled solution about a body and the computer storage requirements for the radiative transport program, the radiating inviscid flow program, and the boundary layer program are 56000_8, 115000_8, and 256000_8, respectively. No attempt has been made to combine the programs into a single computer program because of the large storage requirements and the large computational time.

The effect of the boundary-layer displacement thickness on the inviscid flow solution and subsequent effect on the boundary layer solution could be accounted for by repeating the series of calculations as required until convergence. The computational time for such a procedure would be excessive. Also, the shape of a body is changing during a high velocity entry due to the ablation of the heatshield. Accounting for these shape changes in a solution would require an extensive series of iterations. In the present study, the body shape is the shape prior to entry.

The rate and elemental mass fractions for the mass injection of the ablation products into the boundary layer can be either prespecified or

calculated during a solution for steady-state ablation of a heatshield. The equations for the wall boundary conditions in the boundary layer solution includes the necessary mass and energy balances for steady-state ablation. Steady-state ablation is a good representation of the ablation phenomena at entry conditions where significant radiative heating is present and is better than a specification of the mass injection rate. Steady-state ablation is used for the representation of the ablation of the heatshield for the Venusian entry solutions.

Radiating, Inviscid Flow Field Solution

A time-asymptotic technique is used for the solution of the radiating inviscid flow field; therefore, the analysis is based on the equations of conservation of mass, momentum, and energy for unsteady flow. The conditions for which the present analysis is carried out are that the flow is axisymmetric, inviscid, and nonconducting; the gas is in local thermodynamic and chemical equilibrium; the tangent slab approximation is valid for the radiative transport; and, the shock wave is a discrete surface.

The conservation equations expressed in vector notation are

Mass:

$$\frac{\partial \rho}{\partial t} + \nabla \cdot (\rho \vec{V}) = 0 \tag{3}$$

Momentum:

$$\frac{\partial \vec{V}}{\partial t} + \vec{V} \cdot \nabla \vec{V} - \frac{1}{\rho} \nabla p = 0 \tag{4}$$

Energy:

$$\rho\frac{\partial h}{\partial t} + \rho\vec{V}\cdot\nabla h + \nabla\cdot\vec{q}^{R} - \frac{\partial p}{\partial t} - \vec{V}\cdot\nabla p = 0 \tag{5}$$

Equations 3 thru 5 are for a general, orthogonal, curvilinear coordinate system. The coordinate system for high speed entries can be either body oriented (direct method) or shock orientated (inverse method). The body-orientated, coordinate system as shown in Figure 3 is used in the present analysis.

Equations 3 thru 5 are transformed to the present, body-orientated, coordinate system by using relationships for vector operations as given in reference 74. The necessary metric coefficients, g_i, for the coordinate transformation are determined from the length of a differential line element and the general expression is

$$(d\ell)^2 = g_1^{\,2}(dx_1)^2 + g_2^{\,2}(dx_2)^2 + g_3^{\,2}(dx_3)^2 \tag{6}$$

The expression for the present s, y, ϕ coordinate system is

$$(d\ell)^2 = \lambda^2(ds)^2 + (dy)^2 + r^2(d\phi)^2 \tag{7}$$

Comparing this expression to the general expression, the required metric coefficients are

$$\left.\begin{aligned} g_1 &= \lambda \\ g_2 &= 1 \\ g_3 &= r \end{aligned}\right\} \tag{8}$$

where

$$\left.\begin{aligned} r &= y\cos\theta + \int_0^s \sin\theta\, ds \\ \lambda &= 1 + Ky \end{aligned}\right\} \tag{9}$$

$$K = \frac{d\theta}{ds} \qquad (9)(\text{concl.})$$

The angle θ is a function of the coordinate s and the magnitude of the angle and the functional relation to s is known from the specification of the body shape.

By knowing the metric coefficients and using the relationships given in reference 74, the vector operations in equations 3 thru 5 can be carried out and the equations determined for the present coordinate system. Applying the axisymmetric conditions that the velocity and all gradients in the ϕ direction are zero, the conservation equations become

Mass:

$$\frac{\partial \rho}{\partial t} + \frac{1}{\lambda}\frac{\partial(\rho u)}{\partial s} + \frac{\rho u}{r}\sin\theta + \frac{\partial(\rho v)}{\partial y} + \rho v\left(\frac{K}{\lambda} + \frac{\cos\theta}{r}\right) = 0 \qquad (10)$$

s-momentum:

$$\frac{\partial u}{\partial t} + \frac{u}{\lambda}\frac{\partial u}{\partial s} + v\frac{\partial u}{\partial y} + \frac{Kuv}{\lambda} + \frac{1}{\rho\lambda}\frac{\partial p}{\partial s} = 0 \qquad (11)$$

y-momentum:

$$\frac{\partial v}{\partial t} + \frac{u}{\lambda}\frac{\partial v}{\partial s} + v\frac{\partial v}{\partial y} - \frac{Ku^2}{\lambda} + \frac{1}{\rho}\frac{\partial p}{\partial y} = 0 \qquad (12)$$

Energy:

$$\frac{\partial h}{\partial t} + \frac{u}{\lambda}\frac{\partial h}{\partial s} + v\frac{\partial h}{\partial y} - \frac{1}{\rho}\frac{\partial p}{\partial t} - \frac{u}{\rho\lambda}\frac{\partial p}{\partial s} - \frac{v}{\rho}\frac{\partial p}{\partial y} + \frac{1}{\rho}\left[\frac{\partial q^R}{\partial y} + q^R\left(\frac{K}{\lambda} + \frac{\cos\theta}{r}\right)\right] = 0 \qquad (13)$$

The bracketed term of equation 13 is the divergence of the radiative flux with the application of the tangent slab approximation. In the tangent slab approximation, the derivative of the radiative flux in the y direction is considered in the solution but the derivative in the s

direction is neglected. The parameters in this section of the report are non-dimensionalized by

$$\left.\begin{aligned} s &= \frac{s'}{Rn'} & p &= \frac{p'}{\rho_\infty' V_\infty'^2} & q^R &= \frac{q^R}{\rho_\infty' V_\infty'^3} \\ y &= \frac{y'}{Rn'} & h &= \frac{h'}{V_\infty'^2} & t &= \frac{t'}{(Rn'/V_\infty')} \\ r &= \frac{r'}{Rn'} & \rho &= \frac{\rho'}{\rho_\infty'} \end{aligned}\right\} \qquad (14)$$

where the subscript ∞ refers to the free stream value and the prime to dimensional quantities.

The value of y at the shock wave will vary with the s location around the body and will also vary with time because the shock wave is moving during the solution until a steady-state solution (final solution) is obtained. It is convenient in the solution to fix the location of the shock wave and this is accomplished by the transformation

$$\left.\begin{aligned} T &= t \\ S &= s \\ Y &= \frac{y}{\delta} \end{aligned}\right\} \qquad (15)$$

where

$$\delta = f(S, T)$$

The quantity δ is the shock stand-off distance and the transformation of equations 15 gives Y=0 for y=0 and Y=1 for y=δ. The inviscid flow field is now a rectangular coordinate system of length one for the Y-coordinate and a length for the S-coordinate as specified by the body shape. The value of S is zero at the centerline of the body. The differential

relationships to transform equations 10 thru 13 from the s, y, t coordinate system to the S, Y, T system are

$$\left.\begin{aligned} \frac{\partial(\ )}{\partial t} &= \frac{\partial(\ )}{\partial T} - \frac{Y}{\delta}\frac{\partial \delta}{\partial T}\frac{\partial(\ )}{\partial Y} \\ \frac{\partial(\ )}{\partial s} &= \frac{\partial(\ )}{\partial S} - \frac{Y}{\delta}\lambda_\delta \tan\beta \frac{\partial(\ )}{\partial Y} \\ \frac{\partial(\ )}{\partial y} &= \frac{1}{\delta}\frac{\partial(\ )}{\partial Y} \end{aligned}\right\} \qquad (16)$$

The quantity λ_δ is the value of λ evaluated at y equals δ. Hereafter, subscript notation is used to denote partial differentiation with respect to the variables S, Y, and T.

Applying the transformation of equations 16, the conservation equations 10 thru 13 become

Mass:

$$\rho_T = -\left(A\rho_Y + \frac{u}{\lambda}\rho_S - Bu_Y + \frac{\rho}{\lambda}u_S + \frac{\rho}{\delta}v_Y + C\right) \qquad (17)$$

S-momentum:

$$u_T = -\left(Au_Y + \frac{u}{\lambda}u_S - \frac{B}{\rho^2}p_Y + \frac{1}{\rho\lambda}p_S + D\right) \qquad (18)$$

Y-momentum:

$$v_T = -\left(Av_Y + \frac{u}{\lambda}v_S + \frac{1}{\delta\rho}p_Y - E\right) \qquad (19)$$

Energy:

$$h_T = -\left(Ah_Y + \frac{u}{\lambda}h_S - \frac{1}{\rho}p_T - \frac{A}{\rho}p_Y - \frac{u}{\rho\lambda}p_S + \frac{F^R}{\rho}\right) \qquad (20)$$

where

$$A = \frac{v}{\delta} - \frac{Y}{\delta}\delta_T - \frac{uY}{\delta\lambda}\lambda_\delta \tan\beta \qquad (21)$$

$$B = \frac{\rho Y}{\delta\lambda}\lambda_\delta \tan\beta \qquad (22)$$

$$C = \frac{\rho u}{r} \sin\theta + \rho v \left(\frac{K}{\lambda} + \frac{\cos\theta}{r}\right) \tag{23}$$

$$D = \frac{Kuv}{\lambda} \tag{24}$$

$$E = \frac{Ku^2}{\lambda} \tag{25}$$

$$F^R = \frac{1}{\delta} q_Y^R + q^R \left(\frac{K}{\lambda} + \frac{\cos\theta}{r}\right) \tag{26}$$

$$\lambda = 1 + K\delta Y \tag{27}$$

$$\lambda_\delta = 1 + K\delta \tag{28}$$

The mass equation, equation 17, is now changed from density as the dependent variable to pressure as the dependent variable. This is accomplished by using the state equation in the functional form

$$h = h(p,\rho)$$

to obtain the differential relations

$$\left.\begin{aligned} h_T &= \left(\frac{\partial h}{\partial p}\right)_\rho p_T + \left(\frac{\partial h}{\partial \rho}\right)_p \rho_T \\ h_S &= \left(\frac{\partial h}{\partial p}\right)_\rho p_S + \left(\frac{\partial h}{\partial \rho}\right)_p \rho_S \\ h_Y &= \left(\frac{\partial h}{\partial p}\right)_\rho p_Y + \left(\frac{\partial h}{\partial \rho}\right)_p \rho_Y \end{aligned}\right\} \tag{29}$$

Using the differential relations of equations 29 and combining equations 17 and 20, a new equation for the conservation of mass is obtained in the form

Mass:

$$p_T = -\left[Ap_Y + \frac{u}{\lambda} p_S + P_3\left(\frac{\rho}{\lambda} u_S - Bu_Y + \frac{\rho}{\delta} v_Y + C\right) - \frac{F^R}{P_1 \rho}\right] \tag{30}$$

where

$$P_1 = \frac{1}{\rho} - \left(\frac{\partial h}{\partial p}\right)_\rho \tag{31}$$

$$P_3 = \frac{1}{P_1}\left(\frac{\partial h}{\partial \rho}\right)_p \tag{32}$$

The values for the thermodynamic variables of ρ, P_1, and P_3 are determined by the conditions of chemical equilibrium for the gas with the specification of the elemental mass fractions of the gas and the two thermodynamic state variables of pressure and enthalpy. The dependent variable in the mass equation was changed from density to pressure as the dependent variable because density cannot be used as one of the specified thermodynamic state variables in the chemical equilibrium program used in the present study. Any two of the equations 17, 20, or 30 can be used in the inviscid flow solution depending on the method used for the thermodynamic state.

The basic equations for the solution of the radiating, inviscid flow field are equations 18 thru 28 and equations 30 thru 32. The terms

$$\frac{\rho u \sin\theta}{r}, \quad \frac{\rho v \cos\theta}{r}, \text{ and } \frac{q^R \cos\theta}{r}$$

which appear in equations 23 and 26 are indeterminant at the centerline, S=0, and are evaluated by the L'Hospital rule.

The solution for the location of the shock wave and the flow field variables along the shock wave (Y=1) is by a method using a quasi, one-dimensional, unsteady characteristic solution and the Rankine-Hugoniot equations for a moving shock. This method is discussed by Moretti and

Abbett (ref. 6) and by Callis (ref. 7). A derivation of the equations for the characteristic solution is presented in Appendix A. The equation for a right running characteristic is

$$\frac{dY}{dT} = A + \frac{\sqrt{P_3}}{\delta} \tag{33}$$

and the compatibility equation is

$$\frac{dv}{dT} + \frac{1}{\rho\sqrt{P_3}} \frac{dp}{dT} = C_2 + \frac{C_3}{\rho\sqrt{P_3}} \tag{34}$$

where

$$C_2 = -\left(\frac{u}{\lambda} v_S - E\right) \tag{35}$$

$$C_3 = -\left[\frac{u}{\lambda} p_S + P_3\left(\frac{\rho}{\lambda} u_S + C\right) - \frac{F^R}{P_1\rho} - P_3 Bu_Y\right] \tag{36}$$

The set of derived equations for the radiating, inviscid flow field about a blunt axisymmetric body is solved by the numerical methods presented below. In addition to the complete body solution, a separate solution for only the stagnation point of a blunt body was obtained in the present study and the equations are presented in Appendix B.

The concept of the time-asymptotic technique is to assume initial values for the flow field variables and then to increment the variables in time until the variables are invarient with time. Thus, the evolution of the flow in time is followed until the flow obtains a steady-state condition. The numerical method used in the present study to obtain a solution is based on the two-step method of MacCormack and a description of the numerical analysis for the method is given in references 57 and 58.

At time T the value of a variable is known at all locations in the flow field. The advancement of a variable from time T to T+ΔT (one iteration) is given by

$$f(S,Y,T+\Delta T) = f(S,Y,T) + f_T^{ave}\Delta T \tag{37}$$

where

$$f_T^{ave} = (f_T^1 + f_T^2)/2 \tag{38}$$

The symbol f represents the variable p, u, v, or h and the superscripts 1 and 2 refer to the first and second step in the two-step process. The time derivative, f_T, of the variable is calculated from the unsteady equations (equations 18, 19, 20, or 30) with finite differences used for the spatial derivatives. The calculation of f_T^{ave} and the advancement from T to T+ΔT is a two-step process as follows:

1. Compute f_T^1 at time T from the unsteady equations using forward differences for the spatial derivatives. Advance f by

$$f_{n+1} = f_n + f_T^1\Delta T \tag{39}$$

2. Compute f_T^2 at n+1 from the unsteady equations using the variables f_{n+1} and backward differences for the spatial derivatives. Then, compute the average value of the time derivative, f_T^{ave}, by equation 38 and advance the variable, f, to time T+ΔT by equation 37.

Step 1 is applied to each variable p, u, v and h at all S, Y locations before proceeding to step 2.

A modification to the basic method of MacCormack for the spatial derivatives is used in the present study. In the basic method, two-point, forward finite differences are used for the first step and two-

point, backward differences are used for the second step along all coordinates. In the present method, three-point, central finite differences are used for the derivatives with respect to the S-coordinate for both steps in the two-step process. Three-point, forward differences on the first step and three-point, central differences on the second step are used for the derivatives of h and u with respect to the Y-coordinate. The derivatives of p and v with respect to the Y-coordinate are the basic method of two-point forward on the first step and two-point backward on the second step. A Taylor series expansion is used for the derivation of the finite difference equations for unequal spacing of the nodal points along each coordinate. The same equations are also valid when equally spaced points are specified.

The above numerical method is used for all nodal points except the nodal points along the shock wave (Y=1). The flow field variables at the nodal points along the shock wave and the location of the shock wave are calculated by a numerical method using the equations from the quasi, one-dimensional, characteristics analysis and the Rankine-Hugoniot equations for a moving shock wave. The numerical method is illustrated by the diagram in Figure 4. At time T all the quantities are known and the properties at D, δ, and δ_T are desired at time T+ΔT. The solution procedure is as follows:

1. Assume a δ_T at time T+ΔT and use trapezoidal integration to determine δ by

$$\delta(T+\Delta T) = \delta(T) + \left[\delta_T(T) + \delta_T(T+\Delta T)\right]\frac{\Delta T}{2} \qquad (40)$$

The angle β is calculated by

$$\tan \beta(T+\Delta T) = \left(\frac{1}{\lambda_\delta} \frac{\Delta\delta}{\Delta S}\right)_{T+\Delta T} \tag{41}$$

2. The properties of p, u, v, and h at point D are calculated from the Rankine-Hugoniot equations for a moving shock with the known free-stream properties, the assumed δ_T, and calculated β.

3. Point B is located from the characteristics equation (eq. 33) by

$$\Delta Y = \left(A + \frac{\sqrt{P_3}}{\delta}\right)_{ave} \Delta T \tag{42}$$

where averaged properites of points B and D are used for the integration. The properties at point B are averaged properties of points A and C.

4. A value of v at point D is computed from the integration of the compatability equation (eq. 34) from point B to point D using averaged properties

$$v_D = v_B + \left(C_2 + \frac{C_3}{\rho\sqrt{P_3}}\right)_{ave} \Delta T - \left[\left(\frac{1}{\rho\sqrt{P_3}}\right)_{ave} (P_D - P_B)\right] \tag{43}$$

The value for p_D is the value calculated by the Rankine-Hugoniot equations in step 2.

5. The computed value of v_D from the compatibility equation is compared with the value calculated from the Rankine-Hugoniot equations in step 2. If the values for v_D do not match, then a new value for $\delta_T(T+\Delta T)$ is assumed and steps 1-5 are cycled until convergence.

The numerical method is applied at each time step for each S-coordinate

location beginning with the S=0 location. The method is converged at each S location before proceeding to the next location around the body. A Newton-Raphson method is used for successive guesses for δ_T after the first two guesses.

The value of the shock stand-off distance, δ, at each S location is checked by a mass balance. For the mass balance, the mass flow through a plane in the flow field at the particular S location is equal to the mass flow from the free stream through the shock wave up to the particular S location. The expression for δ from the mass balance is

$$\delta = \frac{r_b^2}{2(SF - r_b \cos \theta)} \tag{44}$$

where

$$SF = \int_0^1 (r\rho u)dY \tag{45}$$

To insure a mass balance for the converged solution, the shock stand-off distance at each S location is adjusted if necessary to the value from equation 44 as the solution approaches convergence.

The size of the time step for the advancement at each iteration is calculated by the use of the characteristic equation (eq. 33) in the form

$$\Delta T \leq \frac{\Delta Y}{A + (\sqrt{P_3}/\delta)} \tag{46}$$

This stability criterion is based on the Courant-Friedricks-Lewy condition and insures that the net slope is less than the characteristics slope for hyperbolic equations (ref. 75, chap. 9). Equation 46 is a

one-dimensional equation being used for a two-dimensional problem; however, the ΔY is smaller than ΔS in the problem and no stability problem was encountered. A time step is calculated at each nodal point in the flow field and the minimum value for the nodal points along a ray at a S-coordinate is used for all the points along that particular S-coordinate. There is a large variation in time steps around the body and using a varying time step around the body requires less iterations for convergnece than using a minimum time step for the entire flow field. Having a different time plane through the flow field did not affect the converged steady-state solution.

The radiative heat flux, the thermodynamic properties, and the solution of the Rankine-Hugoniot equations are calculated by using the computer program of Nicolet (refs. 9 and 32). A modified version of this program is used as subroutines to the computer program developed for the radiating, inviscid flow field. A discussion of the method of calculating the radiative heat flux and the modifications are presented in the sub-section of Radiative Transport. Large computational times are required for the calculation of the radiative heat flux and the thermodynamic properties; however, these parameters do not have to be updated at each iteration. A study was made and it was determined that the thermodynamic properties and radiative heat flux can be calculated every 50 to 100 iterations without affecting the converged solution but greatly reducing the computational time. For the iterations when the thermodynamic subroutine is not used, the density is calculated by

$$\Delta\rho = \Delta h + \frac{\left(P_1 - \frac{1}{\rho}\right)}{P_1 P_3}\Delta p \tag{47}$$

with the thermodynamic properties P_1 and P_3 held constant. The properties P_1 and P_3 are calculated by

$$P_1 = \frac{\bar{T} c_p}{\rho a^2 \left[\left(\frac{\partial \ln M}{\partial \ln \bar{T}}\right)_p - 1\right]} \tag{48}$$

$$P_3 = a^2 \tag{49}$$

where $\bar{T}$ is temperature, a is sonic velocity, M is molecular weight, and c_p is specific heat. The non-dimensionalization of the properties is given by

$$\bar{T} = \frac{\bar{T}'}{\bar{T}'_s} \qquad a = \frac{a'}{V'_\infty} \qquad c_p = \frac{c'_p}{(V'^2_\infty / \bar{T}'_s)} \tag{50}$$

where the subscript s refers to the conditions behind a normal shock. The expressions are derived from equations 31 and 32 by using thermodynamic relations. The necessary properties for calculating P_1 and P_3 by equations 48 and 49 are available from the thermodynamic subroutine. Pressure and enthalpy which are calculated by the unsteady equations are used as the two specified, thermodynamic state variables for the thermodynamic subroutine and the radiative heat flux subroutine. The solution of the Rankine-Hugoniot equations for a moving shock wave is calculated by the usual Rankine-Hugoniot equations with the velocities on either side of the shock made relative to a fixed shock location. As mentioned, a solution for the Rankine-Hugoniot equations is included in the program of Nicolet.

The initial values to begin a solution are calculated by assuming the shock wave is stationary and the shock stand-off distances around

the body are equal to the shock stand-off distance at the centerline (S=0). The value at the centerline is calculated by a correlation from reference 76 of $\delta = .78/\rho_s$ where ρ_s is the nondimensional density behind a normal shock and δ is the nondimensional stand-off distance. The flow field variables for the nodal points along the shock wave are calculated from the Rankine-Hugoniot equations. The variables for the wall nodal points are calculated by assuming an isentropic expansion along the body with a Newtonian pressure distribution. Values for intermediate points in the flow field are calculated by linear interpolation of the shock and body values.

The convergence of a solution is determined by checking the change in enthalpy between iterations. The percentage change in enthalpy between two successive iterations must be less than a specified small value and this criterion must be met for a specified number of iterations. The enthalpy at the body, shock, and midpoint along a ray at each S location is checked.

A computer program was developed for the numerical solution of the radiating, inviscid flow field. The program is written in FORTRAN IV language for CDC 6000 series computers. A listing of the program is given in Appendix C.

Boundary Layer Solution

The boundary layer equations are for a nonsimilar, multicomponent boundary layer with mass injection, unequal diffusion coefficients, and arbitrary chemical species. The solution of the equations is by a

numerical, integral matrix method and there is an existing computer program for the solution called BLIMP. Many types of complex, reactive boundary layer problems can be solved by the program and numerous publications are required for a complete description of the program and the concepts and methods used in a solution. A brief discussion is presented of the basic method and of the modifications to the program made in the present study. A list of the significant publications is given after the discussion of the basic method.

The present discussion of the basic method is from reference 8. The boundary layer equations for an s, y coordinate system of a blunt, axisymmetric body (see Figure 3) are

Mass:

$$\frac{1}{r_b}\frac{\partial(\rho u r_b)}{\partial s} + \frac{\partial(\rho v)}{\partial y} = 0 \tag{51}$$

s-momentum:

$$\rho u \frac{\partial u}{\partial s} + \rho v \frac{\partial u}{\partial y} = \frac{\partial}{\partial y}\left[\left(\mu + \rho\varepsilon_m\right)\frac{\partial u}{\partial y}\right] - \frac{\partial p}{\partial s} \tag{52}$$

y-momentum:

$$\frac{\partial p}{\partial y} = 0 \tag{53}$$

Energy:

$$\rho u \frac{\partial H}{\partial s} + \rho v \frac{\partial H}{\partial y} = -\frac{\partial}{\partial y}\left(q^C + q^R\right) \tag{54}$$

where

$$H = h + \frac{u^2}{2} \tag{55}$$

Species:

$$\rho u \frac{\partial \bar{K}_i}{\partial s} + \rho v \frac{\partial \bar{K}_i}{\partial y} = \frac{\partial}{\partial y}\left(\rho\varepsilon_d \frac{\partial \bar{K}_i}{\partial y} - j_i\right) \tag{56}$$

The species' conservation equation is solved in terms of elemental mass fraction, $\bar{K}_i$, rather than the species' mole fraction by the application of the Shvab-Zeldovich transformation. This transformation eliminates the chemical source term for chemical equilibrium and reduces the number of species' conservation equations from the number of species to the number of elements. For a boundary layer with ablation products injection, the number of species is typically from 20 to 50 whereas the number of elements is only 2 to 6.

The complexity of using unequal diffusion coefficients for a multicomponent mixture is reduced by a bifurcation approximation for the binary diffusion coefficients. The approximation is expressed as

$$D_{ij} \approx \frac{\bar{D}}{F_i F_j} \tag{57}$$

where $\bar{D}$ is the self-diffusion coefficient of a reference specie and F_i, F_j are the diffusion factors for species i and j. The F_i of a specie for a given chemical system can be determined by finding the set of diffusion factors that gives the minimum total system residual error and a method is presented in reference 77. The bifurcation approximation permits the diffusive flux of element i to be expressed explicitly in terms of properties and gradients of element i and of the system as a whole, but not of other elements. Also, the I(I-1)/2 binary diffusion coefficients are replaced by I diffusion factors where I is the number of chemical species.

The diffusional mass flux of element i in the species' conservation equation (eq. 56) can be expressed as

$$j_i = -\frac{\rho \bar{D} \mu_2}{\mu_1 M}\left[\frac{\partial \bar{Z}_i}{\partial y} + (\bar{Z}_i - \bar{K}_i)\frac{\partial \ln \mu_2}{\partial y}\right] \tag{58}$$

by use of the bifurcation approximation and the definition of the new quantities

$$\left.\begin{aligned} Z_j &= \frac{M_j \bar{x}_j}{F_j \mu_2} & \bar{Z}_i &= \sum \alpha_{ij} Z_j \\ \mu_1 &= \sum \bar{x}_j F_j & \mu_2 &= \sum \frac{M_j \bar{x}_j}{F_j} \end{aligned}\right\} \tag{59}$$

The subscript j refers to species and the subscript i refers to elements. The quantity α_{ij} is the mass fraction of element i in species j and Z_j is a quantity which for unequal diffusion lies between a mass fraction and a mole fraction for species j.

The convective heat flux term q^C in the energy equation (eq. 54) is the sum of heat flux due to conduction, diffusion, turbulence, and dissipation of kinetic energy. Using the bifurcation approximation for the heat flux due to diffusion, the convective heat flux can be expressed by

$$q^C = -\left\{(\rho\epsilon_m + \mu)\frac{\partial(u^2/2)}{\partial y} + (k + \rho\epsilon_h c_p)\frac{\partial \bar{T}}{\partial y} + \rho\epsilon_d\left(\frac{\partial h}{\partial y} - c_p \frac{\partial \bar{T}}{\partial y}\right) + \frac{\rho \bar{D} \mu_2}{\mu_1 M}\left[\frac{\partial \bar{h}}{\partial y} - \bar{c}_p \frac{\partial \bar{T}}{\partial y} + (\bar{h} - h)\frac{\partial \ln \mu_2}{\partial y}\right]\right\} \tag{60}$$

where

$$\bar{h} = \sum Z_j h_j \qquad \bar{c}_p = \sum Z_j c_{p_j} \tag{61}$$

The turbulent transport terms in the equations are expressed in the Boussinesq form of eddy viscosity, eddy diffusion, and eddy

conductivity. If turbulent transport is considered, the turbulent transport properties are included in the boundary layer equations when a prespecified Reynolds number is exceeded. The Reynolds number is based on edge properties and momentum thickness. A transition region between laminar flow to turbulent flow is not included.

The boundary conditions at the boundary layer edge are the specifications of u, H, and $\bar{K}_i$ and their derivatives with respect to the y-coordinate. The wall boundary conditions allow for the possibility of solving numerous types of problems and thus specification of different variables. However, all the variations include zero slip at the wall, $u_w=0$, and involves in some form the assignment of values for mass injection rate, $(\rho v)_w$; wall enthalpy or wall temperature, h_w or $\bar{T}_w$; and elemental mass fractions at the wall, $\bar{K}_{i,w}$.

The equations of the wall boundary conditions for energy balance and elemental mass balance allow a solution for steady-state ablation of a heatshield. The energy balance is

$$-q_w^C - q_w^R - \sigma\varepsilon_w\bar{T}_w^4 - (\rho v)_w h_w + m_g h_g + m_c h_c - q_{cond} = 0 \qquad (62)$$

where the subscripts g and c refer to the pyrolysis gas and char for ablation and q_{cond} is the heat conducted into the ablation material at the wall surface. For steady-state ablation

$$m_g h_g + m_c h_c - q_{cond} = m_a h_a^o \qquad (63)$$

where m_a is the total ablation rate, m_g plus m_c, and h_a^o is the heat of

formation of the undecomposed ablation material. Noting that

$$(\rho v)_w = m_a \tag{64}$$

then the surface energy balance for steady-state ablation is

$$-q_w^C - q_w^R - \sigma \epsilon_w \bar{T}_w^4 + m_a (h_a^o - h_w) = 0 \tag{65}$$

The elemental mass balance is

$$m_g \bar{K}_{i,g} + m_c \bar{K}_{i,c} - (\rho v)_w \bar{K}_{i,w} - j_{i,w} = 0 \tag{66}$$

and, for steady-state ablation

$$m_g \bar{K}_{i,g} + m_c \bar{K}_{i,c} = m_a \bar{K}_{i,a} \tag{67}$$

thus, the elemental mass balance for steady-state ablation is

$$m_a (\bar{K}_{i,a} - \bar{K}_{i,w}) - j_{i,w} = 0 \tag{68}$$

A solution for steady-state ablation does not require knowledge of the in-depth response of the ablation material but only the surface interactions between the boundary layer and the ablation material. From equations 65 and 68, it is shown that the additional properties of the elemental mass fractions and heat of formation of the undecomposed ablation material and the wall emissivity are all that is required for a steady-state ablation solution. The solution of the surface balances gives the basic boundary conditions of injection rate, enthalpy, and elemental mass fractions at the wall.

An ξ, η coordinate system is used for the actual solution of the boundary-layer equations by the transformations of

$$\left.\begin{aligned} \xi &= \int_0^s u_e \rho_e \mu_e r_b^2 \, ds \\ \eta &= \frac{r_b u_e}{\sqrt{2\xi}} \int_0^y \rho \, dy \end{aligned}\right\} \tag{69}$$

and a stream function of

$$f - f_w = \int_0^\eta \frac{u}{u_e} \, d\eta \tag{70}$$

The transformed equations will not be presented.

The numerical procedure for the solution of the boundary layer equations is an integral matrix method. The boundary layer is divided into strips in the normal direction (η coordinate) and the conservation equations are integrated across the strips. Across a strip, the primary dependent variables of velocity, total enthalpy, and elemental mass fractions and their derivatives with respect to η are related by Taylor series expansions with cubic or quadratic fits. Implicit, finite difference expressions are used for the derivatives in the streamwise direction (ξ coordinate). The set of simultaneous equations which includes the Taylor series, the conservation equations, and the boundary conditions are solved by general Newton-Raphson iteration using a matrix inversion technique involving successive matrix reductions.

Many aspects of the BLIMP program have been left out in the above discussion. Further information for the boundary layer method and the

BLIMP computer program is presented in the following references. The solution for the boundary layer equations is given in references 8, 18, 78, and 79. The solution is for an arbitrary, multicomponent gas mixture and the method for the thermodynamic properties for chemical equilibrium is given in reference 80 and the method for the mixture transport properties is given in reference 81. A method for considering a boundary layer for a blunt body solution with entropy layer is presented in reference 82. Information on the turbulent transport model is given in references 79, 82, and 83. User's manuals for the BLIMP program are references 84 to 86. The description of a companion analysis for in-depth response of an ablative heatshield is given in reference 87.

Modifications to the BLIMP program were necessary in the present study to clarify the coupling of radiative heating and to make the boundary layer edge conditions compatible with the inviscid flow field. The radiative heating was included in the formulation of the energy equation and in the coding of the BLIMP program; however, the values for the radiative heating were set to zero in the program and no provision was made to input the values. The term $(q^C + q^R)$ was considered as being only convective heating, since q^R was set to zero, and was used in expressions in the program which are only applicable for convective heating. When the radiative heating, q^R, is included in the term $(q^C + q^R)$ these expressions are invalid. There was a provision for inputing radiative heating to the wall, unattenuated by the boundary layer, for use in the wall energy balance for steady-state ablation. The convective heating for the energy balance was represented by the

term ($q^C + q^R$) at the wall and if the radiative heating through the layer is included in the term by q^R then the radiative heating at the wall is accounted for twice and the energy balance is invalid. The BLIMP program was modified by re-defining certain expressions to clarify the difference between convective and radiative heating and to properly input the radiative heating at the nodal locations.

The derivatives for the edge boundary conditions are set in the BLIMP program as the usual boundary layer edge condition of

$$\left(\frac{\partial u}{\partial y}\right)_e = 0 \qquad \left(\frac{\partial H}{\partial y}\right)_e = 0 \qquad \left(\frac{\partial \bar{K}_i}{\partial y}\right)_e = 0$$

These boundary conditions consider that u, H, and $\bar{K}_i$ are invariant with y in the inviscid layer. The edge conditions of zero for the velocity and total enthalpy gradients may not be of suffieient accuracy and may give incorrect results for the boundary layer solution because of non-adiabatic effects when radiative transport is present and when an entropy layer is present in the inviscid flow field of a blunt body. There are several methods in BLIMP for considering the effect of an entropy layer for a blunt body and for these methods the derivatives are specified by appropriate values and not set to zero. However, the methods did not consider the effect on the derivatives for a non-adiabatic inviscid flow field from radiative transport and were not appropriate for the present study. The BLIMP program was modified in the present study so that the derivatives of velocity and total enthalpy with respect to the y coordinate can be specified by inputs and correctly transformed to the η coordinate. Also, a modification was made for specifying the total

enthalpy at the boundary layer edge around the body. These modifications allow for equating the boundary layer edge values with the values of the radiating, inviscid flow field at the match point in the flow field.

Radiative Transport Solution

The solution of the radiative transport is for a nongray gas with molecular band, continuum, and atomic line transitions. A detailed frequency dependence of the absorption coefficients is used in the integration over the radiation spectrum and the tangent slab approximation is used for integration over physical space. An existing computer program (RAD/EQUIL) by Nicolet (refs. 9 and 32) is used for the calculation of the radiative transport. The present section presents a brief discussion of the method and the modifications to the computer program when used as subroutines for the radiating, inviscid flow field solution.

The tangent slab approximation treats the radiative transport as a one-dimensional problem in the direction normal to the body. Thus, the equations for the radiative transport are derived for a gas confined between two infinite parallel boundaries and the property gradients of the gas are considered as zero except in the normal direction between the boundaries. For the present problem, the boundaries are the shock and the body and the normal direction is perpendicular to the body. The tangent slab approximation is applied locally at each location around the body. Note, the tangent slab approximation is used only for the radiative transport calculations and not for the gradients of the thermodynamic state and flow properties for the flow field solution.

The radiative heat flux across a surface at a point in the gas layer is

$$dq_\nu^R = I_\nu \cos \gamma \, d\Omega \tag{71}$$

where I_ν is the intensity, γ is the angle between a ray and the normal, and Ω is the solid angle. The basic equation for the intensity gradient along a ray for a gas in local thermodynamic equilibrium is

$$\frac{dI_\nu}{d\ell} = \mu_\nu (B_\nu - I_\nu) \tag{72}$$

where μ_ν is the linear absorption coefficient corrected for induced emission and B_ν is the Planck function. The solution of equations 71 and 72 at a point y in the gas layer for the directional, radiative heat flux is given by Nicolet in the form

$$\left.\begin{aligned} q_\nu^{R,+}(y) &= \pi \int_0^{\epsilon_b^+} B_\nu(\epsilon_\nu^+) \, d\epsilon_\nu^+ \\ q_\nu^{R,-}(y) &= \pi \int_0^{\epsilon_b^+} B_\nu(\epsilon_\nu^-) \, d\epsilon_\nu^- \end{aligned}\right\} \tag{73}$$

where heat fluxes into the slab at the boundaries are neglected. The net flux at point y is

$$q^R(y) = \int_0^\infty q^{R,+}(y) \, d\nu - \int_0^\infty q^{R,-}(y) \, d\nu \tag{74}$$

The plus sign in the superscripts referes to the heat flux in the direction toward the shock and the negative sign for the flux toward the body.

Nicolet solves the flux equation in a Planck function, B_ν, and emissivity, ε_ν, coordinate system where

$$\tau_\nu = \int_0^y \mu_\nu \, dy \tag{75}$$

$$\left.\begin{aligned} \varepsilon_\nu^+ &= 1 - 2E_3(\tau_\nu - t_\nu), \quad t_\nu \leq \tau_\nu \\ \varepsilon_\nu^- &= 1 - 2E_3(\tau_\nu - t_\nu), \quad t_\nu \geq \tau_\nu \end{aligned}\right\} \tag{76}$$

where t_ν are the dummy values of optical depth and $E_n(z)$ is the exponential integral of order n. For the solution by Nicolet, the exponential integral of third order is approximated by

$$E_3(z) \approx \frac{\exp(-2z)}{2} \tag{77}$$

and the expressions for emissivity become

$$\left.\begin{aligned} \varepsilon_\nu^+ &\approx 1 - \exp\,[2(t_\nu - \tau_\nu)] \\ \varepsilon_\nu^- &\approx 1 - \exp\,[2(\tau_\nu - t_\nu)] \end{aligned}\right\} \tag{78}$$

The spectral absorption coefficient for a gas mixture is in general

$$\mu_\nu = \sum \mu_i^C(\nu) + \sum \mu_j^L(\nu) \tag{79}$$

where the first term is the continuum contribution with a summation over all continuum transitions and the second term is the line contribution with a summation over all line transitions. The absorption coefficients are calculated in the RAD/EQUIL program and the theoretical expressions,

approximations, and experimental data of the various transitions for the species are given in detail in the report of Nicolet (ref. 9). Transitions of the species N, C, H, O, H^-, C^-, N^-, O^-, H_2, C_2, N_2, O_2, NO, CO, CN, and N_2^+ are considered for the radiative transport.

In the computer program, the radiative heating is separated into heating due to continuum transitions and line transitions. The continuum contribution is calculated by using only the first term of equation 79 for the spectral absorption coefficient and then the line contribution is calculated by

$$q_\nu^{R,L} = q_\nu^R - q_\nu^{R,C} \tag{80}$$

where the total absorption coefficient is used for the q_ν^R value. The molecular transitions are treated as an "equivalent" continuum process by a bandless model in which the bands within each band system are smeared by

$$\bar{\mu}_\nu = \frac{\int_{\Delta\nu} \mu_\nu \, d\nu}{\Delta\nu} \tag{81}$$

where the frequency increments $\Delta\nu$ are selected so that $\bar{\mu}_\nu$ varies smoothly over the frequency spectrum of the band system. The molecular transitions are included in the continuum contribution to the radiative flux.

For the continuum calculations, the frequency spectrum in terms of photon energy ($h*\nu$) is divided into 48 frequency nodal points over the range 0 to 15 ev. The frequency nodal points are not equally spaced over the spectrum but are spaced to resolve the frequency variation of the absorption coefficient especially at photoionization edges. The

number of node points, frequency range, and spacing are inputs to the program and the above values were used in the present study.

The line grouping technique is used for the atomic line transitions. In this technique, the line transitions near a specified frequency value are grouped together and the radiative heating is given as that from the line group. However, each line within the group is treated individually and can assume unshifted Lorentz or Doppler line shapes or a combination of the two with the half widths including the Stark, resonance, and Doppler effects. The frequency grid for each line is composed of 13 nodal points and the grid is dependent upon the characteristics of the gas layer as well as the individual line. Twenty line groups with a total of 134 lines are used in the present study. The line groups are not connected over the frequency spectrum, but are spaced according to the frequency locations of the line transitions.

The thermodynamic properties and species concentrations required for the calculation of the spectral absorption coefficients and Planck functions are calculated in the computer program by a chemical equilibrium method from the specification across the spatial grid of the enthalpy (or temperature), pressure, and elemental mass fractions. Only the species as given above are used for the radiative transport calculations; but, additional species can be included in the chemical equilibrium calculation. A method for the solution of the Rankine-Hugoniot equations for shock waves is also included in the program. The methods for the chemical equilibrium solution and the Rankine-Hugoniot solution are given in the report by Nicolet. The calculation of the thermodynamic state is consistent throughout the fully-coupled solution because the

chemical equilibrium method is the same in both the RAD/EQUIL and the BLIMP programs.

Briefly, the solution procedure for the radiative transport is that the chemical equilibrium calculations are made for the specified spatial grid. The spectral absorption coefficients, Planck functions and optical depths are calculated. Then the emissivities are calculated and the transformation to the B_ν, ε_ν coordinates is made by knowing B_ν and ε_ν as a function of y. The heat flux equations are then integrated. Cubic integration formulas are used for all integrations except for the frequency integration of the continuum flux. These integrals are evaluated by linear formulas because of the discontinuity at photoionization edges.

The RAD/EQUIL computer program is used for the calculation of the radiative transport through the total layer from the coupling of the boundary layer to the inviscid layer. This is step 3 in the calculation procedure. Also, a modified version of the RAD/EQUIL program is used as a subroutine in the computer program for the radiating, inviscid flow field solution. The following comments refer to the modified version. A separation between the subroutines for the radiative transport calculations and the chemical equilibrium calculations was made in order that the chemical equilibrium calculations can be performed without calculating the radiative transport. The chemical equilibrium subroutine was modified by the addition of a routine to calculate the necessary thermodynamic properties for the evaluation of the P_1 and P_3 properties required for the inviscid flow solution. The required addition was

taken from the chemical equilibrium version in the BLIMP computer program. The method for calculating thermodynamic derivatives for the chemical equilibrium version in BLIMP is given in reference 80. Also, the storage requirement was reduced by deleting options which were not required, by reducing the maximum number of spatial nodal points, and by reducing the maximum number of chemical species in the chemical equilibrium solution. The modified version of the RAD/EQUIL program was then mated to the computer program for the radiating, inviscid flow field solution.

RESULTS AND DISCUSSION

A computational method has been developed for the fully-coupled solution of nongray, radiating gas flow with ablation product effects about blunt bodies during planetary entries. Application of the developed method is shown by results for Venusian entries. There are no published results for a fully-coupled solution of the radiating flow about ablating, planetary entry bodies; therefore, the validity of the present method is shown by comparing the results from solutions to subcomponents of the method with published results of corresponding solutions.

The present method for the solution of an inviscid flow field is compared with existing methods for both non-radiating and radiating gas flows about blunt bodies during Earth reentry. Results from solutions by the present method for the radiating, inviscid flow about blunt bodies are also presented for planetary entries. The present method for a fully-coupled solution with ablation product effects is compared with an existing method for the stagnation point of blunt bodies for Earth reentry. Results from the present method are then presented for the fully-coupled solution about blunt bodies for Venusian entries.

Several comments are given about the presentation of the results. In the present coordinate system, the radiative heating directed toward the shock wave is positive and the radiative heating directed toward the body is negative. However, the radiative heating rates at the wall are given by positive values in the presentation of results. As stated in

the section of Radiative Transport Solution, the radiation contributions by molecular band transitions are included in the continuum contribution to the radiative heating. The total contributions of molecular band transitions and continuum transitions are referred to by continuum processes. The line grouping technique is used for the atomic line transitions and the spectral distributions for the line transitions are given by the contribution of the line group and not by the individual lines.

Non-Radiating, Inviscid Air Solution

The present method for an inviscid flow field has been used to obtain a solution for the nonradiating flow about a spherically capped, conical body during an Earth reentry. The results are presented in Figure 5 and are compared with results by the method of Inouye et al. (ref. 88). The method of reference 88 is considered to be one of the more accurate methods and provides a good means of evaluating the accuracy of the present method for an inviscid flow field solution.

The solution is for the free-stream conditions and body shape given in Figure 5(a). The results for the shock shape at the forward region of the body and the location of the sonic line are presented in Figure 5(b). Figure 5(c) presents the results for the shock shape at the downstream region of the body. Because the thickness of the shock layer is much smaller than the dimensions of the body, a better means of comparing the shock shape is the shock stand-off distance and these

results are presented in Figure 5(d). The results for the shock stand-off distance illustrate the inflection points in the shock shape around the body. The results from the present method are in good agreement with the results by the method of reference 88 for the shock shape, especially considering the inflection points, and for the sonic line location.

The results for the distribution of tangential velocity and pressure along the body are presented in Figures 5(e) and 5(f), respectively. The results from the present method are in good agreement with the results by the method of reference 88 even in the region of the over-expansion of the flow at the sphere-cone junction.

The good agreement between the present results and those by the method of reference 88 indicates the present method provides a good solution for the inviscid flow about a blunt body. Radiating flow is not treated by the method of reference 88.

Radiating, Inviscid Solutions About Blunt Bodies

Results are presented from solutions of the radiating, inviscid gas flow about blunt bodies during planetary entry. The present results for solutions of entries into the Earth's atmosphere are compared with existing methods.

The present method is compared with the method of Callis (ref. 3) for an Earth reentry and the results are presented in Figure 6. The free-stream conditions and body shape are given in Figure 6(a). The

distributions of the wall pressure and the shock stand-off distance are presented in Figures 6(b) and 6(c), respectively. The two methods are in good agreement for these parameters. The distribution of wall, radiative heating rate is presented in Figure 6(d). The results by the two methods are in reasonable agreement at the forward region of the body; however, there is a considerable difference between the methods at the downstream region of the body. The results by Callis are greater by a factor of two than the present results at the downstream region.

An analysis was done to explain the difference between the methods. The thermodynamic profiles of temperature and pressure and the shock stand-off distances from the results by Callis were used as inputs to the radiative transport program, (RAD/EQUIL), used in the present method. The results of this calculation are compared with the present results in Figure 6(e). As shown by the data, the distributions of wall, radiative heating rate is now in good agreement at the downstream region. A similar type of analysis had to be used by Suttles (ref. 89) in comparing his results with Callis for large stand-off distances at the stagnation point of blunt bodies. The radiative heating rates by Callis were greater than those of Suttles for larger stand-off distances.

Results from the present method and the method of Callis are in good agreement for nonradiating flow solutions. The difference between the methods for radiating flow is attributed to the radiation models. The radiation model used by Callis (refs. 3 and 7) was developed by Olstad (refs. 2 and 26) and is based on a "step-model" approximation for the frequency dependence of the absorption coefficient. It is

possible that this radiation model by Olstad treats the radiating gas as being too transparent.* Thus, more radiation is transmitted to the body and this effect would be more noticeable the greater the shock stand-off distance.

The present method was used to calculate the radiative heating rate to the stagnation point of a blunt body for a range of nose radii and the results are compared with the method of Callis (ref. 7) in Figure 7. The same radiation model was used by Callis in references 3 and 7. The results by Callis are greater than the present results and the difference increases with the shock stand-off distance (nose radius).

A solution was obtained for the same conditions as previously given in Figure 6(a), except the nose radius was increased to 2.0 meters. The distribution of radiative heating rate is presented in Figure 8. The results of Callis are 50 percent greater than the present results at the forward region of the body as well as the downstream region.

The stagnation-point heating rates from solutions by the present method and the method of Callis are compared with the methods of references 73 and 89 in Table I for two nose radii. The methods of references 73 and 89 can only be used for the flow in the subsonic region of a blunt body. For the smaller nose radius, the results agree within 15 percent. For the larger nose radius, the present results and those by references 78 and 89 agree within 5 percent; but, the result by Callis is 50 percent greater. The radiation model (RATRAP, ref. 30) used by

---

*Personal Communications with Dr. W. B. Olstad, Langley Research Center, Hampton, Virginia.

references 73 and 89 treats the frequency dependence of absorption coefficient in detail as does the present radiation model (RAD/EQUIL, ref. 9). As stated in the section Radiation Transport Modeling, Suttles (ref. 32) made a comparison of these radiation models and concluded that the RAD/EQUIL program was the better model. The present method is in agreement with other methods which use a detailed radiation model.

The previously available results for the radiating, inviscid flow about blunt bodies have been provided by the analysis of Callis (ref. 3) and Olstad (ref. 2). The step-model approximation developed by Olstad was used in both methods for the treatment of radiation. Olstad uses an approximate method for the solution of the flow field and the method is inverse, shock shape specified, rather than direct, body shape specified, as the present method. For these reasons, the present method was not compared with the method of Olstad. Since the same radiation model was used by Olstad and Callis, the results of Olstad should not agree with results by the present method.

The difference in the results between the present method and the method of Callis (ref. 3) for the radiative heating rates is attributed to the different radiation models used in the methods. The radiation model used in the present method treats the frequency dependence of the absorption coefficient in detail and is a more accurate model than the step model used by Callis. From the above analysis, it is concluded that the present method provides a good solution for the radiating, inviscid gas flow about blunt bodies.

Callis (ref. 3) and Olstad (ref. 2) state that the nondimensional, radiative heating rate distributions along blunt bodies are nonsimilar

with respect to body angle and nose radius. Suttles (ref. 89) states that the nondimensional, radiative heating rate distribution along the body at the subsonic region of flow for hemispheres to be relatively insensitive to the size of the nose radius. These results are based on entries into an air atmosphere. The heating rates along the body are nondimensionalized by the stagnation-point value, $q_w^R/q_{w,o}^R$, and the distance along the body is nondimensionalized by the nose radius, s/Rn.

The present method was used to investigate the above mentioned trends. The results presented are for spherically-capped, conical bodies since this is the body shape presently being considered for planetary entries. However, the present method is not restricted to this type of body shape. Results from stagnation-point solutions are also presented.

Results of radiative heating distributions from solutions for entries into different atmospheres and different entry conditions are presented in Figure 9. The results for the two entry conditions of the CO_2-N_2 mixture are representative of entry tó Venus and the results for the H_2-He mixture are representative of entry to Jupiter. Note that the distributions are highly nonsimilar for the different cases. The results for case C and D are for the same atmosphere but different entry conditions; but, the distributions are nonsimilar. The present method can be readily used for entries into atmospheres other than air.

A comparison of the stagnation-point, radiative heating rates for entries in air and in a $.90CO_2$-$.10N_2$ mixture (by volume) is presented

in Figure 10. The radiative heating in the CO_2-N_2 mixture is much greater than in air at the lower velocities; but, the results are comparable at the higher velocities. The difference at the lower velocities is due to the molecular band radiation from the red and violet bands of cynrogen, CN(R) and CN(V), and the fourth positive band of carbon dioxide, CO (4+), in the CO_2-N_2 mixture. The atomic species are dominant at the higher velocities, greater temperature behind the shock wave, and the radiation from the continuum and line transitions is greater than from the molecular band systems.

As the radiating gas flows around a body there are two effects which can influence the radiative heating to the body. The volume of radiating gas increases, increased shock stand-off distance, which will increase the radiative heating. This effect is offset by the decrease in temperature as the gas expands around the body. The distributions of radiative heating along spherically-capped, conical bodies for entry in an air atmosphere are presented in Figure 11 for different body angles. The distributions are nonsimilar and the nondimensional radiative heating is greatest for the largest body angle. The shock stand-off distances and temperatures at a location on the conical portion of the body are also presented. Both the temperature and shock stand-off distance are greater for the larger body angle; thus, the greater the radiative heating. Note that the dimensional, stagnation-point heating rate is insensitive to the downstream body angle for spherically-capped, conical bodies. These results are in agreement with the trends presented by Callis (3) and Olstad (4).

The effect of body angle on the nondimensional, radiative heating distribution for entries to Venus is presented in Figure 12 for two entry conditions. As for air entry, the radiative heating rates along the conical region of the body are greater for the larger cone angle. Also, the stagnation-point, radiative heating rate is insensitive to the cone angle. As previously stated, the nondimensional, radiative heating distribution is nonsimilar with respect to entry conditions. For the 60° body, the radiative heating rates along the downstream region of the body exceed the stagnation-point value at the lower velocity entry. At the higher velocity entry, the radiative heating rate increases along the downstream region but does not exceed the stagnation-point value.

The effect of nose radius on the nondimensional, radiative heating distributions for an entry in air is presented in Figure 13. The distributions are slightly nonsimilar for the downstream region of the body. Callis (ref. 3) and Olstad (ref. 2) state the distributions to be nonsimilar and the present results are in agreement. However, the results of Callis and Olstad indicate a greater nonsimilarity than shown by the present results for an air entry. The reason is probably due to the radiation model used by Callis and Olstad which might be too transparent as previously discussed. In which case, the nose radius would have a greater effect than shown by the present results. Suttles (ref. 89) states the distributions along the subsonic flow region of the body to be similar with respect to nose radius. The present results are in agreement with Suttles since the distributions are similar for the forward region of the body, $s/Rn<0.4$.

The effect of nose radius on the nondimensional, radiative heating distributions for entries to Venus is presented in Figure 14. The distributions are slightly nonsimilar for the downstream region of the body for the lower velocity entry. However, the distributions are highly nonsimilar for the higher velocity entry. For both entries, the distributions are similar at the forward region of the body up to approximately the sphere-cone junction.

The present results are based on a limited range of entry conditions and body shapes. This same situation applies to the studies by Callis (ref. 3), Olstad (ref. 2), and Suttles (ref. 89) for entries only in an air atmosphere. Based on the present results, the following trends seem to be generally prevalent. The nondimensional, radiative heating distributions ($q_w^R/q_{w,o}^R$ versus s/Rn) are nonsimilar with respect to entries in different atmospheres and with respect to entries in the same atmosphere at different entry conditions. The distributions are also nonsimilar with respect to body angle and nose radius. Extreme caution should be exercised in attempting to extrapolate the results from known distributions to other entry conditions or body shapes for which solutions have not yet been obtained, For large body angles, the radiative heating rates to the downstream region of a body can exceed the stagnation point value for certain entry conditions.

The exact composition of the Venusian atmosphere is unknown at present. The most recent data indicates the composition to be predominately CO_2 with up to 10 percent by volume of N_2. The effect of gas

composition for CO_2-N_2 mixtures on the radiative heating to the stagnation-point of a body is presented in Figure 15 for two entry conditions. For the higher velocity entry, the radiative heating rate varies by only 25 percent over the range of CO_2 content with the higher values occurring for the greater percentage of CO_2. For the lower velocity entry, the radiative heating rate can vary by a factor of 6 over the range of CO_2 content. This is due to the domination of radiation by the molecular band transitions of CO(4+), CN(V), and CN(R) at the lower velocity. For the composition of present interest for Venusian entry (less than 10 percent N_2), the effect of composition on the stagnation-point, radiative heating rate is negligible at the higher velocity; but, a 22 percent difference occurs with composition at the lower velocity.

Fully-Coupled, Stagnation Point, Solutions for Earth Reentry

The present method has been used to obtain fully-coupled solutions at the stagnation point of blunt bodies for Earth Reentry. The solutions are for mass injection at the wall of air and ablation products. The results from the present method are compared with the results given by Garrett (ref. 19).

The solutions were obtained for the free-stream conditions and mass injection rates presented in Table II. These conditions are representative of a manned spacecraft reentering the Earth's atmosphere after exploration of Mars. For the solutions, the wall conditions of the temperature and the rate and composition of the injected gas were prespecified. This procedure was used to be consistent with the method of

Garrett. The results from the present method and the results given by Garrett are presented in Table II.

The present results agree with the results of Garrett within 5 percent for the mass injection of ablation products and within 10 percent for the mass injection of air. This good agreement is better than has been previously shown in comparing any two methods (see ref. 19). As shown by the results, the mass injection of ablation products is twice as effective as the mass injection of air in reducing the radiative heatinging to the wall. The mass injection of ablation products reduced the radiative heating to the wall by 40 percent at the larger blowing rate.

The present results for the temperature profile and the radiative flux profile through the gas layer for a solution are compared with the results of Garrett in Figure 16. The specified conditions are given in Figure 16(a) and the temperature profile and radiative flux profile are given in Figure 16(b) and 16(c), respectively. The present results are in good agreement with the results of Garrett. For the present solution, spectral distributions of radiative heating toward the wall due to continuum processes and due to line processes are presented in Figures 16 (d) and 16(e) respectively. Spectral distributions were not given in the thesis by Garrett.

For the continuum processes, practically all radiation beyond 11 eV is absorbed within the boundary layer and is attributed to the atomic species being at a lower temperature in the boundary layer than in the inviscid layer. There is a slight absorption of radiation within the boundary layer between the spectral range of 4 to 10 eV but the effect

is offset by increased radiation emission in the spectral range of 1 to 4 eV. For the line processes, the radiation is sharply reduced in the spectral region of 7 to 11 eV. Part of this reduction for the line groups at 7.1, 8.4 and 9.4 eV is due to the absorption by the fourth positive band system of carbon monoxide, CO(4+). The carbon monoxide is present in the boundary layer from the mass injection of ablation products. The present results for the spectral regions of absorption, or increased emission, within the boundary layer are in agreement with the results given in reference 28.

The good agreement of the present results with those given by Garrett (ref. 19) shows that the present method for a fully-coupled solution with ablation product effect provides a good solution at the stagnation point of a blunt body for Earth reentry. The method by Garrett can only be used at the stagnation point of a blunt body and has not been used for entries in atmospheres other than air.

Fully-Coupled Solutions for Venusian Entry

The present method was used to obtain solutions at typical conditions for unmanned, scientific probes during Venusian entry. One mission currently under study is a multi-probe entry with one large probe and three small probes which are spherically-capped, conical bodies. A description of this type of mission is presented in references 61 to 64. The entry probes are released from a spacecraft and are targeted to different locations on Venus.

The entry parameters and body shapes listed below were used to calculate nominal trajectories for use in the present analysis. The only small probe considered herein is the one entering at the steepest entry angle.

	Large Probe	Small Probe
Entry velocity, km/s	11.06	11.06
Entry angle, degrees	-42	-56
W/C_dA, kg/m^2	78.5	125.7
Weight, kg	158.8	22.7
Nose radius, m	.3429	.1397
Body half-angle, degrees	60	45
Base diameter, m	1.3716	.4064

The atmospheric model used for the Venusian atmosphere is that presented in reference 62 and the gas composition is 97 percent carbon dioxide and 3 percent nitrogen by volume. The calculated entry trajectories are presented in Figure 17.

The radiative heating rates at the stagnation point of the bodies were calculated along the trajectories to determine the location of peak radiative heating. The "stagnation-point" version of the developed, radiating inviscid flow program was used for these calculations. The results are presented in Figure 18 for the large and small probes. Even though the nose radius is smaller, the radiative heating to the small probe is greater due to the deeper penetration in the denser regions of the atmosphere at higher velocities. Solutions for the radiating, inviscid flow around the bodies were then obtained at the peak heating conditions and the stagnation-point values of radiative heating rates from these solutions are also presented in Figure 18. It is at these conditions for peak radiating heating that fully-coupled solutions with

ablation product effects were obtained for the radiating gas flow around the large and small probes. Hereafter, the solutions are referred to as large and small probes.

The ablation of the heatshield for the fully-coupled solution is represented by steady-state ablation of a carbon-phenolic material with elemental mass fractions of carbon, 0.851; oxygen, 0.110; hydrogen, 0.035; and nitrogen, 0.004. The ablation rates are solved for as part of the fully-coupled solution and are not prespecified.

The results from the fully-coupled solutions for the large and small probes are presented in Figures 19 and 20, respectively. The distribution along the body of radiative heating, convective heating, ablation rate, aerodynamic shear, and momentum thickness Reynolds number are presented. The spectral distribution of radiative heat flux due to continuum processes is also presented for two body locations.

For the large probe, the ablation rate decreases along the body in the nose region and reaches a nearly constant value along the afterbody (Figure 19(d)). As shown in Figure 19(c), the convective heating rate decreases along the afterbody but the radiative heating rate increases to values which exceed the stagnation-point value. The radiative heating to the wall is greater than the convective heating along the entire body. The total heating rate, radiative plus convective, along the afterbody is 30 to 40 percent less than the stagnation-point value. Thus, the decrease in convective heating rate along the afterbody negates the effect of the increase in radiative heating rate. The wall temperature resulting from the steady-state ablation is 3600^{o}K, within 2 percent, along the body.

For the small probe, there is a decrease in the ablation rate along the afterbody (Figure 20(d)) and both the convective and radiative heating rates decrease along the afterbody (Figure 20(c)). The convective heating rate is greater than the radiative heating rate along the entire body. This result is opposite to the result obtained for the large probe. The total heating rate along the afterbody of the small probe is 40 to 60 percent less than the stagnation-point value. The wall temperature resulting from the steady-state ablation is 3700°K, within 2 percent, along the body.

The radiative heating rates from inviscid, radiating solutions are compared with the results for the fully-coupled solutions with steady-state ablation in Figures 19(b) and 20(b) for the large and small probes, respectively. The radiative heating rates from the fully-coupled solutions are less than the values from the inviscid, radiating solutions by 9 and 17 percent, respectively, for the large and small probes at the stagnation point of the bodies. These percent reductions are nearly constant along the bodies. The reduction in radiative heating is due to absorption of radiation within the boundary layer.

Spectral distributions of radiative heating toward the body due to continuum processes are presented in Figures 19(g) and 20(g), respectively, for the large and small probes. The spectral distributions are presented for the stagnation point and an afterbody location. As shown by the results, the absorption of radiation within the boundary layer occurs in the spectral range of 5 to 10 eV and is due to self absorption

of the fourth positive band system of carbon monoxide, CO(4+). At the stagnation point of the small probe there is a slight increase in radiative heating within the boundary layer at 2.5 eV and is due to the Swan band system of diatomic carbon, $C_2(S)$. A similar effect was noted at the other body locations for both the large and small probes, but the effect was too small to be presented in the figures. The radiative heating due to line processes was less than ten percent of the total radiative heating at these entry conditions and spectral distributions are not presented.

The fully-coupled solutions assumed laminar flow in the boundary layer. Shown in Figures 19(f) and 20(f) are the distributions of momentum thickness Reynolds number around the bodies. If the critical value for transition to turbulent flow is about 200, then the boundary layer would be turbulent along the afterbody for both the large and small probes. This could have an appreciable effect on the distribution of convective heating, ablation rate, and aerodynamic shear.

A fully-coupled solution for the large probe with a turbulent boundary layer was obtained and the results are compared with the laminar case in Figure 21. A critical value of 200 for the momentum thickness Reynolds number was used for transition to turbulent flow. As expected, the convective heating rates, ablation rates, and aerodynamic shears increased with transition to turbulent flow. The distribution along the body of radiative heating was essentially the same for both laminar and turbulent flow; thus, the turbulent boundary layer did not appear to further attenuate the radiative heating even though the

boundary-layer thickness was 80 percent greater than for laminar flow. This phenomenon can be explained with the wall spectral distributions presented in Figure 21(d) for the turbulent and laminar solutions. For the turbulent boundary layer, there is an increase in the self absorption of the CO(4+) band system in the spectral range of 5 to 8 eV but this effect is offset by an increased emission of the C_2(S) band system at 2.5 eV and the red band system of cynrogen, CN(R), at .6 to 2 eV. The spectral distribution at the boundary layer edge is essentially the same for both the turbulent and laminar boundary layers and was presented in Figure 19(g). While the radiative heating rates along the afterbody of the large probe are the same for a turbulent or a laminar boundary layer, the wall spectral distribution of the radiation is different for the two cases. It should not be inferred that the radiative heating to the body will be the same for a laminar or turbulent boundary layer for other entry conditions or body shapes.

A fully-coupled solution was obtained for free-stream conditions representative of a higher entry velocity than the nominal trajectories and the results are presented in Figure 22. The free-stream conditions and body shape are given in Figure 22(a). The body shape is the same as the large probe except the nose radius is slightly smaller. Hereafter, this case is referred to as the high velocity entry.

As shown in Figure 22(c), the radiative heating rate is greater than the convective heating rate along the entire body. Unlike the large probe, there is only a slight increase in the radiative heating along the afterbody. The convective heating rate at the stagnation

point is slightly less than the values just downstream of the stagnation point and is due to an increased effect of blockage of convective heating by the mass injection of the ablation products. As shown in Figure 22(d), the ablation rate decreases along the body in the nose region. The ablation rate and total heating rate are nearly constant along the afterbody. The wall temperature resulting from the steady-state ablation is 3750°K, within 1 percent, along the body.

There is significant absorption of radiation within the boundary layer for the high velocity entry as shown by a comparison of results between the fully-coupled solution and an inviscid, radiating solution in Figure 22(b). The reduction in radiative heating rate is 25 percent at the stagnation point and 25 to 30 percent along the afterbody. Spectral distributions of radiative heating toward the body due to continuum processes are presented in Figure 22(g) for the stagnation point and an afterbody location. For the continuum processes, most of the absorption within the boundary layer occurs in the spectral region of 5 to 10 eV and is due mainly to self absorption of the CO(4+) band. There is an increase in radiative flux at 2.5 eV and is due to the C_2(S) band. At the stagnation point there is absorption at photon energies greater than 10 eV and this absorption is attributed to atomic species within the cooler regions of the boundary layer. There is also absorption at the photoionization edge of carbon at 8.5 eV.

The radiative flux due to line processes is 50 percent of the total radiative flux at the nose region of the body and decreases to only 20 percent along the afterbody. Spectral distributions of the radiative

heating due to line processes for two locations at the nose region are presented in Figure 22(h). Absorption of line radiation within the boundary layer occurs only for the line groups in the ultraviolet at 7.1, 8.4, and 9.4 eV. The line radiation in the visible and infrared regions of the spectral, less than 2 eV, is not attenuated within the boundary layer.

The present results have shown that the radiative heating toward the body is attenuated in the boundary layer for Venusian entries. This attenuation will reduce the radiative heating to the body by 10 to 20 percent at entry conditions and body shapes which are presently considered as nominal. The reduction can be as large as 30 percent at higher velocity entries. The radiative heating toward the body is attenuated in the boundary layer at the downstream region of the body as well as at the stagnation point of the body.

SUMMARY AND CONCLUSIONS

A method is presented for the solution of the fully-coupled, nongray radiating gas flow about an ablating, planetary entry body. The solution is for a gas in chemical equilibrium and arbitrary gas mixtures can be considered. The treatment of radiation accounts for molecular band, continuum, and atomic line transitions with a detailed frequency dependence of the absorption coefficient. The ablation of the entry body is solved as part of the solution for a steady-state ablation process.

Application of the developed method is shown by results at typical conditions for unmanned, scientific probes during entry to Venus. The radiative heating toward the body is attenuated in the boundary layer for Venusian entries. This attenuation will reduce the radiative heating to the body by 10 to 20 percent at entry conditions and body shapes which are presently considered as nominal. The reduction can be as large as 30 percent at higher velocity entries. The attenuation of radiation within the boundary layer is primarily due to the self absorption of the fourth positive band system of carbon monoxide, CO(4+), in the radiation spectral region of 5 to 10 eV. At high velocity entry, the attenuation of radiation also occurs for line transitions in the radiation spectral region of 7 to 10 eV.

Prior studies of fully-coupled solutions with ablation product effects have been for the stagnation point of a body for Earth reentry and have shown that the boundary layer with injection of ablation products is effective in reducing the radiative heating to the body. The

present results show that the boundary layer over an ablating body will reduce the radiative heating to the body for entries to Venus. Furthermore, the attenuation of radiation within the boundary layer occurs at downstream regions of the body as well as the stagnation point of the body.

Present results from a study of the radiating, inviscid flow about spherically-capped, conical bodies during planetary entries show that the nondimensional, radiative heating distributions ($q_w^R/q_{w,o}^R$ versus s/Rn) to be nonsimilar with respect to entries in different atmospheres and with respect to entries in the same atmosphere at different entry conditions. The distributions are also nonsimilar with respect to nose radius and downstream body angle. Therefore, extreme caution should be exercised in attempting to extrapolate the results from known distributions to other entry conditions for which solutions have not yet been obtained. The radiative heating rates to the downstream region of the body can exceed the stagnation-point value for certain entry conditions and body shapes.

EXTENSION OF PRESENT RESEARCH

An immediate extension of the present research can be made in the following areas:

1. Additional fully-coupled solutions are needed for a better evaluation of the thermal environment for Venusian entries. Solutions with a turbulent boundary layer are needed for the small probe and for higher velocity entries.

2. Solutions are needed for body shapes other than spherically-capped, conical bodies for Venusian entries. Future design may dictate a different shape and the results would be useful in evaluating the effects of such a change in shape.

3. A study is needed for the effect of composition for CO_2-N_2 mixtures on the radiative heating distribution along a body for Venusian entries.

4. Use the present results and results from additional solutions to develop correlations which can be easily used in parametric design studies for Venusian entries.

5. The present computational method needs to be extended to include a transient ablation analysis.

6. Use the present method to begin studies of entries to Saturn. Saturn is characteristic of the giant planets (Jupiter, Saturn, Uranus, and Neptune) and probably will be the first chosen for exploration by entry probes.

TABLE I. - STAGNATION-POINT, RADIATIVE HEATING RATES FOR AIR ENTRY.

$V_\infty = 14.55$ km/s

$\rho_\infty = 2.252 \times 10^{-4}$ kg/m^3

$p_\infty = 16.16$ N/m^2

Method	$q^R_{w,o}$, MW/m^2	
	Rn = .3427 m	Rn = 3.427 m
Present method	16.17	28.80
Callis, Ref. 3	18.71	45.47
Suttles, Ref. 89	18.38	27.26
Falanga and Sullivan, Ref. 73	18.73	28.44

TABLE II. - RESULTS FROM FULLY-COUPLED, STAGNATION-POINT SOLUTIONS WITH MASS INJECTION FOR AIR ENTRIES.

(a) V_∞ = 15.25 km/s ; ρ_∞ = 2.72 x 10^{-4} kg/m^3 ; p_∞ = 17.76 N/m^2

Rn = 3.048 m ; $\overline{T}_w$ = 3600° K

Injected gas		$q^R_{w,o}$, MW/m^2	
$(\rho v)_w$, kg/m^2-s	Composition	Present method	Garrett, Ref. 19
0	-	3980	4150
.415	air	3375	3740
.830	air	3090	3490
.415	ablation products*	2870	2770
.830	ablation products*	2560	2460

* $\overline{K}_C$=.9207; $\overline{K}_O$=.0491; $\overline{K}_H$=.0216; $\overline{K}_N$=.0086

(b) V_∞ = 15.25 km/s ; ρ_∞ = 1.77 x 10^{-4} kg/m^3 ; p_∞ = 12.26 N/m^2

Rn = 2.56 m ; $\overline{T}_w$ = 3840° K

Injected gas		$q^R_{w,o}$, MW/m^2	
$(\rho v)_w$, kg/m^2-s	Composition	Present method	Garrett, Ref. 19
0	-	2307	2540
.205	ablation products*	1710	1620

* $\overline{K}_C$=.923; $\overline{K}_O$=.058; $\overline{K}_H$=.018; $\overline{K}_N$=.001

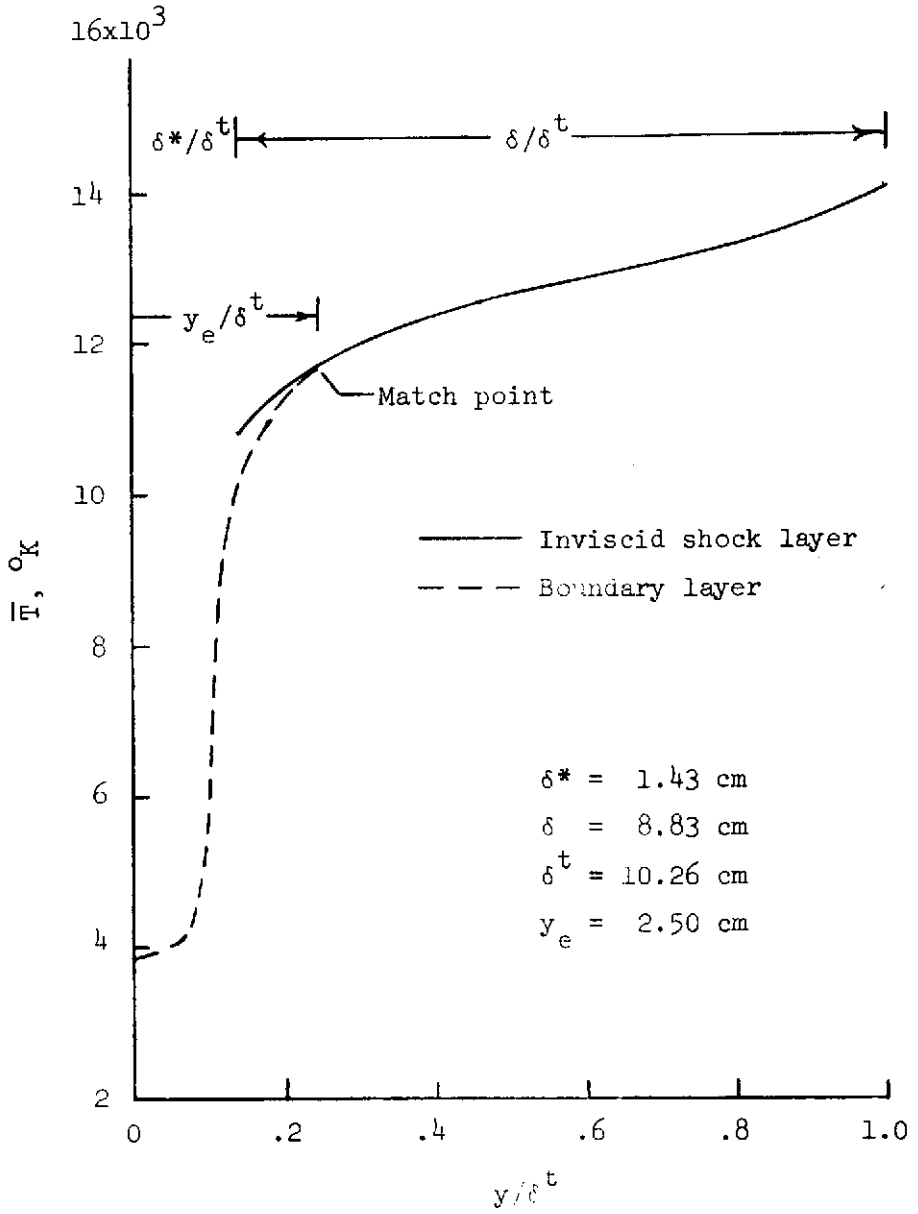

Figure 1. - Illustration of the mating of the boundary layer solution to the inviscid layer solution.

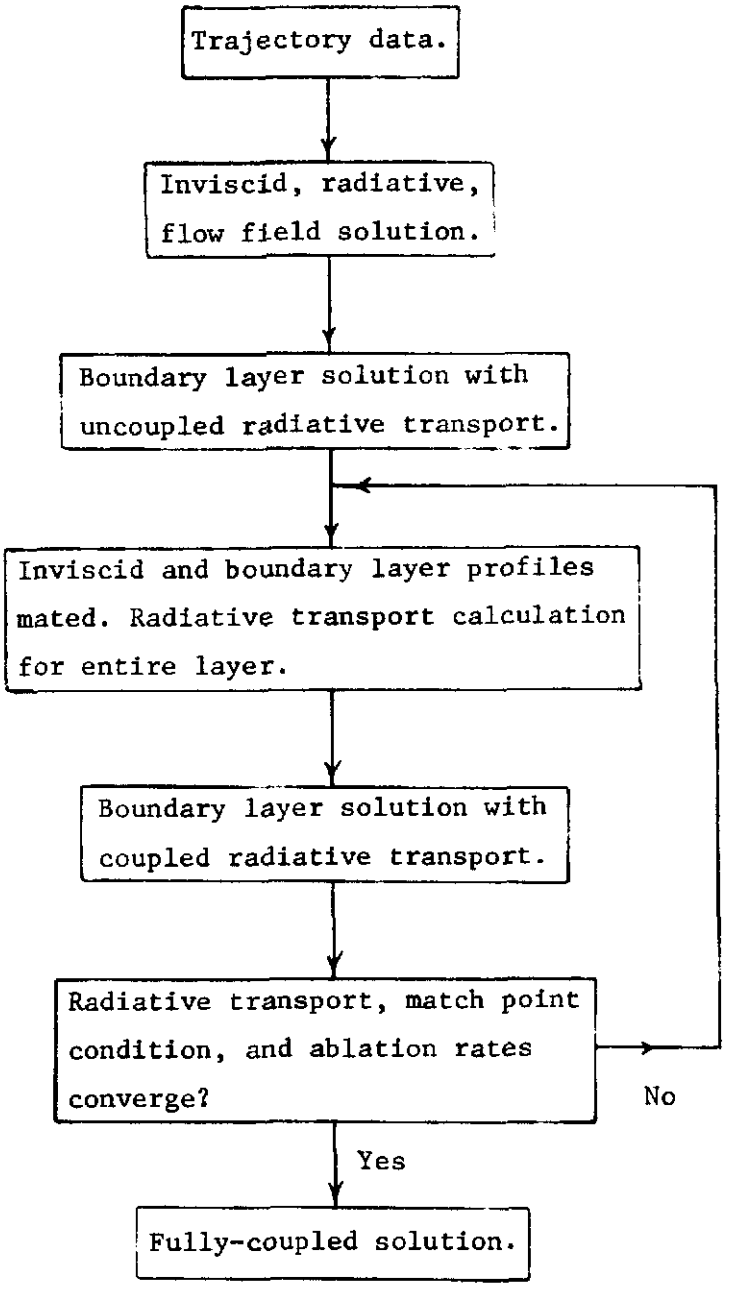

Figure 2. - Calculation procedure for the fully-coupled, radiating, flow field solution.

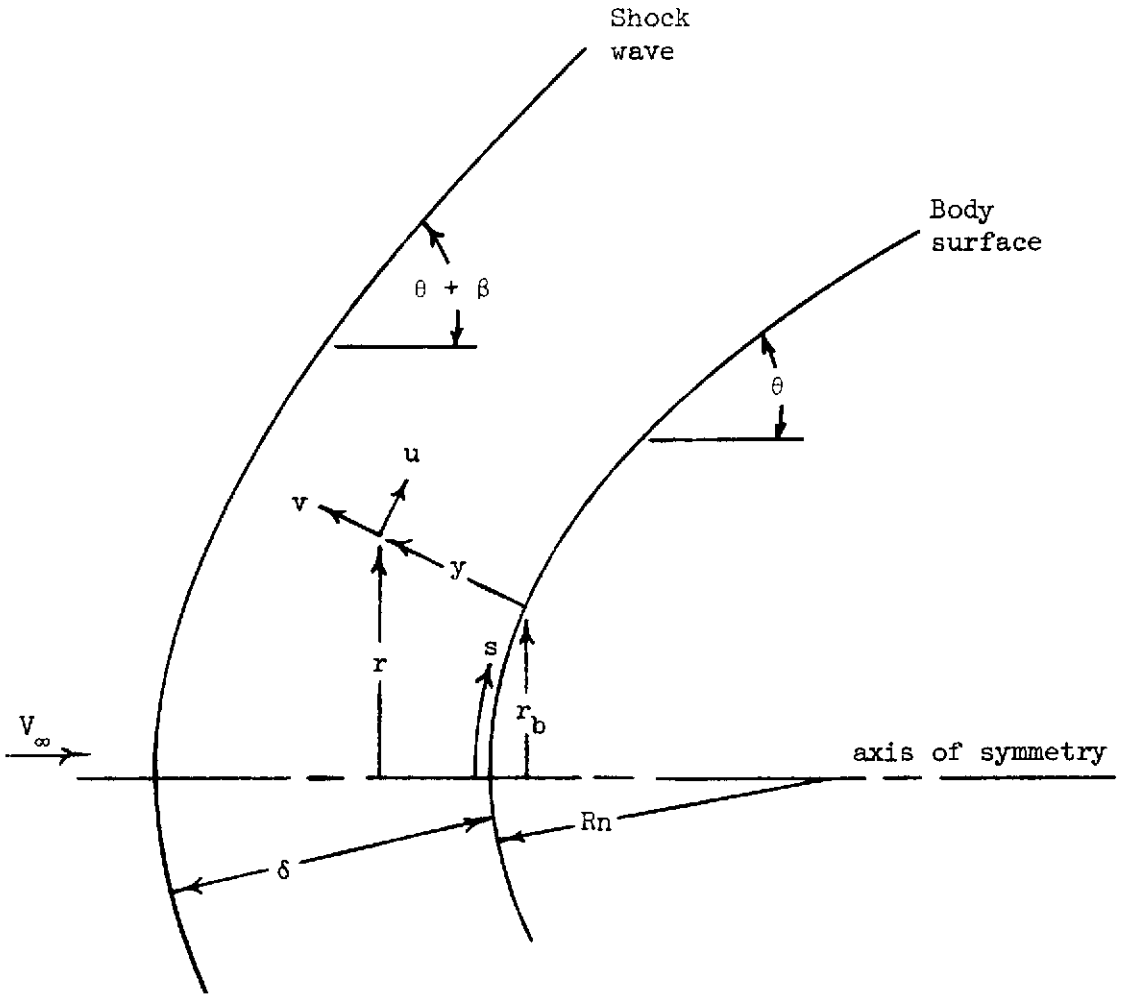

Coordinates

s - Distance along body surface from axis of symmetry.

y - Distance perpendicular to body surface.

ϕ - Angle measured in plane normal to axis of symmetry.

Figure 3. - Flow field coordinate system for axisymmetric blunt body.

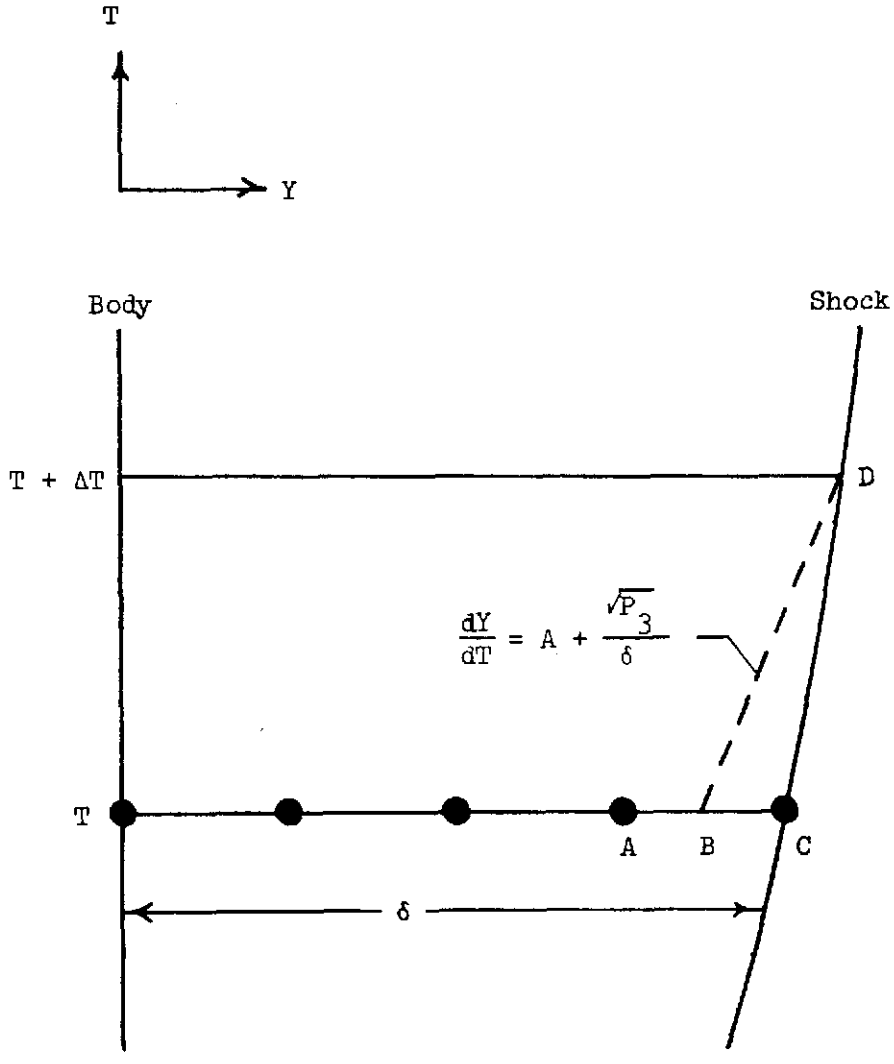

Figure 4. - Schematic of use of unsteady characteristics at shock wave.

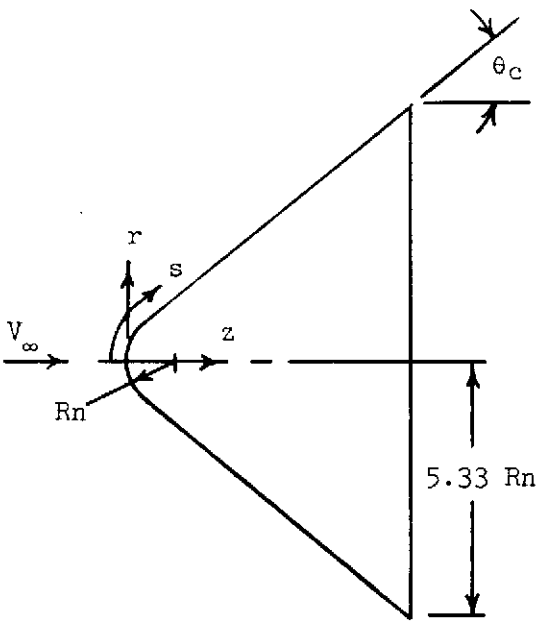

Gas composition by volume

.79 N_2 - .21 O_2 (air)

V_∞ = 12.192 km/s

ρ_∞ = 3.15 x 10^{-4} kg/m^3

p_∞ = 22.6 N/m^2

h_∞ = 0.0 J/kg

Rn = 2.0 m

θ_c = 40°

(a) Free-stream conditions and body shape.

Figure 5. - Nonradiating, inviscid flow solution around a blunt body. Present method is compared with the method of Inouye et al. (ref. 88).

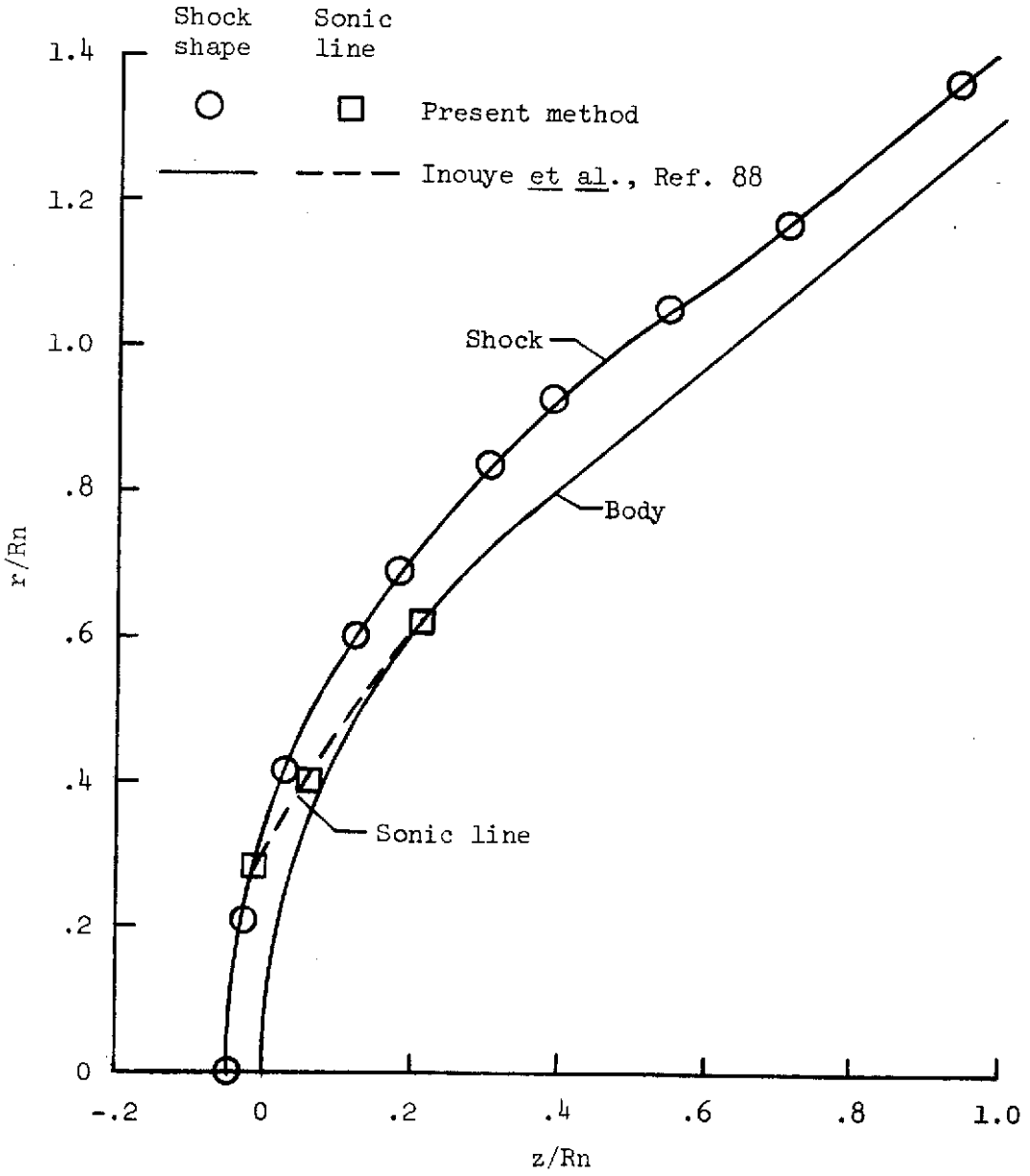

(b) Shock shape at forward region of body and sonic line location.

Figure 5. - Continued.

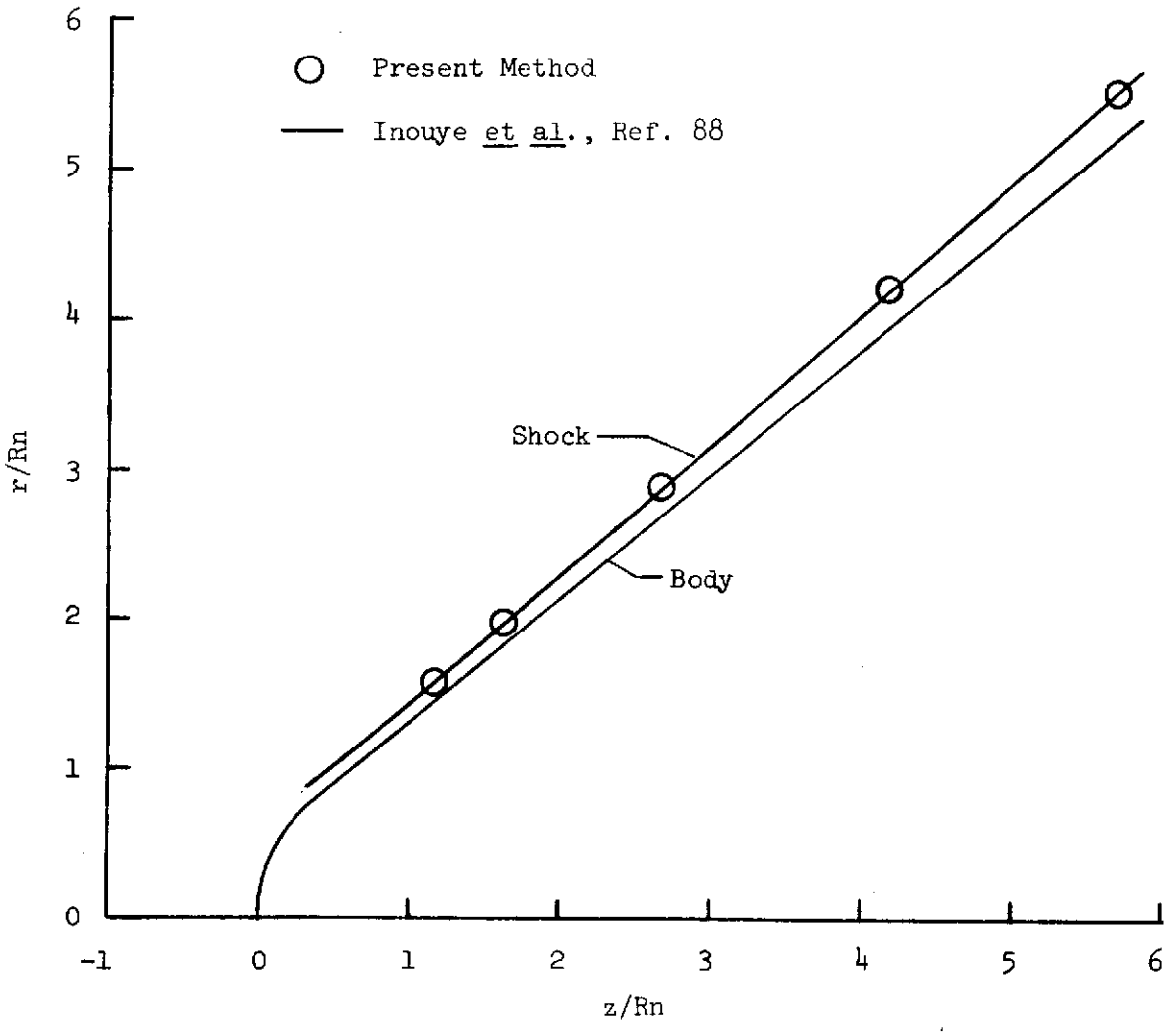

(c) Shock shape at downstream region of body.

Figure 5. - Continued.

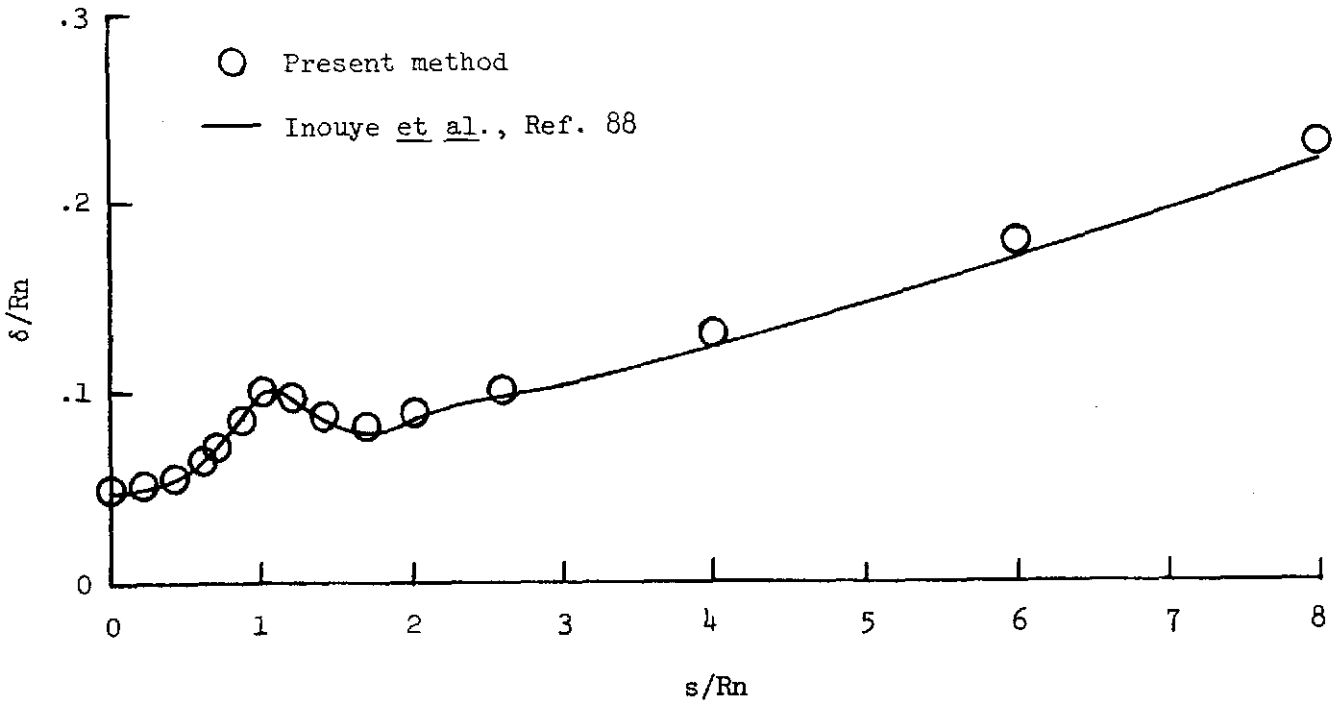

(d) Shock stand-off distance around body.

Figure 5. - Continued.

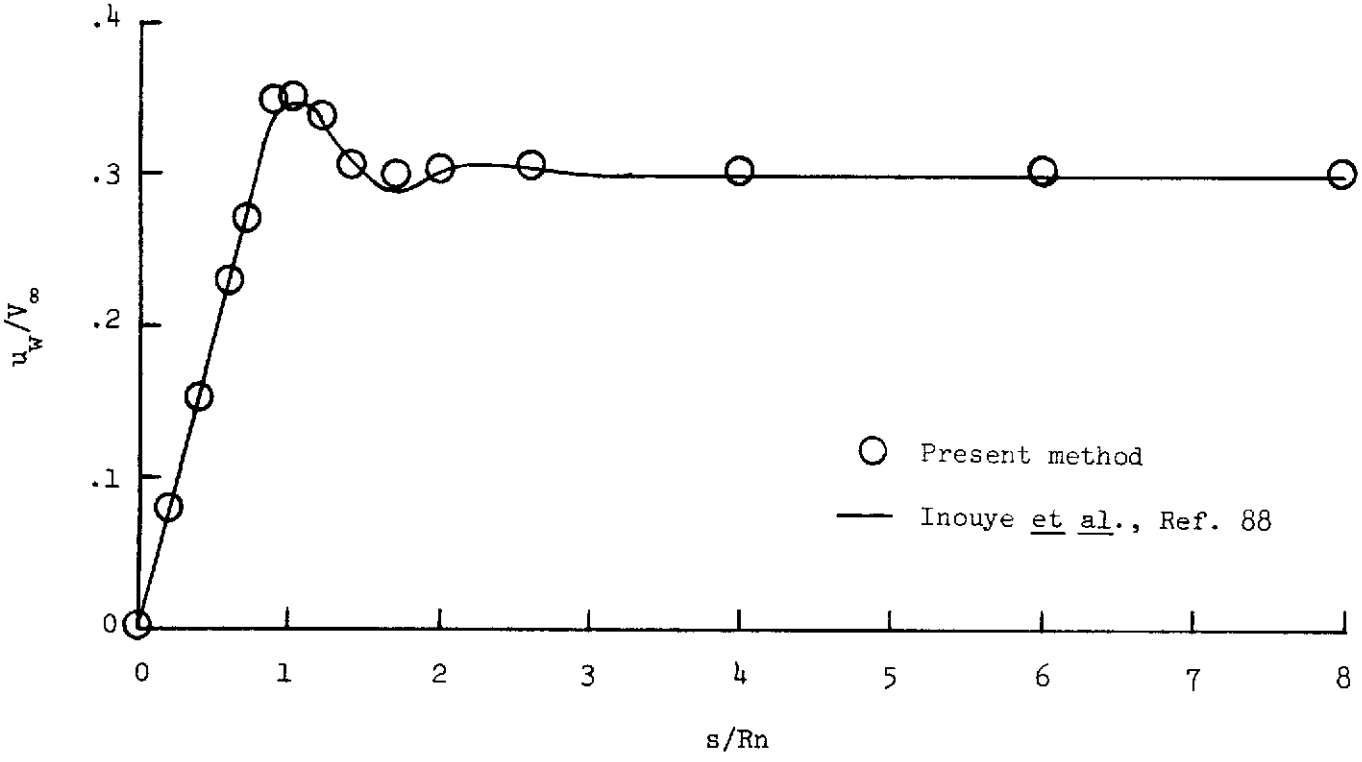

(e) Velocity distribution along body.

Figure 5. - Continued.

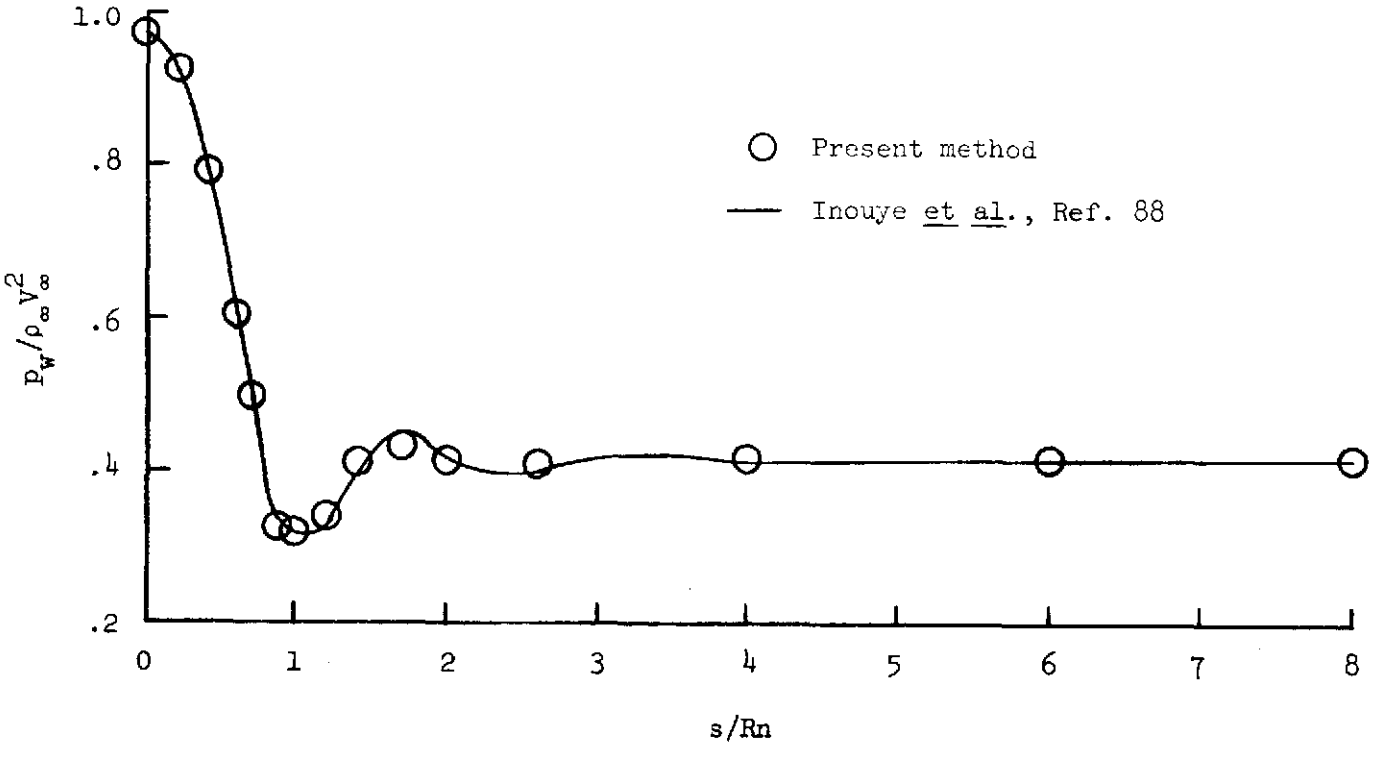

(f) Pressure distribution along body.

Figure 5. - Concluded.

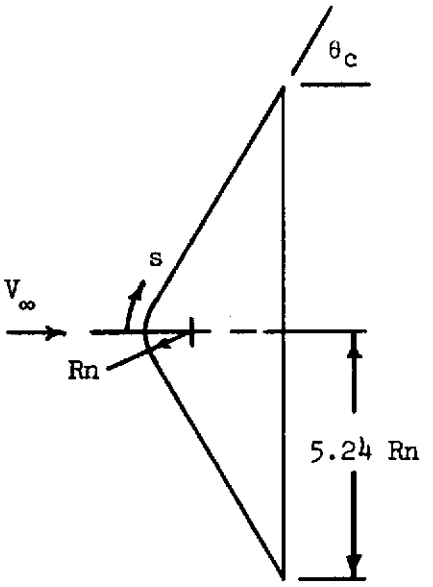

Gas composition by volume

.79 N_2 - .21 O_2 (air)

V_∞ = 12.20 km/s

ρ_∞ = 2.74 x 10^{-4} kg/m^3

p_∞ = 20.0 N/m^2

h_∞ = 0.0 J/kg

Rn = 0.20 m

θ_c = 60°

(a) Free-stream conditions and body shape.

Figure 6. - Radiating, inviscid flow solution about a blunt body during Earth reentry. Present method is compared with the method of Callis (ref. 3).

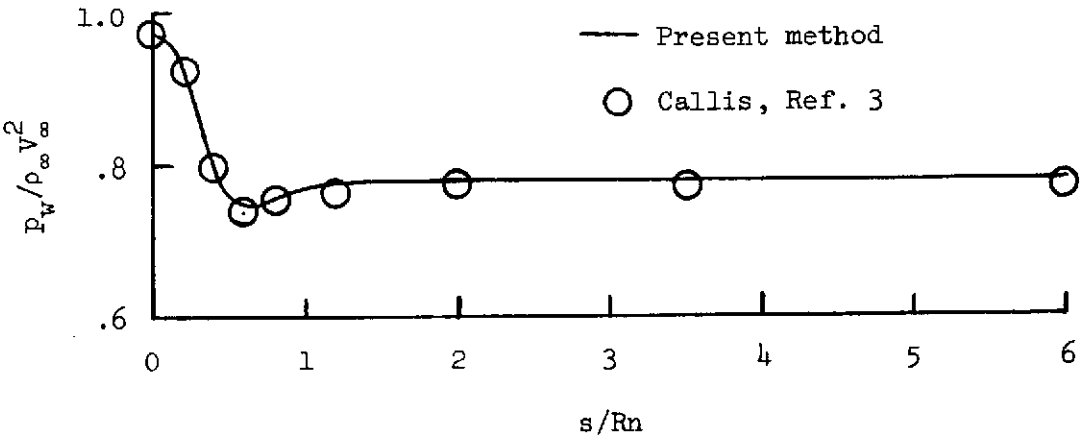

(b) Pressure distribution along body.

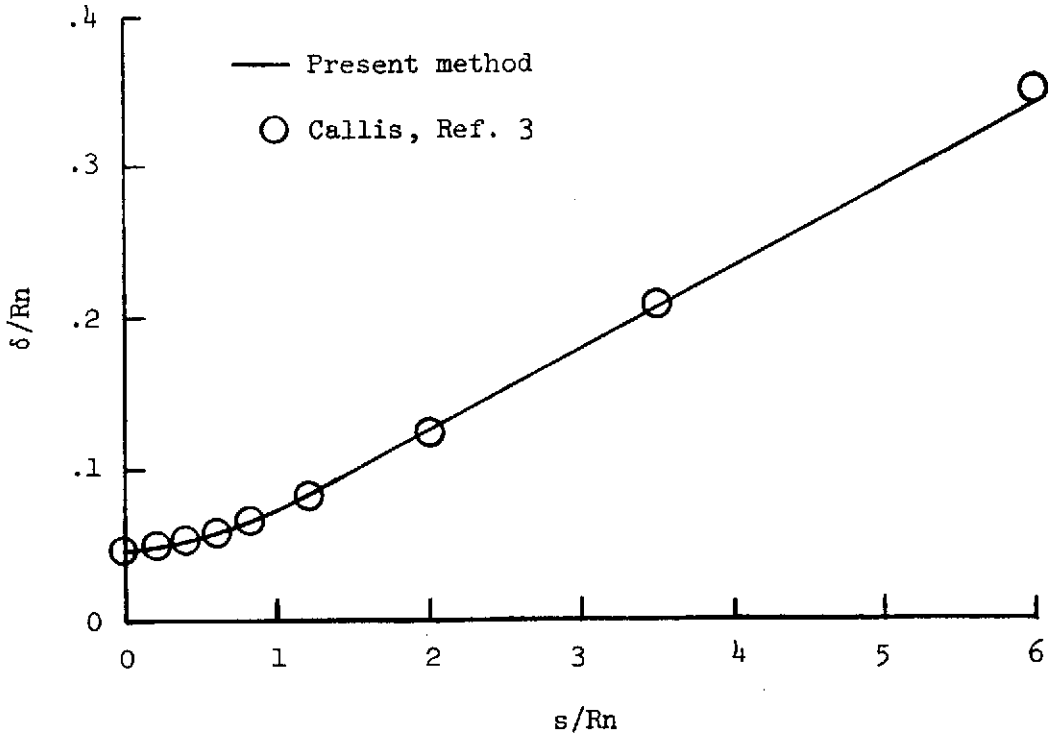

(c) Shock stand-off distance around body.

Figure 6. - Continued.

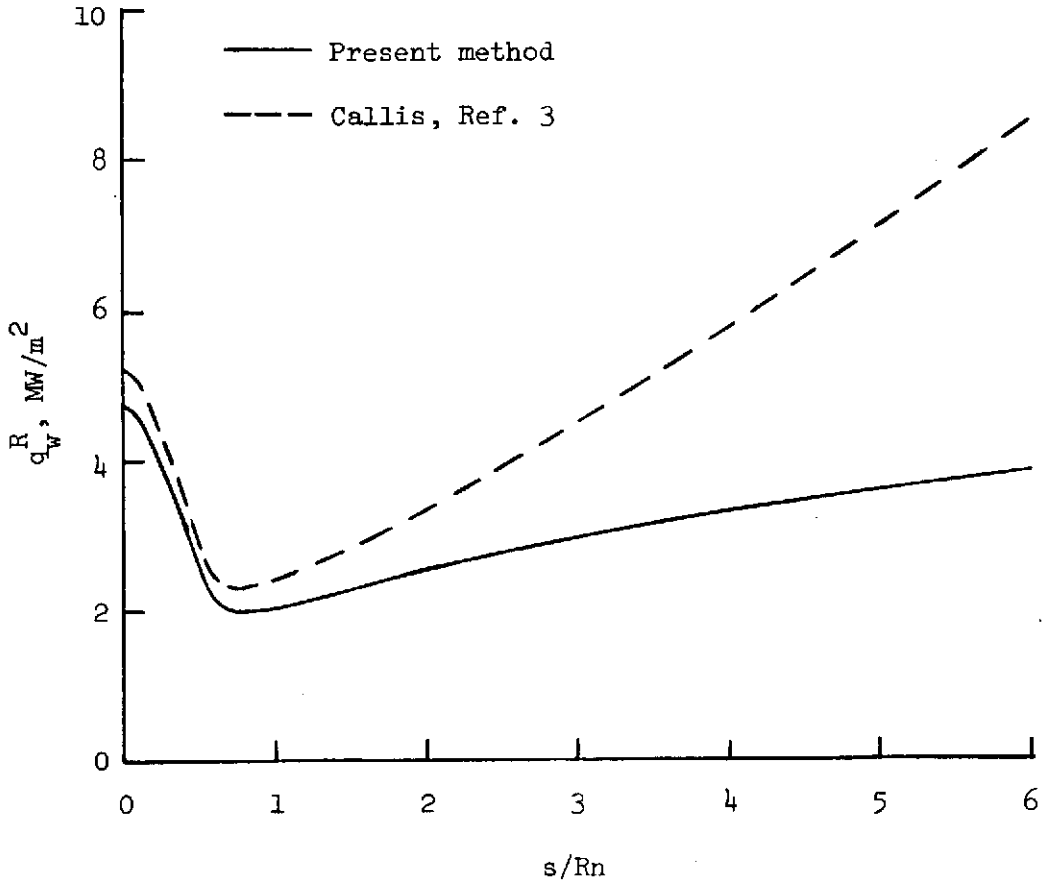

(d) Radiative heating along body.

Figure 6. - Continued.

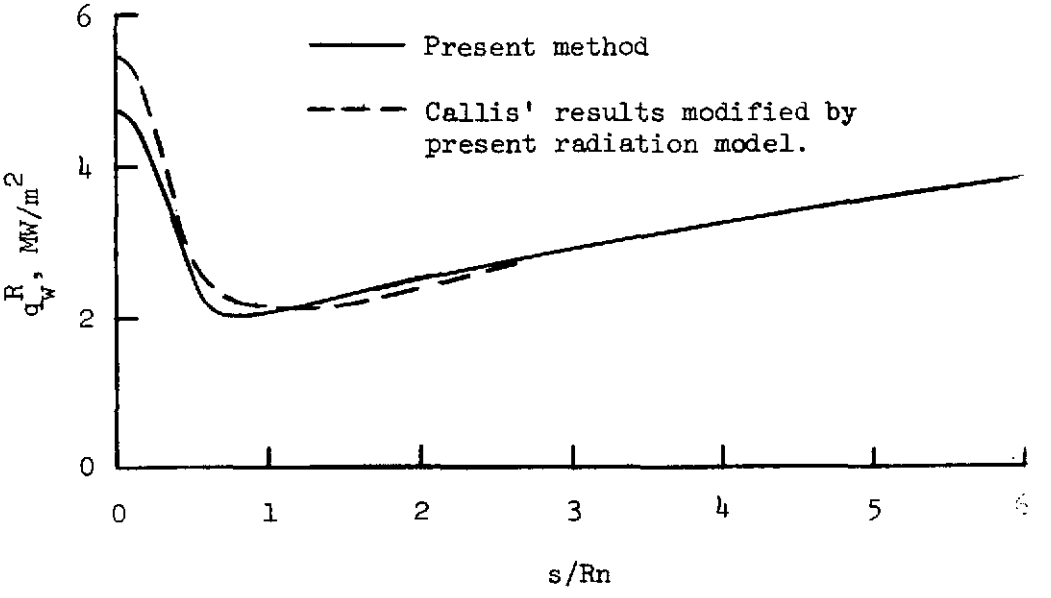

(e) Radiative heating along body. Callis' results modified.

Figure 6. - Concluded.

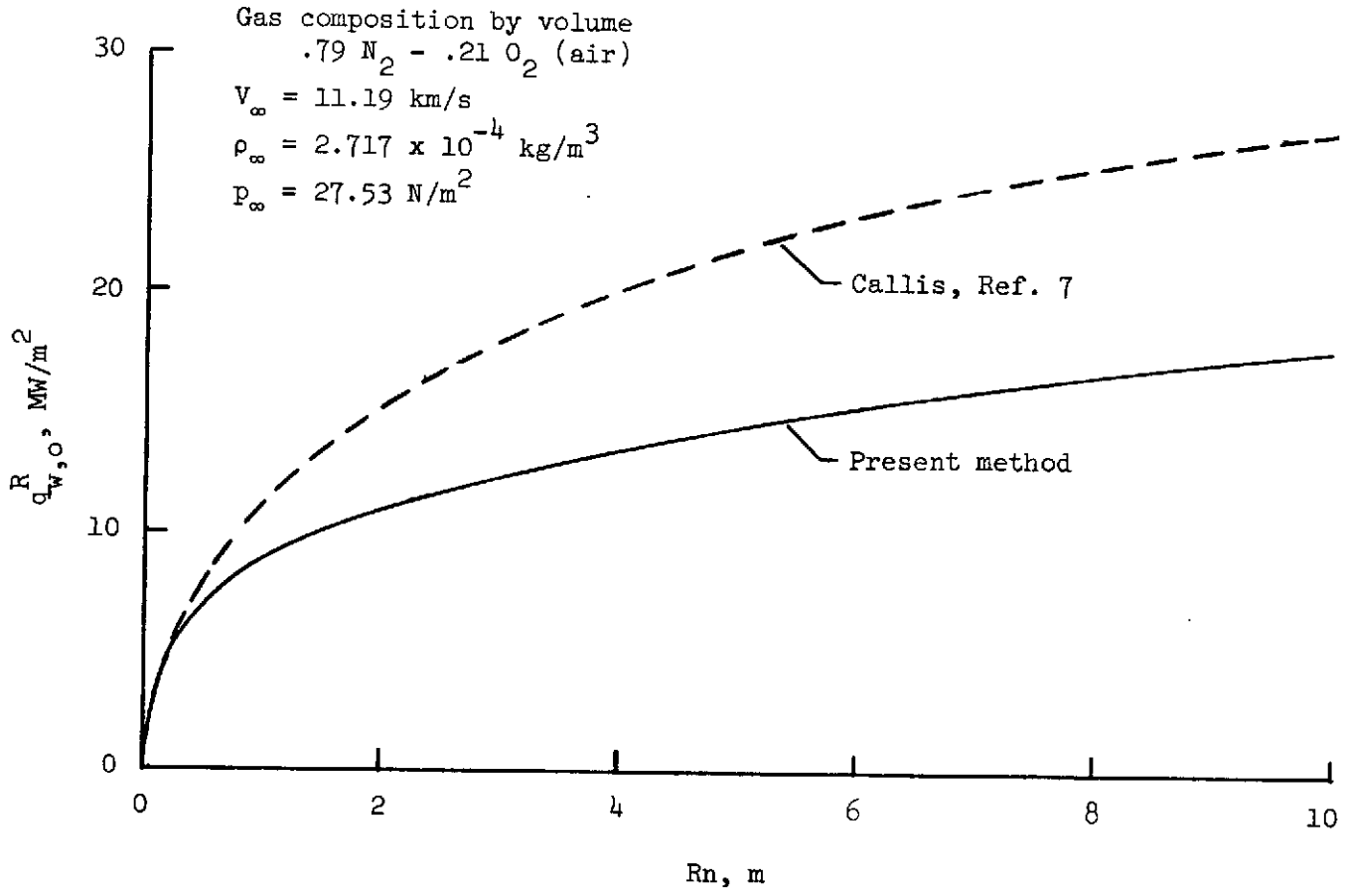

Figure 7. - Stagnation-point, radiative heating rates in an air atmosphere as a function of nose radius. Present results are compared with the method of Callis (ref. 7).

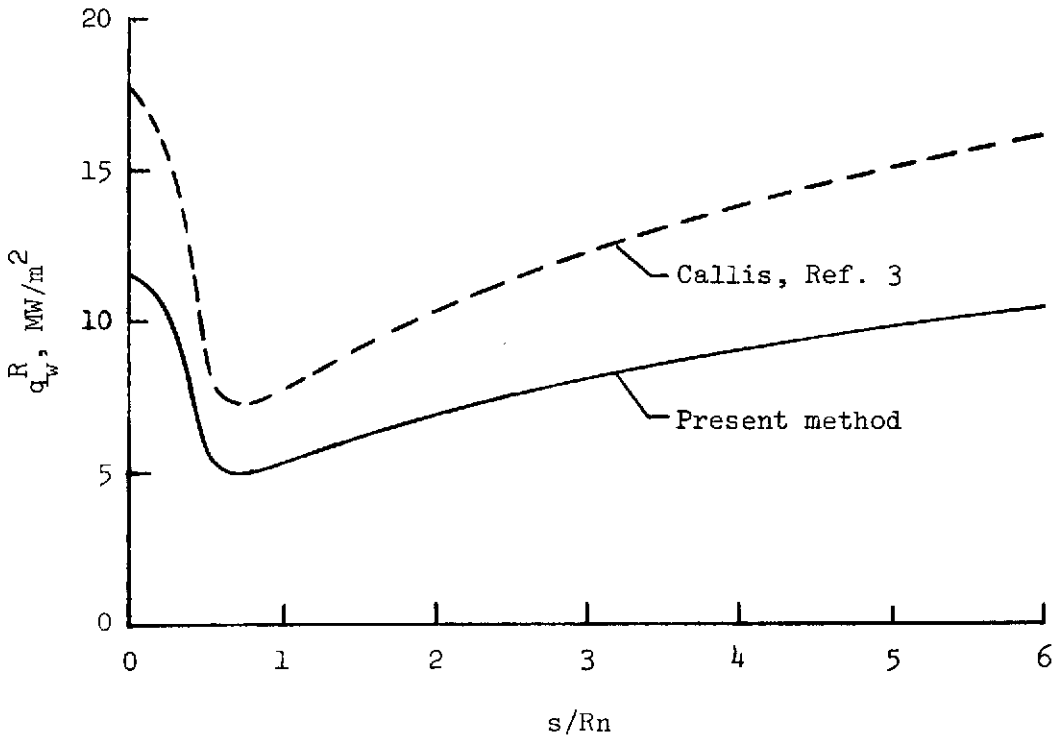

Figure 8. - Radiative heating distribution for free-stream conditions and body shape given in Figure 6(a) except Rn=2.0 m. Present results are compared with the method of Callis (ref. 3).

Case	Gas Composition*	V_∞, km/s	ρ_∞, kg/m^3	p_∞, N/m^2	h_∞, MJ/kg	$q^R_{w,o}$, MW/m^2
A	.79 N_2 - .21 O_2	12.200	2.744×10^{-4}	20.01	0	5.78
B	.85 H_2 - .15 He	50.000	5.700×10^{-3}	0	0	9668.00
C	.90 CO_2 - .10 N_2	8.740	3.294×10^{-3}	130.59	-8.43	4.44
D	.90 CO_2 - .10 N_2	11.175	2.850×10^{-3}	117.30	-8.43	35.70

* by volume

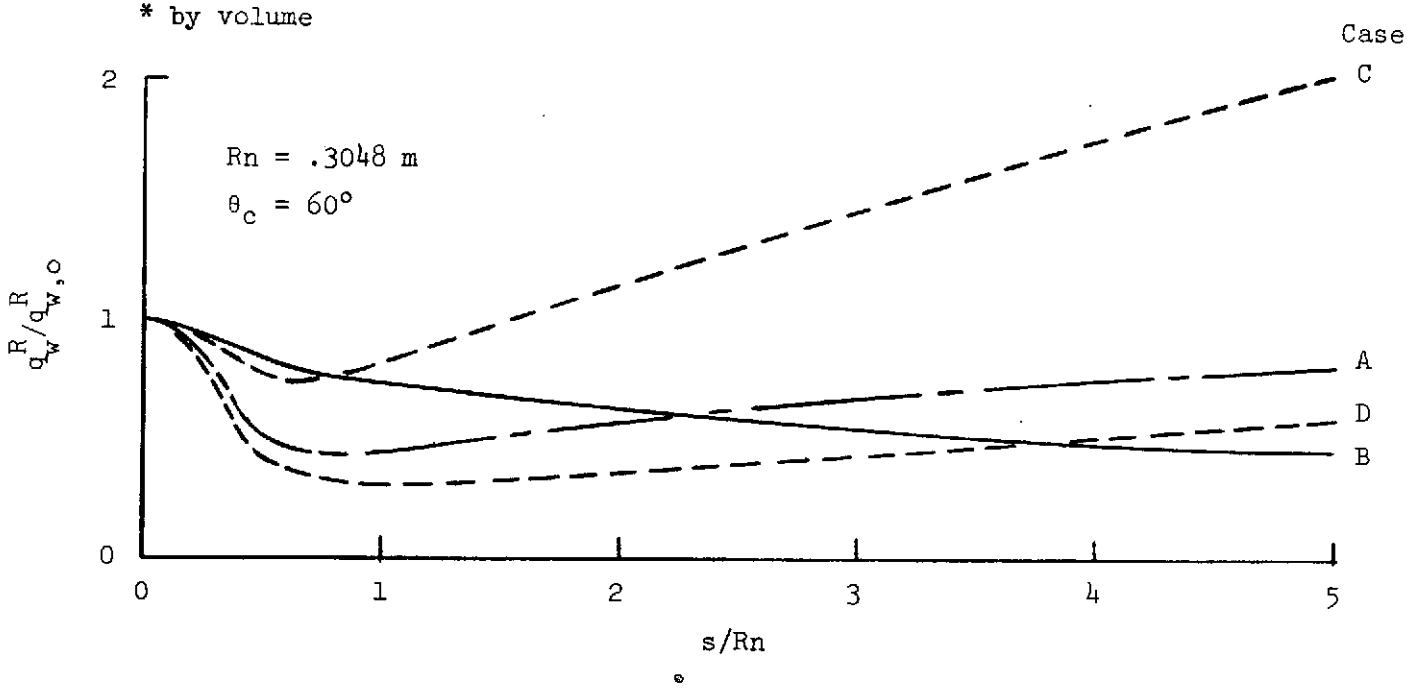

Figure 9. - Radiative heating distributions along a spherically-capped, conical body from radiating, inviscid flow solutions for entries in different atmospheres and different free-stream conditions.

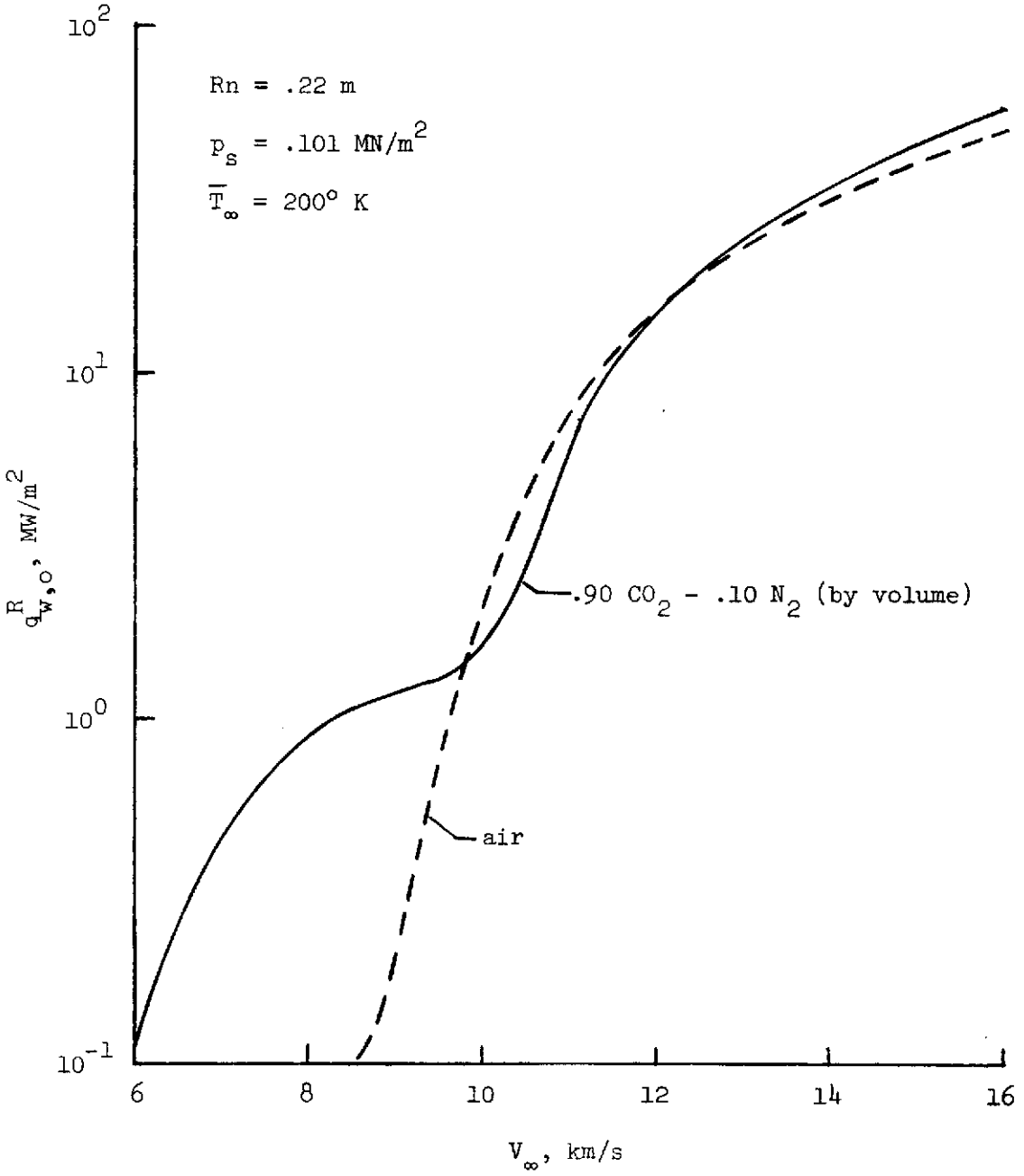

Figure 10. - A comparison of the stagnation-point, radiative heating rates for entries in air and in a .90 CO_2 - .10 N_2 (by volume) gas mixture.

θ_c	$q^R_{w,o}$, MW/m^2	δ_o/Rn	at s/Rn=3.0		
			δ/Rn	$\overline{T}_\delta/\overline{T}_s$	$\theta+\beta$
60°	11.39	.0435	.1893	.9058	63.33°
55°	11.35	.0434	.1606	.8514	57.77°
50°	11.33	.0434	.1382	.7644	52.23°
45°	11.33	.0435	.1155	.6276	46.59°

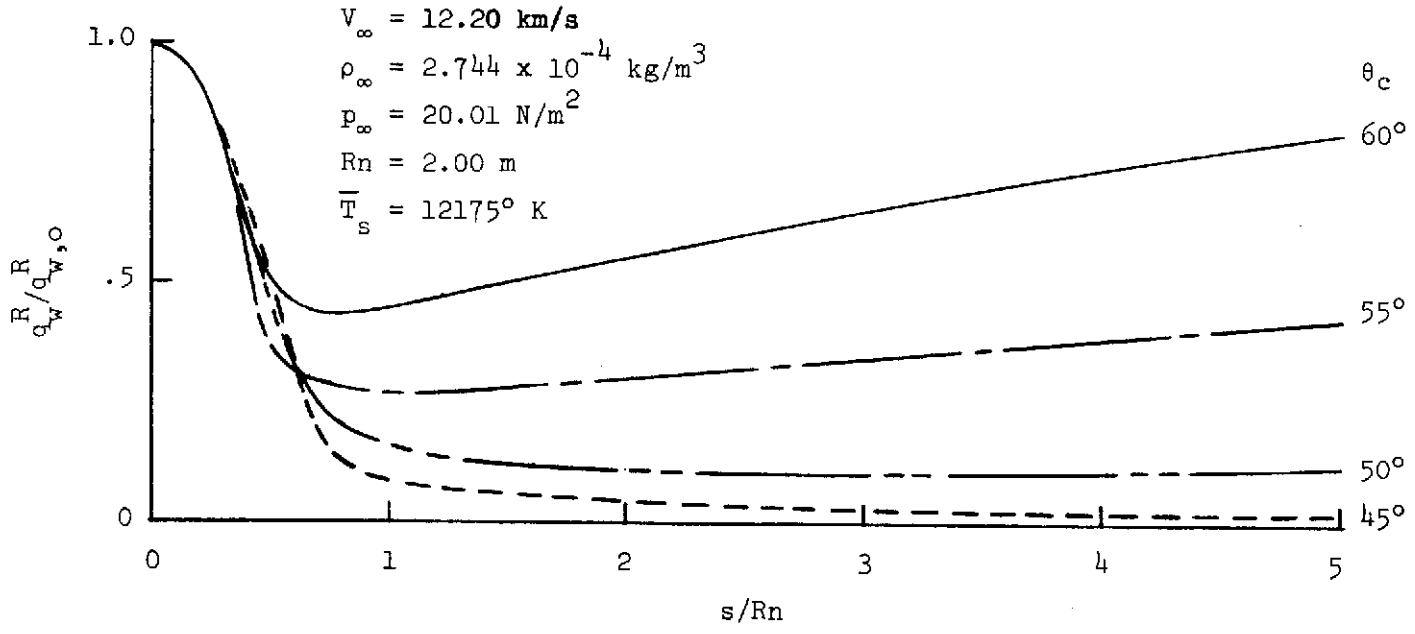

Figure 11. - The distribution of radiative heating along spherically-capped, conical bodies for entry in air.

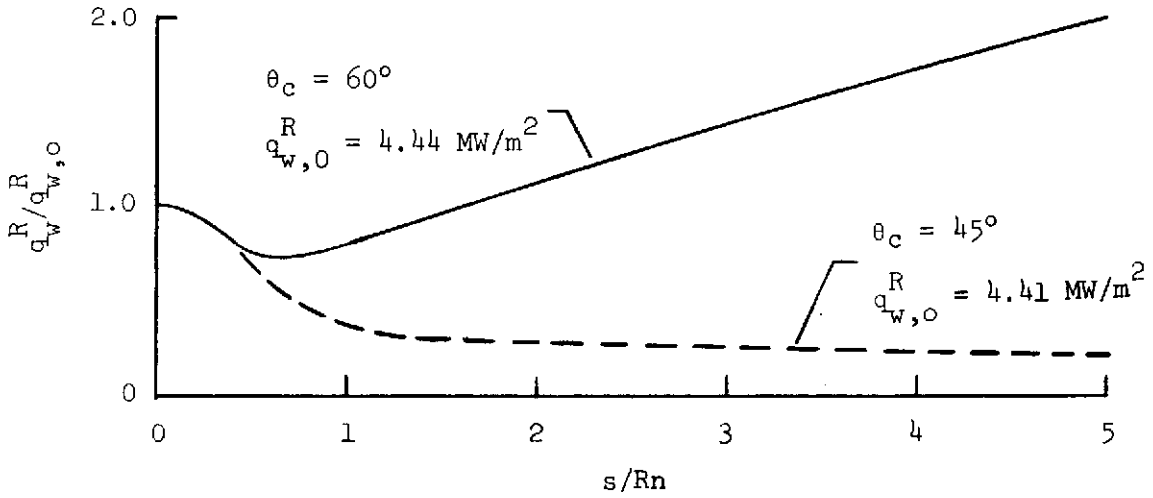

(a) V_∞ = 8.740 km/s ; ρ_∞ = 3.294 x 10^{-3} kg/m^3 ; p_∞ = 130.6 N/m^2

h_∞ = -8.43 MJ/kg ; Rn = .3048 m

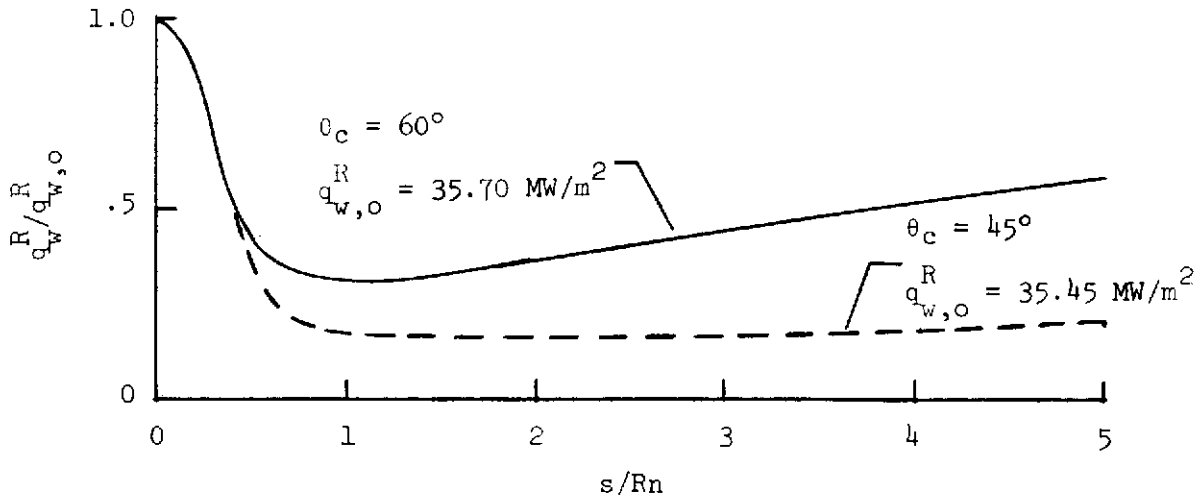

(b) V_∞ = 11.175 km/s ; ρ_∞ = 2.850 x 10^{-3} kg/m^3 ; p_∞ = 117.3 N/m^2

h_∞ = -8.43 MJ/kg ; Rn = .3048 m

Figure 12. - The distribution of radiative heating along spherically-capped, conical bodies for entry in a .90 CO_2 - .10 N_2 (by volume) gas mixture.

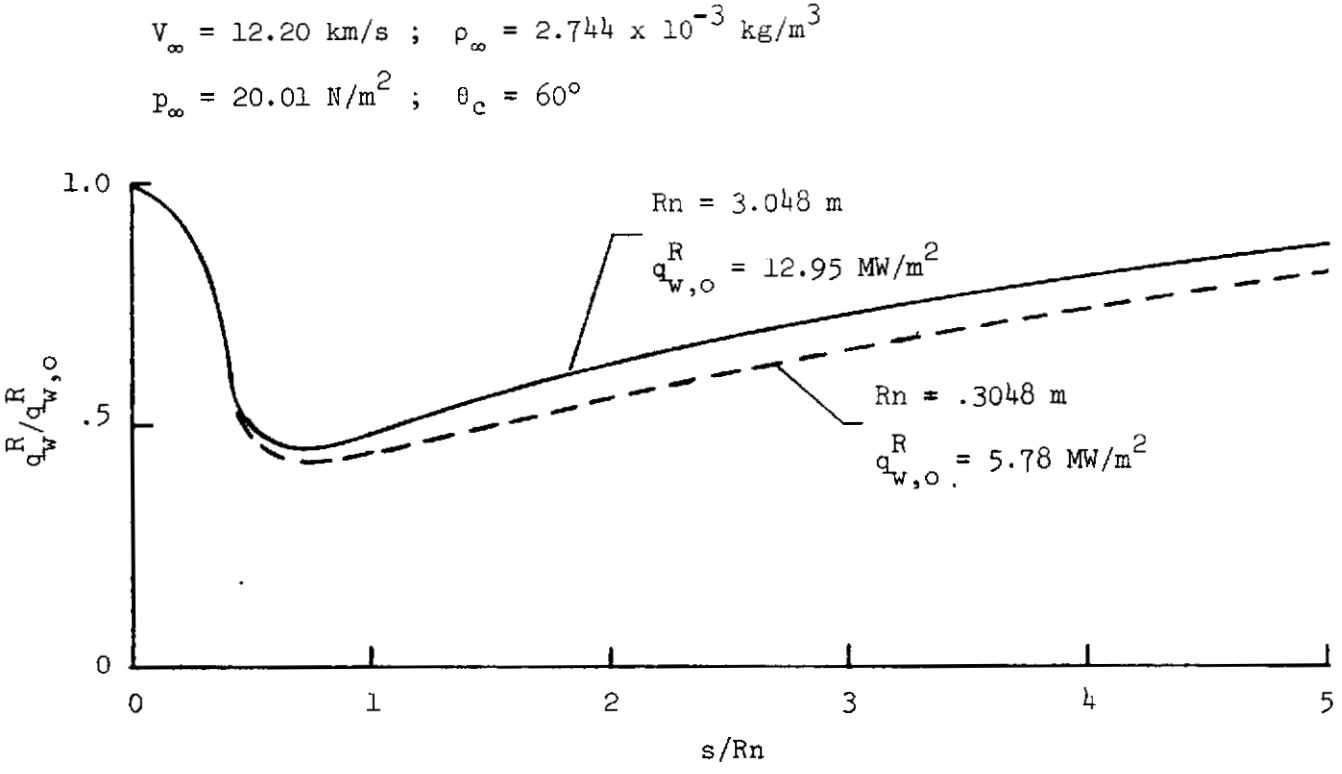

Figure 13. - The effect of nose radius on the distribution of radiative heating along a spherically-capped, conical body for entry in air.

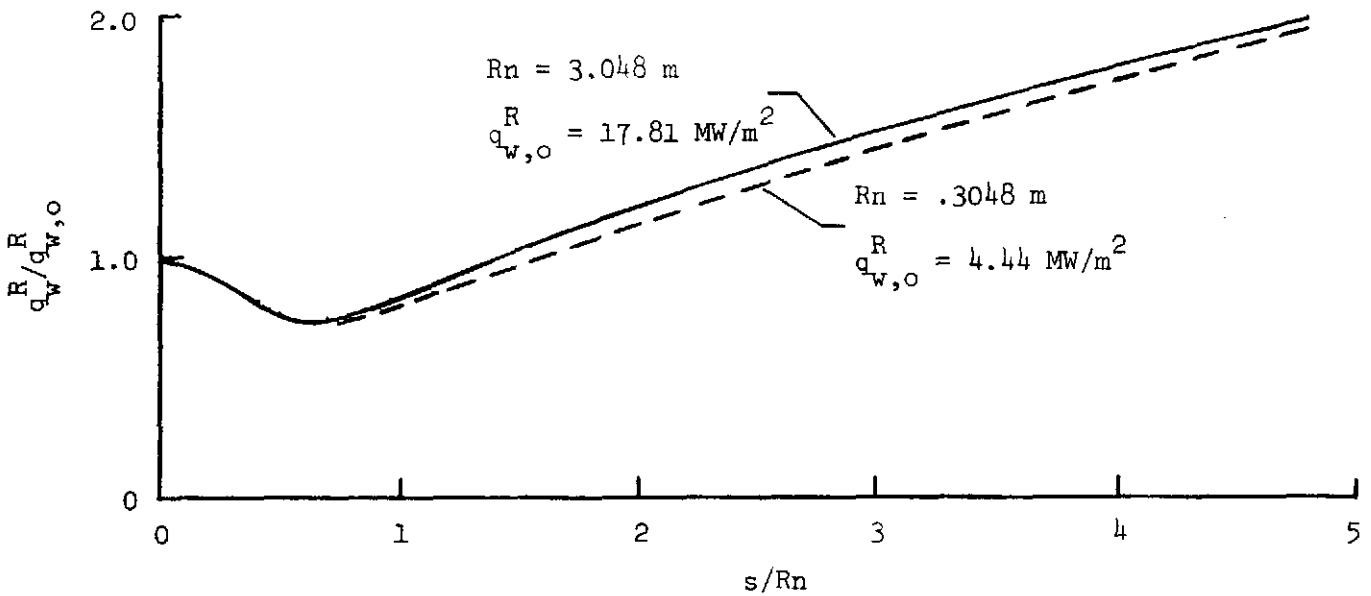

(a) V_∞ = 8.740 km/s ; ρ_∞ = 3.294 x 10^{-3} kg/m^3 ; p_∞ = 130.6 N/m^2

h_∞ = -8.43 MJ/kg ; θ_c = 60°

Figure 14. - The effect of nose radius on the distribution of radiative heating along a spherically-capped, conical body for entry in a .90 CO_2 - .10 N_2 (by volume) gas mixture.

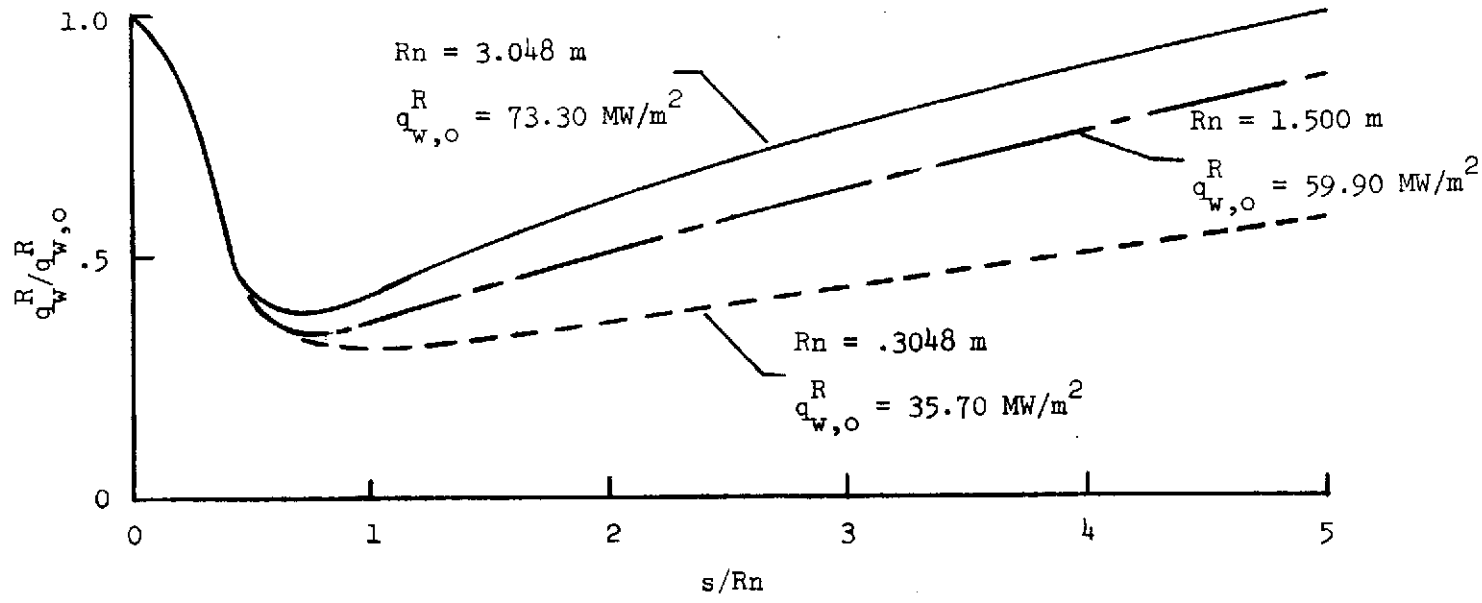

(b) V_∞ = 11.175 km/s ; ρ_∞ = 2.850 x 10^{-3} kg/m^3 ; p_∞ = 117.3 N/m^2

h_∞ = -8.43 MJ/kg ; θ_c = 60°

Figure 14. - Concluded.

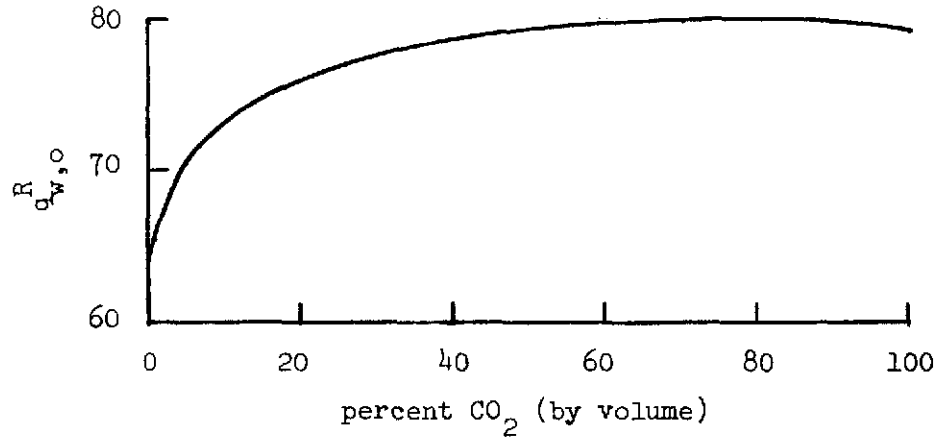

(a) V_∞ = 12.0 km/s ; ρ_∞ = 2.99 x 10^{-3} kg/m^3

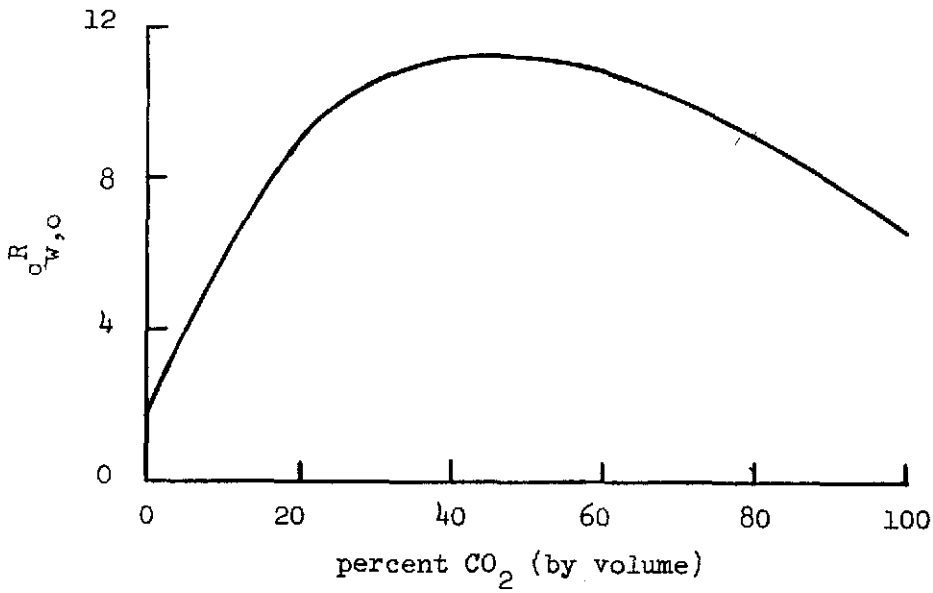

(b) V_∞ = 9.0 km/s ; ρ_∞ = 5.31 x 10^{-3} kg/m^3

Figure 15. - Stagnation-point, radiative heating rates in CO_2 - N_2 gas mixtures. Rn=.3048 m

Gas composition by volume

$.79\ N_2 - .21\ O_2$ (air)

$V_\infty = 15.250$ km/s

$\rho_\infty = 1.77 \times 10^{-4}$ kg/m^3

$p_\infty = 12.3$ N/m^2

$h_\infty = 0.0$ J/kg

Rn = 2.56 m

Specified wall conditions

$\overline{T}_w = 3840$ °K

$(\rho v)_w = .205$ kg/m^2-s

Elemental mass fractions of injected gas:

Carbon	.923
Oxygen	.058
Hydrogen	.018
Nitrogen	.001

(a) Free-stream conditions and specified wall conditions.

Figure 16. - Fully-coupled, stagnation-point solution for Earth reentry. Present method is compared with the method of Garrett (ref. 19).

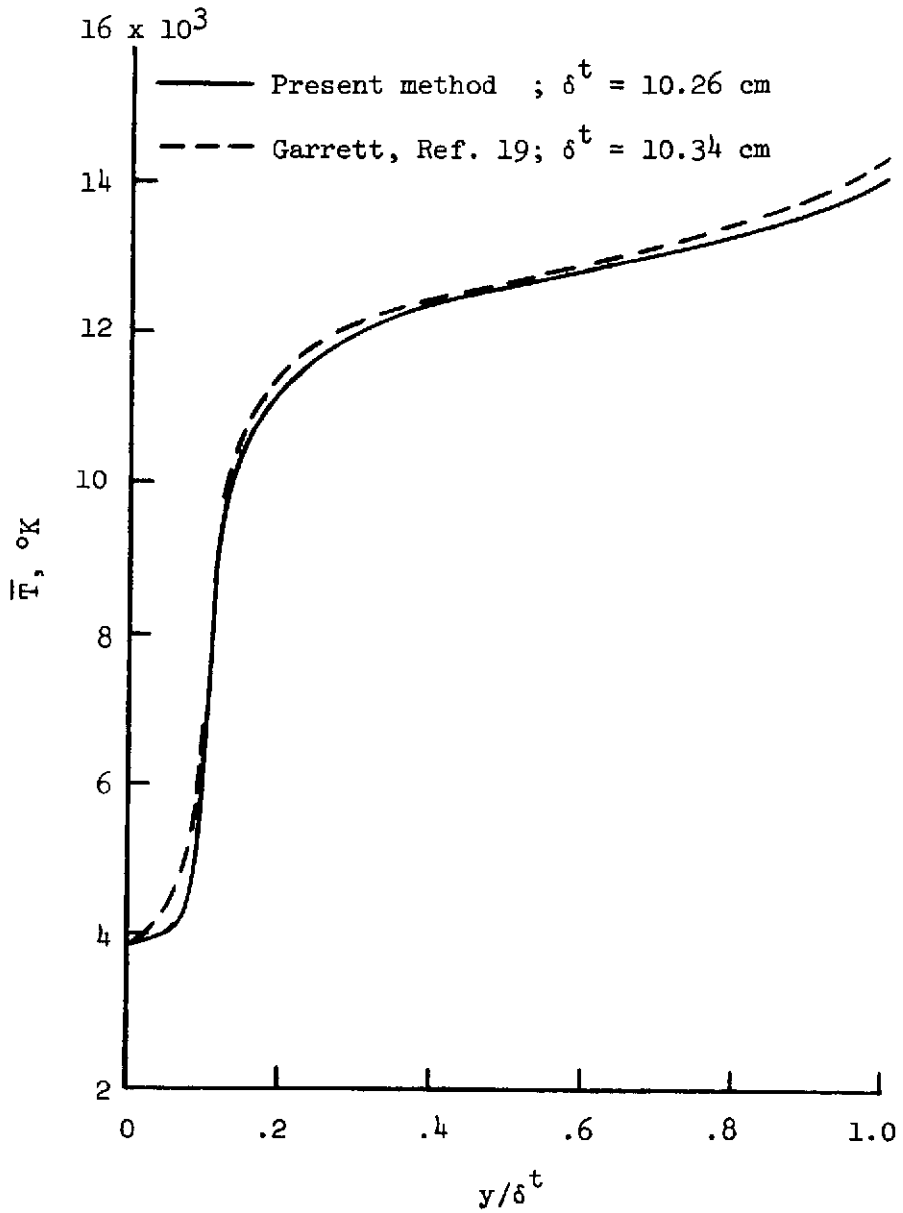

(b) Temperature profile through layer.

Figure 16. - Continued.

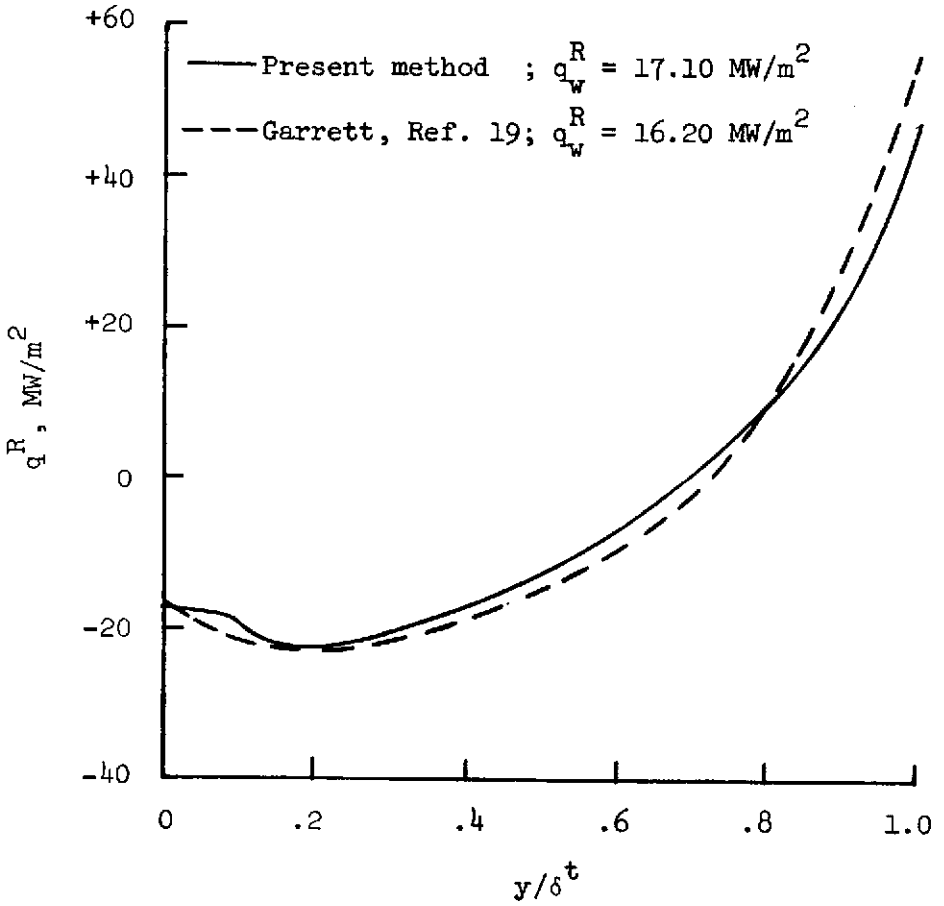

(c) Radiative heating profile through layer.

Figure 16. - Continued.

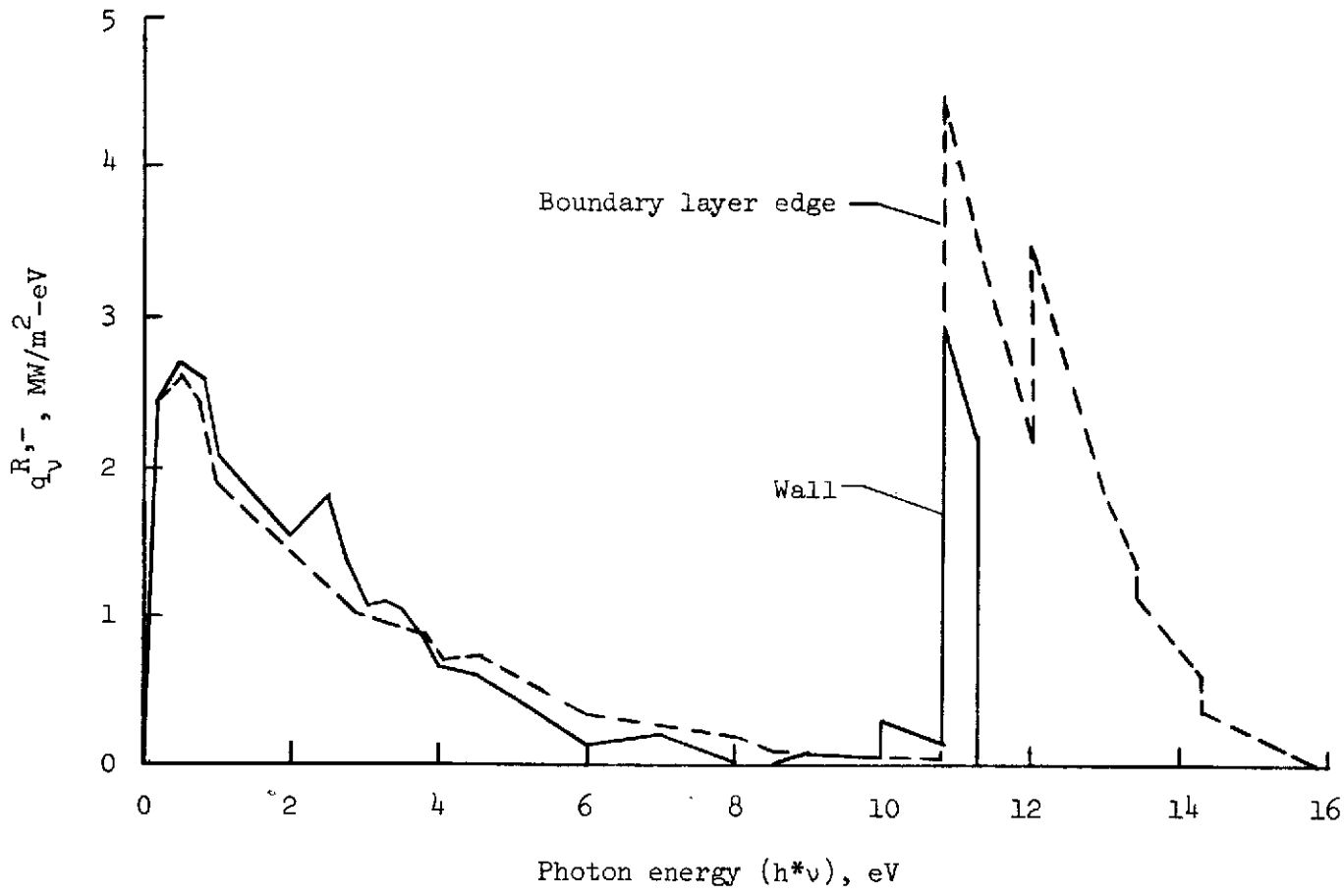

(d) Spectral distribution of radiative heating toward the body due to continuum processes.

Figure 16. - Continued.

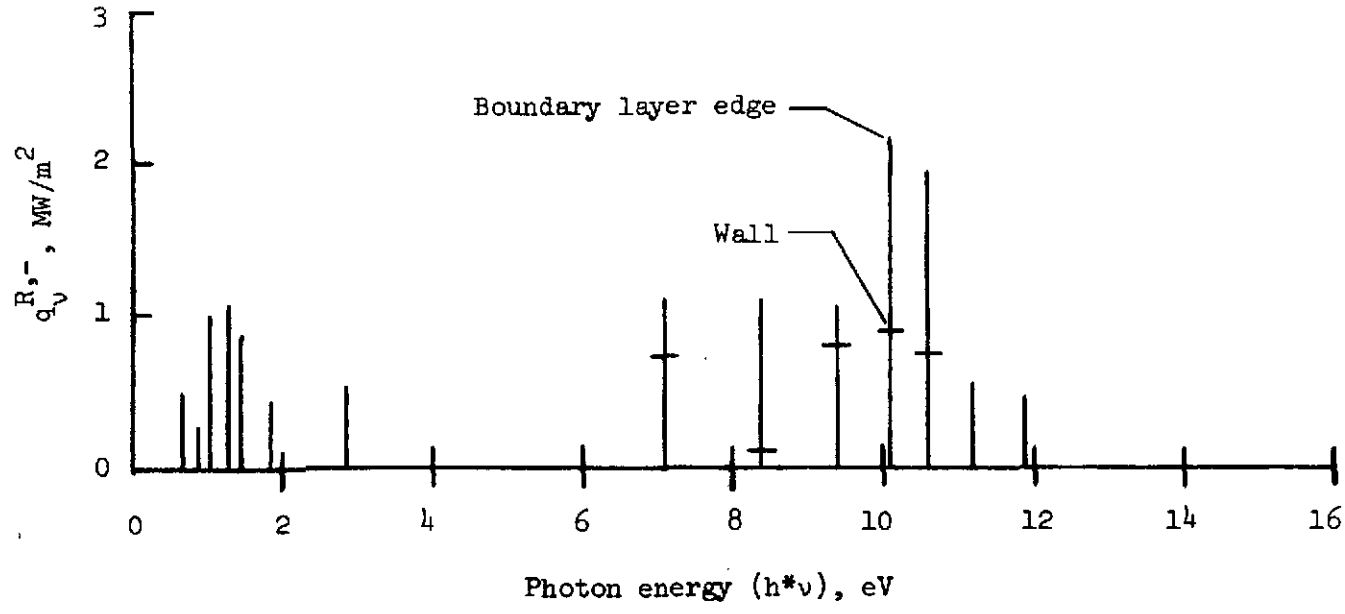

(e) Spectral distribution of radiative heating toward the body due to line processes.

Figure 16. - Concluded.

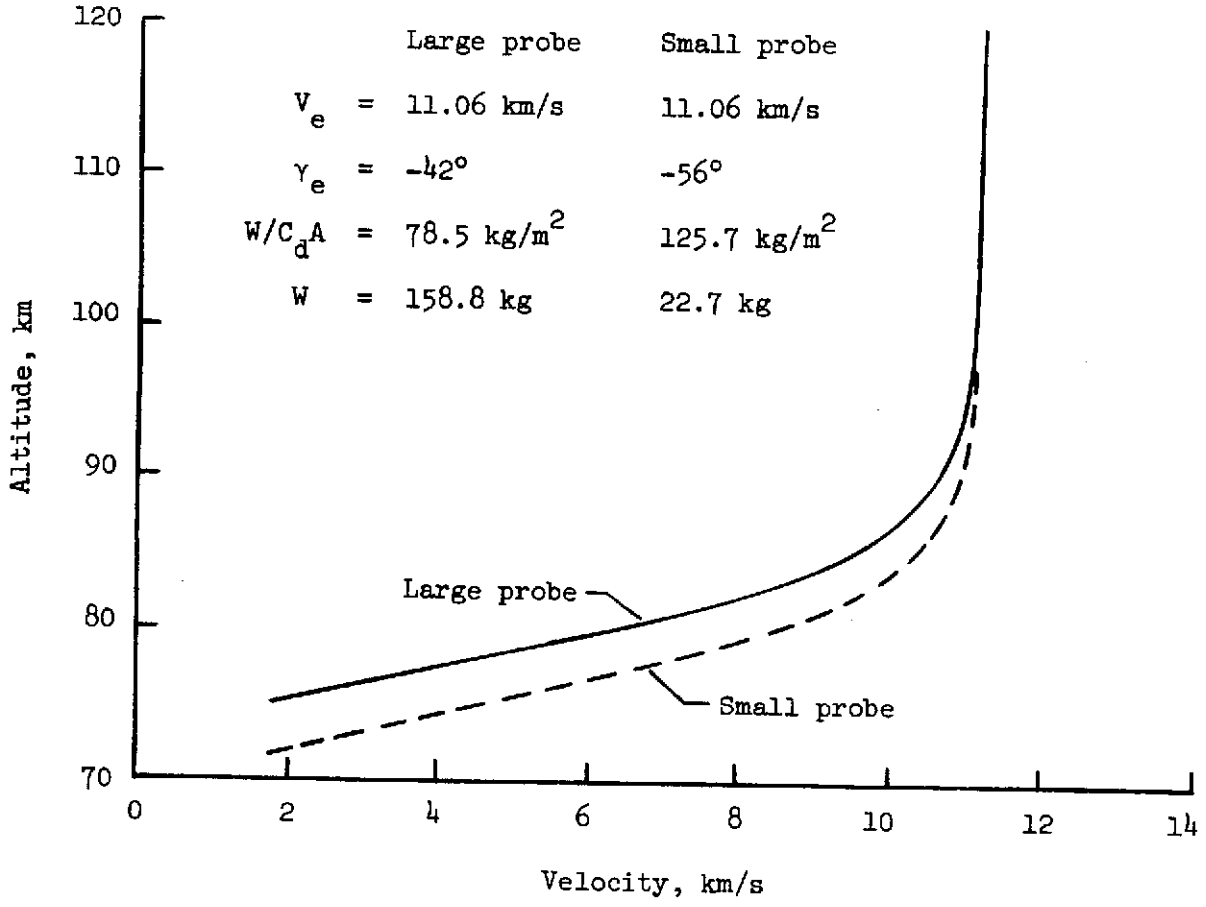

Figure 17. - Trajectories for large and small probes during entry to Venus.

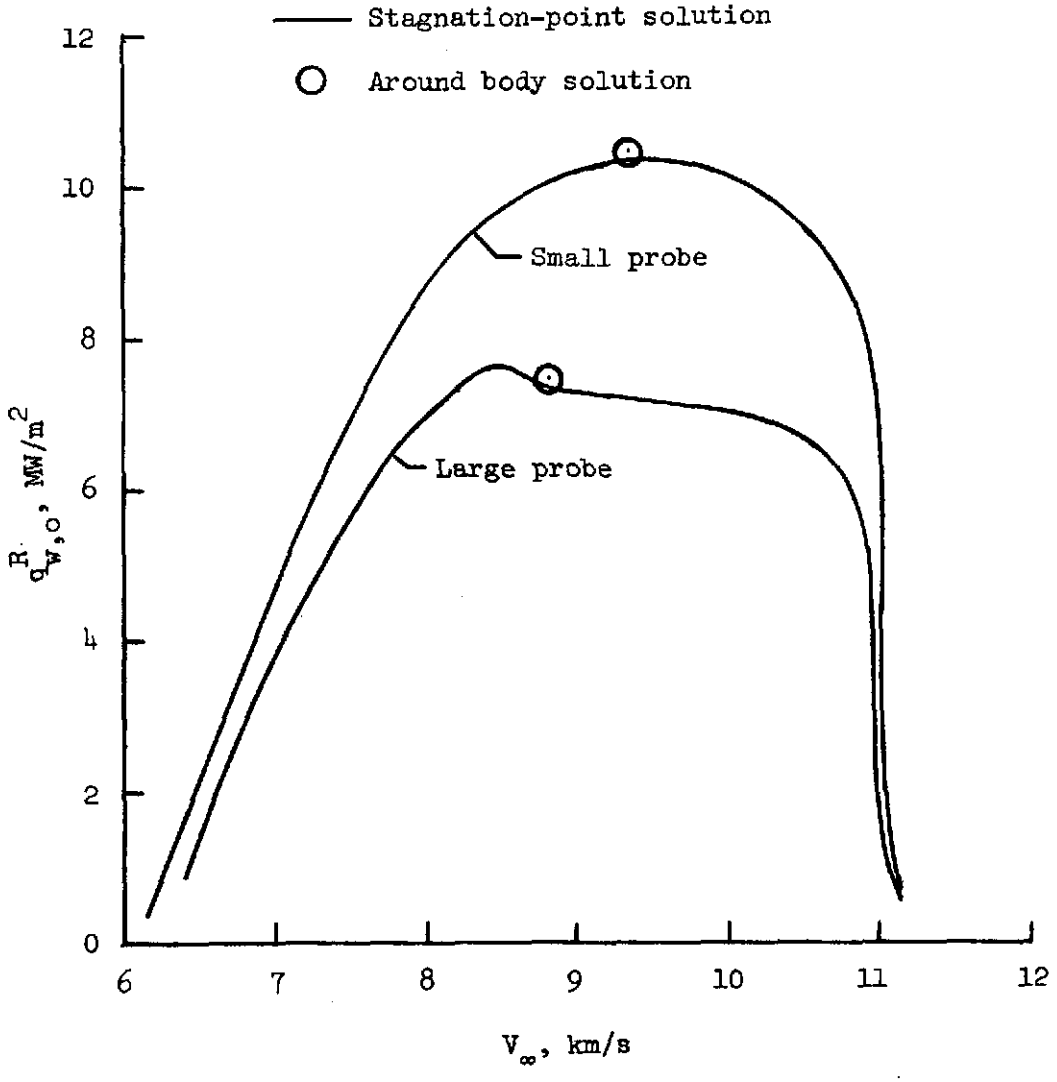

Figure 18. - Stagnation-point, radiative heating rates along entry trajectories for large and small probes. Results from radiating, inviscid flow solutions.

Gas composition by volume
.97 CO_2 - .03 N_2

V_∞ = 8.803 km/s

ρ_∞ = 5.79 x 10^{-3} kg/m^3

p_∞ = 200.1 N/m^2

h_∞ = -8.86 MJ/kg

Rn = 0.3429 m

θ_c = 60°

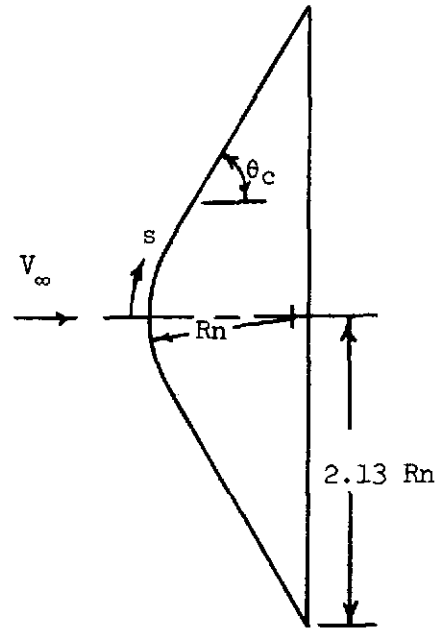

(a) Free-stream conditions and body shape.

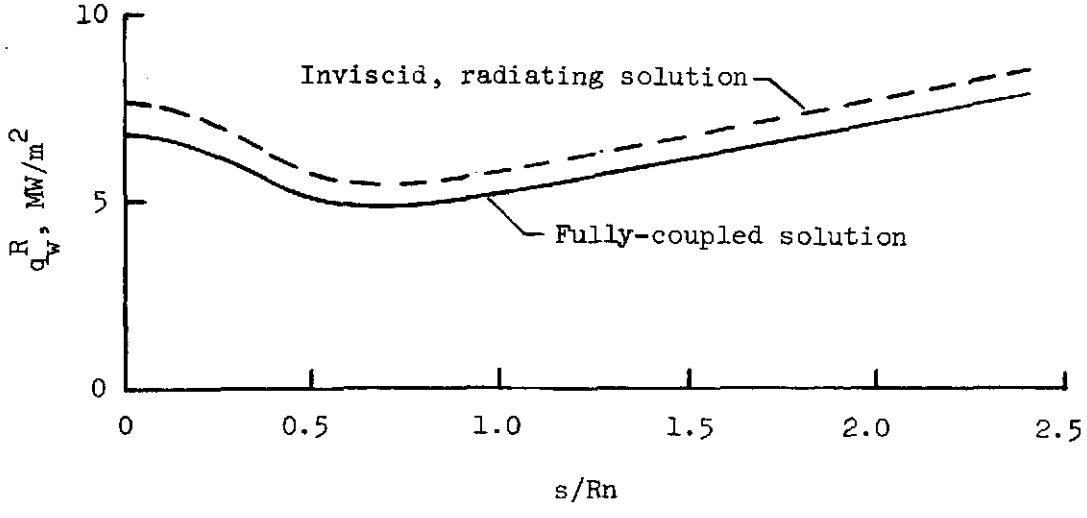

(b) Comparison of radiative heating.

Figure 19. - Fully-coupled, radiating flow solution with steady-state ablation of carbon-phenolic heatshield for large probe.

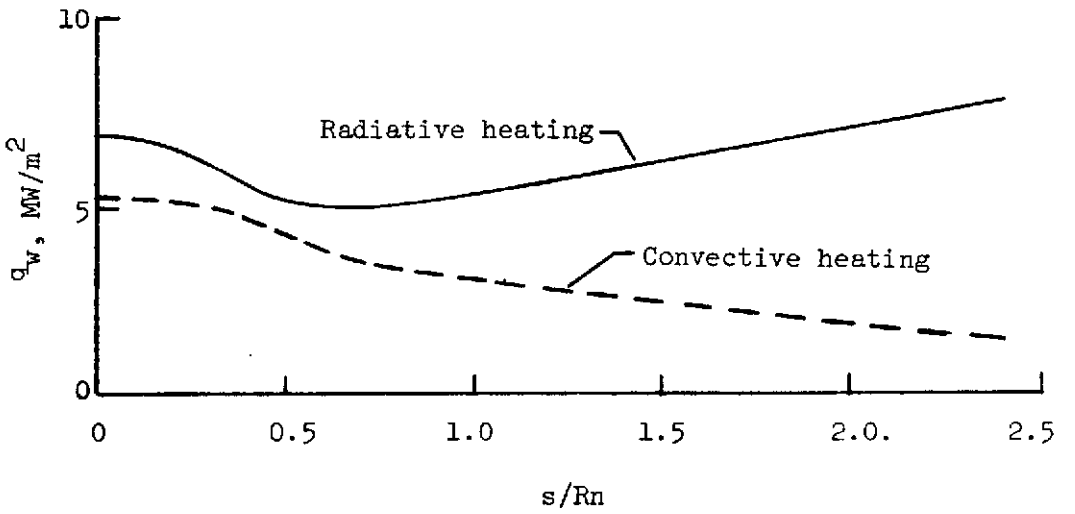

(c) Radiative and convective heating distribution.

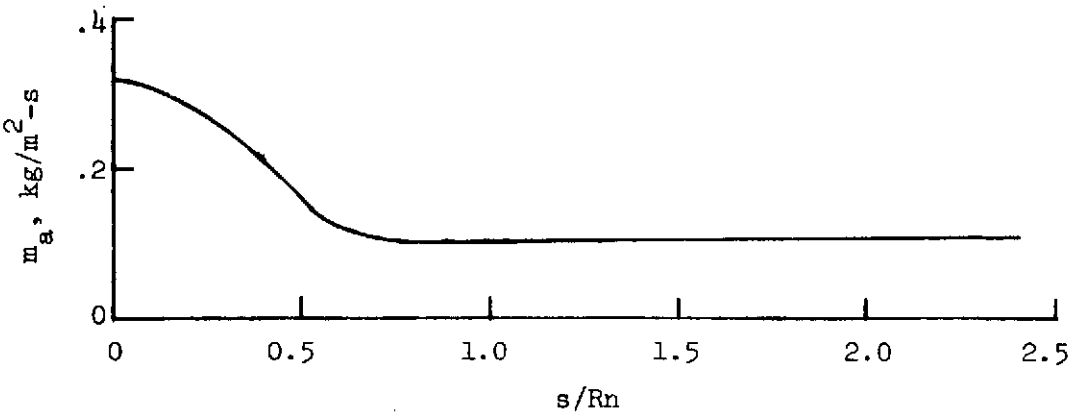

(d) Ablation rate distribution.

Figure 19. - Continued.

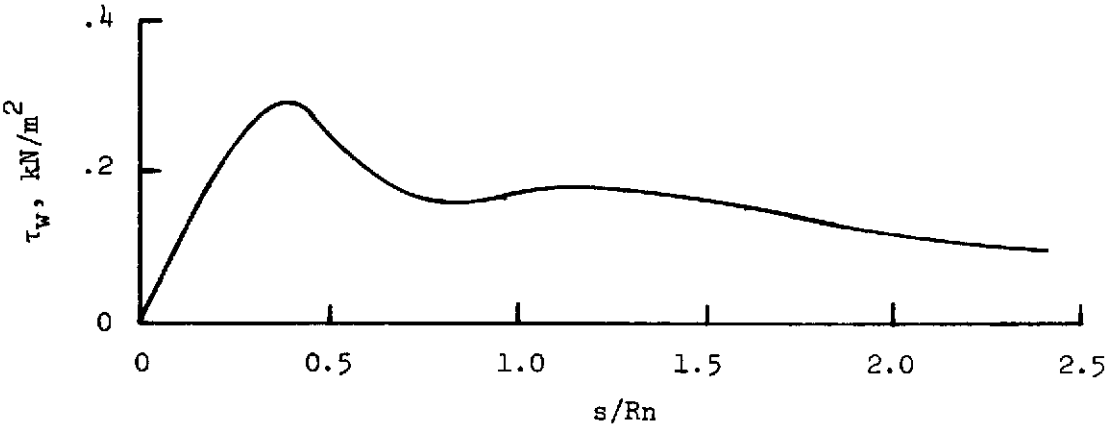

(e) Aerodynamic shear distribution.

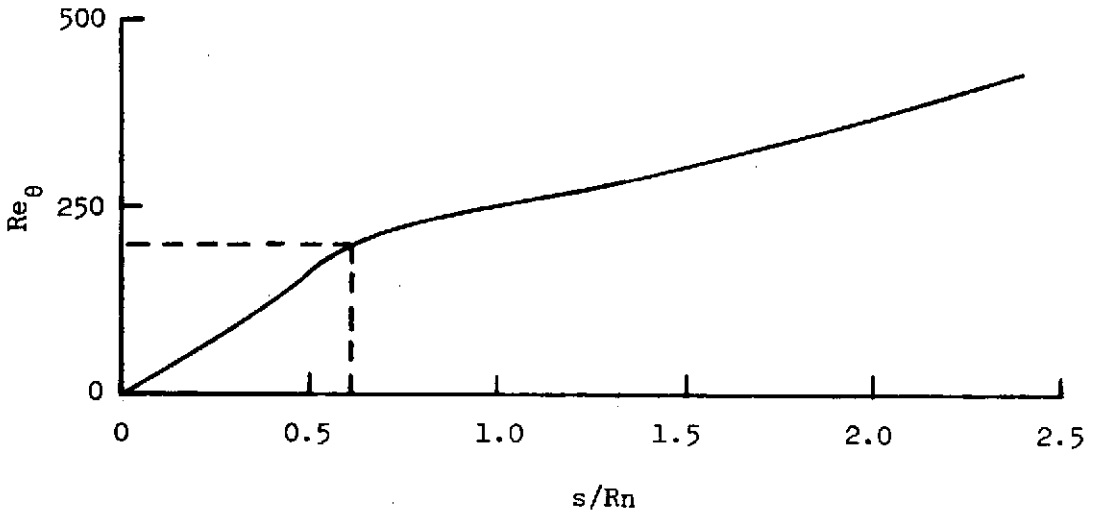

(f) Momentum thickness Reynolds number distribution.

Figure 19. - Continued.

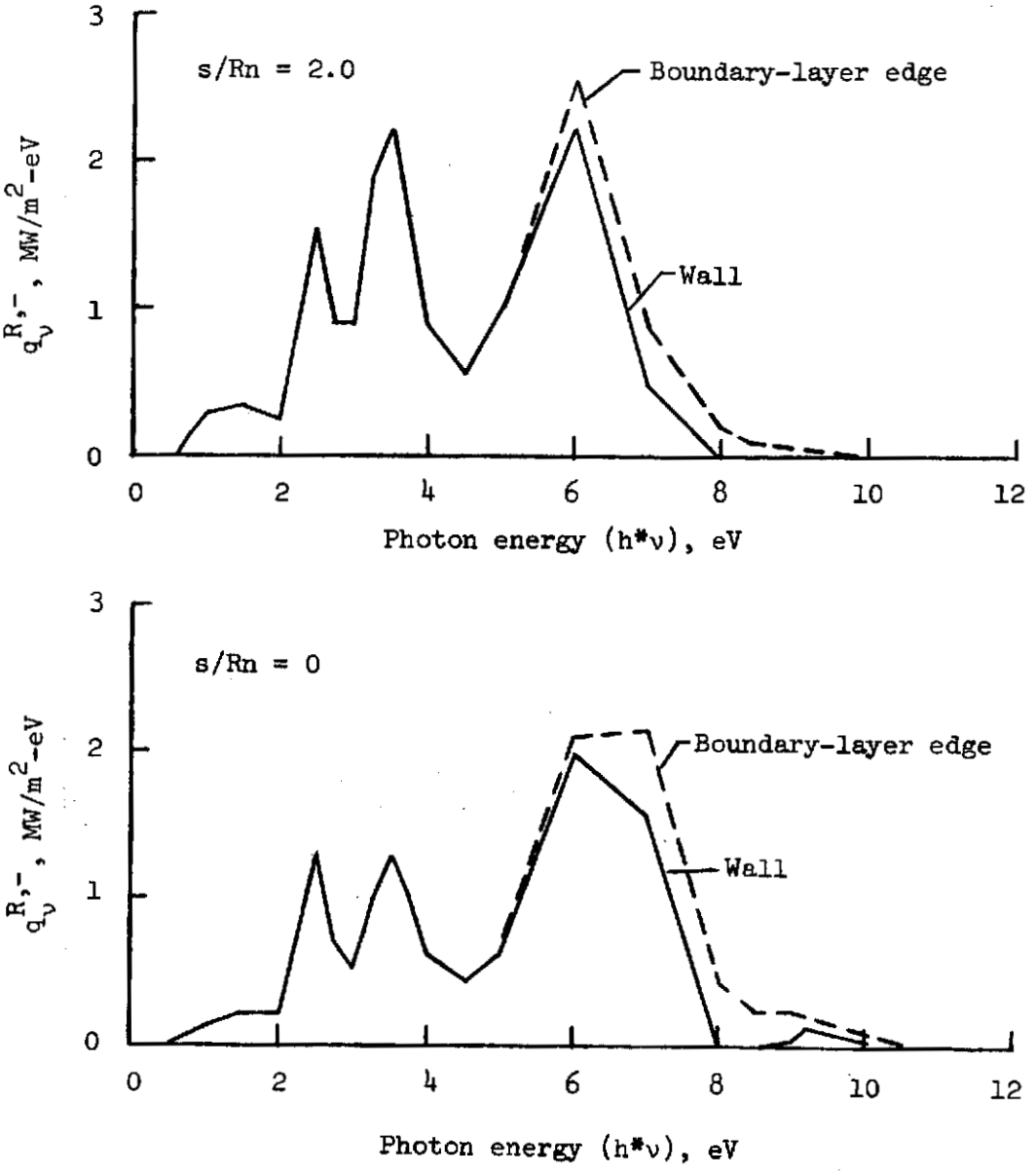

(g) Spectral distribution of radiative heating toward the body due to continuum processes.

Figure 19. - Concluded.

Gas composition by volume
.97 CO_2 - .03 N_2

V_∞ = 9.331 km/s

ρ_∞ = 9.32 x 10^{-3} kg/m^3

p_∞ = 330.4 N/m^2

h_∞ = -8.86 MJ/kg

Rn = 0.1397 m

θ_c = 45°

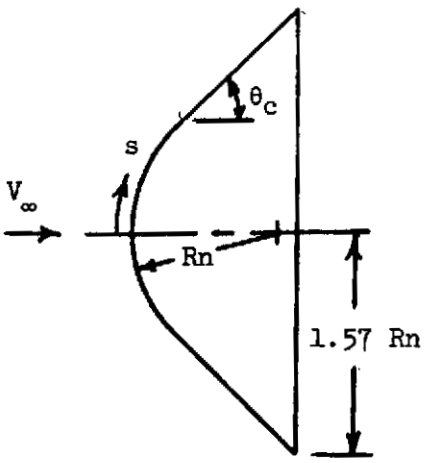

(a) Free-stream conditions and body shape.

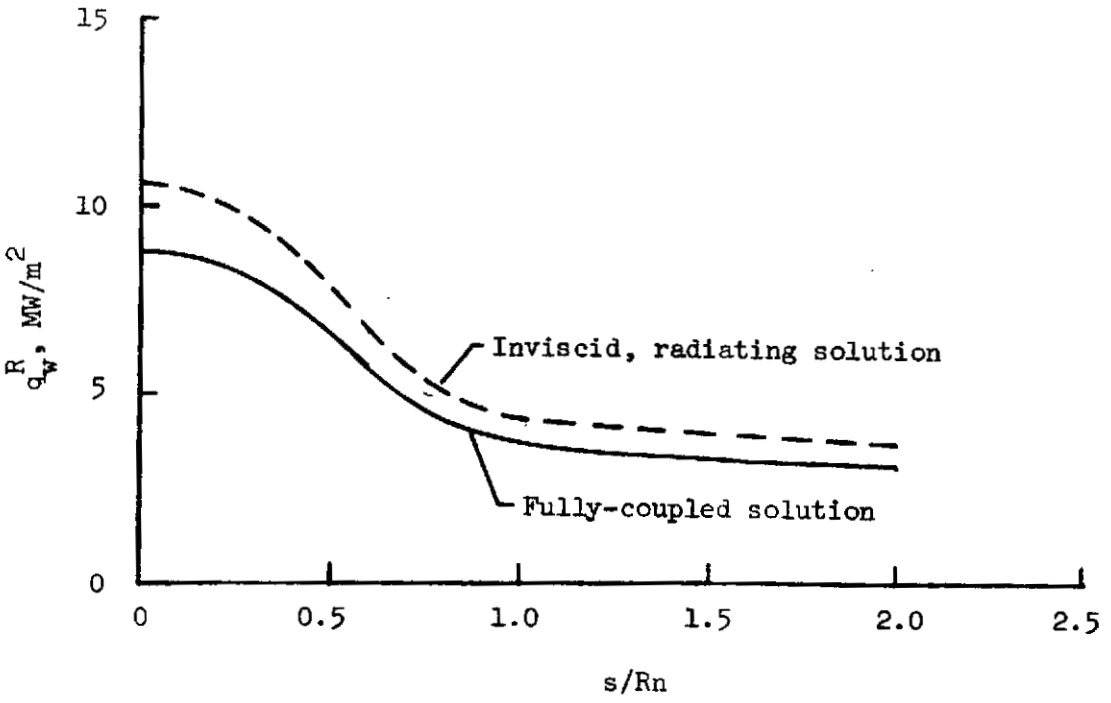

(b) Comparison of radiative heating.

Figure 20. - Fully-coupled, radiating flow solution with steady-state ablation of carbon-phenolic heatshield for small probe.

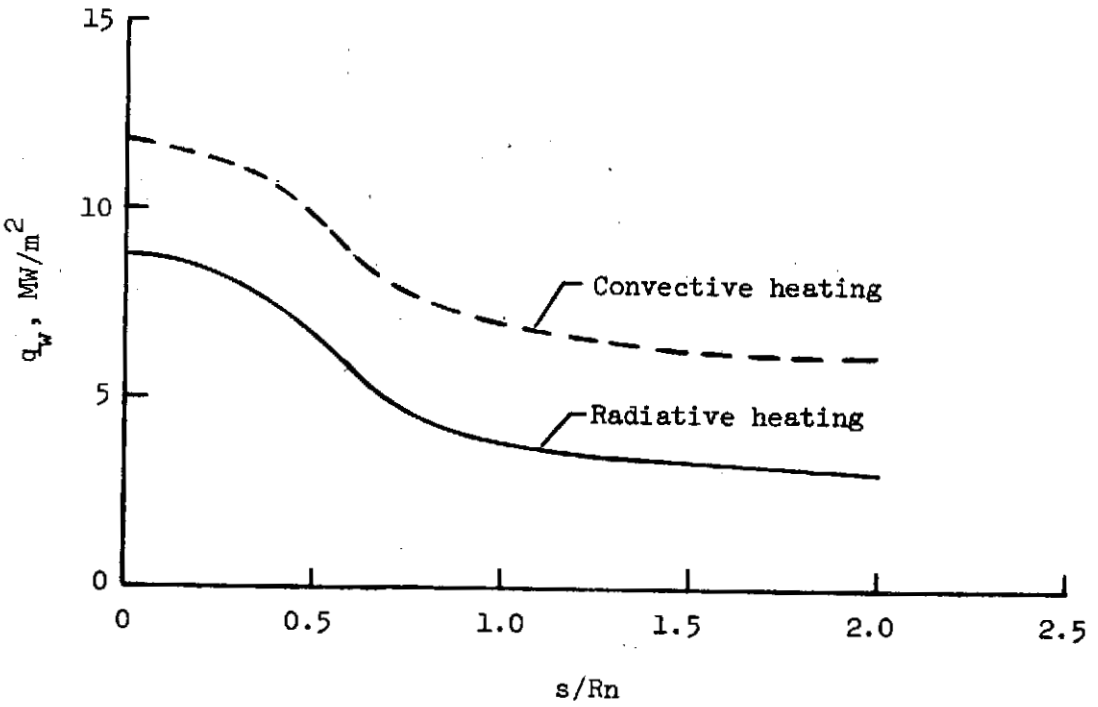

(c) Radiative and convective heating distribution.

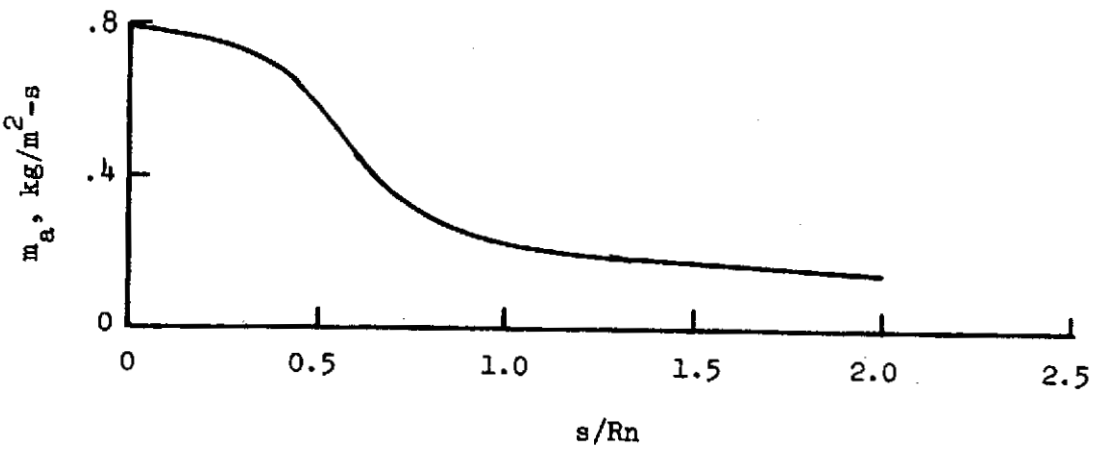

(d) Ablation rate distribution.

Figure 20. - Continued.

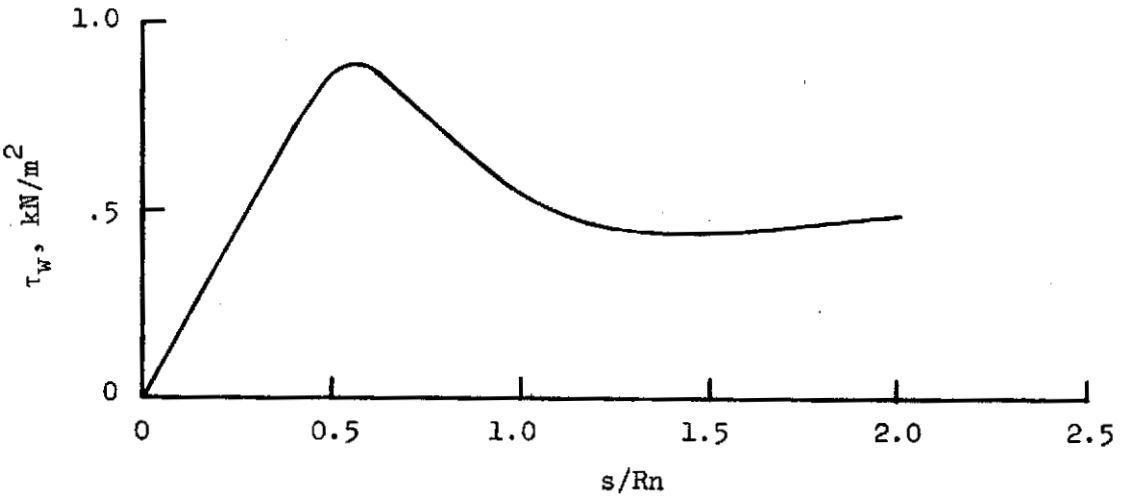

(e) Aerodynamic shear distribution.

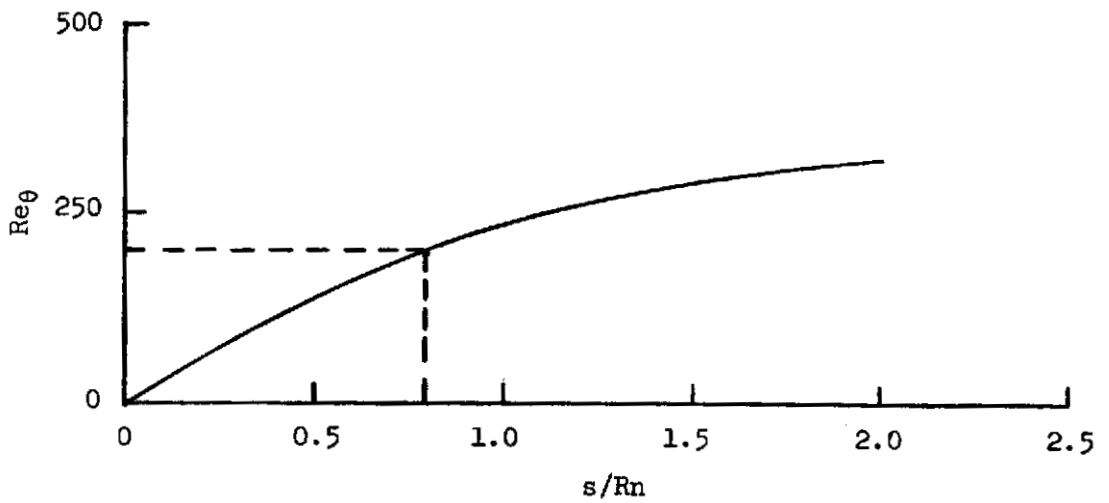

(f) Momentum thickness Reynolds number distribution.

Figure 20. - Continued.

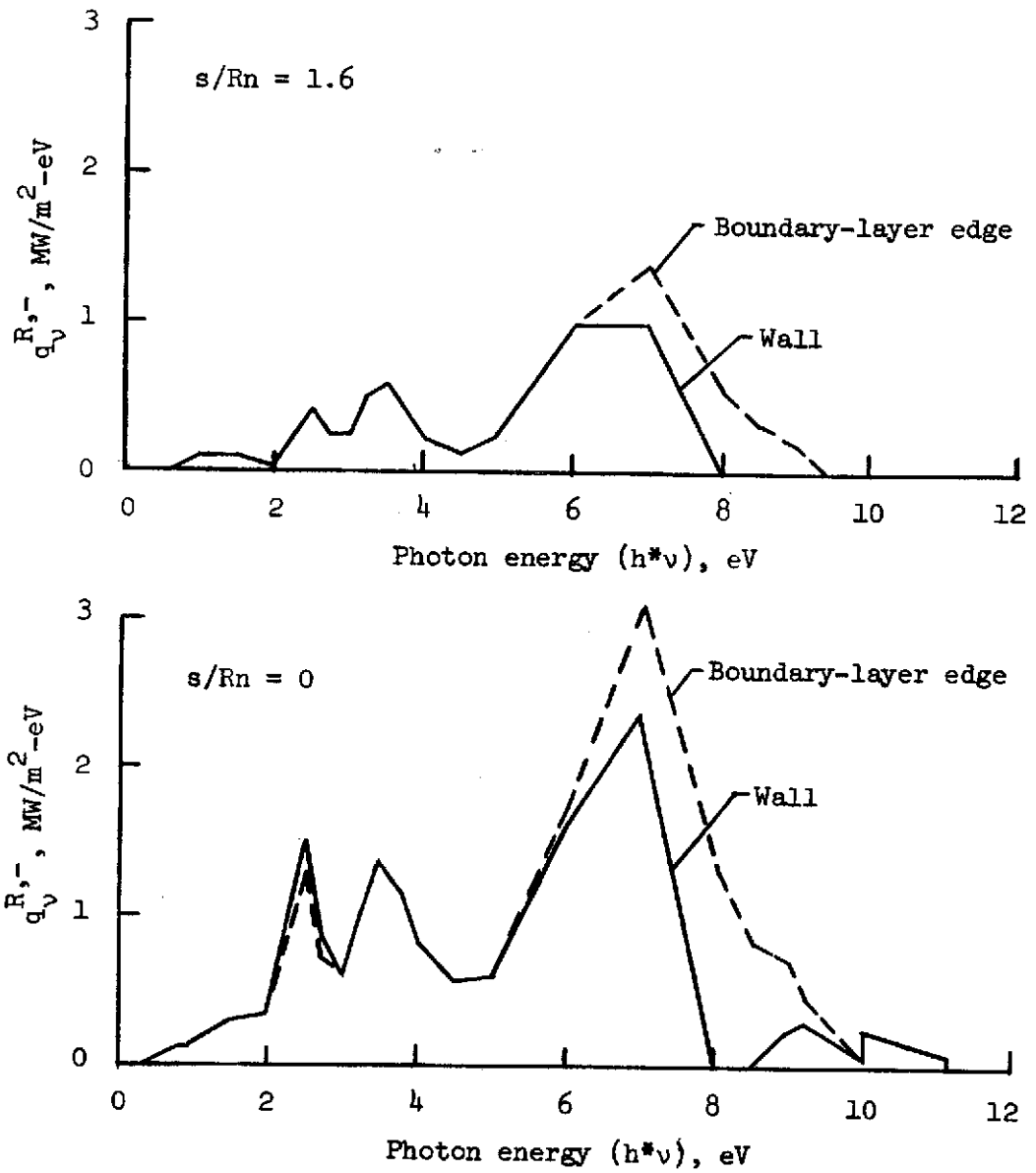

(g) Spectral distribution of radiative heating toward the body due to continuum processes.

Figure 20.- Concluded.

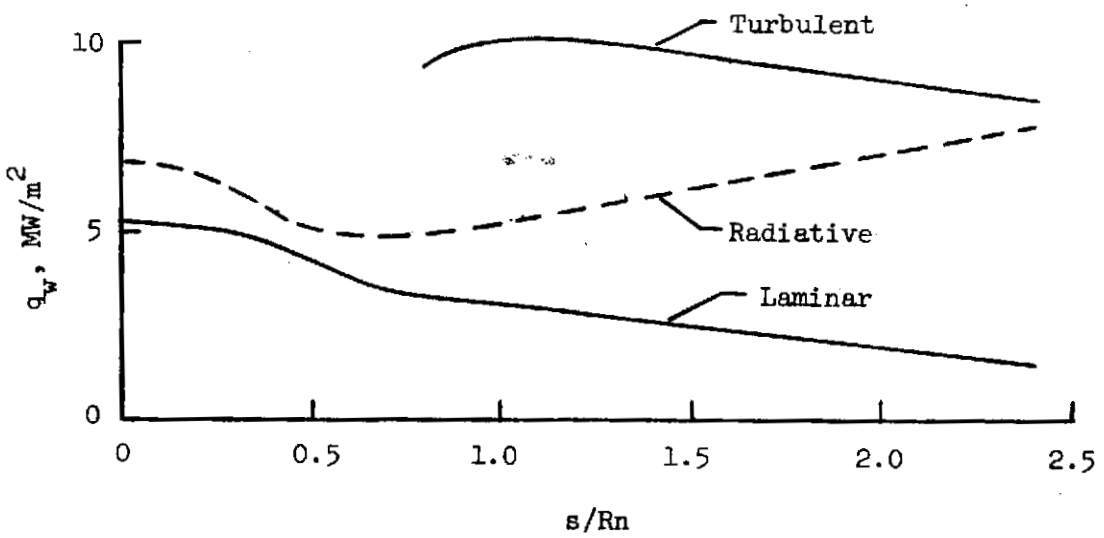

(a) Heating rate distribution.

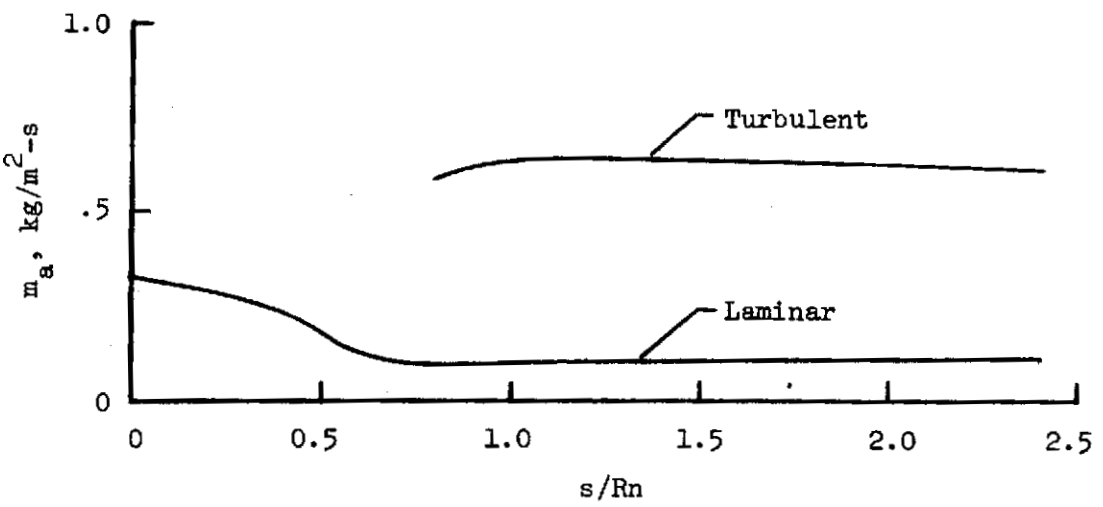

(b) Ablation rate distribution.

Figure 21. - Comparison between a turbulent and laminar boundary layer for fully-coupled solution for large probe.

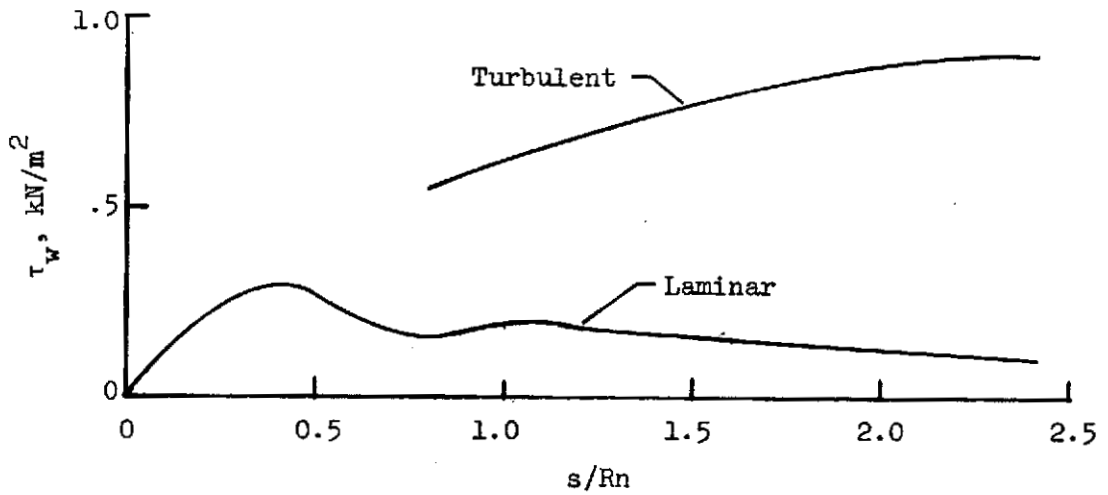

(c) Aerodynamic shear distribution.

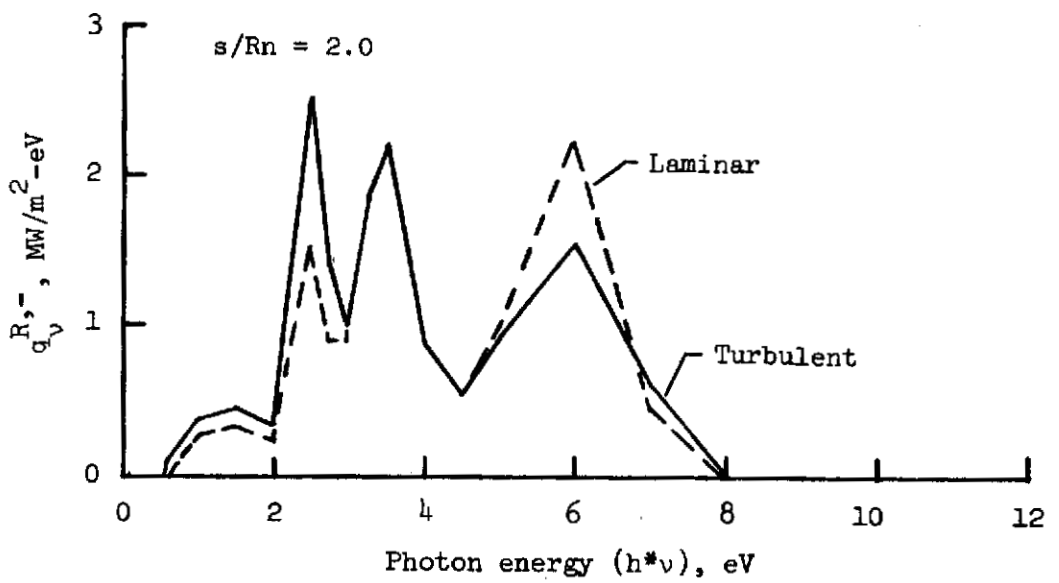

(d) Spectral distribution at the wall of radiative heating toward the body due to continuum processes.

Figure 21. - Concluded.

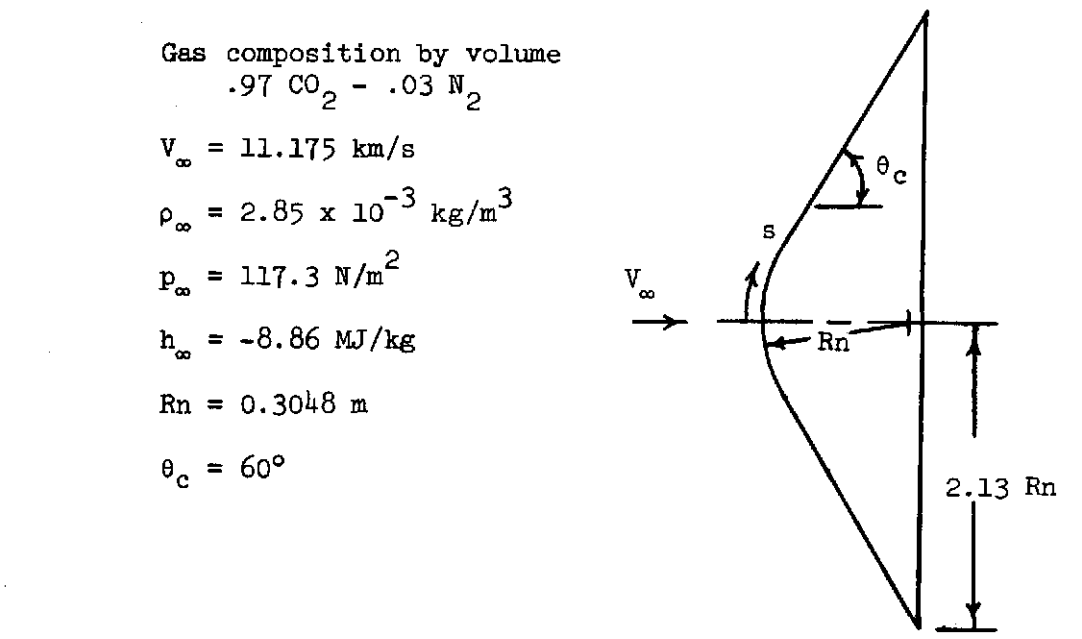

(a) Free-stream conditions and body shape.

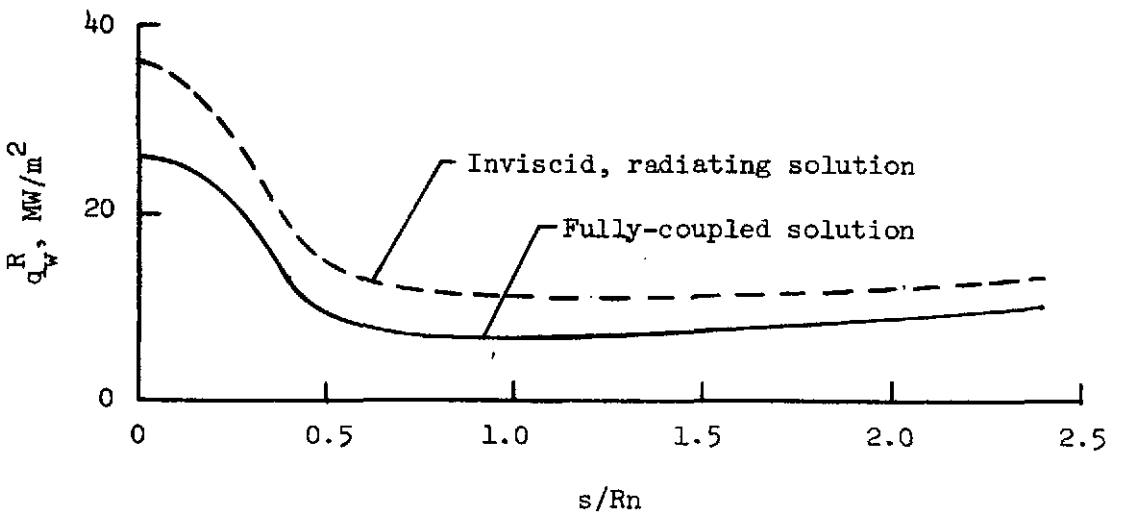

(b) Comparison of radiative heating.

Figure 22. - Fully-coupled, radiating flow solution with steady-state ablation of carbon-phenolic heatshield for high velocity entry.

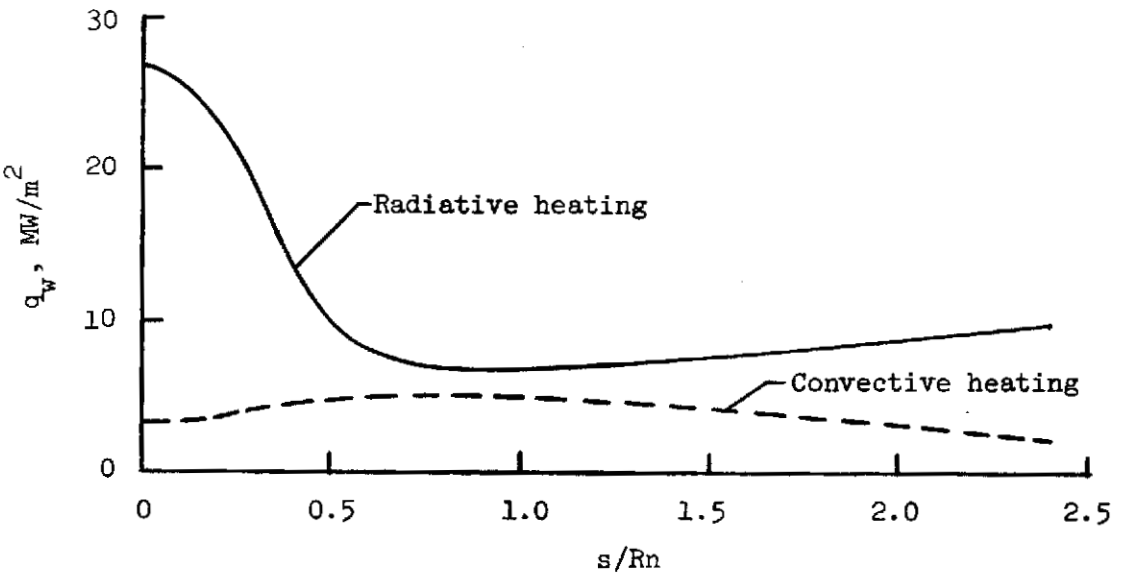

(c) Radiative and convective heating distribution.

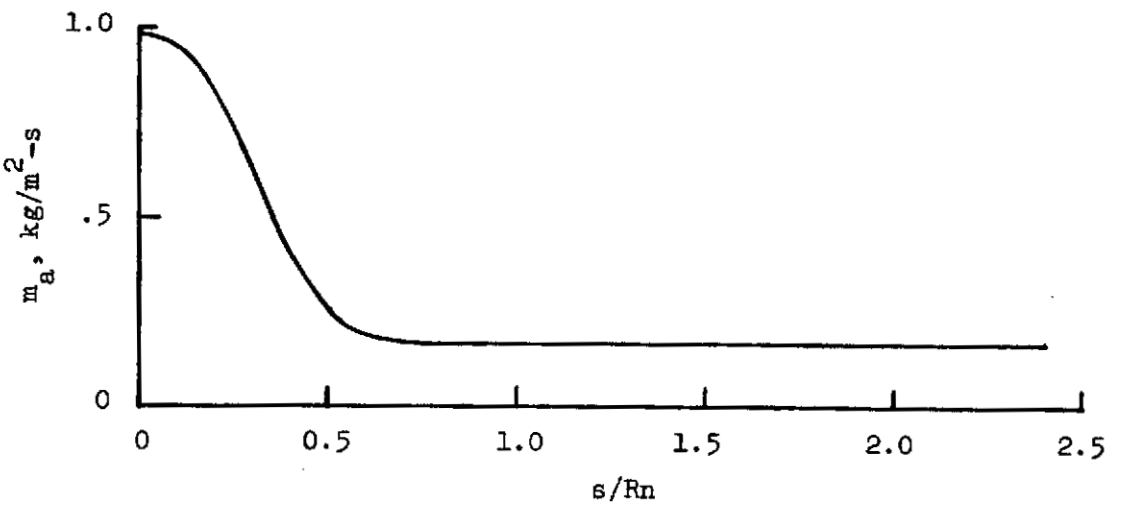

(d) Ablation rate distribution.

Figure 22. - Continued.

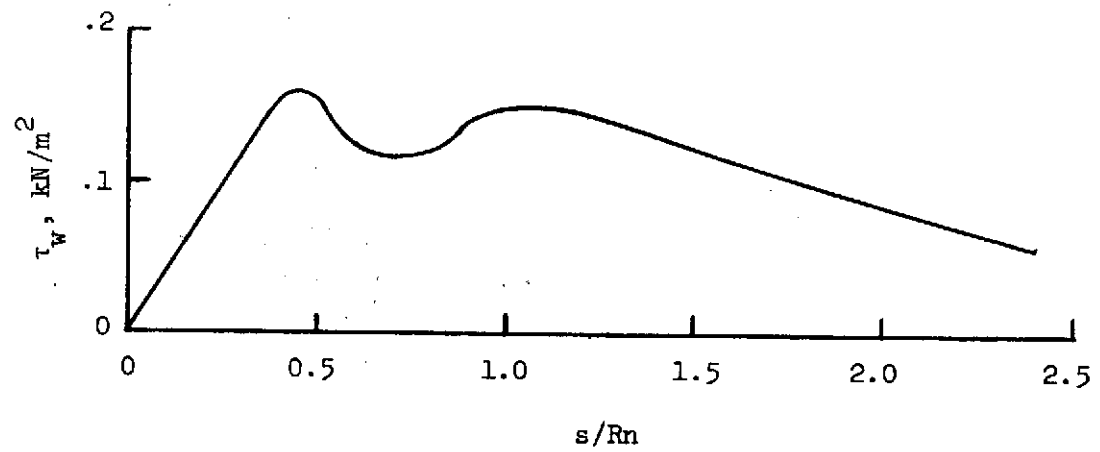

(e) Aerodynamic shear distribution.

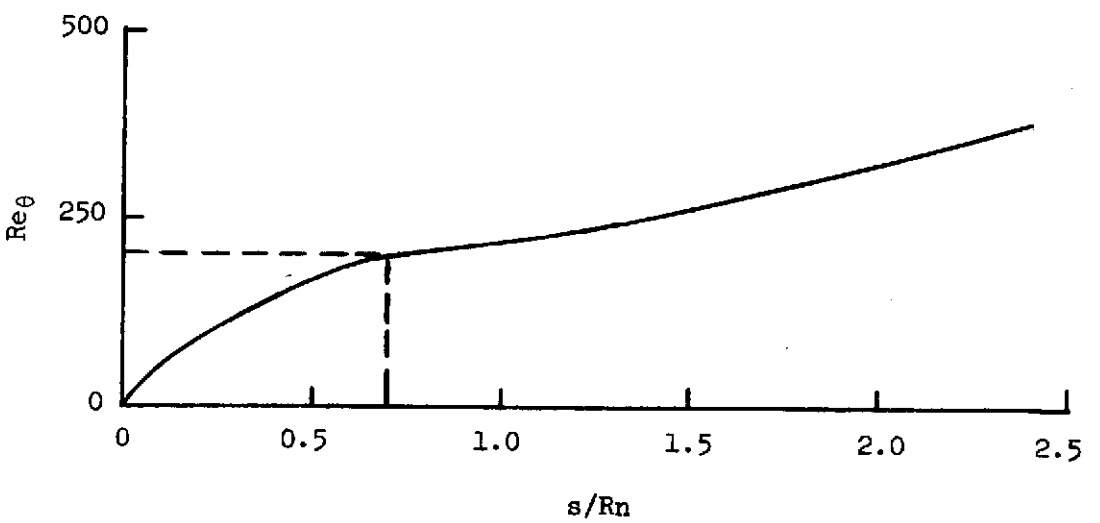

(f) Momentum thickness Reynolds number distribution.

Figure 22. - Continued.

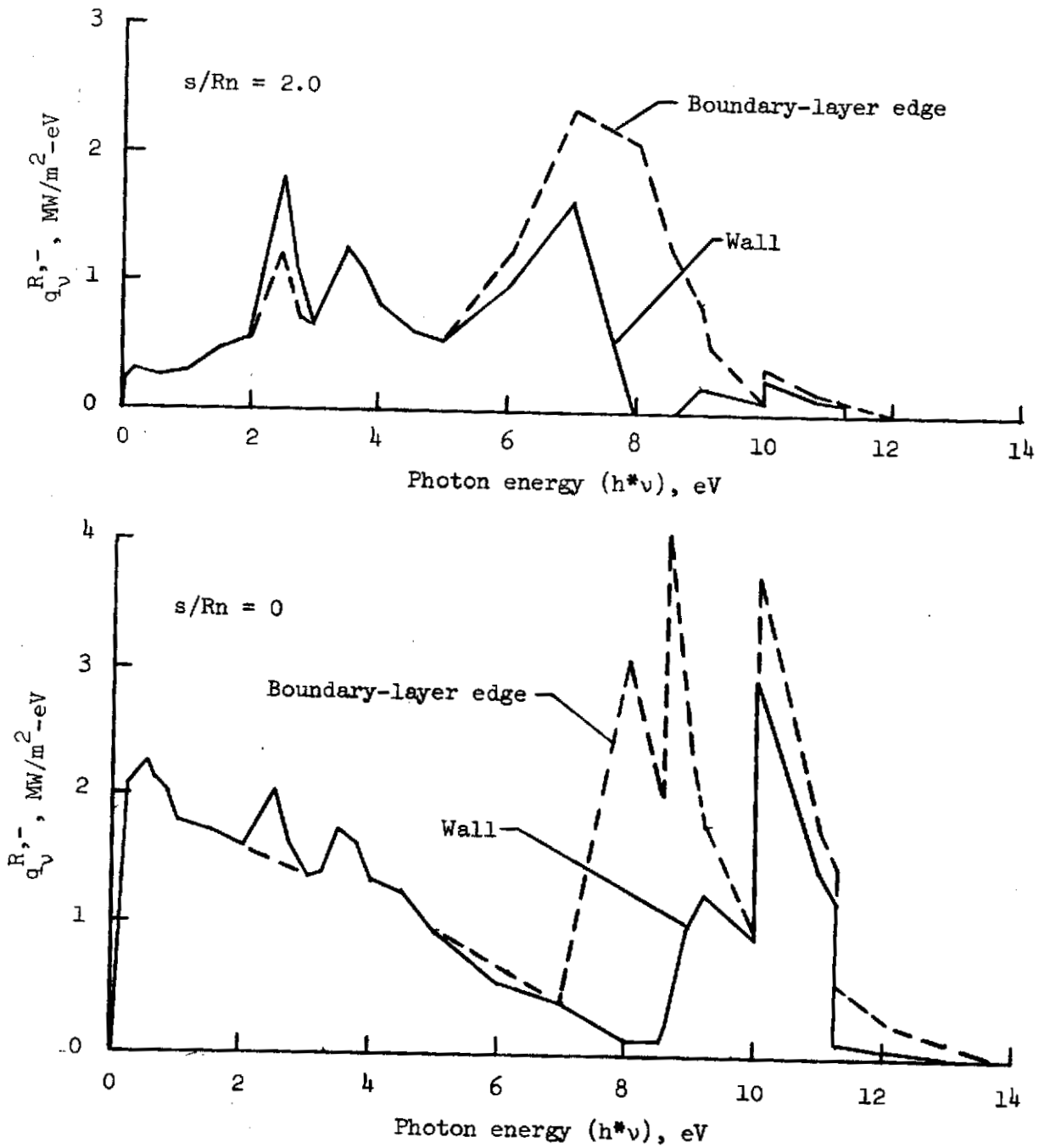

(g) Spectral distribution of radiative heating toward the body due to continuum processes.

Figure 22. - Continued.

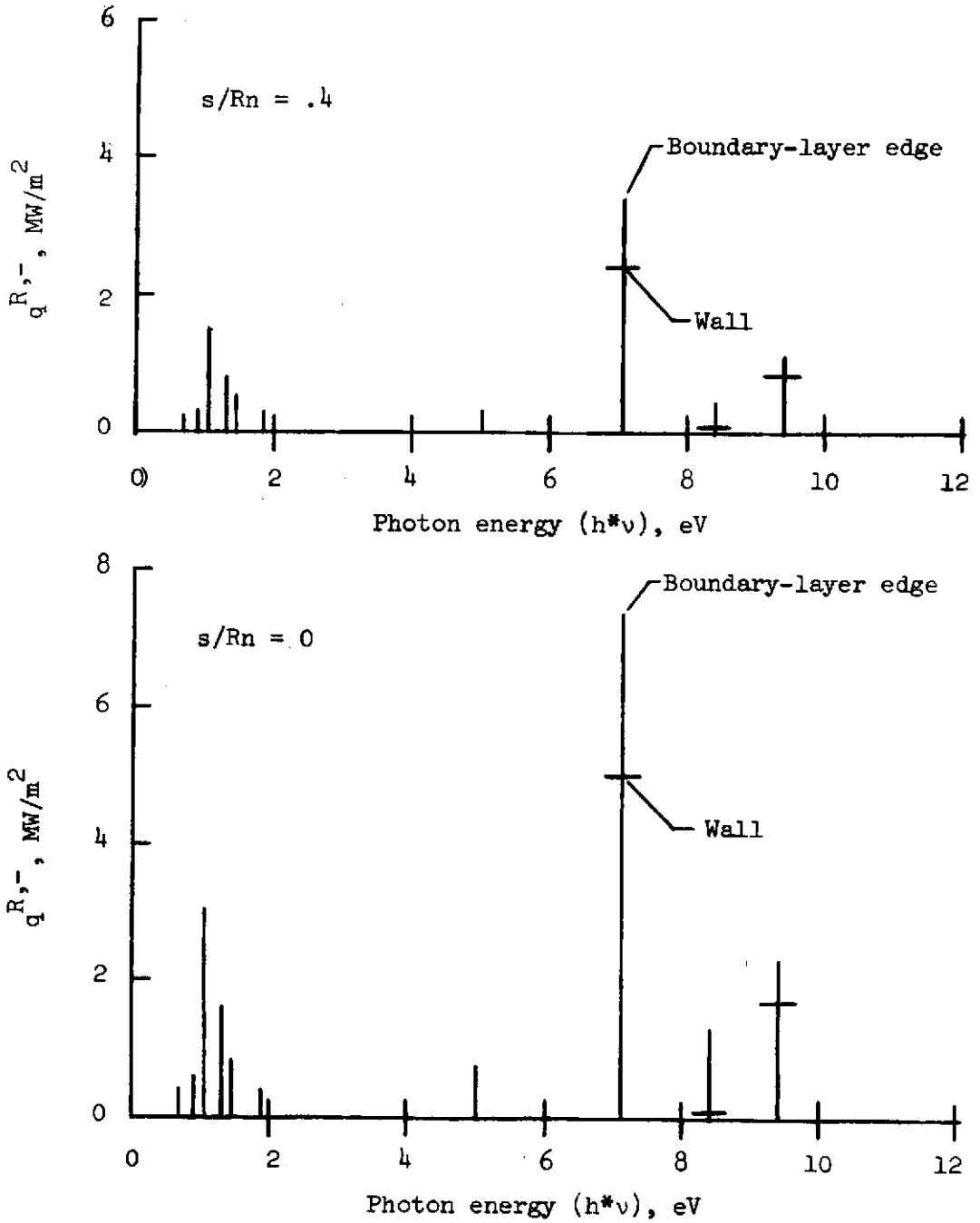

(h) Spectral distribution of radiative heating toward the body due to line processes.

Figure 22. - Concluded.

LIST OF REFERENCES

1. Hirschfelder, Joseph O.; Curtis, Charles F.; and Bird, Byron R. 1964. Molecular Theory of Gases and Liquids. John Wiley and Sons, Inc., New York.

2. Olstad, Walter B. 1971. Nongray Radiating Flow about Smooth Symmetric Bodies. AIAA J., vol. 9, no. 1: 122-130.

3. Callis, Linwood B. 1971. Coupled Nongray Radiating Flows about Long Blunt Bodies. AIAA J., vol. 9, no. 4: 553-559.

4. Page, William A. 1971. Aerodynamic Heating for Probe Vehicles Entering the Outer Planets. AAS Paper No. AAS-71-144.

5. Anderson, John D., Jr. 1969. An Engineering Survey of Radiating Shock Layers. AIAA J., vol. 7, no. 9: 1665-1675.

6. Moretti, Gino; and Abbett, Michael. 1966. A Time-Dependent Computational Method for Blunt Body Flows. AIAA J., vol. 4, no. 12: 2136-2141.

7. Callis, Linwood B. 1969. Solutions of Blunt-Body Stagnation Region Flows with Nongrey Emission and Absorption of Radiation by a Time-Asymptotic Technique. NASA Technical Report, NASA TR R-399.

8. Barlett, Eugene P.; and Kendall, Robert M. 1968. An Analysis of the Coupled Chemically Reacting Boundary Layer and Charring Ablator. Pt. III - Nonsimilar Solution of the Multicomponent Laminar Boundary Layer by an Integral Matrix Method. NASA Contractor Report, NASA CR-1062.

9. Nicolet, W. E. 1970. Advanced Methods for Calculating Radiation Transport in Ablation-Product Contaminated Boundary Layers. NASA Contractor Report, NASA CR-1656.

10. Walberg, Gerald D.; and Sullivan, Edward M. 1970. Ablative Heat Shields for Planetary Entries - A Technology Review. Presented at the ASTM/IES/AIAA Space Simulation Conference, Gaithersburg, Maryland.

11. Allen, H. Julian. 1964. Hypersonic Aerodynamic Problems of the Future, Chap. 1. In Wilbur C. Nelson (ed.). The High Temperature Aspects of Hypersonic Flow. Macmillan Co., New York.

12. Allen, H. Julian; Seiff, Alvin; and Winovich, Warren. 1963. NASA Technical Report, NASA TR R-185.

13. Penner, S. S.; and Olfe, Daniel B. 1968. Radiation and Reentry. Academic Press, New York.

14. Eggers, Alfred J., Jr. 1959. The Possibility of a Safe Landing, Chap. 13. In Howard S. Seifert (ed.), Space Technology. John Wiley and Sons, New York.

15. Lees, Lester. 1959. Recovery Dynamics - Heat Transfer at Hypersonic Speeds in a Planetary Atmosphere, Chap. 12. In Howard S. Seifert (ed.), Space Technology. John Wiley and Sons, New York.

16. Ehricke, Krafft A. 1959. Interplanetary Operations, Chap. 8. In Howard S. Seifert (ed.), Space Technology. John Wiley and Sons, New York.

17. Steg, L.; and Lew, H. 1964. Hypersonic Ablation, Chap. 32. In Wilbur C. Nelson (ed.), The High Temperature Aspects of Hypersonic Flow. Macmillan Co., New York.

18. Kendall, Robert M; Rindal, Roald A.; and Bartlett, Eugene P. 1967. A Multicomponent Boundary Layer Chemically Coupled to an Ablating Surface. AIAA J., vol. 5, no. 6: 1063-1071.

19. Garrett, Lloyd Bernard. 1971. An Implicit Finite Difference Solution to the Viscous Radiating Shock Layer with Strong Blowing. Unpublished Ph.D. Thesis, Department of Mechanical and Aerospace Engineering, North Carolina State University at Raleigh. University Microfilm, Ann Arbor, Michigan.

20. Kennet, H.; and Strack, S. L. 1961. Stagnation Point Radiative Heat Transfer. ARS J., vol. 31, no. 3: 370-372.

21. Koh, J. C. Y. 1962. Radiation From Nonisothermal Gases to the Stagnation Point of a Hypersonic Blunt Body. ARS J., vol. 32, no. 9: 1374-1377.

22. Hoshizaki, H.; and Lasher, L. E. 1968. Convective and Radiative Heat Transfer to an Ablating Body. AIAA J., vol. 6, no. 8: 1441-1449.

23. Chien, Kuei-Yuan. 1971. Application of the S_n Method to Spherically Symmetric Radiative-Transfer Problems. AIAA Paper No. 71-466.

24. Wilson, K. H. 1971. Evaluation of One-Dimensional Approximations for Radiative Transport in Blunt Body Shock Layers. LMSC N-EE-71-3, Lockheed Missiles and Space Co., Sunnyvale, California.

25. Boughner, Robert Eugene. 1969. Theoretical Predictions of Non-Gray Radiant Heat Transfer in High Temperature Nonisothermal CO_2-N_2 Mixtures. Unpublished Ph.D. Thesis, Mechanical Engineering Dept., Purdue University. University Microfilm, Ann Arbor, Michigan.

26. Olstad, Walter B. 1968. Blunt-Body Stagnation-Region Flow with Nongray Radiation Heat Transfer - A Singular Perturbation Solution. NASA Technical Report, NASA TR R-295.

27. Page, William A.; Compton, Dale L.; Borucki, William J.; and Cliffone, Donald L. 1968. Radiative Transport in Inviscid Nonradiabatic Stagnation-Region Shock Layers. AIAA Paper No. 68-784.

28. Smith, G. Louis; Suttles, John T.; Sullivan, Edward M.; and Graves, Randolph A., Jr. 1970. Viscous Radiating Flow Field on an Ablating Body. AIAA Paper No. 70-218.

29. Rigdon, W. S.; Dirling, R. B., Jr.; and Thomas, M. 1970. Stagnation Point Heat Transfer During Hypervelocity,Atmospheric Entry. NASA Contractor Report, NASA CR-1462.

30. Wilson, K. H. 1967. RATRAP - A Radiation Transport. Code. 6-77-67-12, Lockheed Missiles and Space Co., Sunnyvale, California.

31. Thomas, M. 1967. The Spectral Linear Absorption Coefficient of Gases - Computer Program SPECS (H 189). Douglas Report DAC-59135, McDonnell-Douglas Astronautics Co., Western Division, Santa Monica, California.

32. Nicolet, W. E. 1969. User's Manual for the Generalized Radiation Transfer Code (RAD/EQUIL). Aerotherm Report No. UM-69-9, Aerotherm Corp., Mountain View, California.

33. Suttles, John T. 1971. Comparison of the Radiative Flux Profiles and Spectral Detail from Three Detailed Nongrey Radiation Models at Conditions Representative of Hypervelocity Earth Entry. NASA Technical Memorandum, NASA TM X-2447.

34. Vincenti, Walter G.; and Kruger, Charles H., Jr. 1967. Introduction to Physical Gas Dynamics. John Wiley and Sons, New York.

35. Penner, S. S. 1959. Quantitative Molecular Spectroscopy and Gas Emmissivities. Addison-Wesley Publishing Co., Reading, Massachusetts.

36. Wilson, K. H.; and Grief, R. 1968. Radiation Transport in Atomic Plasmas. J. Quant. Spectry. Radiative Transfer, vol. 8, no. 4: 1061-1986.

37. Goulard, R. 1964. Fundamental Equations of Radiation Gas Dynamics, Chap. 27. In Wilbur C. Nelson (ed.), The High Temperature Aspects of Hypersonic Flow. Macmillan Co., New York.

38. Goulard, R.; and Goulard, M. 1960. One-Dimensional Energy Transfer in Radiant Media. Int. J. Heat Mass Transfer, vol. 1: 81-91.

39. Goulard, R.; Boughner, R. E.; Burns, R. K.; and Nelson, H. F. 1968. Radiating Flows During Entry into Planetary Atmospheres. IAF Paper No. RE70.

40. Howe, John T.; and Viegas, John R. 1963. Solutions of the Ionized Radiating Shock Layer, Including Reabsorption and Foreign Species Effects and Stagnation Region Heat Transfer. NASA Technical Report, NASA TR R-159.

41. Hoshizaki, H.; and Wilson, K. H. 1965. Viscous Radiating Shock Layer About a Blunt Body. AIAA J., vol. 3, no. 9: 1614-1622.

42. Hoshizaki, H.; and Wilson, K. H. 1967. Convective and Radiative Heat Transfer During Superorbital Entry. AIAA J., vol. 5, no. 1: 23-35.

43. Chin, Jin H. 1968. Radiation Transport for Stagnation Flows Including the Effect of Lines and Ablation Layer. AIAA Paper No. 68-664.

44. Wilson, K. H. 1970. Massive Blowing Effects on Viscous Radiating, Stagnation-Point Flow. AIAA Paper No. 70-203.

45. Burns, Raymond K.; and Oliver, Calvin C. 1968. Downstream Radiation Flux to Blunt Entry Vehicles. AIAA J., vol. 6, no. 12: 2452-2453.

46. Chou, Y. S. 1971. Locally Nonsimilar Solutions for Radiating Shock Layer about Smooth Axisymmetric Bodies. LMSC N-EE-71-2, Lockheed Missiles and Space Co., Sunnyvale, California.

47. Maslen, S. H. 1964. Inviscid Hypersonic Flow Past Smooth Symmetric Bodies. AIAA J., vol. 2, no. 6: 1055-1061.

48. Tauber, Michael E. 1969. Atmospheric Entry into Jupiter. J. Spacecraft, vol. 6, no. 10: 1103-1109.

49. Tauber, Michael E. 1971. Heat Protection for Atmospheric Entry into Saturn, Uranus, and Neptune. AAS Paper No. AAS-71-145.

50. Tauber, Michael E.; and Wakefield, Roy M. 1970. Heating Environment and Protection during Jupiter Entry. AIAA Paper No. 70-1324.

51. Perry, James C.; and Pasiuk, Lionel. 1966. A Comparison of Solutions to a Blunt Body Problem. AIAA J., vol. 4, no. 8: 1425-1426.

52. Barnwell, Richard W. 1971. A Time-Dependent Method for Calculating Supersonic Angle-of-Attack Flow about Axisymmetric Blunt Bodies with Sharp Shoulders and Smooth Nonaxisymmetric Blunt Bodies. NASA Technical Note, NASA TN D-6283.

53. Bohachevsky, Ihor O.; and Mates, Robert E. 1966. A Direct Method for Calculation of the Flow about an Axisymmetric Blunt Body at Angle of Attack. AIAA J., vol. 4, no. 5: 776-782.

54. VonNeumann, J.; and Richtmyer, R. D. 1950. A Method for the Numerical Calculation of Hydrodynamic Shocks. J. Appl. Phys., vol. 21: 232-237.

55. Lax, Peter D. 1954. Weak Solutions of Nonlinear Hyperbolic Equations and their Numerical Computation. Commun. Pure Appl. Math., vol. VII, no. 1: 159-193.

56. Lax, Peter D.; and Wendroff, Burton. 1964. Difference Schemes for Hyperbolic Equations with High Order of Accuracy. Commun. Pure Appl. Math, vol. XVII, no. 3: 381-398.

57. MacCormack, Robert W. 1969. The Effect of Viscosity in Hypervelocity Impact Cratering. AIAA Paper No. 69-354.

58. MacCormack, Robert W. 1970. Numerical Solution of the Interaction of a Shock Wave with a Laminar Boundary Layer. In Maurice Holt (ed.), Proceedings of the Second International Conference on Numerical Methods in Fluid Dynamics, 151-163. Springer-Verlag, New York.

59. Moretti, Gino; and Abbett, Michael. 1966. A Fast, Direct and Accurate Technique for the Blunt Body Problem. Technical Report No. 583, General Applied Science Laboratories, Westbury, N. Y.

60. Anderson, John D., Jr. 1970. Time-Dependent Solutions of Nonequilibrium Nozzle Flows - A Sequel. AIAA J., vol. 8, no. 12: 2280-2282.

61. National Academy of Sciences. 1970. Venus, Strategy for Exploration. Report of a Study by the Space Science Board. National Academy of Sciences, Washington, D. C.

62. Ames Research Center. 1972. Pioneer Venus. Report of a Study by the Science Steering Group. Ames Research Center, Moffett Field, California.

63. Ainsworth, J. E. 1970. Comprehensive Study of Venus by Means of a Low-Cost Entry-Probe and Orbiter Mission-Series. Report X-625-70-203, Goddard Space Flight Center, Greenbelt, Maryland.

64. Marcotte, Paul G. 1971. Planetary Explorer, Phase A Report and Universal Bus Description. Goddard Space Flight Center, Greenbelt, Maryland.

65. Jaworski, W.; and Nagler, R. G. 1970. A Parametric Analysis of Venus Entry Heat-Shield Requirements. Technical Report 32-1468, Jet Propulsion Laboratory, Pasadena, California.

66. Nagler, Robert G. 1970. A Systematic Review of Heat-Shield Technology for Extraterrestrial Atmospheric Entry. Technical Report 32-1436, Jet Propulsion Laboratory, Pasadena, California.

67. Norman, Herbert C.; and Hart, Paul M. 1968. Mission Influence on the Aerothermodynamic Environment for a Venus Entry Vehicle. AAS Paper No. 68-4-6.

68. Strauss, Eric L.; and Sparhawk, H. E. 1968. Ablative Heat Shields for Planetary Entry Vehicles. AAS Paper No. 68-8-5.

69. Spiegel, Joseph M.; Wolf, Fred; and Zeh, Dale W. 1968. Simulation of Venus Atmospheric Entry by Earth Re-Entry. AIAA Paper No. 68-1148.

70. Anon. 1968. Models of Venus Atmosphere (1968). NASA Special Publication, NASA SP-8011.

71. Deacon, H. J., Jr.; and Rumpel, W. F. 1971. Radiative Transfer Properties of a Shocked Venus Model Atmosphere. J. Spacecraft, vol. 8, no. 2: 177-182.

72. Livingston, F. R.; and Williard, J. 1971. Planetary Entry Body Heating Rate Measurements in Air and Venus Atmospheric Gas up to T=15,000 K. AIAA J., vol. 9, no. 3: 485-492.

73. Falanga, Ralph A.; and Sullivan, Edward M. 1970. An Inverse-Method Solution for Radiating, Nonadiabatic, Equilibrium Inviscid Flow over a Blunt Body. NASA Technical Report, NASA TN D-5907.

74. Hughes, William F.; and Gaylord, Eder W. 1964. Basic Equations of Engineering Science. Schaum Publishing Company, New York.

75. Isaacson, Eugene; and Keller, Herbert Bishop. 1966. Analysis of Numerical Methods. John Wiley and Sons, New York.

76. Inouye, Mamoru. 1965. Blunt Body Solutions for Spheres and Ellipsoids in Equilibrium Gas Mixtures. NASA Technical Note, NASA TN D-2780.

77. Graves, Randolph A., Jr. 1970. Diffusion Model Study in Chemically Reacting Air Couette Flow with Hydrogen Injection. NASA Technical Note, NASA TR R-349.

78. Kendall, Robert M.; and Bartlett, Eugene P. 1968. Nonsimilar Solution of the Multicomponent Laminar Boundary Layer by an Integral-Matrix Method. AIAA J., vol. 6, no. 6: 1089-1097.

79. Kendall, Robert M; Anderson, Larry W.; and Aungier, Ronald H. 1972. Nonsimilar Solution for Laminar and Turbulent Boundary-Layer Flows over Ablating Surfaces. AIAA J., vol. 10, no. 9: 1230-1236.

80. Kendall, Robert M. 1968. A General Approach to the Thermochemical Solution of Mixed Equilibrium-Nonequilibrium, Homogeneous or Heterogeneous Systems. Pt. V - An Analysis of the Coupled Chemically Reacting Boundary Layer and Charring Ablator. NASA Contractor Report, NASA CR-1064.

81. Bartlett, Eugene P.; Kendall, Robert M; and Rindal, Roald A. 1968. A Unified Approximation for Mixture Transport Properties for Multicomponent Boundary-Layer Applications. Pt. IV - An Analysis of the Coupled Chemically Reacting Boundary Layer and Charring Ablator. NASA Contractor Report, NASA CR-1063.

82. Grose, Ronald D.; and Kendall, Robert M. 1970. A Nonsimilar Solution for Laminar and Turbulent Boundary Layer Flows Including Entropy Layers and Transverse Curvature. NASA Contractor Report, NASA CR-73481.

83. Anderson, Larry W.; and Kendall, Robert M. 1970. A Nonsimilar Solution for Multicomponent Reacting Laminar and Turbulent Boundary Layer Flows Including Transverse Curvature. Technical Report No. AFWL-TR-69-106, Air Force Weapons Laboratory, Kirtland AFB, New Mexico.

84. Anderson, Larry W.; Bartlett, Eugene P.;and Kendall, Robert M. 1970. User's Manual - Volume I - Boundary Layer Integral Matrix Procedure (BLIMP). Technical Report No. AFWL-TR-69-114, Vol. I. Air Force Weapons Laboratory, Kirtland AFB, New Mexico.

85. Anderson, Larry W.; and Kendall, Robert M. 1970. User's Manual - Volume II - Boundary Layer Integral Matrix Procedure (BLIMP). Technical Report No. AFWL-TR-69-114, Vol. II. Air Force Weapons Laboratory, Kirtland AFB, New Mexico.

86. Anderson, Larry W.; and Morse, Howard L. 1971. User's Manual - Volume I - Boundary Layer Integral Matrix Procedure (BLIMP). Technical Report No. AFWL-TR-69-114. Vol. I (Supp.). Air Force Weapons Laboratory, Kirtland AFB, New Mexico.

87. Moyer, Carl B.; and Rindal, Roald A. 1968. Finite Difference Solution for the In-Depth Response of Charring Materials Considering Surface Chemical and Energy Balances. Pt. II - An Analysis of the Coupled Chemically Reacting Boundary Layer and Charring Ablator. NASA Contractor Report, NASA CR-1061.

88. Inouye, Mamoru; Rakich, John V.; and Lomax, Harvard. 1965. A Description of Numerical Methods and Computer Programs for Two-Dimensional and Axisymmetric Supersonic Flow Over Blunt-Nosed and Flared Bodies. NASA Technical Note, NASA TN D-2970.

89. Suttles, John T. 1969. A Method of Integral Relations Solution for Radiating, Nonadiabatic, Inviscid Flow over a Blunt Body. NASA Technical Note, NASA TN D-5480.

APPENDIX A

UNSTEADY CHARACTERISTICS SOLUTION

A quasi, one-dimensional unsteady characteristics solution is used for the shock points in the radiating, inviscid flow field solution. The present method for this solution is similar to the methods given by Callis (ref. 7) and by Moretti and Abbett (ref. 6). A brief development of the equations is given below and further details are available in the above mentioned reports.

In the analysis, the pertinent quantities considered are the normal component of the velocity and the Y-coordinate. Since the tangential velocity is unchanged across a shock wave, the tangential velocity is not considered a pertinent quantity and the S-momentum equation is neglected. Consequentially, the equations for mass, Y-momentum, and energy are considered as quasi, one-dimensional equations modified by forcing terms on the RHS of the equations. The forcing terms are the terms in the equations which do not contain derivatives, which contain derivatives with respect to the S-coordinate, and which contain the tangential velocity.

The mass equation (eq. 17) is written as

$$\rho^*_T + A\rho^*_Y + \frac{1}{\delta} v_Y = C_1 \tag{A1}$$

where the asterisk refers to the natural logarithm of ρ that is differentiated. The Y-momentum equation (eq. 19) is written as

$$v_T + Av_Y + \frac{1}{\rho\delta} p_Y = C_2 \tag{A2}$$

In the inviscid flow field analysis, the mass equation in terms of density and the energy equation in terms of enthalpy were combined to form a new equation in terms of pressure. This combined equation replaced the mass equation; however, in the characteristics development, the combined equation is used for the energy equation. Thus, the energy equation (eq. 30) is written as

$$p_T + Ap_Y + \frac{\rho P_3}{\delta} v_Y = C_3 \tag{A3}$$

The forcing terms are

$$C_1 = -\left(\frac{u}{\lambda} \rho_S^* - \frac{B}{\rho} u_Y + \frac{1}{\lambda} u_S + \frac{C}{\rho}\right) \tag{A4}$$

$$C_2 = -\left(\frac{u}{\lambda} v_S - E\right) \tag{A5}$$

$$C_3 = -\left[\frac{u}{\lambda} p_S + P_3 \left(\frac{\rho}{\lambda} u_S + C\right) - \frac{F^R}{P_1 \rho} - P_3 B u_Y\right] \tag{A6}$$

The forcing terms are considered as known quantities and the characteristics equations and the compatibility equations are solved for by standard procedure.

The differential relations for the variables ρ, p, and v of the independent variables Y and T are

$$\rho_T^* \, dT + \rho_Y^* \, dY = d\rho^* \tag{A7}$$

$$v_T \, dT + v_Y \, dY = dv \tag{A8}$$

$$p_T \, dT + p_Y \, dY = dp \tag{A9}$$

The equations A1 to A3 and A7 to A9 written in matrix form are

$$\begin{vmatrix} \rho_T^* \\ \rho_Y^* \\ v_T \\ v_Y \\ p_T \\ p_Y \end{vmatrix} \times \begin{vmatrix} dT & dY & 0 & 0 & 0 & 0 \\ 0 & 0 & dT & dY & 0 & 0 \\ 0 & 0 & 0 & 0 & dT & dY \\ 1 & A & 0 & \frac{1}{\delta} & 0 & 0 \\ 0 & 0 & v_T & A & 0 & \frac{1}{\rho\delta} \\ 0 & 0 & 0 & \frac{\rho P_3}{\delta} & 1 & A \end{vmatrix} = \begin{vmatrix} d\rho^* \\ dv \\ dp \\ C_1 \\ C_2 \\ C_3 \end{vmatrix} \tag{A10}$$

The characteristics equations are found by setting the associated coefficient determinant equal to zero.

$$\begin{vmatrix} dT & dY & 0 & 0 & 0 & 0 \\ 0 & 0 & dT & dY & 0 & 0 \\ 0 & 0 & 0 & 0 & dT & dY \\ 1 & A & 0 & \frac{1}{\delta} & 0 & 0 \\ 0 & 0 & v_T & A & 0 & \frac{1}{\rho\delta} \\ 0 & 0 & 0 & \frac{\rho P_3}{\delta} & 1 & A \end{vmatrix} = 0 \tag{A11}$$

The solution of equation A11 is a cubic in dY/dT and the characteristics equations are

$$\frac{dY}{dT} = A \tag{A12}$$

$$\frac{dY}{dT} = A \pm \frac{\sqrt{P_3}}{\delta} \tag{A13}$$

Equation A12 is a trivial solution and is neglected. The compatibility equations are found by substituting a column of the associated coefficient determinant by the RHS of equation A10 and the determinant is set

equal to zero.

$$\begin{vmatrix} dT & dY & 0 & d\rho^* & 0 & 0 \\ 0 & 0 & dT & dv & 0 & 0 \\ 0 & 0 & 0 & dp & dT & dY \\ 1 & A & 0 & C_1 & 0 & 0 \\ 0 & 0 & v_T & C_2 & 0 & \frac{1}{\rho\delta} \\ 0 & 0 & 0 & C_3 & 1 & A \end{vmatrix} = 0 \qquad \text{(A14)}$$

The solution of equation A14 is

$$\left(\frac{dY}{dT} - A\right)\frac{dv}{dT} + \frac{1}{\rho\delta}\frac{dp}{dT} = \left(\frac{dY}{dT} - A\right)C_2 + \frac{C_3}{\rho\delta} \qquad \text{(A15)}$$

and substituting for $\frac{dY}{dT}$ from equation A13, the compatibility equations are

$$\frac{dv}{dT} \pm \frac{1}{\rho\sqrt{P_3}}\frac{dp}{dT} = C_2 \pm \frac{C_3}{\rho\sqrt{P_3}} \qquad \text{(A16)}$$

From equations A13 and A16, the right running characteristic is used in the solution for the shock points and the equations are

$$\frac{dY}{dT} = A + \frac{\sqrt{P_3}}{\delta} \qquad \text{(A17)}$$

$$\frac{dv}{dT} + \frac{1}{\rho\sqrt{P_3}}\frac{dp}{dT} = C_2 + \frac{C_3}{\rho\sqrt{P_3}} \qquad \text{(A18)}$$

APPENDIX B

STAGNATION-POINT SOLUTION FOR RADIATING, INVISCID FLOW FIELD

The equations for the radiating, inviscid flow field around an axisymmetric blunt body are reduced so that they are applicable for only a stagnation-point solution. Note, the equations presented in this section are not used for the stagnation point of the complete body solution but are used in a separate program when only a stagnation-point solution is required.

The following conditions, from symmetry of the body, exist at the stagnation line.

$$\left.\begin{array}{lll} u = 0 & v_S = 0 & \beta = 0 \\ u_Y = 0 & h_S = 0 & \theta = \pi/2 \\ \rho_S = 0 & p_S = 0 & K = 1 \end{array}\right\} \tag{B1}$$

With these conditions, the equations for mass, Y-momentum, and energy (eqs. 30, 19, and 20) become

mass:

$$p_T = -\left[Ap_Y + P_3\left(\frac{2\rho}{\lambda}u_S + \frac{\rho}{\lambda}v_Y + \frac{2\rho v}{\lambda}\right) - \frac{F^R}{P_1\rho}\right] \tag{B2}$$

Y-momentum:

$$v_T = -\left(Av_Y + \frac{1}{\rho\delta}p_Y\right) \tag{B3}$$

energy:

$$h_T = -\left(Ah_Y - \frac{1}{\rho}p_T - \frac{A}{\rho}p_Y + \frac{F^R}{\rho}\right) \tag{B4}$$

The equation for S-momentum (eq. 18) is degenerate at the stagnation line; but, by differentiation of equation 18 with respect to S and applying the symmetry conditions the following equation is obtained

S-momentum:

$$u_{ST} = -\left(Au_{SY} + \frac{1}{\lambda} u_S^2 + \frac{v}{\lambda} u_S + \frac{1}{\rho\lambda} p_{SS}\right) \tag{B5}$$

The S derivative of the tangential velocity, u_S, is used in the stagnation-point solution rather than the tangential velocity. The parameters in the equations are

$$A = \frac{v}{\delta} - \frac{Y}{\delta} \delta_T \tag{B6}$$

$$F^R = \frac{1}{\delta} q_Y^R + \frac{2}{\lambda} q^R \tag{B7}$$

$$\lambda = 1 + \delta Y \tag{B8}$$

In order to solve the set of equation an expression is needed for p_{SS}. An approximation for this parameter is taken from Newtonian theory

$$p_{SS} = -2 \tag{B9}$$

The characteristic equation and the compatibility equation for the unsteady characteristic solution at the shock location become

$$\frac{dY}{dT} = A + \frac{\sqrt{P_3}}{\delta} \tag{B10}$$

$$\frac{dv}{dT} + \frac{1}{\rho\sqrt{P_3}} \frac{dp}{dT} = \frac{C_3}{\rho\sqrt{P_3}} \tag{B11}$$

where

$$C_3 = -\left[\frac{2\rho}{\lambda} P_3 (u_S + v) - \frac{F^R}{P_1\rho}\right] \tag{B12}$$

The equations presented in this section are non-dimensionalized by the expression given in equation 14. Indeterminate terms were evaluated by the L'Hospital rule.

APPENDIX C

COMPUTER PROGRAM FOR RADIATING, INVISCID FLOW FIELD SOLUTION

A program listing and a description of inputs are given for the computer program developed for the radiating, inviscid flow field solution. The program is written in FORTRAN IV language for CDC 6000 series computers. In order to run the program, all variables have to be initially set to zero by means external to the program. A system subroutine called by a SETCORE control card is used for this external initialization for the computer system used in the present study.

The inputs and printed outputs for a sample case are also given. The sample case is a radiating solution for a .97 CO_2 - .03 N_2 (by volume) gas composition. The body shape is a hemispherical nose, .3048 meter radius, with a 60° half-angle, conical afterbody.

PROGRAM LISTING

```
      PROGRAM  SUTFLO(INPUT,OUTPUT,TAPE5=INPUT,TAPE6=OUTPUT,PUNCH)
      REAL K
      COMMON/SUT2/    Y(11),S(15),K(15),THETA(15),BETA(15),RB(15),
     1DELTA(15),DELTAY(15),XB(15)
      COMMON/SUT3/   XMOI(15,11),UI(15,11),VI(15,11),PI(15,11),HI(15,11),
     1T(15,11),SX(15,11),VA(15,11),VAMI(15,11),PI(15,11),HHI(15,11),
     2TAUI(15,11)
      COMMON/SUT4/ RHOBE(15,11),UBE(15,11),VBT(15,11),PBE(15,11),
     1HBI(15,11),DELS1(15),DELS2(15),DELS3(15),DELS4(15),DELS5(15),
     2DELY1(11),DELY2(11),DELY3(11),DELY4(11),DELY5(11)
      DIMENSION DELY6(11),DELYT(11),DELYB(11)
      DIMENSION DELS4(15),DELST(15),DELSB(15)
      COMMON/SUT5/ RHOT(15,11),UT(15,11),VT(15,11),PT(15,11),HT(15,11)
      COMMON/SUT6/   DP(15,11),UHI(15,11),QHI(15,11),QDI(15,11)
     1                ,QWT(15),QWC(15),QWL(15)
      COMMON/SUT7/ VEL2(15),SA22(15)
      COMMON/RAD/AHY900,AHVLE(25),SKEP(45)          ,DELTR,GPSI(56),PPI900),
     1PHYI299,PHYCI501,PHMM(25),PHPP(25),PEMI(11),PIPI(11),PLI,PL2,PLO,
     2FLGI,GAMP(300),GEE(561,41),(40),RZII4),WAFS,WBLP,ND1300),MTC,NICMI11
     3),MIMYC,*MIY,MJI59),MY,PAES(111),TPE(11),WOLI(1),XMOL,XDT,111,TDELT
     4,YY(11),CASE(5),TMSWE(501,TMSWL(25) ,TW
      COMMON/LINE/HVL(500),R1,R2,YLCH(11),YLCP(11),KMM(8,11),MRF,TA(99)
     1,M1,XMOL(300) ,QUP(900)
      COMMON/RADCOR/PRE(18,11),TT(11),VM(11),HHE(11),SP(1,11,8)
     1                ,THETR,SV1,SP1,SR1,MSS
      COMMON/INTCOR/KR(20),M,N
      COMMON/EQPCOR/PSC(1( 63),(SC(063),PSC2(24),(SC(186,15,
     1              (BC2(42)      ,PSC3) 249)   ,(PSC3(669),
     2              (SC5(N),PSC4,(SC4,PSC5( 945),(SP2,PARDA(31),FAMDB(51)
     3              ,ESP,*ICX,PSC6(3),*IN,KOUT,K4A(20),PSCF( 81
      COMMON/SUTCOM/TKS,PRS,WRKS,HFPKS,SIPKS,RHKS,CPPKS,CSPKS,ALPKS,
     1BETHKS,GAMKS,VEL,SA2,KYS
      DIMENSION GF(11)
      DIMENSION XQS(10)
      DIMENSION CCE(3,5)
      DIMENSION CHE(3,3)
      DIMENSION IKSUI(0),ITCUE(5),IRCUE(5)
      DIMENSION YAUMS(15)
      NAMELIST/NAME1/ MF,PF,RMOF,HF,RN,KYS,KSE,Y
      NAMELIST/NAME2/ TIPRAC,TKSC,CC1,CCF,ICC,IKSP,(OUTPN,(OUTF,(YC,(RC,
     1IKSU,(TCU,IRCU,NCTS,LSC,CC1
      READ(5,9401 KQS(10,KQS(2),KQS(3),KOS(6),<OS(9),CASE
  940 FORMAT(5(1,15A5)
      WORAD = KQS(3)
      MDEL = KQS(2)
      READ(5,NAME1)
      READ(5,911) (THETA(KS),SI(KS),RB(KS),RB(KS),K(KS), KS=1,KSE)
  911 FORMAT(5F15.7)
      LS = -1
      LSC = 1900
      CCS = .0005
      TIPRAC = .8
      IKSC=900
      CC1 = .0001
      CCF = .95
      ICC = 90
      IKSP = 1900
      TOUTN = 100
      TOUTP = 99
      ITC = 50
      IRC = 100
      IKSUI(1 = 100
      IKSU(2) = 200
      IKSU(3) = 400
      IKSU(4) = 600
      IKSU(5) = 800
      ITCUE(1) =ITC
      ITCUE(2) =ITC
      ITCUE(3) =ITC
      ITCUE(4) =ITC
      ITCUE(5) =ITC
      IRCUE(1) = IRC
      IRCUE(2) = IRC
      IRCUE(3) = IRC
      IRCUE(4) = IPC
      IRCUE(5) = IPC
      NCTS = 0
      IF(KQS(1).EQ.0)  GO TO 4
      READ(5,NAME2)
    4 CONTINUE
      IKSUE0 = IKSP
      RFADI5,9905) (KS,TAUT,ITI,TRI,TO,J9
      (F(IKS,EQ.0)  GO TO 9901
      READ(5,9906) (BETA(KS), KS=1,KSE)
      READ(5,9906) (DELTA(KS), KS=1,KSE)
      READ(5,9906) (DELTAT(KS), KS=1,KSE)
      DO 9945  KS=1,KSE
      DO 9945  KY=1,KYS
      READ(5,9906) PIKS,KY),RHOIKS,KY),HCKS,KY),UIKS,KY),VEKS,KY),
     1VA(KS,KY),PEIKS,KY),QDERS,KY)
 9945 CONTINUE
 9905 FORMAT(I9,E13.8,I9,I9,E14.8,I9)
 9906 FORMAT(5E15.8)
      IF(MDEL.EQ.0) GO TO 9991
      CI = ABS(DELTAT(1))
      IF(IKS.GE.LSC.AND.CI.LE.CCS)  LS=0
 9991 CONTINUE
      KYS1=KYS-1
      KSE1 = KSE-1
      KYC = KYS/2
      XCC1 = 3.*KSE
      IOUT = IOUTP
      TC = 0
      CALL INPUT
      IF(NORAD.EQ.0)  GO TO 11
      NY = KYS
      NI = NY
      NIC = NY
      DO 03   I=1,NY
      NICNE(I) = I
      YYE(I) = Y(I)
   03 CONTINUE
      DO 3  I=1,20
      KR(I) = 0
    3 CONTINUE
      KR(3) = 1
      KR(5) = KOS(4)
      KR(6) = -KOS(9)
      KR(7) = 1
      KR(11) = 1
      KR(12) = 1
      CALL RADIN
   11 CONTINUE
      SV1 = VF/.3048
      SP1 = PF/101325.
      SR1 = RMOF/16.018463
      HSS = HF*(1.8/4184.)
      WRITE(6,900) CASE
  900 FORMAT(1H1,///2X,4CASE - ,15A5)
      WRITE(6,955) VF,RMOF,PF,HF,RN
  955 FORMAT(///2X,*FREESTREAM PARAMETERS*,5X,*VELOCITY = *,E11.4,1X,
     1*M/S*,/20X,*DENSITY = *,E11.4,1X,*KG/M3*,/20X,*PRESSURE = *,
     2E11.4,1X,*N/M2*,/20X,*ENTHALPY = *,E11.4,1X,*J/KG*,/20X,*NOSE RADI
     3US = *,E11.4,1X,*M*,)
      WRITE(6,956)
  956 FORMAT(///2X,*BODY SHAPE, NONDIMENSIONAL BY NOSE RADIUS*,
     1                    /10X,*K*,5X,6X,*S*,9X,*RBODY*,7X,*YBODY*,
     2/2X,*THETA*,7X,*K*)
      WRITE(6,957) (KS,SI(KS),RB(KS),RB(KS),THETA(KS),K(KS), KS=1,KSE)
  957 FORMAT(10X,E2.3X,F8.6,3X,F8.4,3X,F8.4,3X,F8.4,3X,F8.4)
      DO 5  I=1,10
      KQS(I)=0
    5 CONTINUE
      KQS(1)=1
      KQS(2)=1
      KQS(3)=KQS(2)
      DELS1(1) = SI2I-SI(1)
      DELS2(1) = DELS(1)
      DELS3(1) = 1.
      DELS4(1) = 1.
      DELS5(1) = 1./DELS2(1)
      DELS1(KSE) = SIKSE)-SI(KSE1)
      DELS2(KSE) = DELS1(KSE)
      DELS3(KSE) = 1.
      DELS4(KSE) = 1.
      DELS5(KSE) = 1./DELS1(KSE)
      DO 81   KS=2,KSE1
      DELS1(KS) = SIKS+1)-SI(KS)
      DELS2(KS) = SI(KS)-SI(KS-1)
      DELS3(KS) = (DELS1(KS)*DELS1(KS))/(DELS2(KS)*DELS2(KS))
      DELS4(KS) = DELS3(KS)-1.
      DELS5(KS) = 1./(DELS1(KS)+(DELS3(KS)*DELS2(KS)))
   81 CONTINUE
      DELY1(1) = Y(2)-Y(1)
      DELY2(1) = DELY1(1)
      DELY5(1) = 1.
      DELY4(1) = 1.
      DELY6(1) = 1./DELY1(1)
      DELY1(KYS) = Y(KYS)-Y(KYS1)
      DELY2(KYS) = DELY1(KYS)
      DELY3(KYS) = 1.
      DELY4(KYS) = 1.
      DELY5(KYS) = 1./DELY1(KYS)
      DO 40  KY=2,KYS1
      DELY1(KY) = Y(KY+1)-Y(KY)
      DELY2(KY) = Y(KY)-Y(KY-1)
      DELY3(KY) = (DELY1(KY)*DELY1(KY))/(DELY2(KY)*DELY2(KY))
      DELY4(KY) = DELY3(KY)-1.
      DELY5(KY) = 1./(DELY1(KY)+(DELY3(KY)*DELY2(KY)))
   40 CONTINUE
      DO 86  KY=1,KYS
      IF(KY.GE.KYS1) GO TO 87
      G1 = DELY1(KY) + DELY1(KY+1)
      DELY6(KY) = (G1*G1)/(DELY1(KY)*DELY1(KY))
      DELY7(KY) = DELY6(KY) - 1.
      DELY8(KY) = 1./(G1-(DELY6(KY)*DELY1(KY)))
      GO TO 86
   87 CONTINUE
      G1 = DELY2(KY) + DELY2(KY-1)
      DELY6(KY) = (G1*G1)/(DELY2(KY)*DELY2(KY))
      DELY7(KY) = DELY6(KY) - 1.
      DELY8(KY) = 1./(G1-(DELY6(KY)*DELY2(KY)))
   86 CONTINUE
      DO 89  KS=1,KSE
      IF(KS.GT.2) GO TO 88
      G1 = DELS1(KS) + DELS1(KS+1)
      DELS6(KS) = (G1*G1)/(DELS1(KS)*DELS1(KS))
      DELS7(KS) = DELS6(KS) - 1.
      DELS8(KS) = 1./(G1-(DELS6(KS)*DELS1(KS)))
      GO TO 89
   88 CONTINUE
      G1 = DELS2(KS) + DELS2(KS-1)
      DELS6(KS) = (G1*G1)/(DELS2(KS)*DELS2(KS))
      DELS7(KS) = DELS6(KS) - 1.
      DELS8(KS) = 1./(G1-(DELS6(KS)*DELS2(KS)))
   89 CONTINUE
      IF(KS.NE.0)  GO TO 9992
      IT1 = 0
      IP1 = 0
      KS = 0
      TAUT = 0.
      J9 = 1
      DO 13  KS=1,KSE
      KQS(5)=1
      IF(KS-1) 14,14,15
   14 THETR=0.
      DPPA(1) = 0.
      TT(1)=1.8000.
      PPES(1)=1.0
      CALL EQUILIBQS,1,PRES(1)
      VEL2(1) = VEL*.3048/VF
      SA22(1) = SA2
      RHOTE(KY5) = (RHKRS*16.018463)/RMOF
      DPLTA(1) = 0.78/RMOE1.KYS)
      TO=TRS
      HE1,KYS) = (HEPRS*6186.)/(VF*VF)
      P(1,KY5) = (PRS*101325.)/(RMOF*VF*VF)
      VE1,KY5) = -VEL*COS(SA2)*.3048/VF
      UE1,KY5) = 0.
      HC1,1) = HE1,KY5) + (VE1,KY5)*VE1,KY5)/2.)
      P11,1) = P41,KY5) + (RMOE1.KY5)*VE1,KY5)*VE1,KY5)/2.)
      UE1,1) = 0.
      VI1,1) = 0.
      GO TO 16
   15 TT(1) = 1.8*TKS
      PPES(1) =PKS
      THETR = 1.5707963 - THETA(KS)
      CALL EQUILIBQS,1,PRES(1))
      VEL2(KS) = VEL*.3048/VF
      SA22(KS) = SA2
      HEKS,KY5) = (HEPRS*6186.)/(VF*VF)
      PEKS,KY5) = (PRS*101325.)/(RMOF*VF*VF)
      VEKS,KY5) = -VEL*COS(SA2)*.3048/VF
      UEKS,KY5) = VEL*SIN(SA2)*.3048/VF
      P(KS,1) = P(E,1)*COS(THETR)*COS(THETR)
      HCKS,1) = HCNS-1,1)*(P(EKS,1)/P(KS-1,1))**GAMRA)
      UEKS,1) = SQRT(2.0*(HE1,1)-HEKS,1))
      VEKS,1) = 0.
   16 CONTINUE
      KQS(9)= 0
```

```
      DO 18 KY=1,KYS
      P(KS,KY) = P(KS,1) + (1P(KS,KYS)-P(KS,1))*Y(KY)
      H(KS,KY) = H(KS,1) + (1H(KS,KYS)-H(KS,1))*Y(KY)
      U(KS,KY) = U(KS,1) + (1U(KS,KYS)-U(KS,1))*Y(KY)
      V(KS,KY) = V(KS,KYS)*Y(KY)
      VH(KY) = (H(KS,KY)*VF*VF/2324.6666
      PRES(KY) = (P(KS,KY)*RHOF*VF*VF)/101325.
      CALL EQUIL(RQS,KY,PRES(KY))
      IF(KY.EQ.1)  GAMA=(GAMK-1.)/GAMK$
      HH(KY) = 1.8*HP(KS
      TE(KY) = TK$
      RHO(KS,KY) = (RHRKSP16.0184A3)/RHOF
      T(KS,KY)   =  TKS/TO
      SR(KS,KY)  = (SIRKS*A186.    1*( TO/1VF*VF)
      VA(KS,KY)  =  SQRT(1831.4*GAMA$P(KS/WRKS)/VF
      WR(KS,KY)  = WRKS
      G3 = (UTKS,KY)*UU(KS,KY))+(V(KS,KY)*VV(KS,KY))
      VAM(KS,KY) =  SQRT(G3)/VA(KS,KY)
      G3 = (TKS*CSPKSP*4184.1/(VF*VF)
      PL(KS,KY)= G3/( RHO(KS,KY)*VA (KS,KY)*VA (KS,KY)*1A(LFRS- 1.3)
   18 CONTINUE
      IF(KS,EQ.1) GO TO 23
      C2 = RB(KS) + (DELTA(KS)*COS(THETA(KS)))
      C1 = RB(KS)*RHO(KS,1)*U(KS,1)
      C2 = C2*RHO(KS,KYS)*U(KS,KYS)
      C1 = (C1 + C2)/2.
      C2 = (C1 - (RB(KS)*COS(THETA(KS))))**2.
      DEL TA(KS) = RB(KS)*RB(KS)/C2
   23 CONTINUE
      DELTA(KS) = 0.
      IF(NOPAD.EQ.0) GO TO 11
      DELTR = DELTA(KS$*RN*100.
      CALL RADICAL
      DNC(KS) = (P(KE(1)*10000.1/(RHOF*VF*VF*VF)
      DNL(KS) = (TL(PE(1)*10000.1/(RHOF*VF*VF*VF)
      DNT(KS) = DNC(KS) + DNL(KS)
      DO 19 KY=1,KYS
      DP(KS,KY)=(DP(KE(KY)+TL(KE(KY))*10000.)/(RHOF*VF*VF*VF)
      DN(KS,KY)=(DP(PE(KY)+TL(PE(KY))*10000.1/(RHOF*VF*VF*VF*VF
      DN(KS,KY)=  DP(KS,KY)-DN(KS,KY)
   19 CONTINUE
      DD(KS,1) = (DN(KS,2)-DN(KS,1))/DEL Y(1)
      DD(KS,KYS) = (DN(KS,KYS)-DN(KS,KYS-1))/DELY2(KYS)
      DO 20  KY=2,KYS1
      DD(KS,KY) = (DN(KS,KY+1)+(C)EL Y4(KY)*DN(KS,KY))-(DELY5(KY)*DN(KS,
     1KY-1))*DELY5(KY)
   20 CONTINUE
      IF(KS.GT.1) GO TO 24
      DO 27  KY=1,KYS
      G1 = R11/(1.0+(R11)*Y(KY)*DELTA(1))
      DN(1,KY) = (DD(1,KY)/DELTA(1)) + (2.*G1*DN(1,KY))
   27 CONTINUE
      GO TO 25
   24 CONTINUE
      S2 = COS(THETA(KS))
      DO 22   KY=1,KYS
      R = RB(KS) + (Y(KY)*G2)
      G1 = K(KS)/(1.0+(K(KS)*Y(KY)*DELTA(KS)))
      DN(KS,KY) = (DD(KS,KY)/DELTA(KS)) + ((G1*(G2/R))*DN(KS,KY))
   22 CONTINUE
   25 CONTINUE
   11 CONTINUE
      DO 26  KS=2,KSFL
      G1 = 1.0 + (K(KS)*DELTA(KS))
      S1 =(DELTA(KS+1) *(DEL(S4(KS)*DELTA(KS)) -(DELS3(KS)*DELTA(KS-1)))*
     1DELS5(KS)
   26 BETA(KS) = ATAN(S1/G1)
      G1 = 1.0 + (K(KSE)*DELTA(KSE))
      S1 = (-(DELS7(KSE)*DELTA(KSE)) +(DELS6(KSE)*DELTA(KSE-1)) -
     1DELTA(KSE-2))*DELS8(KSF)
      BETA(KSE) = ATAN(S1/G1)
 9992 CONTINUE
      C1 = VF
      C2 = RHOF
      C3 = C1*C1
      C4 = C2*C3
      C5 = C4*C1
      C6 = TO
      C7 = C3/TO
      C8 = C4/C1
      WRITE(4,960) C1,C2,C3,C4,C5,C6,C7,C8,C9
  960 FORMAT(//2X,35HPARAMETERS FOR NONDIMENSIONAL(EA5ON,/78,
     14HVF =,E12.5,4H M/S,/78,
     26HRHOF =,E12.5,6H KG/M3,/78,
     37HVF*VF =,E12.5, 5H J/KG,/78,
     432HRHOF*VF*VF =,E12.5,5H N/M2,/78,
     515HRHOF*VF*VF =,E12.5,5H M/M2,/78,
     66HTS =,E12,9,2H K,/78,
     718HVF*VF/TS =,E12.5, 9H J/(KG-K),/78,
     8HRN =,E12.5,2H M,/78,
     97HRN/VF =,E12.5, 2H S)
      WRITE(6,965) PIE,KYS),(RHO(I,KYS),HE(,KYS),T(I,KYS),VE(,KYS),
     1VM(I,KYS),SX(I,KYS),V4E(,KYS)
  965 FORMAT(//2X,*NORMAL SHOCK PROPERTIES - NONDIMENSIONAL*,/78,**PRESSU
     1RE =*,F6.4,/78,*DENSITY =*,F6.2,/78,*ENTHALPY =*,F6.4,/78,*TEMPERA
     2TURE =*,F6.5,/78,*VELOCITY = *,F6.4,/78,*MOLECULAR WT. =*,F6.2,/78
     3,*ENTROPY =*,F6.5,/78,*SONIC VELOCITY =*,F6.4,///)
      WRITE(6,NAME2)
    1 CONTINUE
      IOUT = IOUT + 1
      IF(IOUT-IOUTM)  431,430,430
  430 CONTINUE
      IOUT = 0
      CALL OUTPUT(IKS,TAUT,KSF,KYS)
  431 CONTINUE
      IKS = IKS + 1
      DO 700  KS=1,KSE
      G1 = 1.0 + (K(KS)*DELTA(KS))*Y(KY)*DP(KS)
      DO 700  KY=1,KYS
      G2 = 1.0 + (K(KS)*Y(KY))*DELTA(KS))
      G3 = (V(KS,KY) - (Y(KY)*DELTA(KS)) - (U(KS,KY)*V(KY)*G1/G2) +
     1VA(KS,KY))/DELTA(KS)
      TAU(KS,KY) = DELY(KY)/G3
      G4 = DELY2(KY)/G3
      IF(G4-LT.TAU(KS,KY))  TAU(KS,KY)=G4
      TAU(KS,KY) = TAU(KS,KY)*TYIP*4C
      TAU(KS,KY) = ABS(TAU(KS,KY))
  700 CONTINUE
      TAUM= TAU(1,1)
      DO 711  KS=1,KSE
      TAUMS(KS) = TAU(KS,1)
      DO 710  KY=1,KYS
      IF(TAU(KS,KY).LT.TAUMS(KS))  TAUMS(KS)=TAU(KS,KY)
  710 CONTINUE
      IF(TAUMS(KS).LT.TAUM)  TAUM=TAUMS(KS)
  711 CONTINUE
      IF(NCTS.EQ.0)  GO TO 1701
      DO 1700  KS=1,KSE
 1700 TAUMS(KS) = TAUM
 1701 CONTINUE
      TAUT = TAUT + TAUM
      UTE(,1) = 0.
      VTE(,1) = 0.
      Y3 = ((DELY2(E)*VTE(,I)) -(DELY4(I)*VE(,2)) +V(I,3))*DELY8(I)
      S2 = U(2,1)/S(2)
      PT(E,I) =   -(VA(I,I)*VA(I,I)*RHO(I,I)*(E2.*E2)*V(S)/DELTA(I))))
      I = (QQ(I,1)/(P(I),I))*RHO(I,1)))
      TT(I,I) = (P(I),I)- QQ(I,I))/RHO(I,I)
      RHO(I,I) = (P(I),I)*(PS(I,I)-(1./RHO(I,I)))*PT(I,I))/(P(I),I)*
     1DELY8(KY)
      LVA(I,I)*VA(I,I)
      DO 91   KY=2,KYS1
      S2 = U(S,KY)/S(2)
      IF(KY.EQ.KYS1) GO TO 9101
      Y3 = (V(I,KY+1)-V(I,KY))/DELY1(KY)
      Y4 = (P(I),KY+1)-P(I,KY))/DELY1(KY)
      Y5 = ((DELY7(KY)/RHO(I,KY))*(DELY6(KY)*RHO(I,KY+1)) +RHO(I,KY+2))*
     1DELY8(KY)
      GO TO 9102
 9101 CONTINUE
      Y3 = (V(I,KY+1)*(DELY4(KY)*V(I,KY))-(DELY3(KY)*V(I,KY-1)))*
     1DELY5(KY)
      Y4 = (P(I,KY+1)*(DELY4(KY)*P(I,KY))-(DELY3(KY)*P(I,KY-1)))*
     1DELY5(KY)
      Y5 = (-(DELY7(KY)*RHO(I,KY)) +(DELY6(KY)*RHO(I,KY+1)) -RHO(I,KY-2))*
     1DELY8(KY)
 9102 CONTINUE
      G6 =(V(I,KY)- (Y(KY)*DELY8(I)))/DELTA(I)
      G1 = 1.0 + (K(I)*V(KY)*DELTA(I))
      UT(I,KY) =  0.
      VT(I,KY) =  -(G6*Y3)  -(Y4/(RHO(I,KY)*DELTA(I)))
      PT(I,KY) =  -(G6*Y4)  -(VA(I,KY)*VA(I,KY)*(E2.*RHO(I,KY))*S2/G1))+
     1((RHO(I,KY)*Y5)/DELTA(I))*(2.*E(I)*RHO(I,KY)*V(I,KY)/G1))) +
     2((RHO(I,KY)/P(I,KY)*RHO(I,KY)))
      HT(I,KY) =  -(G6*Y5) +((P(I,KY)*(G6*Y4))- QQ(I,KY))/RHO(I,KY))
      RHOT(I,KY) = (HT(I,KY)-(P(I,KY)*(1./RHO(I,KY))))*PT(I,KY))/
     1E(I,KY)*VA(I,KY)*VA(I,KY))
   91 CONTINUE
      DO 90   KS=2,KSF
      Y3 = ((DELY7(I)*V(KS,I)) -(DELY4(I)*V(KS,2)) +V(KS,3))*DELY8(I)
      TP(KS,KS,KYS)  GO TO 191
      S2 = U(KS,1)*(.1) +(DELS4(KS)*U(KS,I)) -(DELS3(KS)*U(KS-1,I)))*
     1DELS5(KS)
      S6 = (P(KS,1)*(.1) +(DELS4(KS)*P(KS,I)) -(DELS3(KS)*P(KS-1,I)))*
     1DELS5(KS)
      S9 = (H(KS,1)*(.1) +(DELS4(KS)*H(KS,I)) -(DELS3(KS)*H(KS-1,I)))*
     1DELS5(KS)
      GO TO 291
  191 CONTINUE
      S2 = (-(DELS7(KS)*U(KS,I)) +(DELS6(KS)*U(KS-1,I)) -U(KS-2,I))*
     1DELS8(KS)
      S6 = (-(DELS7(KS)*P(KS,I)) +(DELS6(KS)*P(KS-1,I)) -P(KS-2,I))*
     1DELS8(KS)
      S9 = (-(DELS7(KS)*H(KS,I)) +(DELS6(KS)*H(KS-1,I)) -H(KS-2,I))*
     1DELS8(KS)
  291 CONTINUE
      S4 = (RHO(KS,I)*U(KS,I)*SIN(THETA(KS)))/RB(KS)
      UT(KS,I) =  -(U(KS,I)*S2) -(S4/RHO(KS,I))
      RT(KS,I) = 0.
      PT(KS,I) = -((U(KS,I)*S2) +(V(A(KS,I)*VA(KS,I)*(C)*RHO(KS,I)*S2)+(
     1RHO(KS,I)*V)/DELTA(KS)))+G6)) +(QQ(KS,I)/(P(KS,I)*RHO(KS,I)))
      HT(KS,I) = -(U(KS,I)*S9) +(P(I(KS,I)/RHO(KS,I)))
      UR(I,I) =(QQ(KS,I)/RHO(KS,I))
      RHOT(KS,I) = (HT(KS,I)+((P(KS,I)-(E(./RHO(KS,I)))*PT(KS,I)))/(
     1P(KS,I)*VA(KS,I)*VA(KS,I))
   90 CONTINUE
      DO 101 KS=2,KSF
      DO 101 KY=2,KYS1
      IF(KS.EQ.KSE)   GO TO 1101
      S2 = (U(KS+1,KY) +(DELS4(KS)*U(KS,KY)) -(DELS3(KS)*U(KS-1,KY)))*
     1DELS5(KS)
      S6 = (P(KS+1,KY) +(DELS4(KS)*P(KS,KY)) -(DELS3(KS)*P(KS-1,KY)))*
     1DELS5(KS)
      S9 = (H(KS+1,KY) +(DELS4(KS)*H(KS,KY)) -(DELS3(KS)*H(KS-1,KY)))*
     1DELS5(KS)
      GO TO 2101
 1101 CONTINUE
      S2 = (-(DELS7(KS)*U(KS,KY)) +(DELS6(KS)*U(KS-1,KY)) -U(KS-2,KY))*
     1DELS8(KS)
      S6 = (-(DELS7(KS)*P(KS,KY)) +(DELS6(KS)*P(KS-1,KY)) -P(KS-2,KY))*
     1DELS8(KS)
      S9 = (-(DELS7(KS)*H(KS,KY)) +(DELS6(KS)*H(KS-1,KY)) -H(KS-2,KY))*
     1DELS8(KS)
 2101 CONTINUE
      IF(KY.EQ.KYS2) GO TO 1011
      Y3 = ((V(KS,KY+1)-V(KS,KY))/DELY1(KY)
      Y4 = (P(KS),KY+1)-P(KS,KY))/DELY1(KY)
      Y5 = ((DELY7(KY)*U(KS,KY)) -(DELY6(KY)*U(KS,KY+1)) +U(KS,KY+2))*
     1DELY8(KY)
      GO TO 1012
 1011 CONTINUE
      Y2 = (-(DELY7(KY)*U(KS,KY)) +(DELY6(KY)*U(KS,KY-1)) -U(KS,KY-2))*
     1DELY8(KY)
      Y3 = ((V(KS,KY+1)+(DELY4(KY)*V(KS,KY))-(DELY3(KY)*V(KS,KY-1)))*
     1DELY5(KY)
      Y4 = ((P(KS,KY+1)+(DELY4(KY)*P(KS,KY))-(DELY3(KY)*P(KS,KY-1)))*
     1DELY5(KY)
      Y5 = (-(DELY7(KY)*H(KS,KY)) +(DELY6(KY)*H(KS,KY+1)) +H(KS,KY+2))*
     1DELY8(KY)
 1012 CONTINUE
      G4=  1.0+(K(KS)*Y(KY)*DELTA(KS))
      G2= 1.0+(K(KS)*DELTA(KS))
      R = RB(KS) + (Y(KY)*DELTA(KS)*COS(THETA(KS)))
      G3= (Y(KY)*G2*TAN(THETA(KS)))/G1
      S4= (V(KS,KY)-(Y(KY)*DELTA(KS))-(U(KS,KY)*R)*3)/DELTA(KS)
      S5= (RHO(KS,KY)*G3)/DELTA(KS)
      S6=  (RHO(KS,KY)*U(KS,KY)*SIN(THETA(KS)))/R)+((RHO(KS,KY)*V(KS,KY)*
     1(K(KS)*S)/DELTA(KS))/R))
      S7= (RHO(KS)*UR(KS,KY)*V(KS,KY))/G1
      S8= (RHO(S)*UR(KS,KY)*U(KS,KY))/G1
      UT(KS,KY)=-((G4*Y2)+((U(KS,KY)*S2/G1))-((G5*Y4)/(RHO(KS,KY)*RHO(KS,
     1KY)))  + (S4/(RHO(KS,KY)*G1)) + G7)
      VT(KS,KY)=-((G4*Y3)+(U(KS,KY)*S3/G1))+(Y4/(DELTA(KS)*RHO(KS,KY)))-
     1 G8)
      PT(KS,KY)=-((G4*Y4)+(U(KS,KY)*S6/G1))+((VA(KS,KY)*VA(KS,KY))*((RHO(
     1KS,KY)*S2/G1)-(G5*Y2)+(RHO(KS,KY)*S3/DELTA(KS)))+G8))-(DO(KS,KY)/(
     2P(KS,KY)*RHO(KS,KY))))
      HT(KS,KY)=-((G4*Y5)+(U(KS,KY)*S5/G1))-(P(KS,KY)/RHO(KS,KY))-((G4*Y4
     1/RHO(KS,KY))-((U(KS,KY)*S4)/(RHO(KS,KY)*G1)))+(QQ(KS,KY) /RHO(KS,KY
     2)))
      RHOT(KS,KY) = (HT(KS,KY) + ((P(KS,KY)*(1./RHO(KS,KY)))*PT(KS,KY))
     1/(P(KS,KY)*VA(KS,KY)*VA(KS,KY))
  101 CONTINUE
      IF(NOEL.EQ.01 GO TO 4200
      IF(LS) 4200,4300,4400
 4200 CONTINUE
      JSTOP = 0
      TAUM = TAUMS(1)
      CG1 = RHO(1,KYS)
      CG2 = VE(,KYS)
      CG3 = P(I,KYS)
      CG4 = ME(,KYS)
      CG5 = DELTA(1)
      CG6 = DELTA(1)
```

```
      I = 0
      DO 249  KY=KYS1,KYS
      I = I+1
      GI =  1.0 + (KEL)*EXY1*DELTA(I)
      G4 =  (VEL,KY)- EYEKY1*DELTAT(I))/DELTA(I)
      CHI(1,I) =  G4 + (VAI1,KY1/DELTA(I)
      CHI2,I) = 1./RHO(I,KY1*VA(I,KY1)
      S2 =   UI2,KY1/S(I2)
      CHI3,I) =  -(I2.*RHOI)*EXI*VAI),KY1*VA(I,KY1/GI)*(S2* EKE(I)*UI),
     1KY1)))  + IOO(I,KY1/(PI(I,KY1*RHOI(,KY1))
      CHI3,I) = CHI3,I)*EMC2,I)
  249 CONTINUE
  239 CONTINUE
      JSTOP = JSTOP + 1
      IFIJSTOP.GE.2) GO TO 470
      GO TO 475
  470 KS = 1
  471 WRITE(6,495) KS,EKS,JSTOP
  495 FORMAT(1H1,//////LOR,*SHOCK PROPERTIES DID NOT CONVERGE IN 25 ITE
     1RATIONS*,///13X,*BODY LOCATION =*,F7.3,3X,**THE ITERATIONS =*,I4,
     23X,*SHOCK ITERATIONS =*,I3)
      CALL OUTPUT(IKS,TAUT,KSE,KYS)
      STOP
  475 CONTINUE
      DELTAG = DELTA(I) + (ICG6*DELTAT(II)*.5*TAUM)
      IFIJSTOP.EQ.1)  GO TO 240
      SYI =  (1.* DELTAT(I))*(VF/.3046)
      CQS(S) = 1
      THETR = 0.
      TT(I) =  TI(,KYS)*TO*1.8
      PRES(I) =  (PI(,KYS)*RHOF*VF*VF)/101325.
      CALL EQUIL(EQS,1,PRES(I))
      VEL2(I) = VEL*.3048/VF
      SA22(I) = SA2
      CG2 =  -(VEL*.3048/VFI + DELTAT(I)
      CG1 =  (RHRKS*16.018863)/RHOF
      CG3 = (PKS*101325.)/(RHOF*VF*VF)
      CG4 = (HIPKS*4184.)/(VF*VF)
  240 CONTINUF
      G9 =  1.0 + (KIKS)*DELTAG)
      CHI(1,3) = (CG2-DELTAT(I)*VAI(,KYS))/DELTAG
      CHI(2,3) = 1./(CG1*VAI(,KYS))
      CHI3,3) =  -(I2.0*CG1*VAI(,KYS)*VAI(,KYS0/GI)*(S2*(KE3)*CG2))
     1+ EQI(,KYS)/(PI(EI,KYS)*CG1))
      CHI3,3) = CHI3,3)*CHI(2,3)
      SYI = (I1.0-YI(KYS))*(I2./TAUM)- CHI(,3)-CHI(,I3)) + (YIKYS)*
     1(CHI(,2)-CHI(,I3))
      SY2 = (2.*II.0-YI(KYS))*(I2./TAUM) + CHI(,2) -CHI(,3)
      SY1 =  SYI/SY2
      SY2 = (SYI-YIKYS))*(1.0-Y(KYS))
      C4  =  VEI,KYS3)*(SY2*VEI,KYS)-VFI,KYS))3
      C5  =  PI(,KYS0)*(SY2*(PI(,KYS)-PI(,KYS)))
      C6 = (CHI(2,3) *CHI2,3) +(SY2*(CHI(2,2)-CHI(2,I))*/2.
      C7 = (CHI(3,3)+CHI3,3))*(SY2*(CHI(,2)-CHI(2,I))))/2.
      C9 = C4 + (CI*TAUM)- (C6*(CG3)-C5))
      C10 = ABS((CG2-C9)/CG2)
      IF(CIO-.0001) 236,236,235
  235 CONTINUE
      IFIJSTOP.GT.3)  GO TO 234
      ERR2 = CG2 - C9
      DTAT2 = DELTAT(I)
      DELTA(I) =  1.2*DELTAT(I)
      IF(DELTAT(I).EQ.0.) GO TO 238
      GO TO 239
  238 DELTAT(I) = -.002
      GO TO 239
  234 CONTINUE
      ERR1 = ERR2
      DTAT1 = DTAT2
      ERR2 = CG2 - C9
      DTAT2 = DELTAT(I)
      DELTAT(I) = DTAT2 - ((ERR2*(DTAT2-DTAT1))/(ERR2-ERR1))
      GO TO 239
  236 DELTA(I) = DELTAG
      RHOR(I,KYS) = CG1
      UR(I,KYS) = 0.
      VB(I,KYS) = CG2
      PB(I,KYS) = CG9
      HB(I,KYS) = CG4
      DO 350  KS=2,KSE
      JSTOP = 0
      TAUM = TAUM(KS)
      CG5 = DELTA(KS)
      CG6 = DELTA(KS)
      G2 =(1.0 + (K(KS)*DELTA(KS))**AN(RETA(KS))
      I = 0
      DO 349   KY=KYS1,KYS
      I = I+1
      IFIKS.EQ.KSE)  GO TO 2200
      S2 = (UIKS+1,KY)*(DELSA(KS)*UIKS,KY))-(DELSB(KS)*UIKS-1,KY))*
     1DELS5(KS)
      S3 = (VIKS+1,KY)+(DELS6(KS)*VIKS,KY))-(DELS3(KS)*VIKS-1,KY))*
     1DELS5(KS)
      S4 = (PIKS+1,KY)+(DELSA(KS)*PIKS,KY))-(DELS5(KS)*PIKS-1,KY))*
     1DELS5(KS)
      GO TO 2201
2200 S2=(-(DELS7(KSE)*UIKSE,KY)) +(DELS6(KSE)*UI(KSE),KY)) -UIKSE-2,KY)
     1)*DELS8(KSE)
      S3=(-(DELS7(KSE)*VIKSE,KY)) +(DELS6(KSE)*VIKSE),KY)) -VIKSE-2,KY)
     1)*DELS8(KSE)
      S4=(-(DELS7(KSE)*PIKSE,KY)) +(DELS6(KSE)*PIKSE,KY)) -PIKSE-2,KY)
     1)*DELS8(KSE)
2201 CONTINUE
      IF(KY.EQ.KYS)  GO TO 2210
      Y2 = (UIKS,KY+1)+(DELY6(KY)*UIKS,KY))-(DELY5(KY)*UIKS,KY-1))*
     1DELY5(KY)
      GO TO 2211
2210 Y2=(-(DELY7(KYS)*UIKS,KYS)) +(DELY6(KYS)*UIKS,KYS)) -UIKS,KYS-1
     1)*DELY8(KYS)
2211 CONTINUE
      S1 =  1.0 + (K(KS)*Y(KY)*DELTA(KS))
      R = RHOIKS) + (Y(KY)*DELTA(KS)*COS(THETA(KS)))
      G3 = (Y(KY)*G2)/G1
      G4 = (VIKS,KY)- (Y(KY)*DELTA(KS))- (UIKS,KY)*GB))/DELTA(KS)
      G5 = (RHOIKS,KY)*G3)/DELTA(KS)
      G6 = (RHOIKS,KY)*UIKS,KY)*SIN(THETA(KS))/R)
     1*(SIN(KS)/G1)+(COS(THETA(KS))/R))3
      G8 =  R(KS)*UIKS,KY)*UKS,KY)/G1
      CHI(,I) =  G4 + (VAIKS,KY)/DELTA(KS))
      CHI2,I) = 1./(RHOIKS,KY)*VAIKS,KY))
      G3 =  -(UIKS,KY)*S3/G1)+G8
      G7 =  -(UIKS,KY)*S4/G1) -(VAIKS,KY)*VAIKS,KY)*(ERHOIKS,KY)*S2/G1)
     1+G8)) +(ODIKS,KY)/(PIKS,KY)*RHOIKS,KY))) + (VAIKS,KY)*VAIKS,KY)*
     2DS*Y2)
      CHI3,I) = G3 + (GT*CHI2,I))
  349 CONTINUE
  339 CONTINUE
      JSTOP = JSTOP +1
      IFIJSTOP.GT.25) GO TO 471
      DELTAG =  DELTA(KS) +((CG4*DELTAT(KS))*.5*TAUM)
      G1 = 1.0 + (K(KS)*DELTAG)
      IFIKS.GT.2) GO TO 460
      S1 = (DELTAG-DELTA(I))*(2./SE2))
      GO TO 461
460 S1 = (-(DELS7(KS)*DELTAG) +(DELS6(KS)*DELTA(KS-1)) -DELTA(KS-2))*
      IDELS8(KS)
  461 RETA(KS) = ATAN(S1/G1)
      SYI =  1. + 2.*DELTAT(KS)*SIN(THETA(KS))) + (DELTAT(KS)*
     1DELTAT(KS))
      SYI =   SQRT(SYI)*VF/.3048
      GAMMA =  (DELTAT(KS)*COS(THETA(KS)))/(1.+(DELTAT(KS)*SINE
     1THETA(KS)))
      THETR = 1.5707963 -THETA(KS)-BETA(KS)- ATAN(GAMMA)
      KQS(S) = 1
      TT(I)= TIKS,KYS)*TO*1.8
      PRES(I) =  PIKS,KYS)*RHOF*VF*VF/101325.
      CALL EQUIL(KQS,1,PRES(I))
      VEL2(KS) = VEL*.3048/VF
      SA22(KS) = SA2
      GAMMA =   SA2 + BETA(KS)
      CG7 =   -(VEL*COS(GAMMA)*.3048/VF) + DELTAT(KS)
      CG2 =   VEL*SIN(GAMMA)*.3048/VF
      CG1 =   RHRKS*16.018863/RHOF
      CG3 =  (PKS*101325.)/(RHOF*VF*VF)
      CG4 =  (HIPKS*4184.)/(VF*VF)
      R = RB(KS) + (DELTAG*COS(THETA(KS)))
      S3 =   TAN(BETA(KS))
      G4 =  (CG2 -DELTAT(KS)*(- CG7*G3))/DELTAG
      G9 =   CG1*G3/DELTAG
      G6 =  (CG1*CG7*SIN(THETA(KS)))/R) + (CG1*CG2*(COS(I
     1COS(THETA(KS))/RB))
      G8 =  KIKS)*CG7*CG7/G1
      CHI(1,3) =  G4 + (VAIKS,KYS)/DELTAG)
      CHI(2,3) = 1./(CG1*VAIKS,KYS))
      G3 =   -(CG7*S3/G1)+G8
      G7 =  -(CG7*G4/CG1) + (VAIKS,KYS)*VAIKS,KYS))*((CG1*S2/G1)+G6)) +
     1(OOIKS,KYS)/(PIKS,KYS)*RHOIKS,KYS))) + (VAIKS,KYS)*VAIKS,KYS)*G5*Y2)
      CHI(9,3) = G3 + (GT*CHI(2,3))
      SYI = (1.0-YIKYS))*(I2./TAUM)-CHI(,3)-CHI(,I3))+ (Y(KYS))*
     1(CHI(1,2)-CHI(,I3))
      SY2 = (2.0*(1.0-Y(KYS))/TAUM) + CHI(,2) -CHI(,3)
      SY1 =  SYI/SY2
      SY2 = (SYI-Y(KYS))/(1.0-Y(KYS))
      C4 = VEKS,KYS)*(SY2*(VEKS,KYS)-VFKS,KYS)))
      C5 = PIKS,KYS)*(SY2*(PIKS,KYS)-PI(KS,KYS)))
      C6 = (CHI(2,3) + CHI2,I3 + (SY2*(CHI(2,2)-CHI(2,I)))/2.
      C7 = (CHI(3,3)+CHI3,I)*(SY2*(CHI(3,2)-CHI(2,I)))/2.
      C9 = C4 + (C1*TAUM)- (C6*(CG3-C5))
      C10 = ABS((CG7-C9)/CG2)
      IF(CIO-.0001) 336,336,335
  335 CONTINUE
      IFIJSTOP.GT.3)  GO TO 334
      ERR2 = CG2 - C9
      DTAT2 = DELTAT(KS)
      DELTAT(KS) = 1.2*DELTAT(KS)
      IF(DELTAT(KS).EQ.0.) GO TO 338
      GO TO 339
  338 DELTAT(KS) = -.002
      GO TO 339
  334 CONTINUE
      ERR1 = ERR2
      DTAT1 = DTAT2
      ERR2 = CG2 - C9
      DTAT2 = DELTAT(KS)
      DELTAT(KS) = DTAT2 - ((ERR2*(DTAT2-DTAT1))/(ERR2-ERR1))
      GO TO 339
  336 DELTAT(KS) = DELTAG
      RHOR(I,KYS) = CG1
      UR(KS,KYS) = CG7
      VB(KS,KYS) = CG2
      PB(KS,KYS) = CG5
      HB(KS,KYS) = CG4
  350 CONTINUE
      DO 351   KS=1,KSE
      RHO(KS,KYS) = RHOB(KS,KYS)
      U(KS,KYS) = UB(KS,KYS)
      V(KS,KYS) = VB(KS,KYS)
      P(KS,KYS) = PB(KS,KYS)
      H(KS,KYS) = HB(KS,KYS)
  351 CONTINUE
      C1 = ABS(DELTAT(1))
      IF(KS.GE.LSC.AND.C1.LE.CCS)  LS=0
      GO TO 4500
 4100 CONTINUE
      DELTAT(1) = 0.
      RO(KY) 1 = 1
      SYI = VF/.3048
      THETR = 0.
      TT(I) = TI(,KYS)*TO*1.8
      PRES(I) = PI(,KYS)*RHOF*VF*VF/101325.
      CALL EQUIL(KQS,1,PRES(I))
      VEL2(I) = VEL*.3048/VF
      SA22(KS) = SA2
      V(I,KYS) = -VEL2(I)
      U(I,KYS) = 0.
      RHO(I,KYS) = RHRKS)*16.018863/RHOF
      P(I,KYS) = (PKS)*101325.)/(RHOF*VF*VF)
      H(I,KYS) = (HIPKS*4184.)/(VF*VF)
 4400 CONTINUE
      DO 107  KS=2,KSE
      G2 = RB(KS) + (DELTA(KS)*COS(THETA(KS)))
      SP(I) = 0.
      G3 = RB(KS)*RHOIKS,I)*UIKS,I)
      DO 106  KY=2,KYS
      R = RB(KS) + (Y(KY)*(G2-RHO(KS)))
      G4 = RHHOIKS,KY)*UIKS,KY)
      SP(KY) = (((G4*C3)*.5*DELY2(KY)) + SP(KY-1)
      G3 = G4
  106 CONTINUE
      DP(I,KS) = 0.
      G5 = (SP(KYS)-(RB(KS)*COS(THETA(KS)))*2.
      DELTA(KS) = RO(KS)*RHO(KS)/G5
  107 CONTINUE
      DO 108  KS=2,KSE)
      G1 = 1.0 + (K(KS)*DELTA(KS))
      S1 =(DELS7(KS)*DELTA(KS-1)) -(DELS6(KS)*DELTA(KS-1))
     1 -DELTA(KSE-2))*DELS8(KSE)
      BETA(KSE) = ATAN(S1/G1)
      DO 109  KS=2,KSE
      G1 = 1.0 + (K(KS)*DELTA(KS))
      S1 = (-(DELS7(KS)*DELTA(KS-1)) +(DELS6(KSE)*DELTA(KSE-1))
     1 -DELTA(KSE-2))*DELS8(KSE)
      BETA(KSE) = ATAN(S1/G1)
      DO 109  KS=2,KSE
      G1 = 1.0 + (K(KS)*DELTA(KS))
      S1 = (-(DELS7(KS)*DELTA(KS-1)) +(DELS6(KS)*DELTA(KS-1))
     1 -DELTA(KS-2))*DELS8(KS)
      BETA(KS) = ATAN(S1/G1)
      KQS(S) = 1
      SYI = VF/.3048
      THETR = 1.5707963 - THETA(KS) - BETA(KS)
      TT(I) = TI(KS,KYS)*TO*1.8
      PRES(I) = PI(KS,KYS)*RHOF*VF*VF/101325.
      CALL EQUIL(KQS,1,PRES(I))
      VEL2(KS) = VEL*.3048/VF
      SA22(KS) = SA2
      GAMMA = SA2 + BETA(KS)
      V(KS,KYS) = -VEL2(KS)*COS(GAMMA)
      U(KS,KYS) = VEL2(KS)*SIN(GAMMA)
      RHO(KS,KYS) = RHRKS*16.018863/RHOF
      P(KS,KYS) = (PKS*101325.)/(RHOF*VF*VF)
      H(KS,KYS) = (HIPKS*4184.)/(VF*VF)
  109 CONTINUE
      IF(LS.EQ.+1) GO TO 4500
      LS = +1
```

```
      WRITE(6,4130)
 4130 FORMAT(1HL,/////////20X,10H**********,///20X,*PROGRAM WAS SWITCHE
     1D TO MASS BALANCE OPTION*,///20X,10H**********)
      CALL OUTPUT(IKS,TAUT,KSF,KYS)
 4500 CONTINUE
      DO 103   KS=1,KSE
      TAUM = TAUMS(KS)
      DO 105   KY=1,KYSI
      RHOB(KS,KY) = RHO(KS,KY)
      UBI(KS,KY)    =   UI(KS,KY)
      VBI(KS,KY)    =  VI(KS,KY)
      PBI(KS,KY) = PI(KS,KY)
      HBI(KS,KY) = HI(KS,KY)
      RHO(KS,KY) = RHOBI(KS,KY) + (RHOT(KS,KY)*TAUM)
      UI(KS,KY) = UBI(KS,KY) + (UT(KS,KY)*TAUM)
      VI(KS,KY) = VBI(KS,KY) + (VT(KS,KY)*TAUM)
      PI(KS,KY) = PBI(KS,KY) + (PT(KS,KY)*TAUM)
      HI(KS,KY) = HBI(KS,KY) + (HT(KS,KY)*TAUM)
  103 CONTINUE
      Y8 = (DELYT(1)*VI(1,1)) -(DELY6(1)*VI(1,2)) +V(1,3))*DELY8(1)
      S2  = UI2.(3/S(2)
      T4          -(VR(3,1)*VA(1,1)*RHO(1,1)*EI2.*S2)+(Y8/DELTA(1)))
     1 + (QO(1,1)/(PI(1,1)*RHO(1,1)))
      T5      = (T4-QO(1,1))/RHO(1,1)
      T3 = (T5+((PLE(1,1)-E1./RHO(1,1))*T6))/(PI(1,1)*VA(1,1)*VA(1,1))
      RHOT(1,1) = (RHOT(1,1)+T1)/2.
      PT(1,1) = (PT(1,1)+T4)/2.
      HT(1,1) = (HT(1,1)+T5)/2.
      DO 95  KY=2,KYS1
      S2 = UI2.KY3/S(2)
      Y3 = (V(1,KY3-V(1,KY-1))/DELY2(KY)
      Y4 = (P(1,KY1-P(1,KY-1))/DELY2(KY)
      Y5 = (V(1,KY+1)*DELY4(KY)*V(1,KY))-(DELY3(KY)*V(1,KY-1))*
     1DELY5(KY)
      IF(KY.EQ.2) Y5 = ((DELY7(2)*V(1,2)) -(DELY6(2)*V(1,3))*V(1,1)*
     1DELY8(2)
      IF(KY.EQ.KYSI) Y5 =(-(DELY7(KY)*V(1,KY))+(DELY6(KY)*V(1,KY-1))
     1-V(1,KY-2))*DELY8(KY)
      IF(KY.EQ.KYSI) Y4 =(-(DELY7(KY)*P(1,KY))+(DELY6(KY)*P(1,KY-1))
     1-P(1,KY-2))*DELY8(KY)
      G4 =(V(1,KY)- (Y(KY)*DELTAT(1))1)/DELTA(1)
      G1 = 1.0 + (K(1)*Y(KY)*DELTAT(1))
      T3          -(G4*Y3)  -(Y4/RHO(1,KY))+DELTA(1)(3))
      T4          -(G4*Y4)  -(Y4(1,KY)*VA(1,KY)*(2.*RHO(1,KY)*S2/G1))+
     1(RHO(1,KY)*Y3/DELTA(1))+(2.*K(1)*RHO(1,KY)*VI1,KY)/G1))) +
     2(QO(1,KY)/(PI(1,KY)*RHO(1,KY)))
      T5 = -(G4*Y5) +((E1*(G4*Y4-QO(1,KY)))/RHO(1,KY))
      T1 = (T5+(P(1),KY1-(1./RHO(1,KY)))+Y4))/PI(1,KY)*
     2VA(1,KY)*VA(1,KY))
      RHOT(1,KY) = (RHOT(1,KY)+T1)/2.
      VT(1,KY) = (VT(1,KY)+Y3)/2.
      PT(1,KY) = (PT(1,KY)+T4)/2.
      HT(1,KY) = (HT(1,KY)+T5)/2.
   95 CONTINUE
      DO 96  KS=2,KSE
      IF(KS.EQ.KSE) GO TO 9660
      S2 = (UI(KS+1,1) +(DELS4(KS)*UI(KS,1)) -(DELS3(KS)*UI(KS-1,1)))*
     1DELS5(KS)
      S4 = (P(KS+1,1) +(DELS4(KS)*P(KS,1)) -(DELS3(KS)*P(KS-1,1)))*
     1DELS5(KS)
      S5 = (HI(KS+1,1) +(DELS4(KS)*HI(KS,1)) -(DELS3(KS)*HI(KS-1,1)))*
     1DELS5(KS)
      GO TO 9661
 9660 CONTINUE
      S2 = (-(DELS7(KS)*UI(KS,1)) +(DELS6(KS)*UI(KS-1,1)) -UI(KS-2,1))*
     1DELS8(KS)
      S4 = (-(DELS7(KS)*P(KS,1)) +(DELS6(KS)*P(KS-1,1)) -P(KS-2,1))*
     1DELS8(KS)
      S5 = (-(DELS7(KS)*HI(KS,1)) +(DELS6(KS)*HI(KS-1,1)) -HI(KS-2,1))*
     1DELS8(KS)
 9661 CONTINUE
      Y3 = ((DELY7(1)*VI(KS,1)) -(DELY6(1)*VI(KS,2)) +VI(KS,3))*DELY8(1)
      G6 = (RHO(KS,1)*UI(KS,1)*SI*VI(KS,1))*RB(KS)
      T2          -(UI(KS,1)*S2)  -(S6/RHO(KS,1))
      T4          -(UI(KS,1)*S6)  -((VA(KS,1)*VA(KS,1)*(RHOI(KS,1)*S2)+(
     1RHOI(KS,1)*Y3/DELTA(KS)))+G6))  +(QO(KS,1)/(PI(KS,1)*RHO(KS,1)))
      T5 = -(UI(KS,1)*S6) +(T4/RHO(KS,1)) +(UI(KS,1)*S6/RHO(KS,1)) -
     1 (QO(KS,1)/RHO(KS,1))
      T1 = (T5+((PI(KS,1)-(1./RHO(KS,1)))*T6))/(PI(KS,1)*VA(KS,1)*
     1VA(KS,1))
      RHOT(KS,1) = (RHOT(KS,1)+T1)/2.
      UT(KS,1) = (UT(KS,1)+T2)/2.
      PT(KS,1) = (PT(KS,1)+T4)/2.
      HT(KS,1) = (HT(KS,1)+T5)/2.
   96 CONTINUE
      DO 102   KS=2,KSE
      DO 102   KY=2,KYSI
      IF(KS.EQ.KSE) GO TO 1021
      S2 = (UI(KS+1,KY) +(DELS4(KS)*UI(KS,KY)) -(DELS3(KS)*UI(KS-1,KY)))*
     1DELS5(KS)
      S3 = (VI(KS+1,KY) +(DELS4(KS)*VI(KS,KY)) -(DELS3(KS)*VI(KS-1,KY)))*
     1DELS5(KS)
      S4 = (PI(KS+1,KY) +(DELS4(KS)*PI(KS,KY)) -(DELS3(KS)*PI(KS-1,KY)))*
     1DELS5(KS)
      S5 = (HI(KS+1,KY) +(DELS4(KS)*HI(KS,KY)) -(DELS3(KS)*HI(KS-1,KY)))*
     1DELS5(KS)
      GO TO 1022
 1021 CONTINUE
      S2 = (-(DELS7(KS)*UI(KS,KY)) +(DELS6(KS)*UI(KS-1,KY)) -UI(KS-2,KY))*
     1DELS8(KS)
      S3 = (-(DELS7(KS)*VI(KS,KY)) +(DELS6(KS)*VI(KS-1,KY)) -VI(KS-2,KY))*
     1DELS8(KS)
      S4 = (-(DELS7(KS)*PI(KS,KY)) +(DELS6(KS)*PI(KS-1,KY)) -PI(KS-2,KY))*
     1DELS8(KS)
      S5 = (-(DELS7(KS)*HI(KS,KY)) +(DELS6(KS)*HI(KS-1,KY)) -HI(KS-2,KY))*
     1DELS8(KS)
 1022 CONTINUE
      Y2          = (UI(KS,KY+1)+(DELY4(KY)*UI(KS,KY))-(DELY5(KY)*UI(KS,KY-1)
     1))*DELY3(KY)
      Y3          = (VI(KS,KY)-VI(KS,KY-1))/DELY2(KY)
      Y4          = (PI(KS,KY)-PI(KS,KY-1))/DELY2(KY)
      Y5          = (HI(KS,KY+1)+(DELY4(KY)*HI(KS,KY))-(DELY5(KY)*HI(KS,KY-1)
     1))*DELY3(KY)
      IF(KY.EQ.2)  Y2 = ((DELY7(2)*UI(KS,2)) -(DELY6(2)*UI(KS,3))
     1+UI(KS,1))*DELY8(2)
      IF(KY.EQ.2)  Y5 = ((DELY7(2)*HI(KS,2)) -(DELY6(2)*HI(KS,3))
     1+HI(KS,1))*DELY8(2)
      IF(KY.EQ.KYS1)  Y3=(-(DELY7(KY)*VI(KS,KY))+(DELY6(KY)*VI(KS,KY-1))
     1-VI(KS,KY-2))*DELY8(KY)
      IF(KY.EQ.KYS1)  Y4=(-(DELY7(KY)*PI(KS,KY))+(DELY6(KY)*PI(KS,KY-1))
     1-PI(KS,KY-2))*DELY8(KY)
      G1= 1.0+(K(KS)*Y(KY)*DELTA(KS))
      G2= 1.0+(K(KS)*DELTA(KS))
      R = RB(KS) + (Y(KY)*DELTA(KS)*COS(THETA(KS)))
      G3= (Y(KY)*G2*TAN(BETA(KS)))/G1
      G4= (VI(KS,KY)-(Y(KY)*DELTAT(KS)))-EU(KS,KY)*G3))/DELTA(KS)
      G5= (RHO(KS,KY)*G3)/DELTA(KS)
      G6=  (RHO(KS,KY)*UI(KS,KY))+SIN(THETA(KS)))/RI+((RHO(KS,KY)*VI(KS,KY))
     1*(COS(THETA(KS)))/RI))
      G7= (K(KS)*UI(KS,KY)*VI(KS,KY))/G1
      G8= (K(KS)*UI(KS,KY)*UI(KS,KY))/G1
      T2=-((G4*Y2)+(UI(KS,KY)*S2/G1)-((G5*Y4)/(RHO(KS,KY1**RHO(KS,KY))))
     1+(S4/(RHO(KS,KY1*G1)) + G7)
      T3=-((G4*Y3)+(UI(KS,KY)*S3/G1)+(Y4/(DELTA(KS)*RHO(KS,KY))))- G8)
      T4=-((G4*Y4)+(UI(KS,KY)*S4/G1)+(1VA(KS,KY1*VA(KS,KY1)+(RHO(KS,KY)
     1*S2/G1)-(DS*Y2)+(RHO(KS,KY)*Y3/DELTA(KS)))+G6))-(QO(KS,KY)/(PI(KS.
     2 KY)*RHO(KS,KY))))
      Y5=-((G4*Y5)+(UI(KS,KY)*S5/G1)-(T6/RHO(KS,KY)))-(G4*Y4/RHO(KS,KY))
     1-((UI(KS,KY)*S4)/(RHO(KS,KY)*G1))+(QO(KS,KY) /RHO(KS,KY)))
      T1 = (T5 + ((P(KS,KY+(1./RHO(KS,KY))))*T6))/(PI(KS,KY)*VA(KS,KY)
     1*VA(KS,KY))
      RHOT(KS,KY) = (RHOT(KS,KY)+T1)/2.
      UT(KS,KY) = (UT(KS,KY)+T2)/2.
      VT(KS,KY) = (VT(KS,KY)+T3)/2.
      PT(KS,KY) = (PT(KS,KY)+T4)/2.
      HT(KS,KY) = (HT(KS,KY)+T5)/2.
  102 CONTINUE
      DO 105   KS=1,KSE
      TAUM = TAUMS(KS)
      DO 105   KY=1,KYSI
      RHO(KS,KY) = RHOBI(KS,KY) + (RHOT(KS,KY)*TAUM)
      UI(KS,KY) = UBI(KS,KY) + (UT(KS,KY)*TAUM)
      VI(KS,KY) = VBI(KS,KY) + (VT(KS,KY)*TAUM)
      PI(KS,KY) = PBI(KS,KY) + (PT(KS,KY)*TAUM)
      HI(KS,KY) = HBI(KS,KY) + (HT(KS,KY)*TAUM)
  105 CONTINUE
      IF(IRS-IKSU)JP)1 709,709,708
  708 ITC = ITCUT(J9)
      IRC = IRCUT(J9)
      J9 = J9 +1
  709 CONTINUE
      IT1 = IT1 + 1
      IR1 = IR1 + 1
      IF(ITC-IT1) 715,715,716
  715 IT1 = 0
  716 CONTINUE
      IF(IRC-IR1) 713,713,716
  713 IR1 = 0
      IT1 = 0
  716 CONTINUE
      IF(IT1) 790,790,035
  790 CONTINUE
      KSS1S1=0
      DO 800  KS=1,KSE
      DO 805  KY=1,KYS
      HH(KY)= (HI(KS,KY)*WP*VF)/2324.4444
      PRES(KY)= (PI(KS,KY)*RHOF*VF*WP  )/101325.
      CALL EQUEL(H01,KY,PRES(KY))
      HHKY= 1.0* HIPS
      TEE(KY) = TKS
      RHOI(KS,KY) = (RHKS*16.018463)/RHOF
      TEKS,KY)  = TKS/TO
      SX(KS,KY) = (S/PKS*4184.)*TO/(VF*VF)
      WH(KS,KY) = WHS
      VAI(KS,KY) =  SQRT(8814.39*GAMS*PKS/WHKS)/VF
      S3 = (UI(KS,KY1*UI(KS,KY))+(VI(KS,KY1*VI(KS,KY))
      XAMI(KS,KY)=  SQRT(S3)/VAI(KS,KY)
      S3 = (TKS*CSPKS*4184.3/(VF*VF)
      PI(KS,KY) =  G3/(RHO(KS,KY)*96 (KS,KY)*VA (KS,KY)*(AL(KS-1.)
  805 CONTINUE
      IF(NOBAD.EQ.0)  GO TO 818
      IF(IN1) 810,810,811
  810 CONTINUE
      INADCK = IRS
      DEL18 = DELTA(KS)*AN*100.0
      CALL RADICAL
      QWE(KS) = (FIP(I(I)*10000.)/(RHOF*VF*VF*VF)
      QWI(KS) = (FLCP(I)*10000.)/(RHOF*VF*VF*VF)
      QWT(KS) = QWE(KS) + QWI(KS)
      DO 820 KY=1,KYS
      QP(KS,KY)=((EPH(KY)*FLCH(KY))*10000.)/(RHOF*VF*VF*VF)
      QWE(KS,KY)=((EPIP(KY)*FLCP(KY))*10000.)/(RHOF*VF*VF*VF)
      QWI(KS,KY)=  QP(KS,KY)-QWE(KS,KY)
  820 CONTINUE
      QO(KS,1) = ((QELY7(1)*QN(KS,1)) -(DELY6(1)*QN(KS,2)) +QN(KS,3))*
     1DELY8(1)
      QO(KS,KYS) =(-(DELY7(KYS)*QN(KS,KYS))) +(DELY6(KYS)*QN(KS,KYS1))
     2-QN(KS,KYS-2))*DELY8(KYS)
      DO 120  KY=2,KYS1
      QO(KS,KY) =  (QN(KS,KY+1)+(DELY6(KY)*QN(KS,KY))-(DELY5(KY)*QN(KS,
     1KY-1)))*DELY8(KY)
  120 CONTINUE
      IF(KS.GT.1) GO TO 124
      DO 121   KY=1,KYS
      G1 = KE(1)*(1.0+(K(1)*Y(KY))*DELTA(1))
      QO(1,KY) = (QO(1,KY)/DELTA(1)) + 12.*G1*QN(1,KY))
  121 CONTINUE
      GO TO 125
  124 CONTINUE
      G2 = COS(THETA(KS))
      DO 122  KY=1,KYS
      R = RB(KS) + (Y(KY)*G2)
      G1 = KE(KS)*(1.0+(K(KS)*Y(KY))*DELTA(KS))
      QO(KS,KY) = (QO(KS,KY)/DELTA(KS))) + ((G1+(G2/R1))*QN(KS,KY))
  122 CONTINUE
  125 CONTINUE
  811 CONTINUE
  800 CONTINUE
      IF(NOBAD.EQ.0)  INADCK = IRS
  835 CONTINUE
      IF(IRS-IRSC) 360,361,365
  365 CONTINUE
      KCC = 0.
      DO 370   KS=1,KSE
      CC(1,KS) = EH(KS,1)-CC(1,KS))/CC(1,KS)
      CC(2,KS) = EH(KS,KYS1-CC(2,KS))/CC(2,KS)
      CC(3,KS) = (HI(KS,KYC)-CC(3,KS))/CC(3,KS)
      DO 369   I=1,3
      IF(ABS(CC(I,KS)).LE.CC8)  KCC = KCC + 1.
  369 CONTINUE
      KCC = KCC/ICC)
      IF(KCC-CCF) 374,375,375
  374 CONTINUE
      IC = IC + 1
      IF(IC-ICC) 361,380,380
  380 CONTINUE
      IF(INADCK.EQ.IKS) GO TO 361
      INCC = IKS-ICC
      IF(INADCK-IA(CC) 361,361,361
  374 CONTINUE
      IC = 0
  361 CONTINUE
      DO 362   KS=1,KSE
      CC(1,KS) = HIKS,1)
      CC(2,KS) = HIKS,KYS)
      CC(3,KS) = HI(KS,KYC)
  362 CONTINUE
  380 CONTINUE
      IF(IEB-IKSF) 1901,1900,1900
 1900 CONTINUE
      CALL OUTPUT(IKS,TAUT,KSF,KYS)
      PUNCH 9909,  IRS,TAUT,(T(I,IR),TO,J9
      PUNCH 9906,  (BETA(IR),  KS=1,KSF)
      PUNCH 9906,  (DELTA(KS),  KS=1,KSE)
      PUNCH 9906,  (DELTAT(KS),  KS=1,KSE)
      DO 9940  KS=1,KSE
      DO 9940  KY=1,KYS
      PUNCH 9906,  PIKS,KY),RHO(KS,KY),HI(KS,KY),UI(KS,KY1,VI(KS,KY),
     1VA(KS,KY),PI(KS,KY),QO(KS,KY)
```

```
 9940 CONTINUE
      STOP
 1401 CONTINUE
      GO TO 1
  381 CONTINUE
      IKS = -IKS
      CALL OUTPUT(IKS,TAUT,KSF,KYS)
      STOP
      END

      SUBROUTINE OUTPUT(IKS,TAUT,KSF,KYS)
      REAL K
      COMMON/SUT2/   YE(11),SI(15),K1(51,THETA(15),BETA(15),RB(15),
     1DELTA(15),DELTAT(15),RB1(15)
      COMMON/SUT3/   RHO(15,11),U(15,11),V(15,11),P(15,11),HE(15,11),
     1TE(15,11),SX(15,11),VA(15,11),VAM(15,11),PI(15,11),WM(15,11),
     2TAU(15,11)
      COMMON/SUT4/ RHOB1(15,11),UB1(15,11),VB1(15,11),PB1(15,11),
     1HB1(15,11),DELSI(15),DELS2(15),DELS3(15),DELS4(15),DELS5(15),
     2DELY1(11),DELY2(11),DELY3(11),DELY4(11),DELY5(11)
      COMMON/SUT5/ RHOF(15,11),UF(15,11),VF(15,11),PF(15,11),HF(15,11)
      COMMON/SUT6/   QM(15,11),QM1(15,11),QM2(15,11),QD(15,11)
     1               ,QNTE(15),QNC(15),QWL(15)
      COMMON/SUT7/ VEL2(15),SA22(15)
      DIMENSION SF(11)
      I = 1
      J = KYS
      IF(IKS) 14,13,13
   13 CONTINUE
      WRITE(6,1050) IKS,TAUT
 1050 FORMAT(1H1,//2X,9HNON-CONVERGED OUTPUT*,10X,*ITERATIONS =*,I4,10X,
     1*TIME =*,E10.3,////)
      GO TO 15
   14 CONTINUE
      WRITE(6,1051) IKS,TAUT
 1051 FORMAT(1H1,///2X,9HCONVERGED OUTPUT*,10X,*ITERATIONS =*,I4,10X,
     1*TIME =*,E10.3,////)
   15 CONTINUE
      DO 1300   KS=1,KSF
      C1=RB(KS)-(UELTA(KS) * SIN(THETA(KS)))
      C2=RB(KS)+(UELTA(KS) * COS(THETA(KS)))
      IF(KS-EQ.1) GO TO 1296
      SF(1) = 0.
      C3 = RB(KS)*RHOB(KS,1)*UB(KS,1)
      DO 1295  KY=2,KYS
      R = RB(KS) + 0.5*(Y(KY)+(C2-RB(KS)))
      C4 = RHOB(KS,KY)*UB(KS,KY)
      SF(KY) = (C4+C3)*.5*DELY2(KY)) + SF(KY-1)
      C3 = C4
 1295 CONTINUE
      AMF = (C2*C2)/2.*DELTA(KS)
      C9 = (SF(KYS) -(RB(KS)*COS(THETA(KS)))**2.
      DELTAN = RB(KS)*RB(KS)/C9
      GO TO 1297
 1296 CONTINUE
      DO 1298  KY=1,KYS
 1298 SF(KY) = 0.
      AMF = 0.
      DELTAN = DELTA(1)
 1297 CONTINUE
      WRITE(6,9711 KS,SI(KS),THETA(KS),BETA(KS),DELTA(KS),DELTAT(KS),
     1RB(KS),RB1(KS),C1,C2,QNTE(KS),QWL(KS),QM1(KS)
  971 FORMAT(//2X,*BODY STATION *,I3,*X,*,E8.4,5X,*THETA =*,F8.4,5X
     1,*BETA =*,F8.4,5X,*DELTA =*,F7.4,5X,*DELTAT =*,E10.3,///2X,22H
     2*RBOD =*,F8.4,5X,*VBOD =*,F8.4,5X,*PSHOC =*,F8.4,5X,*VSHOC =*,
     3F8.4,//2X,22H,*QNT =*,E10.3,5X,*QWC =*,F10.5,5X,*QWL =*,E10.3,//)
      WRITE(6,972) VEL2(KS),SA22(KS)
  972 FORMAT(2X,22H,*VEL2 =*,F10.5,5X,*SA22 =*,E10.3,///)
      WRITE(6,1101 (KY, KY=1,J)
      WRITE(6,1102)          (V(KY)          ,KY=1,J)
      WRITE(6,1103)          (P(KY),KY)      ,KY=1,J)
      WRITE(6,1104)          (RHO(KS,KY)     ,KY=1,J)
      WRITE(6,1105)          (H(KS,KY)       ,KY=1,J)
      WRITE(6,1106)          (U(KS,KY)       ,KY=1,J)
      WRITE(6,1107)          (V(KS,KY)       ,KY=1,J)
      WRITE(6,1108)          (VAM(KS,KY)     ,KY=1,J)
      WRITE(6,1109)          (T(KS,KY)       ,KY=1,J)
      WRITE(6,1110)          (WM(KS,KY)      ,KY=1,J)
      WRITE(6,1111)          (SX(KS,KY)      ,KY=1,J)
      WRITE(6,1112)          (VA(KS,KY)      ,KY=1,J)
      WRITE(6,1113)          (PI(KS,KY)      ,KY=1,J)
      WRITE(6,1114)          (QP(KS,KY)      ,KY=1,J)
      WRITE(6,1115)          (QM(KS,KY)      ,KY=1,J)
      WRITE(6,1116)          (QN(KS,KY)      ,KY=1,J)
      WRITE(6,1117)          (QD(KS,KY)      ,KY=1,J)
      WRITE(6,1118)          (RHOT(KS,KY)    ,KY=1,J)
      WRITE(6,1119)          (U1(KS,KY)      ,KY=1,J)
      WRITE(6,1120)          (V1(KS,KY)      ,KY=1,J)
      WRITE(6,1121)          (P1(KS,KY)      ,KY=1,J)
      WRITE(6,1122)          (T1(KS,KY)      ,KY=1,J)
      WRITE(6,1123)  (TAU(KS,KY),KY=1,J)
      WRITE(6,1124) (SF(KY), KY=1,J)
 1127 FORMAT(2X,7HSF          ,11(1PE10.3,1X))
      WRITE(6,974) AMF,SF(KYS),DELTAN
  974 FORMAT(//15X,*MASS BALANCE F*,5X,*FREESTREAM =*,E10.3,5X,*SHOCK LAYE
     1R =*,E10.3,5X,*DELTA MASS =*,E10.3)
 1101 FORMAT(2X,10HKY          ,11(I7, 9X))
 1102 FORMAT(2X,3HV          ,11(E10.3,1X))
 1103 FORMAT(2X,3HP          ,11(E10.3,1X))
 1104 FORMAT(2X,7HRHO        ,11(E10.3,1X))
 1105 FORMAT(2X,3HH          ,11(F10.3,1X))
 1106 FORMAT(2X,3HU          ,11(E10.3,1X))
 1107 FORMAT(2X,3HV          ,11(E10.3,1X))
 1108 FORMAT(2X,7HM          ,11(E10.3,1X))
 1109 FORMAT(2X,3HT          ,11(E10.3,1X))
 1110 FORMAT(2X,7HWM         ,11(E10.3,1X))
 1111 FORMAT(2X,7HSX         ,11(E10.3,1X))
 1112 FORMAT(2X,7HVA         ,11(E10.3,1X))
 1113 FORMAT(2X,7HPI         ,11(E10.3,1X))
 1114 FORMAT(2X,7HQP         ,11(E10.3,1X))
 1115 FORMAT(2X,7HQM         ,11(E10.3,1X))
 1116 FORMAT(2X,7HQN         ,11(E10.3,1X))
 1117 FORMAT(2X,7HQD         ,11(E10.3,1X))
 1131 FORMAT(2X,7HRHOT       ,11(E10.3,1X))
 1132 FORMAT(2X,7HUT         ,11(E10.3,1X))
 1133 FORMAT(2X,7HVT         ,11(E10.3,1X))
 1134 FORMAT(2X,7HPT         ,11(E10.3,1X))
 1135 FORMAT(2X,7HHT         ,11(E10.3,1X))
 1151 FORMAT(2X,7HTAU        ,11(E10.3,1X))
 1300 CONTINUE
      RETURN
      END

C     * * * * * * * * * * * * * * * * * * * * * * * * * * * * * * * * * *
C
C     SUBROUTINES FOR CHEMICAL EQUILIBRIUM CALCULATIONS AND SOLUTION OF
C     RANKINE-HUGONIOT EQUATIONS.
C
C     * * * * * * * * * * * * * * * * * * * * * * * * * * * * * * * * * *
C

      SUBROUTINE INPUT
      INTEGER FAMDA,FAMDB,CHAR,BLANK
      INTEGER AMDA,AMDB
      COMMON/RADCOM/FRE(31,11),TT(11),YMN(11),HH(11),SPI(1,11,8)
     1               ,THETA,SV1,SP1,SR1,HS
      COMMON /EQMCOM/ RR(31,2),          IFC(31),AT(48),AF(8),WAT(8),
     1               KAT(8),IR(8),IS,KR(LD),CAM(8,1),P,RC(31,2),
     2               RD(31,2),RE(31,2),RP(31,2),T,TK(8,8),TQ(8,8),
     3               TU(31,2),VM(31),VMU(31,8),L2,L3,ITPF,KM2,MCH,MCV,
     4               WM,WTM(31),V1(31),TW(31),ISP2,FAMDA(31),FAMDB(31),
     5               ISP,N,NF31,KIN,KOUT,KAR(20),ATC(8)
      COMMON /EQTCOM/ SEP,MSP,EL,EWL,FLIQ,CPF,IRE,IER,AA,FT3,IN,IL,IT,
     1               MODE,MMELY,SMELY,TMAX,TMIN,MELT,SUMN,SUML,E(84),
     2               E8(8),ERL(8),A(14,14),B(14),EPI(31),ALPC(8),FMU(8),
     3               GAMMC(8),GAMF(8),AC,MC,          CPC,DYE(31),CP(31),
     4               HI31),SB(31),TC(31),WLMC(31),EI3I),TTMIN,TMAX,
     5               FMUS(8),WS,WSS,ISPQ,BC(8),RLMX(8),BY(8),IOC(8),
     6               B1,RKJ,SVA,SVB,SVC,SVD,SUMC,     AW,CNF,EP,IFCJC,
     7               WTG,WTL,JJ(8),BE(8),LCF(8)
      COMMON/SUTCOM/PKS,PKS,WMCS,HEPKS,SIPKS,RHOKS,CPFKS,CSPKS,ALFKS,
     1BETHKS,GAMKS,WELKS,SA2,KYS
      DIMENSION CIJK( 31,1P,TFI)
      DIMENSION ZICPPS(2)
      DIMENSION VMI( 8, 8)
      EQUIVALENCE(FTU( 32),TFI,(VMU,CI)
      DIMENSION SONCE(80), EM(8), JA(7), ALPT(7), TAU(8,8),
     1CC( 8),KPMAI2),RAI2)
      DIMENSION          ICI 8),LIM 8, 8)
  301 FORMAT(1H0)
  302 FORMAT(6E9.4,2F9.0,I1)
 3020 FORMAT(1XAE12.5,F10.4,F11.4,72/1X8E12.5,F10.4,F11.4,12)
  303 FORMAT(1H /1H )
  304 FORMAT(I3,3A4,F9.3,7E8.3)
  306 FORMAT(I7(F3.0,I3), A2,9A4)
      DATA CHAR,BLANK/4HCHAR,4H    /
      KIN = 5
      KOUT = 6
      KPI3)=2
      KP(2) = 1
 3067 M9=0
      P=1.
      VENT=P*1.E-6
      FINT=ALOG(VENT)
      NMR=1.
      READ(KIN,301) IS
      JAT(8)=0
      IX=3
      IF (IS-10) 311,311,399
  311 READ(KIN,3041 (KAT(J), ATA(J), ATBF(J), ATCE(J), WATE(J), ETA(J,I),
     1   I  I=1,8),J=1,15)
      DO 59   J=1,KYS
      DO 59   J=1,IS
      SPI(1,I,J)=ABS(ETA(J,I))
   59 CONTINUE
      DO 49  J=2,IS
      TA(I,I)=0.
   49 CONTINUE
      DO 327 I=1,7
      VA=0.
      DO 322 J=1,IS
      IF(ABS(J)-998 3181,325,3111
 3111 IF(TA(I,J)) 324,322,329
  324 VA=VA-TA(I,K)
      TA(I,K)=-TA(I,K)/WATE(J)
      GO TO 322
  325 VA=VA+TA(I,K)*WATE(J)
  322 CONTINUE
      IF(VA) 326,327,326
  326 DO 323 J=1,IS
  329 TA(I,J)=TA(I,K)/VA
  327 CONTINUE
      K=K+1
      IF(KP(3)) 390,394,394
  394 FFMAX=0.
      AAA=0.
      M=0
      FI=ISP
      J=1
  342 READ(KIN,3061(ALPT(K),JAT(K),K=1,7),SONCE,AMDA,AMDB
      IF(ALPT(1)) 344,399,344
  344 DO 345 K=1,45
  345 C(K)=0.
      DO 349 I=1,7
      IF(JAT(I)) 346,349,346
  346 DO 347 K=1,IS
      IF(JAT(I)-KAT(K)) 347,348,347
  347 CONTINUE
      READ(KIN,3031
      GO TO 342
  348 C(K)=ALPT(I)
  349 CONTINUE
      WT=0.
      L=1
      LAMAX=0
      DO 388 I=1,IS
      IF(C(I)) 387,388,387
  387 LAMAX=LAMAX+L
      WT=WT+C(I) * WAT(I)
  388 L=L+L
      IF(J-ISP) 360,360,369
  360 JM=J+2
      DO 3601 L=1,IS
 3601 C(JL,J)=C(L)
      LAMI(J) = LAMAX
      IF (JM) 320,320,318
  319 DO 314 L=1,JM
      EWL=EWEL*
      UGM=C(JM)
      UWEL,J)=0.
      IF(UGM) 353,316,353
  353 DO 349 I=1,L
  349 UMI(I,J)=UM(I,JJ-UWEL,L)*UGM
      GO TO 342
  316 C(L)=C(L)-TAU(I,L)*UGM
  314 UMI(J,L)=0.
  320 DO 316 I=1,IS
      IF(ABS (C(I))-.0019316,316,317
  317 TAU(I,J)=0.
      DO 396 I=1,JM
  396 VWU(I,I)=-UMI(,J)
      DO 397 I=2,IS
  397 VWU(I,I)=0.
      LAMI(J)=LAMAX
      GO TO 370
  317 IMI(J)=I
      UMI(,J)=UMEL,JI/C(I)
      DO 320 L=1,IS
  320 TAU(L,J)=C(L)/C(I)
      YE=VINT
      K=J
      J=J+1
      IF(J-ISP) 372,372,329
  329 DO 330 L=2,IS
      JM=ISP-L
      IMJ=IMI(JM+1)
      DO 330 K=1,JM
      UGM=TAU(IMJ,K)
      DO 330 I=1,IS
```

```
      330 UME(I,K)=UME(I,K)-UGHPUME(I,J+1)
          DO 333 I=1,IS
      337 IME=IME(I)
          IF(IME)-E) 336,333,336
      336 DO 338 K=1,IS
          V=UME(I,K)
          UMER,IME)=UMER,I)
      338 UMER,I)=V
          IME(I)=IME(IME)
          IME(IME)=IME
          GO TO 337
      333 CONTINUE
C-----ELEMENT -- BASE GAS CORRESPONDENCE
C     INITIALIZE ROW AND COLUMN SUMS
          IG=IS
          DO 403 I=1,IS
          IRE(I)=-1
      401 ICE(I)=-1
C     EVALUATE INITIAL SUMS
          LAND=1
          DO 402 I=1,IS
          DO 403 J=1,IS
          LIME(I,J)=MOD(LAME(J)/LAND,2)
          ICI(J) = ICE(J) + LIME(I,J)
      403 IRI(I)= IRE(I) + LIME(I,J)
      402 LAND=LAND+LAND
C     CHECK FOR ZEROS
      426 EE=0
      404 DO 412 I=1,IS
          IF(ICE(I)-12) 408,405,408
      405 DO 406 J=1,IS
          IF(LIME(J,I)) 407,406,407
      406 CONTINUE
      407 ICI(I)=-1
          IRI(I)=-1
          DO 428 K=1,IS
          LIME(J,I)=0
          IF(LIME(J,K)) 425,427,425
      425 ICE(K)=ICE(K)-1
          LIME(J,K)=0
      427 IF(LIME(K,I)) 422,428,422
      422 LIME(K,I)=0
          IRI(K)=IRE(K)-1
      428 CONTINUE
          GO TO 413
      408 IF(IRE(I)-12) 412,409,412
      409 DO 410 J=1,IS
          IF(LIME(I,J)) 411,410,411
      411 ICE(J)=-1
          IRE(I)=-1
          LIME(I,J)=0
          GO TO 4101
      410 CONTINUE
     4101 DO 410 K=1,IS
          IF(LIME(K,I))424,429,424
      424 IRE(K)=IRE(K)-1
          LIME(K,I)=0
      429 IF(LIME(I,K)) 423,430,423
      423 LIME(I,K)=0
          ICE(K)=ICE(K)-1
      430 CONTINUE
          GO TO 413
      412 CONTINUE
          12=EE+1
          GO TO 404
      413 IG=IG-1
          J=IS+1
          IF(IG) 414,414,426
      414 IF(KP(J)-1) 372,372,415
      415 FAMOA(ES)=AMOA
          FAMOB(ES)=AMOB
          DO 416 I=1,IS
          K=-IRE(I)
          ICI(I)=FAMOA(K)
      416 IMI(I)=FAMOB(K)
          GO TO 372
      369 DO 361 L=1,IS
          VMUI(I,L)=0.
          DO 361 I=1,IS
      361 VMUI(I,L)=VMUI(I,L)+CE(I)*UMI(I,I)
          LAM(CE)=LAMKE
      370 KK=EE
          IE=FI+1
          YC= 0.
  372 RFAQ(KIN,302) (RA(KK),RB(KK,K), RC(KK,K), RQ(KK,K), RE(KK,K),
     1RF(KK,K), ZIGEPS(K), TOLER,K),KP(K),K=1,2)
      IF(KPHAI(I-KPHAE23) 3735,3736,3736
 3733 IF(KPHAI(3+KPHAE23-6) 3734,3737,3736
 3734 WRITE(6,3737) AMOA,AMOB
 3735 FORMAT(////29H BAD PHASE NUMBERING FOR 2&4)
      STOP
 3736 IF(KPHA(3)-1) 3736,3727,3727
 3737 TUI(K,L)=-TUI(K,L)
 3727 CONTINUE
 3722 FAMOA(KK)=AMOA
      FAMOB(KK)=AMOB
      MTM(KK)=MF
      RA(KK,L)= RA(KK,L) + RA(I)
      RB(KK,2) = RB(KK,2) + RA(I)
      N=N+1
      IF(KPHAE3)-1)3734,362,364
  364 ICE(KK)=-1
      VMI(KK)=0.
      YEKK)=YC
      EP(IFE(KK)-TFMAX) 362,362,371
  371 EPMAX=TP(KK)
      GO TO 342
  362 IPC(KK)=0
      VMI(KK)=VINT
      YEKK)=YINT
      GO TO 342
  394 CONTINUE
      DO 375 K=1,4
      DO 375 I=1,IS
      TQI(I,L)=0.
      DO 375 K=1,IS
  375 TQI(I,L)=TQI(I,L)+UMI(I,K)*TP(K,L)
 3752 VMI(N)=0.
      IPC(N)=1
      MTM(N)=1.
      FAMOA(N)=CHAR
      FAMOB(N)=BLANK
      TP(N)=50000.
      RETURN
      END
C
      SUBROUTINE EQUILIBQ,T,PRR)
      INTEGER FN
      INTEGER FAMOA,FAMOB
      COMMON/RADCOM/FRE(3),II),TT(II),VME(II),MME(II),SPE(II,8)
     1                 ,VMETA,SVI,SPI,SRE,45
      COMMON /EQPCOM/ CHE(3),2I,          IFC(3E),AT(48),AIB(E3,MAT(8),
     1               KAT(8),IR(48),IS,RME(OI,LAM(E3I),P,ACC(3),2),
     2               RO(3),2),RF(3),2),RFE(3),2),T,TKE(8,8),TOI(8,8),
     3               TU(3),2),VME(3)),VMU(3),A),L2,E3,ITPP,KR2,HCH,NCV,
```

```
                    4               MR,WTME(3I),XC(3I),YW(3I),ISP2,FAMOA(3I),FAMOB(33),
                    5               ISP,NLME(3),KIN,KOUT,KRR(20),ATC(8)
                     COMMON /EQTCOM/ SIP,HIP,FI,ENL,FLIQ,CPP,IRE,IER,AA,ITS,IN,IL,IT,
                    1               MODE,MMELT,SMELT,TMAX,TMIN,MELT,SUMN,SUML,FRI(9),
                    2               FRE(8),ENLI(8),AE14,14),RE(43,EP(33),ALPE(8),FNUE(8),
                    3               GAMME(8),GAMFE(8),JC,MG,          CPG,DVC3II,CPI33),
                    4               HI3I),SBC5I),TCE3I),VLNK(3II,EE3E),TFMEN,TTMAX,
                    5               PNUE(3I,VS,VSS,ISPD,RC(8),RLNA(8I,BYC(8),TOC(8),
                    6               BI,KKJ,SVA,SVB,SVC,SVD,SUMC,     AV,CMP,EP,IPCJC,
                    7               MTG,WTL,JJE(8),AE(8),LEF(8)
                     COMMON/SUTCOM/TKS,PKS,WMKS,MEPKS,SIPKS,RHOKS,CPPKS,CSPKS,ALFKS,
                    1RETMES,GAMKS,VEL,SAZ,KYS
                     EQUIVALENCE(TUE 32I,TFI,(VMU,CEJ)
                     DIMENSION C3JC 3I,3I),TF(I)
                     DIMENSION APE(36,16),BS(16)
                     DIMENSION 3I(4),KOE3DI
                     EQUIVALENCE(B,K)
                  1 FORMAT(E0I3,3F10.5)
                    3 FORMAT( /8TH  SPECIES  PAR.PRES.     O=LOG-PP       LOG-PP        LO
                     IG=KP      FLAG   ERROR          CP   /(IH2A4,4E13,9,15,2E13.5))
                    7 FORMAT(13,FA.2,11E10.3/9(13E10.3))
                   10 FORMAT(10X1THFRACTION LIQUID =F6.4)
                   42 FORMAT(8F10.4)
                      DTU=500.
                      DTD=DTU
                      TTMIN=250.
                      TTMAX=100000.
                      ITS=0
                      IG=0
                      IMV=0
                      TIDM=1400.
                      TSP=ES+1
                      DO 302 I=1,10
                  302 KB(I)=KOCE3
                      KK=0
                      IF(IRRES)) 304,304,303
                  303 581 = THETA
                      SH1=HS/1.8
                      KK=K-1
                      KP(II=2
                      SVA=(3.3146*581*SVE*COS(SA3))**2/40E09.
                      SVB=SVA*2./1.9869
                      SVC=(SVE*COS(SA))**2/90E08.+SH1
                      SKD=SP1+SVB/(1.3146*SH1)
                      P=SVD
                      GO TO 305
                  304 P=PRR
                  305 MODE=MB(I)
                      KP(6)=-1
                      NZ=51+KP(6)
                      IF (KK(3)-GT-01 IG=1
                      NSP=15
                      IF (KATITS).E3.999 NSP=15-1
                      NSPM1=NSP-1
C*****BOUNDARY LAYER
                  412 ALP(1S)=0.
                      KP(6)=0
                      HEP = MME(I)/3.8
                      ALP(NSP)=1.0
                      IF(ENSPME) 3141,3141,313
                  313 DO 314 K=1,NSPM1
                      ALP(K)=SP1;EE(K)/WTM(K)
                  314 ALPINSP1=ALPINSP1-SP1(E,K)
                 3141 ALPINSP1=ALPINSP1/WTM(NSP)
                      LEF(ES) = 3
                      DO 319 K=1,NSP
                      LEF(I) = 3
                      ARPM=0.
                      IF(KATEE(I-99) 3140,319,3140
                 3140 CONTINUE
                      ARPM=0.
                      DO 315 K=1,NSP
                      DUM=CI)EI,K*ALP(K)
                      ARPM=ARPM+(ARPM,485*DUM)
                  315 ARPM=ARPM-DUM
                      IF (ARPM+.00001*ARPM) 317,317,319
                  317 LEF(IN=KABS(LEF(EI)
                  319 CONTINUE
                      IF (IE-IG) 304,306,350
C*****RECALL STORED VALUES OF BOUNDARY LAYER SOLUTION AND
C     RE-INITIALIZED ONEYED SPECIES
                  350 EE=IE+IG
                      PPM=1,E+APP
                      RINL=ALOG(PPM)
                      DO 354 I=1,N
                      IF(IFC(I)-1) 342,342,341
                  341 IFC(I)=IFC(I)-3
                      GO TO 345
                  342 IF(IFC(I)+1) 343,345,345
                  343 IFC(I)=IFC(I)+3
                  345 IF (IRFC(I)) 348,349,348
                  348 VME(I)=FME(I,IIPP
                      IPC(E)=1
                      YE(I)=0.
                      IF(VME(I)) 347,347,354
                  347 IFC(I)=-1
                      IF (I-IS) 348,348,354
                  348 YE33=PPM
                      GO TO 354
                  349 IF(IPRI(,3II)357,357,352
                  357 VME(I)=0.1*VME(I)*PPM
                      IF(I-(-1) 353,351,353
                  351 VME(I)=PPM
                      GO TO 359
                  352 VME(I)=FME(,EI)*P
                  353 YE(I)=ALOG(VME(I)+1.E-35)
                  354 CONTINUE
                      T=TT(II)/1.8
                      IFCT-T1ON) 355,356,356
                  355 LEF (NSP=EI)=-KABS(LEF(NSP+E))
                  356 WM=SVME(E)
                      II=IT+IG
                      IF (MODE,EQ.0) T=TT(I)/1.8
                      GO TO 393
                  306 VCV=0
                      T=3000.
                      WM=20.
                  393 LAND=1
                      IF(MODE.EQ.0) T=YE(I)/1.8
                      DO 397 K=1,IS
                      IF (LEF(K)) 396,397,397
                  396 DO 396 J=1,N
                      IF(KABS(IFC(J))-1) 389,389,396
                  389 IF(MOD(LAME(J)/LAND,2)) 395,396,395
                  395 VN(J)=0.
                      IFC(J)=IFC(J)-3
                  396 CONTINUE
                      LEF(K)=KABS(LEF(K))
                      J=-IR(K)
                      IF(IFC(J)-1) 3961,3961,397
                 3961 IFC(J)=IFC(J)+6
                  397 LAND=LAND+LAND
                  398 IF(KR(7)-1) 21,21,1902
C*****EVALUATE PROPERTIES
                  170 AAA=1.
```

```
      CPF=CPF/AA
 1702 HG=0.
      HL=0.
      WTL=0.
      DO 1703 J=1,N
      IF(IFCE(J)) 1703,1704,1705
 1704 HG=HG+VN(J)*WT(J)
      GO TO 1703
 1705 HL=HL+VN(J)*WT(J)
      WTL=WTL+VN(J)*WT*C(J)
 1703 CONTINUE
      HIP=(HG+HL)/AA
      VN(11)=AA/P
      TT(11)=TT).6
      DO 195 J=1,N
  195 PRIJ,II)=VN(J)/P
      HH(11)=HIP*1.8
      IF(NA(5)) 510,510,511
  510 CALL RERAY(ISP2,A,0,6,0,0,IG,14)
      ALF=AL2,11/AE1,1)
      CSP=1./SQR(1.+BETA**2)
      BETA=PP(AE2,2)-AE1,2)*RT)-1.
 1933 CSP=CSP/I
      SAN=1.-ALF
      GAN=1./(1.+BETA-1.9869/AA**SAN/CSP**GAMMP1
      CPFKS=CPF
      CSPKS=CSP
      ALFKS=ALF
      BETAKS=BETA
      GAMKS=GAM
  511 CONTINUE
      ITS=-1
 C*****OUTPUT PACKAGE
   10 WM=AA/P
 1902 CONTINUE
      TKS=T
      PKS=P
      WMKS=WM
      SHIP=HIP
      SSIP=SIP
      HEP=0.
      SIP=0.
      DO 20 J=1,N
      HEP=HEP+HE(J)*SIGN(VN(J),WT*(J))
   20 SIP=SIP+ VN(J)*ES(J)-1.9869*Y(J)
      HIP=(HEP+VN(NEL)*(HEL)0+HMFL)/AA
      SIP=(SEP+VN(NEL)*(HEL)0*SMFL)/AA
      RHR=P/TOWM/1.3146
      HIPKS=HIP
      SIPKS=SIP
      OMKS=OM
      IF(NA(5)) 515,515,516
  516 VELSQ= (SQR(SIN(AA))**2  + ((SQR(/RHR)+SQR(VE*RC)/SQR(SA1))**2
      VPL= SQRT(VELSQ)
      SAZ= ASIN(CSV1/VEL*SIN(SA1))
  515 CONTINUE
      IF (FLIQ) 204,203,204
  204 WRITE(KOUT,10) FLIQ
  203 IF (100) 2036,1205,1205
 1203 IF(ITS) 2031,2036,2036
 2031 DO 2033 I=1,N
 2033 VN(I)=VN(I)/P
      DO 2035 I=1,N
 2035 VN(I)=VN(I)*P
      GO TO 2034
 2036 WRITE(KOUT,3) (FAMDA(I),FAMDR(I),VN(I),CV(I),VE(I),VL*W(I),IPC(I),E
     1I),CP(I),I=1,N)
      KPCT8=KPCT8+1
 2034 CONTINUE
      IF(ITS) 11,1021,1021
 1021 HIP=SHIP
      SIP=SSIP
 C*****PRINCIPAL ITERATIVE LOOP
   21 IF(ITS) 109,110,109
  109 IF(NODE) 161,111,110
 1091 ITS=ITS+1
  110 CALL THERM
  111 NODE=KRE(1)
      IQQ=0
      FLIQ=0.
      AA=1.
      CALL WATER
      B1=B(1)
  213 NOE=1
      IF(KR(7)-1) 2101,210,2102
 2102 IQQ=-2
      WRITE(KOUT,2100)(I,I=1,5)
  210 WRITE(KOUT,7) ITS,T,AA,EL,FNL,CMF,(E(I),I=1,15)
 2100 FORMAT (50H1ITS TEMP   PPESSMFT  EQUIL FR  MASSAL ER  SCALE  PE(1),
     1TH MASSAL/90X3(13,7H MASSAL))
 2101 IF(ITS) 2193,221,221
 2103 IF(NODE-1) 170,2104,170
 2104 TMALG=T
      GO TO 170
  221 ITS=ITS+1
      IF(ITS-50) 2219,2219,222
 2219 IF(ITS-47) 22.2222,2222
  222 IF(KRA(10)) 2226,2226,2225
 2225 WRITE(KOUT,2000)
 2000 FORMAT (2//22,50H----FOLLOWING OUTPUT NON-CONVERGENT----------
     1-/90H  ISS,ITEM,II,MITS,ITS,IQQ,KR(6),MIP,SIP,TT(8)),ALP(10),LP(10)
     2/99(1,11))
      WRITE(KOUT,3017) ISS,ITEM,II,MITS,ITS,IQQ,KR(6),MIP,SIP,TT(8))
      WRITE(KOUT,3018) ALP
      WRITE(KOUT,3019) LBP
      WRITE(KOUT,3018) (PRE(I-11),I=1,N)
 3017 FORMAT(2I5,2X1PE12.5)
 3018 FORMAT(2X1P10E11.4)
 3019 FORMAT(2X10(9)
      IQQ=-7
      KRE7)=1
 2226 ITS=-1
      NCV=NCV+1
      NEW=NEV
      IF(NCV-20) 170,170,2220
 2220 MITS=100
      GO TO 170
 2222 KR(7)=3
      IQQ=-2
      GO TO 22
   22 ISPQ=(N+EL-1
      ICT=10
      OUM)=0.
      DO 2205 I=1,ISPQ
 2205 BS(I)=B(I)
      GO TO 2208
 2207 DO 22061=IL,ISPQ
 2206 B(I)=BS(I)
 2208 DO 2204 I=1,ISPQ
      DO 2200 J=1,ISPQ
 2200 APE(I,J)=AC(I,J)
      IF(E-2) 2204,2204,2201
 2201 IF(SPE(E-2)-1) 2204,2204,2202
 2202 NII)=0.
      DO 2203 J=1,ISPQ
 2203 APE(I,J)=0.
      APE(I,I)=1.0
 2204 CONTINUE
      IG=TBO
      CALL RERAY(N,APE(EL,IL),0,B(EL),1,0,IG,14)
      ICT=ICT-1
      IF(ICT-1005 222,2209,2210
 2209 IQQ=-2
 2210 IF(IG) 2212,2221,2221
 2212 IF(INV) 2216,2213,222
 2213 INV = -1
      PTM=PPL*E-5
      DO 2215 I=1,N
      IF(SPCE(I) 2215,2214,2215
 2214 VN(I)=VN(I)*PIN
      Y(I)=ALOG(VN(I)
 2215 CONTINUE
      GO TO 111
 2216 CONTINUE
 2217 ITS=999
      GO TO 111
 C*****IF TRYING TO PUSH THROUGH FMIN OR FMAX -- REINVERT AND DT TO ZERO
 2221 IF(1-TMIN) 2225,227,226
 2225 T=TMIN
      GO TO 1091
  227 IF (XE(1) 228,228,228
  228 IF (T-TMAX) 223,229,2224
 2224 T=TMAX
      GO TO 1091
  229 IF(E(1)) 225,223,228
 C*****IF NEW CONDENSED HAS NEG CORRECTION, DELETE AFTER REINVERT
  223 IF(ERR) 226,252,226
  226 IF(SPE(E(1-1.E-6) 229,218,212
  225 BS(E(E))=-1.E5
      RE(E)=1.E10
      GO TO 2207
 C*****IF S.E. ERROR AND CORRECTION ON T OR COMPLICTING SIGN,REINVERT
  212 IF(NODE-1) 226,213,226
  211 IF(ERE(1)*51*.000011 226,210,219
 C*****N S.E. IF DELTA LN T -GT- .9 REINVERT NO DT IF EL AND FNL ARE SMA
  218 IF(ABS(E(II)-0.91226,226,228
 C*****IF CONVERGED EXCEPT FOR T OR H OR S OPTIONS -- NON CONVERGENT
  228 IF(NODE-1) 2201,214,2280
 2280 IF(EL+100.+FNL-1.E-6) 222,222,2201
 C*****N S.E. OPTION RESULTS IN CONFLICTING ERROR/CORRECTION OR T PUSH
 C*****IF OTHER BALANCES RELATIVELY GOOD, SET T TO TMIN/TMAX AS PER ERROR
  214 IF(ABS(B(I-300.+EL+FNL 3) 2201,215,215
  215 TMIN=T+T(L)/1.E-500.
      TMAX=TMIN=1000.
      IF(B1) 216,216,217
  216 IF(T-TMIN) 170,170,2161
 2160 T=AMAX1(T-DT5,TMIN)
      TTMIN=T
      DTU=DTU/2.
      GO TO 1091
  217 IF(T-TMAX) 2171,170,170
 2171 T=AMIN1(T+TMAX,T+DTU)
      TTMIN=T
      DTU=DTU/2.
      GO TO 1091
 2201 KE(I)=0.
      NODE=0
      IN=IN-1
      IL=2
      GO TO 2207
  224 IF(KR(2)=1.012240,2249,2249
 2240 BS(2)=0.
      A(2,2)=1.E25
      GO TO 2207
 2249 CALL CRECT(NODE)
      TMIN=TMIN
      TMAX=TMAX
      IF(KR(9)-1) 21,21,19
   19 PLEASE=SPEASE
      RETURN
      END

C
      SUBROUTINE CRECT(NOE)
      INTEGER FAMDA,FAMDR
      COMMON/RA4DCOM/PR(3),TE),TE(11),VN(11),HH(11),SPE(),E(,0)
     1                /HETA/SV1,SP1,SR1,HS
      COMMON /EQTCOM/ IE=(3),Z),                IPC(3)),ATA(8),ATB(8),WAT(8),
     1                GA(19),IR(9),55,RR(10),LAN(3)),P,RC(3)),Z),
     2                RO(3),2),HE(3)),ZS),RP(3)),2),T,TR(8),TQ(8),
     3                TQE(8,2),VN(3)),VNU(3),R),L2,L3,TTF,RR2,HF,HV,NCV,
     4                HV,MTH(3)),VE(1),VW(3)),ISP2,FAMDA(3)),FAMDR(3)),
     5                ISP(N,W(3),R1N,KOUT,RRR(20),ATC(8)
     1                SIP,HIP,EL,FNL,FLIQ,CPP,IRP,IER,AA,ITS,IN,IL,IT,
     2                NODE,HRELT,SMELT,TMAX,TMIN,MELT,SUMN,SUME,IB(9),
     3                EB(9),FNLE(3),AE(14),L6),B(14),IP(3)),ALP(9),FNUI(8),
     4                GAMH(9),GAMP(8),JC,NG,                CP0,DV(3)),CP(3)),
     5                HE)3),SPE(3),TC(3),VLMK(3)),ET3),TTMIN,TTMAX,
     6                PNUS(8),WS,WES,ISPQ,BC(49,BLMK(8),BY(8),IBC(8),
     7                WTG,WTL,JJ(8),RE(8),LPF(8)
      DIMENSION C(2( 3),IF,TF(1)
      EQUIVALENCE(TQ( 3),TP),EVMU,CT,J)
      EQUIVALENCE(DVA,DY)
      DIMENSION XA(4)
      DIMENSION CMPF( 3))
      EQUIVALENCE(IR,E)
      CLEAR=AMAX1(1.,ME2(4*ME3)*NG,2*MTG
      SMFL=0.
      SMEG=0.
      DUMP=PP1.E-7
      BUMP=PP1.E-6
      BULP=ALOG(BUMP)
      CMP=1.
    9 K=0
      DO 20 J=2,15
      IF (IB(J)-IB(J-1)) 10,15,20
   10 JA=IB(J)
      IB(J)=IB(J-1)
      IB(J-1)=JA
      K=1
      GO TO 20
   15 IB(J)=1000
   20 CONTINUE
      IF (K) 25,25,9
   25 IB(5)=IB(5)-1000
      M=IB(1)
      M1=1
      L=IB+2
      I=0
      LL=1
      LIM=N+KR(8)
      DO 280 K=1,LIM
      I=I+1
      IF (IB-15) 30,30,65
   30 CONTINUE
      IBC(I)=IBC(I)
      PNUS(I)=0.
      IF (IPCC(I)-3) 35,35,75
```

```
      DYI=XI(I+2)
      IF (IPC(I)+3) 275,40,40
   40 IF (IPC(I)) 205,95,230
   45 IF (IPC(I)+2) 75,50,90
   50 IF (IPC(I)) 70,55,85
   55 VA=E(II)-TC(I)*XE(I)
      DO 65 J=1,IS
      IF (IRC(J)) 60,60,65
   60 VA=VA+VNU(I,J)*E(J+2)
   65 CONTINUE
      DYI=VA
      GO TO 95
   70 IF (IK-IRF) 75,80,15
   75 DYI=0.
      GO TO 275
   80 IPC(I)=1
      DYI=XC(IR)
      GO TO 230
   85 I=I+1
      IF (I-IRP) 90,86,90
   90 DYI=XI(I)
      GO TO 230
   95 HWFG=DWTG+VNE(I)*DYI+WTME(I)
      IF (IPI(I)) 100,195,100
  100 IF (IK-M) 105,145,105
  105 IF (VNE(I)-OUMP) 110,140,140
  110 IF (MOE) 195,195,115
  115 IF (DYI) 120,275,125
  120 IF (VNE(I)/AUMP-.9999995-FMF*DYI) 275,275,130
  125 IF (BUMP/VNE(I)-1.-CMF*DYI) 135,275,275
  130 CMF=(VNE(I)/BUMP-.49999951)/DYI
      GO TO 275
  135 CMF=(BUMP/VNE(I)-1.)/DYI
      GO TO 275
  140 IF (MOE) 175,175,150
  145 MI=MI+1
      M=IRCMI)
  150 IF (DYI) 155,275,160
  155 IF (DYI+CMF+.999) 165,275,275
  160 IF (DYI+CMF-9.) 275,275,170
  165 CMF=-.999/DYI
      GO TO 275
  170 CMF=9./DYI
      GO TO 275
  175 IF (DYI+CMF-2.303) 180,190,190
  180 IF (DYI+CMF+6.9091 185,275,275
  185 CMF=-6.909/DYI
      GO TO 275
  190 CMF=2.303/DYI
      GO TO 275
  195 IF (YCI)-BULP+ABS(DYI*CMF) 275,200,200
  200 CMF=-(YCI)-BULP)/ABS(DYI)
      GO TO 275
C     NON-PRESENT BASE
  205 CONTINUE
  215 IF (YCI)+CMF*DYI-0.1) 275,220,220
  220 DUMI=(1.-YCI))/DYI
      IF (DUMI-.001) 275,275,225
  225 CMF=DUMI
      GO TO 275
  230 DWTG=DWTG+DYI*WTME(I)
      IF (DYI) 235,275,250
  235 IF (VNE(I) 250,250,240
  240 IF (VNE(I)+DYI*CMF) 245,250,250
  245 CMF=-VNE(I)/DYI+1.0000)
  250 CONTINUE
  255 IF (ABS(CMF*DYI)-PI 275,275,270
  270 CMF=P/ABS(DYI)
  275 CMFE(I)=CMF
  280 DYI(K)=DYI
  290 IF (KR(72-1) 315,315,300
  295 FORMAT (1X2(2HX2HVN9X1HYBRE*HVY2X5HSCALF2X1HE9X6HMFC( I9)/(1E66.5E10.
     1 13,13,12,1X,69.5E10.3,F3.1211
  300 WO=1
      WRITE (KOUT,2951 (FRAMRAE(J),VNE(J),YC(J),DYI(J),ELI,CMFE(J),F(J),IPC(J
     1,I=1,J=1,VO)
      WRITE (KOUT,310) (EB(I),I=1,IS)
      WRITE (KOUT,310) (XE(I),I=1,ISP)
      WRITE (KOUT,305) (IRC(I),I=1,IS)
  305 FORMAT (1015)
  310 FORMAT (8E12.4)
  315 CONTINUE
      IF (XI(I)) 320,360,320
  320 XI=XI(I)*CMF
      ABX=ABS(XI(I))
      IF (ABS(XI)-.5) 330,330,325
  325 CMF=.5/ABX
      XI=CMF*XI(I)
  330 IF (XI) 340,360,335
  335 TM=TMAX
      XI=AMIN1(1.2*XI)
      GO TO 345
  340 TM=TMIN
      XI=AMAX1(-0.2,XI)
  345 DTM=(TM-T)/(TMAX*I)
      IF (DTM-1.) 350,355,355
  350 CMF=DTM*CMF
      T=TM
      GO TO 360
  355 T=T/(1.-XI)
  360 AA=AA*EXP(CMF*BE(2))
      MI=1
      M=IRCI)
      WTG=0.
      WTG=0.
      I=1
      L(M)=KR(8)+N
      DO 495 IK=1,LIM
      DYI=CMF*DYI(IK)
      IF (DYE) 395,390,395
  390 IF (IPC(I)) 495,435,405
  395 IF (IPC(I)) 455,400,480
  400 IF (IPI(I)) 405,430,405
  405 IF (M-IK) 410,415,410
  410 IF (MOE) 430,430,420
  415 MI=MI+1
      M=IRCM)
  420 VNC(I)=VNC(I)+E(1,*DYI)
      IF (VNE(I)) 430,430,425
  425 YC(I)=ALOG(VNE(I))
      GO TO 435
  430 YC(I)=YC(I)+DYI
      VNE(I)=EXP(YC(I))
  435 VA=WTME(I)*VNE(I)
      WTG=WTG+VA
      IF (IK-ISP 440,440,445
  440 PNUS(I)=VNE(I)
      GO TO 495
  445 DO 450 K=1,IS
      VA=VNUE(I,K)*VNE(I)
      PNUS(K)=PNUS(K)+VA
  450 CONTINUE
      GO TO 495
C     NON-PRESENT BASE CORRECTIONS AND TESTS
  455 YC(I)=YC(I)+DYI
      IF (YC(I)) 495,460,460
  460 IF (IPC(I)+1) 495,465,465
  465 CONTINUE
  475 YC(I)=0.
      IPC(I)=+1
      GO TO 495
  480 VNE(I)=VNC(I)+DYI
      IF (VNE(I)) 490,490,485
  485 WTG=WTG-VNE(I)*WTME(I)
      GO TO 495
  490 VNE(I)=0.
      IPC(I)=-1
  495 I=I+1
      RETURN
      END
C
      SUBROUTINE THERM
      INTEGER FA
      INTEGER FANQA,FANOR
      COMMON/RADCOM/ER(36),EB,TT(11),VMNE(11,MHE(11),SPE(1,1L,8)
     1                ,THETA,SVI,SPI,SRI,HS
     COMMON /EQPCOM/ RB(31,2),                    IPC(31),ATA(8),ATB(8),MAT(8),
     3               KAT(8),EN(48,IS,KRE(10),LAM(31),P,RCE(31,2),
     2               RDC(31,2),PF(31,7),RE(31,2),T,TK(8),B1,FOR(8),
     3               TUE(31,2),VNC(11),VNE(31,2),IZ,L3,ETFF,KR2,MCH,NEV,
     4               WM,WTME(31),YI(31),YW(31),ISP2,FANOA(31),FANOB(31),
     5               ISP,N,M(5),KFN,KOUT,KRP(20),ATC(8)
      COMMON /EQPCOM2/ SSP,NSP,FL,ENE,FLTQ,CPF,IRF,IER,AA,ITS,IN,IL,ET,
     1               NODE,WHIT,SMELT,TMAX,TMIN,WFLT,SUMN,SUNE,IR(9),
     2               EA(8),FAL(8),AE(4,14),AI,RC(24),TP(31),ALPC(8),PNUC(8),
     3               GAMM(8),GAMC(8),JC,MG,          CPG,DYI(31),CPE(31),
     4               HI(31),SBI(31),TC(31),VLNK(31),EE(31),TTMEN,TFMAX,
     5               PNUS(8),WS,WSS,ISPQ,RE(8),BLNK(8),BYI(8),TBC(8),
     6               B1,KRJ,VA,SVA,SVE,SVD,SUNC,     RV,CMF,FP,IFCJC,
     7               WTG,WTL,JJCE(1,RFE(),EFF(8)
      DIMENSION CE(( $1,1),YF(1)
      EQUIVALENCE(FUI 329,YF),(VNU,(1,1)
    5 NODE=KR(1)
      IF (ITS) 50,10,50
   10 WTG=0.
      WTL=0.
      IF (KR(18)) 40,40,15
   15 IF (IFC(KR(1)-1) 25,20,25
   20 IF (TM-.001-TP(N+1)) 25,25,30
   25 IPC(N+1)=-1
      VNI(N+1)=0.
      DO 35 K=1,IS
   35 VNU(N+1,K)=-FQCK,5)
      WFL=-VNI(N+1)
   40 CONTINUE
      SUNN=0.
      DO 45 I=1,IS
      PNUS(I)=0.
   45 CONTINUE
   50 HMELT=0.
      FLTQ=0.
      SMELT=0.
      WFL(=1
      TMIN=TTMIN
      TMAX=TTMAX
      TFMAX=500.
      VA=ALOG(TF/3000.)
      VB=T-3000.
      VC=(T+3000.)/2.
      VD=T+3000.
      VE=VC/(VD*VD)
      PT=1.986*T
      I=1
      DO 235 IN=1,N
      J=2
      IF (IPC(I)+1) 165,45,45
   85 IF (IPC(I)) 90,95,120
   90 IF (MODE-1) 165,160,165
   95 IF (ITS) 165,100,165
  100 SUMN=SUMN+VNE(I)
      SUNE=SUNE(I)*VNE(I)
      WTG=WTG+DUMI
      IF (II-15) 105,105,110
  105 PNUS(I)=VNE(I)
      GO TO 165
  110 DO 115 K=1,IS
      DUMI=VNUE(I,K)*VNE(I)
      PNUS(K)=PNUS(K)+DUMI
  115 CONTINUE
      GO TO 165
  120 IF (IPC(I)-3) 125,125,165
  125 IF(ITS) 150,145,150
  145 WFL=WFL+VNE(I)*WTME(I)
  150 IF (MODE-1) 165,155,165
  155 TMIN=AMAX1(TMIN,TPC(I))
  160 TPMAX=AMAX1(TPE(I),TPMEX)
  165 IF (IT-ABS(TUE(I,1)) 170,175,175
  170 J=1
  175 CPE(I)=RC(I,J)+TPROC(I,J)*PC(I,J)/(TMC)
      HI(I)=RB(I,J)+VAOPC(C(I,J)+ROT(I,J)*VC(I)*EE(I,J)/VD)
      SBE(I)=RF(I,J)*RC(I,J)*VA+VNO*PC(I,J)*EE(I,J)*VE)
      IF (MODE-2) 210,180,180
  180 IF (IPC(C)-1) 210,185,210
  185 IF (TUE(I,1)) 190,210,210
  190 IF (T-TUE(I,1)) 200,195,206
  195 HMELT=-HE(I)-HMELT
      SMELT=-SE(I)-SMELT
      WFLT=I
      IF (J-2) 210,170,210
  200 TMAX=AMIN1(TMAX,-TUE(I,1))
      GO TO 210
  205 TMIN=AMAX1(TMIN,-TUE(I,1))
  210 PC(I)=HE(I)/RT
      VLNK(I)=TC(I)+SBE(I)/1.98E3
      IF (IR-15) 215,215,220
  215 BLNK(I)=VLNK(I)
      IPC(I)=IPE(I)
      BC(I)=TC(I)
      GO TO 235
  220 DO 230 K=1,IS
      IF (IRC(K)+1) 230,225,225
  225 VLNK(I)=VLNK(I)-VNUE(I,K)*BLNK(K)
      TC(I)=TC(I)-VNUE(I,K)*RC(K)
  230 CONTINUE
  235 I=I+1
      IF (MODE-1) 250,240,250
  240 IF (TFMAX-T) 245,250,250
  245 T=TMAX
      IF(T-500.) 248,248,5
  248 WRITE(KOUT,2401
      STOP
  249 FORMAT(//'38H NO AVAILABLE SURFACE SPECIES. . .STOP)
  250 IF (ITS) 385,255,385
  255 RA=PMIN
  165 SUMN=SUMN/P
      SUML=ALOG(SUMN)
      WTG=WTG/SUMN
      WTL=WTL/SUMN
      SUNC=1.0
  385 RETURN
```

```
      END
C
      SUBROUTINE MATER
      INTEGER FAMOA,FAMOR
      DIMENSION EQC(11),EES(31)
      DIMENSION EBS(14)
      COMMON/RADCOM/FR(31,11),TF(11),VMV(11),HH(11),SP(11,8)
     1             ,THETA,SV1,SP1,SR1,HS
      COMMON /EQPCOM/ CH(31,2),          EFC(31),ATA(8),ATB(8),WAT(8),
     1                KAT(8),IREP(1,5),RR(10),LAM(31),P,RC(31,2),
     2                RO(31,2),HE(31,2),RF(31,2),T,TK(8),TO(8),
     3                TU(31,2),VM(31),VNU(31,8),L2,L3,ITF,KR2,MCH,NCV,
     4                MM,WTM(31),VI(31),VMI(31),ISP2,FAMOA(31),FAMOR(31),
     5                ISP,N,W(3),KIN,KOUT,KKR(20),ATC(8)
      COMMON /EQTCOM/ SIP,MIP,IFL,ENL,FLIQ,CPF,IRE,IER,AA,TTS,IN,IL,IT,
     1                MODE,MMELT,SMELT,TMAX,TMIN,MELT,SUMN,SUML,BB(9),
     2                EB(8),ERR(10),AA(6,6),B(6,1),IP(31),ALP(8),FNU(8),
     3                GAMM(8),GAMF(8),JC,MG,          CPG,DY(31),CPI(31),
     4                W(31),SBI(31),TC(31),VLMER(31),E(31),TMIN,TMAX,
     5                PNUS(8),NS,MSS,ISPQ,BC(8),BLNK(8),BV(8),IBC(8),
     6                R1,KKJ,SVA,SVM,SVC,SVD,SUMC,     MV,CNF,EP,EFCJC,
     7                NTG,WTL,JJ(8),RR(8),LFP(8)
      DIMENSION VLAM(31,11),XI(6)
      DIMENSION CEJ( 31,11,TF(11)
      EQUIVALENCE(TU( 321,TF(1,VMV(1))
      MSS=MS
      DO 5 I=1,IS
    5 IBC(I)=IFC(I)
   40 RV=MSS-WTL/WTG
      IF (RR(7)-1) 70,45,50
   45 IF (ITS) 70,60,70
   50 CONTINUE
      KK(7)=KK(7)-1
      IF (KK(7)-1) 70,60,70
   60 WRITE (KOUT,65) (I,I=1,IS)
   65 FORMAT (50HLISTS TEMP   PRESSMOL  EQUIL FR  MASBAL ER  SCALE  7(13,
     17H MASBAL1/90X3(13,7H MASBAL))
C     INITIALIZE
   70 FL=0.
      SPG=0.
      EP=0
      CPF=0.
      JC=0
      JCS=0
      ISP=IS+1
      ISPQ=IS+2
      B(1)=0.
      B(2)=0.
      A(1,1)=0.
      A(1,2)=0.
      A(2,1)=0.
      A(2,2)=0.
C     -----INITIALIZE CONTRIBUTION OF MOST SIGNIFICANT SPECIES IN EACH M
      DO 75 I=1,IS
      ERR(I)=0.
   75 E(I)=AMAX1(P(I)
      ISP2=ISPQ
C     - - - - MAIN BASE SPECIES LOOP
      DO 125 I=1,IS
      K=2-ERR(I)
      IF (KAT(I))-99) 85,80,85
   80 PNUS(I-2)=0.
C     ZERO MATRIX
   85 DO 90 K=1,ISPQ
   90 A(K,I)=0.
      IF (ITS) 110,95,110
C     NORMALIZE ON PRESSURE ON FIRST PASS
   95 VMI(I-2)=VMI(I-2)/SUMN
      EBL(I-2)=0.
      IF (IBC(I-2)) 110,100,105
  100 Y(K-2)=P(I-2)-SUML
      GO TO 110
  105 VMI(I-2)=VMI(I-2)/SUMC
C     INITIALIZE SOME MORE
  110 A(I,I)=0.
      A(1,I)=0.
      IP(I-2)=0.
C     SET FLAG INDICATING SIGNIFICANCE OF SPECIES IN MASS
C     BALANCE(S) AND INCREMENT COUNT ON SIGNIFICANT SPECIES
      IF (VMI(I-2)-EBL(I-2)) 120,120,115
  115 IP(I-2)=1
C     TREAT BASE SPECIES CONTAINING BUT NOT REPRESENTING NON-PRESENT
C     ELEMENTS IN SAME MANNER AS NON-PRESENT CONDENSED SPECIES
  120 IF (IBC(I-2)+1) 325,125,125
  125 IF (IBC(I-2)) 180,215,130
  130 A(1,1)=1.
      VA=VMI(I-2)
      IF (1ABS(EBC(I-2)-99-1) 135,200,140
  135 A(2,1)=1.0
      GO TO 290
  140 IF (EBC(I-2)-ABS(VA)) 145,150,150
  145 EBC(I-2)=ABS(VA)
      IBC(I-2)=I-2
  150 F(I-2)=E(I-2)-VA
  155 IF (MODE-1) 280,170,280
  170 TMIN=AMAX1(TMIN,TF(I-2))
      IF (T-TF(I-2))+.003) 175,175,180
  175 A(1,1)=1.0E+10
      F(I-2)=-VMI(I-2)*1.0D1E+10
      MODE=0
  180 IF (MODE-1) 185,190,185
  185 IF (KKC(8)) 280,280,190
  190 IF (TF(I-2)+.001-T) 325,195,195
  195 IF (JC) 205,205,200
  200 IF (Y(I-2)-BJC) 325,325,205
  205 BJC=Y(I-2)
      JCS=JC
      TMAX=TF(I-2)
      JC=I-2
      EFCJC=IBC(I-2)
      IF (KR(8)) 210,210,280
  210 A(1,JCS+2)=0.
      A(1,I)=-1.0
      GO TO 325
C     -----GAS PHASE
  215 VA=VMI(I-2)
      CPG=CPG+VA*CP(I-2)
      A(1,1)=VA
      A(2,1)=VA
      EP=EP+VA
  275 ERR(I-2)=ABS(VA)
      IBC(I-2)=I-2
      F(I-2)=F(I-2)-VA
  280 IF (MODE-2) 320,300,285
  285 IF (IBC(I-2)) 325,295,290
  290 MOS=SBI(I-2)
      GO TO 305
  295 MOS=SBI(I-2)-1.98809*Y(I-2)-1.98A9
      GO TO 310
  300 MOS=MI(I-2)
      IF (IBC(I-2)) 325,310,305
  305 A(1,I)=MOS
      GO TO 315
  310 A(1,3)=MOS*VMI(I-2)
  315 A(1,2)=A(1,2)-MOS*VMI(I-2)
  320 CPF=CPF+CP(I-2)*VMI(I-2)
  325 CONTINUE
      DO 330 I=1,IS
      RE(I)=E(I)
  330 BY(I)=Y(I)
      IER=0
      IRE=0
      EER=0.
C     - - - - MAIN NON-BASE SPECIES LOOP
  350 LIM=NKR(8)
      IF (LIM-ISP) 730,355,355
  355 J=ISP
      DO 725 IN=ISP,LIM
      IF (TK-NI) 365,365,360
  360 F(J)=1.E-10
      IF (IFC(J)) 410,725,445
  365 IF (IFC(J)+1) 725,370,370
  370 IF (EFS) 390,375,390
  375 VMI(J)=VMI(J)/SUMN
      IF (EFC(J)) 390,385,380
  380 VMI(J)=VMI(J)/SUMC
      GO TO 390
  385 Y(J)=Y(J)-SUML
  390 F(J)=VLM(J)-Y(J)
      DO 405 I=1,IS
      IF (IBC(I)) 400,400,395
  395 FNU(I)=0.
      GO TO 405
  400 FNU(I)=VNU(J,I)
      F(J)=F(J)+FNU(I)*RY(I)
  405 CONTINUE
  409 EAB=ABS(E(J))
      IF (IFC(J)) 410,490,445
C     CONDENSED SPECIES
  410 EAB=E(J)
  425 IF (E(J)-ERR) 535,535,430
  430 ERR=E(J)
      IF (IER) 435,435,440
  435 ISPQ=ISPQ+1
      IER=ISPQ
  440 IF=IER
      IRE=IN
      GO TO 450
  445 ISPQ=ISPQ+1
      IER=ISPQ
  450 ATB=0.
  460 DO 465 I=1,ISPQ
      A(I,IE)=0.
  465 A(IE,I)=0.
      DO 480 K=1,IS
      DUM=VNU(J,K)
      IF (IBC(K)-1) 470,470,480
  470 A=DUM*VMI(J)
      A(K+2,IE)=DUM1-WTM*PNUS(K)+GAMF(K)*WTG)
      B(K+B(IE))-YA
      IF (ABS(YA)-ER(K)) 480,480,475
  475 B(K)=ABS(YA)
      IR(K)=IN
  480 CONTINUE
      X=IF-ESP
      IF (IN-NP 505,505,485
  485 JJ(EX)=JC
      B(EE)=Y(JC)
      IF (JC-IS) 495,495,490
  490 A(IP,I)=FC(JC)
      B(EE)=E(JC)
  495 JJ(K)=J
      JJ(K)=J
      A(IP,I)=FC(J)
      B(EE)=E(J)
      IF (F+.001-TF(J)) 515,510,510
  510 IF (NKR(8)) 930,930,540
  515 EP(MOF-1) 530,529,580
  525 A(IE,IE)=1.E+10
      B(IE)=-VMI(J)*1.0D1E+10
      MODE=0
  530 IF (MODE-2) 535,575,540
  535 IF (MODE-1) 715,540,715
  540 IF (F-TF(J)-.003) 545,545,560
  545 IF (JC) 555,555,550
  550 IF (E(J)-BJC) 725,725,555
  555 BJC=E(J)
      JC=J
      IFCJC=IFC(JC)
      TMAX=TF(J)
      IF (IRR(8)) 565,560,560
  560 IF (MODE-2) 724,575,580
  564 BC(I)=BJC
      DO 570 K=1,IS
      A(I,K+2)=-FNU(K)
      A(K,I)=FC(J)
  570 CONTINUE
      GO TO 725
  575 MOS=MI(J)
      GO TO 585
  580 MOS=SBC(J)
  585 A(1,IE)=MOS
      A(1,IP)=A(1,2)-VMI(J)*MOS
      CPF=CPF+CP(J)*VMI(J)
      GO TO 715
C     GAS PHASE SPECIES
  590 IP(J)=0
      IF (VMI(J)) 595,715,595
  595 ID=0
      CPG=CPG+VMI(J)*CP(J)
  625 DO 680 K=1,IS
      I=2-ER(K)
      VA=VNU(J,I-2)*VMI(J)
  645 BP(K-2)=BE(I-2)-VA
      ABSVA=ABS(VA)
  650 IF (ABSVA-ER(I-2)) 680,660,655
  655 ID=1
      IF (ABSVA-ER(I-2)) 670,670,665
  660 IF (ABSIVA)-EBL(I-2)) 680,680,670
  665 EBL(I-2)=ABSVA
      IR(I-2)=IN
  670 DO 675 K=3,ISP2
  675 A(I,K)=A(I,K)+VA*FNU(K-2)
      B(I)=B(I)-VA*E(J)
      A(1,1)=A(1,1)-VA*FC(J)
      A(2,I)=A(2,1)+VMI(J)*FNU(I-2)
  680 CONTINUE
      IF (ID) 715,715,685
  685 FP=EP-VMI(J)
      JP(J)=-1
      B(2)=B(2)-VMI(J)*E(J)
      A(2,1)=A(2,1)-VMI(J)*FC(J)
      IF (MODE-2) 710,690,695
  690 MOS=MI(J)*VMI(J)
      GO TO 700
  695 MOS=VMI(J)*(SBC(J)-1.98809*Y(J)-1.98A9)
  700 DO 705 I=1,ISP2
```

```
      705   A(I,I)=HOS*FNU(I-2)+A(I,I)
            A(I,2)=A(I,2)-HOS
            A(I,J)=A(I,J)-HOS*YC(J)
            R(I)=B(I)-HOS*E(J)
      710   CPP=CPP+VN(J)*CP(J)
      715   IF (EL-EABS) 720,725,725
      720   EL=ERR
      725   J=J+1
      730   CONTINUE
            ISP3=ISP+3
            IF (MODE-2) 735,735,760
      735   CPA=CPP*P
            SMALT=SMELT*VN(MELT)
            EHS=AAMHP*A(1,2)
            IF (KKJ+1) 750,740,750
      740   DUM1=SVA/AAMTHT
            EHS=AA*SVC-DUM1*A(1,2)
            HIP=-A(1,2)/AA
            A(1,2)=-AA*SVC-DUM1
            CPA=(CPP+2.*DUM1/T)*AT
            DUM2=SVB/AA*T
            P=P-EP
            EP=0.
            IF (ABS(EHS/AA)-10.) 765,765,740
      745   EPA=P+SVD-DUM2
            A(2,1)=A(2,1)+DUM2
            A(2,2)=-DUM2
      750   IF (KKK2)-MODE) 765,755,765
      755   A(1,2)=-AA*MHP
            GO TO 765
      760   CPA=CPP
            SMALT=SMELT*VN(MELT)
            EHS=AA*SIP+A(1,2)-1.9869*(P-EP)
            A(1,2)=-AA*SIP
      765   B(1)=B(1)+EHS
            R(1,1)=A(1,1)+CPA
            IF (SMALT) 785,785,770
      770   IF (EHS) 785,780,775
      775   EHS=EHS-SMALT
            A(1)=B(1)-SMALT
            IF (EHS) 780,785,785
      780   FLIQ=1.+EHS/SMALT
            MODE=0
            A(1,1)=1.E+10
            T=(N=500.
            T=MAX=5000.
      785   ENL=ABS(EP)/PP*100.
            DO 810 I=3,ISP2
            F(I-2)=B(I)-2)
            ERR(I-2)=ABS(F(I-2)*1.E-7
            IF (IPC(I-2)-1) 799,795,799
      790   NP=N=P+1
            GO TO 810
        795 CONTINUE
      800   EA=E(1-2)
            ARR=ABS(ER)/(ABS(I-2)+1.E-20)
            ENL=AMAX1(ARR,ENL)
            R(I)=A(I)+EP
      810   CONTINUE
            IF (ISP2-ISP01 815,880,880
      815   IV=0
            JJ=0
      C     ADD CONDENSED NONBASE SPECIES TO ARRAY
            DO 840 IF=ISP3,ISPO
            J=IF-(SP2
            J=JJ(J)
            IF (J-IS) 820,820,830
      820   DO 825 K=1,IS
      825   A(IF,K+2)=0.
            A(IF,J+2)=-1.0
            GO TO 840
      830   DO 835 K=1,IS
      835   A(IF,K+2)=-VNU(J,K)
      840   CONTINUE
      C     ELIMINATE TERMS CORRESPONDING TO PRESENT BASE CONDENSED
            DO 855 K=1,IS
            IF (IPC(K)) 855,855,845
      845   DO 850 I=ISP3,ISPO
      850   A(IF,K+2)=0.
      855   CONTINUE
      880   R(2)=EP*R(2)
            IF (MODE-1) 910,890,885
      885   IF (ABS(EHS/A(1,1))-.0001) 910,910,920
      890   IF (IPC(C) 895,900,905
      895   IF (IJC-1)E) 900,905,900
      905   MODE=0
            TMIN=TTMIN
            TMAX=TTMAX
      900   IF (ABS(R(1))-1.E-6) 910,910,920
      910   IF (EL-1.E-6) 915,915,920
      915   IF (FNL-1.E-5) 935,955,920
      920   EN=ISPO
            IL=1
            IF (MODE) 925,925,930
      925   IN=ISPO-1
            IL=2
            EX(1)=0.
      930   RETURN
      935   IT=ITS+1
            ITS=-1
            GO TO 930
            END
      C
            SUBROUTINE RERAY(N,C,MM,D,MNN,LS,IS,ND)
      C     DIRECT INVERSION PROCEDURE  --  C IS REPLACED BY C##-1
            DIMENSION DI(4,8),SDI(80),CI(4,1),LI(80),S(60),LL(60),LLL(60),&S(1)
            KIN=5
            KOUT=6
            MI=M+1
            MP=M+MM
            DO 11 I=1,MP
            LLL(I)=1
            IF(LS(I)) 119,115,112
        112 L(I)=LS(I)
            GO TO 11
        119 L(I)=1
         11 CONTINUE
            IX=-1
            IF(IS+2) 111,109,111
        106 FORMAT(1LH  L(I),I=1,13,5X (3DI3))
        107 FORMAT(15H  I(C(I,J),J=1,I+1),I=1,I3,15H)  BE
           1FORE RERAYS
        108 FORMAT(2X, 11E10.3/(12X, 10E10.3))
        109 WRITE(KOUT,107) MP,MMN,N
            WRITE(KOUT,106)NP,(LI(I),I=1,NP)
            IX=0
            DO 110 I=1,N
        110 WRITE(KOUT,108)(C(I,J),J=1,NP1,(DI(,J),J=1,MMN)
        111 IS=1
      C     TRIANGULATE MATRIX
            DO 19 I=1,N
            DO 160 M=1,NP
        160 S(M)=ABS(C(I,M))
            IF(IS) 18,16,16
        18  IS=0
            SDI(I)=1.
            GO TO 12
      C     REDUCE ROW I BY PRECEEDING ROWS
        16  DO 17 J=2,I
            K=L(J-1)
            DIV=-C(I,K)
            IF(DIV) 161,17,161
       161  C(I,K)=0.
            DO162 M=1,NP
            DIVC=DIV*C(J-1,M)
            S(M)=AMAX1(S(M),ABS(DIVC))
       162  C(I,M)=C(I,M)+DIVC
            IF(MMN) 17,17,163
       163  DO 164 M=1,MMN
       164  DI(,M)=DI(,M)+DIV*DI(J-1,M)
         17 CONTINUE
      C     SEEK MAXIMUN PIVOT
         12 DIV=0.
            DO 13 JJ=1,N
            M=L(JJ)
            IF(ABS (C(I,M))-DIV)13,13,131
       131  DIV=ABS (C(I,M))
            K=M
            J=JJ
         13 CONTINUE
            IF(S(K)) 130,131,130
       130  SDI(I) = DIV/S(K)
            L(J)=L(I)
            L(I)=K
            IF(SDI(I)-1.E-8) 131,131,14
      C     SINGULAR MATRIX RETURN
       131  IS=-1
            WRITE(KOUT,151) (I),L(I),SDI(I),I=1,I)
            RETURN
         14 DIV=C(I,K)
            C(I,K)=1.0
            K=L(L(J)
            LL(J)=LLL(I)
            LLL(I)=K
            LL(K)=1
      C     NORMALIZE ROW
            IF(MMN) 143,143,241
       141  DO 142 J=1,MMN
       142  DI(,J)=DI(,J)/DIV
       143  DO 15 J=1,NP
         15 C(I,J)=C(I,J)/DIV
            IF(IDIV)19,20,19
         19 C(I,K)=0.
            IF(MMN) 191,191,192
       192  DO 193 M=1,MMN
       193  DI(,M)=DI(,M)+DIV*DI(I-1,M)
       198  DO 201 M=1,NP
       201  C(J,M)=C(J,M)+DIV*C(I-1,M)
         20 CONTINUE
      C     INTERCHANGE COLUMNS
            DO 30 I=1,NP
            J=II
         21 J=L(I)
            L(I)=I
            IF(J-1)22,30,22
         22 IF(IS)225,25,25
         23 DO 24 M=1,N
            S(M)=C(M,I)
         24 C(M,I)=C(M,J)
            I=J
            GO TO 21
         25 IF(IS-1)26,26,26
         26 DO 27 M=1,N
         27 C(M,I)=C(M,J)
            I=J
            GO TO 21
         28 DO 29 M=1,N
         29 C(M,I)=S(M)
            IS=0
         30 CONTINUE
      C     INTERCHANGE ROWS
            DO 40 I=1,N
            I=II
         31 J=LL(I)
            LL(I)=I
            IF(J-1)32,40,32
         32 IF(IS)325,33,33
         33 DO 34 M=1,NP
            S(M)=C(I,M)
         34 C(I,M)=C(J,M)
            IF(MMN) 343,343,341
       341  DO 342 M=1,MMN
            SDI(M)=DI(,M)
       342  DI(,M)=DI(,M)
       343  IS=1
            I=J
            GO TO 31
         35 IF(IS-J)36,38,36
         36 DO 37 M=1,NP
         37 C(I,M)=C(J,M)
            IF(MMN) 373,373,371
       371  DO 372 M=1,MMN
       372  DI(,M)=DI(J,M)
       373  I=J
            GO TO 31
         38 DO 39 M=1,NP
         39 C(I,M)=S(M)
            IF(MMN) 393,393,391
       391  DO 392 M=1,MMN
       392  DI(,M)=SDI(M)
       393  IS=0
         40 CONTINUE
            IF(IX) 411,409,411
       407  FORMAT(15H  ((C(I,J),J=1,I+1),I=2MI,10(J),J=1,I3, 6H),I=1,I3,15HI  AF
           1TER RERAY  )
       409  WRITE(KOUT,407) NP,MMN,N
            DO 410 I=1,N
       410  WRITE(KOUT,108)(C(I,J),J=1,NP),(DI(,J),J=1,MMN)
       411  RETURN
            END
      C     * * * * * * * * * * * * * * * * * * * * * * * * * * * * * * * * * *
      C
      C     SUBROUTINES FOR RADIATIVE TRANSPORT CALCULATIONS.
      C
      C     * * * * * * * * * * * * * * * * * * * * * * * * * * * * * * * * * *
      C
            SUBROUTINE RADEN
      C
```

```
C     ... READS IN DATA FOR THE RADIATION TRANSPORT CALCULATION
C
      COMMON/RAD/ANHV(50),AHVL(25),C1,C2,C3,C4,C5,DELTA,EPSI(96),FF(3000),
     1FHV(25),FHVC(50),FHVW(25),FHVP(25),FINI(11),FIPI(11),FL1,FL2,FLG,
     2FLG1,GAMP(300),GEE(56),MI(14),M2(14),NAES,NBLP,ND(300),NIC,NICN(11
     3),NIHVC,NHV,NU(25),NY,PRFS(11),TEE(11),WDLE(11),XMOL,XQ(7,11),YDELT
     4,YY(11),CASE(15),TMSW(50),TMSWL(25) ,TW
      COMMON/LINE/HVL(3001,K1,K2,TLCH(11),TLCPE(11),XNN(10,11),NXI,IA(9)
     1,NI,XNOLE(300) ,GUPE(300)
      COMMON/INTCON/KRI(20),M,N
      COMMON/CONTM/NCRC(20)
      M=5
      N=6
      READ(M,902)NCRC(J),J=1,20)
  902 FORMAT(20I3)
      READ(M,100)NHV,NAES,NXI
  100 FORMAT(6F12.1)
C
C     INPUT TABLES 1,11
C
      READ(M,226) (GFE(I),I=1,NAFS)
      READ(M,226) (EPSE(I),I=1,NAES)
      READ(M,226) (FHVN(I),I=1,N+V)
      READ(M,226) (FHVP(I),I=1,NHV)
      READ(M,226) (FHVE(I),I=1,NHVE)
  226 FORMAT(6F12.4)
      IF(NXII) 50,80,81
   81 READ(M,101) (LBE(I),I=1,NXI)
   80 READ(M,101) (NOET(I,I=1,NHV)
  101 FORMAT(40E2)
      IS=0
      DO 1 I=1,NHV
    1 IS=IS+NU(I)
      READ(M,102)(NOII),HVL(I),FF(I),GAMP(I),XNOLE(I),GUPE(I,I=1,IS)
  102 FORMAT(I2,10X,2E12.1,9E12.3)
      DO 413 I=1,15
      IF(XNOLE(I).EQ.0.) XNOLE(I) = 1.
  413 CONTINUE
      DO 513 I=2,15
      IF(HVLE(I)-HVLE(I-1)) 514,514,513
  514 WRITE(6,4000) HVLE(I)
      STOP
  513 CONTINUE
 4000 FORMAT(23H****LINE CENTER ***  AT ,E9.3,23H IS OUT OF SEQUENCE****)
C
C     INPUT HV VALUES FOR CONTINUUM CALCULATION
C
      READ(M,119) NIHVC
  119 FORMAT(2415)
      READ(M,109) (FHVC(I),I=1,NIHVC)
      DO 582 I=2,NIHVC
      IF(FHVC(I)-FHVC(I-1)) 582,582,580
  582 WRITE(6,4001) FHVC(I)
      STOP
  580 CONTINUE
 4001 FORMAT(21H****CONTINUUM FREQ AT ,F9.3,23H IS OUT OF SEQUENCE****)
  440 DO 355 I=1,NIHVC
      TMSWII = 0.
  355 ANF(I) = 1.
      DO 456 I=1,NHV
      TMSWL(I) = 0.
  456 AHVL(I) = 1.
      RETURN
      END
C
      SUBROUTINE RADIC4L
      COMMON/INTCON/KRI(20),M,N
      COMMON/RAD/ANHV(50),AHVL(25),C1,C2,C3,C4,C5,DELTA,EPSI(96),FF(3000),
     1FHV(25),FHVC(50),FHVW(25),FHVP(25),FINI(11),FIPI(11),FL1,FL2,FLG,
     2FLG1,GAMP(300),GEE(56),MI(14),M2(14),NAES,NBLP,ND(300),NIC,NICN(11
     3),NIHVC,NHV,NU(25),NY,PRFS(11),TEE(11),WDLE(11),XMOL,XQ(7,11),YDELT
     4,YY(11),CASE(15),TMSW(50),TMSWL(25) ,TW
      COMMON/LINE/HVL(3001,K1,K2,TLCH(11),TLCPE(11),XNN(10,11),NXI,IA(9)
     1,NI,XNOLE(300) ,GUPE(300)
      COMMON/CONTM/NCRC(20)
      COMMON/RADCOM/FR(31,11),TT(11),VNN(11),HNE(11),SPE(1,11,8)
     1                ,THETA,SVI,SPI,SPE,HS
      CALL DADIN
      CZ=DELTA*FL1
      CALL MODEM
      CALL CONTM2
      IF(KRI(4)-11) 2,2,3
    2 CALL LINT2
    3 CONTINUE
      RETURN
      END
C
      SUBROUTINE DADIN
      INTEGER FAMDA,FAMOB,ALPHA,BETA
      COMMON/RAD/ANHV(300),AHVL(25),C1,C2,C3,C4,C5,DELTA,EPSI(96),FF(3000),
     1FHV(25),FHVC(50),FHVW(25),FHVP(25),FINI(11),FIPI(11),FL1,FL2,FLG,
     2FLG1,GAMP(300),GEE(56),MI(14),M2(14),NAES,NBLP,ND(300),NIC,NICN(11
     3),NIHVC,NHV,NU(25),NY,PRFS(11),TEE(11),WDLE(11),XMOL,XQ(7,11),YDELP
     4,YY(11),CASE(15),TMSW(50),TMSWL(25) ,TW
      COMMON/LINE/HVL(3001,K1,K2,TLCH(11),TLCPE(11),XNN(10,11),NXI,IA(9)
     1,NI,XNOLE(300) ,GUPE(300)
      COMMON/CONTM/NCRC(20)
      COMMON/INTCON/KRI(20),M,N
      COMMON/RADCOM/FR(31,11),TT(11),VNN(11),HNE(11),SPE(1,11,8)
     1                ,THETA,SVI,SPI,SPE,HS
      COMMON/EOPCOM/FSC(1 03),(SC2(31),(SC2(24),(SC2(16),85,
     1               ESC2(4),P,(SC3( 2403,T,PSC3(640),
     2               ESC3(64),PSC4,ISC4,PSC5( 96),ISP2,PRADE(3),FAMDA(3),
     3               ISP,NICK,(SC6(4 9),KIN,KTMP,KRR(20),PSCT( 8)
      EQUIVALENCE (FMSW(1),AHVL(1),(FMSWL(1),AHVL(1))
C
      DIMENSION ALPHA(15),BETA(7)
      DIMENSION BQ(10) ,FMSW(50),FMSWL(25)
      DATA (ALPHA(J),J=1,15)/2HOH ,2HO ,2HNO,2HN ,2HF-,2HO2,2HN2,2HCO,
     L2HH2,2HC2,2HCN,2HC ,2HC+,2HH ,2HOF/
      DATA (BETA(J),J=1,7)/2HN ,2HC ,2HH ,2HN+,2HO+,2HC+/
 100 FORMAT(6E12.1)
 102 FORMAT(E12.4)
 103 FORMAT(5I5)
 115 FORMAT(24I3)
 225 FORMAT(6E10.3)
 226 FORMAT(6E12.4)
 227 FORMAT(20I1,5F10.3)
 625 FORMAT(,/,47H ****NICN(I) MUST EQ.1 FOR REFLECTING WALLS****)
4010 FORMAT(35H****EXTEND CONTINUUM FREQ RANGE****)
4006 FORMAT(20I3,15A4)
4008 FORMAT(35H****KQC(I)=2 CANNOT BE USED HERE****)
      TW = 0.
      C1=0.
      C3=1.
      FL1=2.
      FL2=2.
      FLG=0.
      FLG1=FL1-1
      IF( KRI(3)-11 174,173,174
  173 KNOL = 0.
      GO TO 176
  174 KNOL = 1.
  176 CONTINUE
      TSML = TS - 1
      KKRI(8) = KRI(8)
      W1 = FHVC(NIHVC)/(32.48.62E-5)
      DO 960 I=1,NY
      IF(W1-TEE(I)) 590,560,560
  590 WRITE(N,4010)
      STOP
  560 CONTINUE
   86 CONTINUE
      IF(NICN(1),EQ.1.OR.KR(53),LT,2) GO TO 640
      WRITE(N,625)
      STOP
  640 CONTINUE
C
C     CALCULATE ELECTRONIC PARTITION FUNCTIONS FOR ATOMS AND IONS
C
      DO 500 I=1,NY
      T1=TEE(I)*8,62E-5
      IRK=0
      NCES=0
C     LOOP FROM 450 TO 495 ESTABLISHES IDENTITY
C     ....8 ELECTRONIC STATES PER SPECIES
  450 IRK=IRK+1
      NICF=0
      XQ(IRK,I)=0.
C     LOOP FROM 475 TO 476 EVALUATES PARTICULAR PARTITION FUNCTION
  475 NCES=NCES+1
      NICE=NICE+1
      XQ(IRK,I)=XQ(IRK,I)+GEE(NCES)*EXP(-EPSI(NCES)/T1)
C     FOLLOWING IF STATEMENT TESTS TO SEE IF TOTAL NUMBER OF ELECTRONIC
C     STATES ( FOR ALL STAGES IN SYSTEM) HAS BEEN EXCEEDED
      IF(NCES.EQ.NAES) GO TO 500
  495 IF(NICE.EQ.8) GO TO 490
  476 GO TO 475
  490 CONTINUE
      YW=MAXOF(HV,NIHVC)
      RETURN
      END
C
      SUBROUTINE MODEM
C     ...OBTAINS SPECIES NUMBER DENSITIES FOR EACH SPATIAL STATION
      INTEGER FAMDA,FAMOB,ALPHA ,BETA
      COMMON/RAD/ANHV(300),AHVL(25),C1,C2,C3,C4,C5,DELTA,EPSI(96),FF(3000),
     1FHV(25),FHVC(50),FHVW(25),FHVP(25),FINI(11),FIPI(11),FL1,FL2,FLG,
     2FLG1,GAMP(300),GEE(56),MI(14),M2(14),NAES,NBLP,ND(300),NIC,NICN(11
     3),NIHVC,NHV,NU(25),NY,PRFS(11),TEE(11),WDLE(11),XMOL,XQ(7,11),YDELT
     4,YY(11),CASE(15),TMSW(50),TMSWL(25) ,TW
      COMMON/LINE/HVL(3001,K1,K2,TLCH(11),TLCPE(11),XNN(10,11),NXI,IA(9)
     1,NI,XNOLE(300) ,GUPE(300)
      COMMON/RADCOM/FR(31,11),TT(11),VNN(11),HNE(11),SPE(1,11,8)
     1                ,THETA,SVI,SPI,SPE,HS
      COMMON /EOPCOM/ CX(31,2),              IFC(31),ATA(8),ATB(8),WATE(8),
     1                KAT(8),IA(8),IS,KR(80),LAM(31),P,RCE(3),Z3,
     2                RD(3),RE(3),RF(3),Z1,T,TA(8,9),TQ(8,8),
     3                TU(31,29,VN(31),VNU(31,8),C2,L3,ITPR,KR9,NCH,NCV,
     4                AP,WINE(3),YE(31,VW(31),ISP2,FAMDA(3),FAMOB(3),
     5                ISP,NICK,NI(3),M,N,KKR(20),ATC(8)
      DIMENSION IN(15)
      DIMENSION ALPHA(15),XNN(10,11),BETA(7)
      DATA (BETA(J),J=1,7)/2HN ,2HC ,2HH ,2HN+,2HO+,2HC+/
      DATA (ALPHA(J),J=1,15)/2HOH,2HO ,2HNO,2HN ,2HF-,2HO2,2HN2,2HCO,
     L2HH2,2HC2,2HCN,2HC ,2HC+,2HH ,2HOF/
C
C     ESTABLISH IDENTITY OF EACH SPECIES
C
      DO 91 J=1,89
      IN(J)=0
      DO 235 I=1,NICK
      IF (FAMDA(I).NE.ALPHA(J)) GO TO 235
      IN(J)=I
      GO TO 91
  235 CONTINUE
   91 CONTINUE
C
C     START DO LOOP ON SPATIAL GRID POINTS
C
      DO 20 I=1,NY
      PRES=PRE(I)
      DO 19 J=1,19
      IJ=IN(J)
      IF (IJ.EQ.0) GO TO 18
      XNN(J,I)=7,3998E21*PRES*FR(IJ,I)/TEE(I)
      GO TO 19
   18 XNN(J,I)=0.
   19 CONTINUE
   20 CONTINUE
C
C.....FORATIVE ION NUMBER DENSITIES
      DO 525 I=1,NY
      T1=8.617E-5*TEE(I)
C.....M-
      XND = 10./EXP(1.E34*EXP(-2.8/T1)*XNN(4,I)
      XNN(16,I) = XND*XNN(5,I)/(4.85E+15*TEE(I)**1.5*EXP(1.22/T
     1I)/9.)
C.....O-
      XNN(17,I)=XNN(2,I)*XNN(5,I)/(4.83E+15*TEE(I)**1.5*EXP(-1.
     148/T1)/(4.*2.*EXP(-0.0353/T1)))
C.....C-
      XNN(19,I) = XNN(12,I)*XNN(5,I)/(4.915E+15*TEE(I)**1.5*EXP(-1
     1.25/T1)/(4.))
C.....H-
      XNN(18,I)=XNN(14,I)*XNN(5,I)/(4.83E+15*TEE(I)**1.5*EXP(-0
     1.754/T1))
C.....N2+ NUMBER DENSITY
C     PARTITION FUNCTION RATIO FROM GILMORE (GOOD FOR 9000.-25000. DEG)
      IF(XNN(4,I).GT.0.) GO TO 526
      XQL(I)=0.
      GO TO 525
  526 CONTINUE
      XQL(I)=2.415E+15*TEE(I)**1.5*12.*10.*5.1E-04*EXP(-1.438E-00*
     1FEE(I)*20)*EXP(-15.576/T1)*XNN(7,I)/XNN(4,I)
  525 CONTINUE
      RETURN
      END
C
      SUBROUTINE CONTM2
      COMMON/RAD/ANHV(50),AHVL(25),C1,C2,C3,C4,C5,DELTA,EPSI(96),FF(300),
     1FHV(25),FHVC(50),FHVW(25),FHVP(25),FEMI(11),FIPI(11),FL1,FL2,FLG,
     2FLG1,GAMP(300),GEE(56),MI(14),M2(14),NAES,NBLP,ND(300),NIC,NICN(11
     3),NIHVC,NHV,NU(25),NY,PRFS(11),TEE(11),WDLE(11),XMOL,XQ(7,11),YDELT
     4,YY(11),CASE(15),TMSW(50),TMSWL(25) ,TW
      COMMON/LINE/HVL(3001,K1,K2,TLCH(11),TLCPE(11),XNN(10,11),NXI,IA(9)
     1,NI,XNOLE(300) ,GUPE(300)
      COMMON/CONTM/NCRC(20)
      COMMON/INTCON/KRI(20),M,N
      DIMENSION FM(11),TAU(11),BEE(11),                FEME(11),FIPI(11),FI
     1NO(11),FIPO(11),FINE(11),FI(11)
      DIMENSION SI(11),SI(11),S2(11)
      DIMENSION XNN(10,11)
      EQUIVALENCE (XNN,XNN)
      EQUIVALENCE (FI(1),FEMB(1)),(FIPI(1),FIPO(1))
      DO 120 II=1,NIC
      IY=NICN(II)
  120 SI(II) = YY(IY)
      HLG = FLG + .00001
      HLG1 = FLG1 + .00001
```

```
      DO 1 LL=1,NIC
      FIEMI(LL)=0.
    1 FIPI(LL)=0.
      DO 50 K=1,NHMC
      REEW = 0.
      KJW = 0.
      DO 30 I=1,NY
      T1=T6EE(I)*6.62E-4
      CALL MU (FMVC(K),T1,XXN(4,I),YXN(2,I),EXN(5,I),ZKN(6,I),ZXN(7,I),
     1XXN(8,I),XXN(9,I),EI,XXN(10,I),I,XYY(I),FI,XXN(12,I),EXN(13,I),
     2XXN(14,I),XXN(15,I),EI,XXN(16,I),EI,XXN(17,I),XXN(18,I),WOL(I),RMOL,
     3FMUE(I))
      BEE(I)=0.
      RQ=FMVC(K)/T1
      IF(AQ-85.) 2,3,3
    3 BEE(I)=0.
      GO TO 30
    2 YEE(I)=5040.*FMVC(K)**3/(EXP(AQ)-1.)
      IF(YEE(I)  10,10,10
   10 BEE(I)=3.1416*YEE(I)
   30 CONTINUE
      CALL TRANS2(NY,YY,NIC,NICH,C2,REF,FMU,S,S1,S2,TAU,FIN,FIP)
      IF(NICH(I).NE.1) GO TO 2755
      XJW = AMV(K) * BEEW + ( 1.-AMVEK) - TMSW(K3) * FIPE(I)
 2755 CONTINUE
      DO 265 LL=1,NIC
      IY = NICHE(LL)
  265 FIMEL(I) = FIMEL(I) + XJW * 3PI-TAU(IY))
      DO 45 LL=1,NIC
      IF(K-1) 9,9,11
   11 FIEMI(LL)=FIEMI(LL)+(FIMEL(I)-FIMOEL(I))*(FMVC(K)-FMVC(K-1))/2.
      FIPI(LL)=FIPI(LL)+(FIMEL(I)+FIMOEL(I))*(FMVC(K)-FMVC(K-1))/2.
    9 FIMOEL(I)=FIMEL(I)
      FIPOEL(I)=FIPEL(I)
   45 CONTINUE
   50 CONTINUE
      RETURN
      END
C
      SUBROUTINE LTNT2
      COMMON/RAD/AMV(65),AMU(225),C1,C2,C3,C4,C5,DELTA,EPSI(90),FF(300),
     1FMV(25),FMVC(501,FMVN(25),FMVP(25),FIMI(11),FIPI(11),FL1,FL2,FLG,
     2FLG1,GAMP(300),GFFE(90),MI(6),MZI(6),MAFS,NBLP,NDI(300),NEC,NICH(11
     3),NIMVC,NMV,NUE(25),NY,PHYS(11),TFEE(11),WOLE(11),XMOL,XQ(7,11),YDELT
     4,YY(11),CASE(15),TMSW(50),TMSWL(25) ,TM
      COMMON/LINE/HVL(300),KL,K2,FLCM(11),TLCPE(11),XNN(18,11),NXL,EA(9)
     1,NE,XMOL(300) ,GUP(300)
      COMMON/CNTR/NCRC(20)
      COMMON/ENTCOM/R(20),M,N
      DIMENSION XXN(14,11)
      DIMENSION BFF(11),FMVS(200),FIIMT(11),FIEPT(11),FIM(11),FIMT(11),P
     1IP(11),PIPTC (11),FMUE(11),S(200),TAUE(11),TAUTE(11),TMUE(11),PSI(11),
     2DIMEL(11,52(20),S1(200),NICH(11),BIPE(11),IYN(20),BIM(11),NIP(11))
      EQUIVALENCE (XXN,XNN)
      DO 320 LL=1,NIC
      IY=NICHE(LL)
  320 SILL) = YY(IY)
      WLGI = FLG1 * .03001
      RR=NY
      DO 30 LL=1,NIC
      PIPEL(I) = 0.
      FIMILL) = 0.
      PIPTE(L) = 0.
      FIMTILL) = 0.
      FIEMT(LL) = 0.
      FIEPT(LL) = 0.
      TLCPE(LL)=0.
   30 TLCPELL)=0.
      K2=0
      DO 50 K=1,NMV
      K1=K2+1
      K2=K2+NUE(K)
      NSL = NUE(K)
      REEW = 0.
      KJW = 0.
      DO 10 I=1,NY
      T1=TFEE(I)*4.62E-4
      RFE(I)=0.
      QW=FMVC(K)/T1
      IF(QW.LT.85.) BEE(I)=5040.*FMV(K)**3/(EXP(QW)-1.)
      IF(NEGE.NE.0 ) BEE(I)=3.1416*BEE(I)
   10 CALL MU (FMV(K),TE,EXN(4,I),EXN(2,I),EXN(5,I),ZKN(6,I),ZXN(7,I),
     1XXN(8,I),XXN(9,I),XXN(10,I),I,YY(I),FI,XXN(12,I),EXN(13,I),
     2XXN(14,I),XXN(15,I),XXN(16,I),XXN(17,I),XXN(18,I),WOL(I),XMOL,
     3FMUE(I))
      CALL TRANS2(NY,YY,NIC,NICH,C2,REF,FMU,S,S1,S2,TAU,FIN,FIP)
      IF(NICH(1).NE.1) GO TO 2755
      XJW = XJW + (1. - AMV(LK) - TMSW(K)) * FIPE(I)
 2755 DO 265 LL=1,NIC
      IY = NICH(LL)
  265 FIMELL) = FIMELL) + XJW * EXPI-TAU(IY))
      CALL FREQ(K,NSHV,FMVS,CFIL)
      NPPL = NSHV/NUE(K)
      DO 6500 JS = 1,NSL
      JJSL(JS) = JS
      KE = K1 - 1 + JJSL(JS)
      DO 6501 LK = 1,NPPL
      L= LR * (JS-1) * NPPL
      KJWL = KJW
      IF(LK.NE.1) GUN=FMVS(L)-FMVS(L-1) 3/2.
      CALL MULE(FMVS(L),SL)
      DO 501 I=1,NY
  501 TMUE(I)=S1(I) * FMUE(I)
      CALL  TRANS2(NY,YY,NIC,NICH,C2,REF,TMU,S,S1,S2,TAUP,XIN ,XIP )
      IF(NICH(1).NE.1) GO TO 2765
      KJWL = KJWL + (1. - AMVL(K) - TMSWL(K)) * XIP(I)
 2765 DO 276 LL=1,NIC
      IY = NICH(LL)
  276 EIMELL) = EIMELL) + KJWL * EXPI-TAUTE(IY))
      DO 302 LL=1,NIC
      IF(LR.EQ.1) GO TO 180
      FIMTILL)=FIMTILL)+(EIMELL)+EIMYILL))   *DUM
      FIPTELL)=FIPTILL)+(EIPELL)+XIPMILL))   *DUM
  180 EIMOELL)=EIMELL)
  302 EIPOELL) = EIPELL)
 6501 CONTINUE
      DO 500 LL=1,NIC
      FIEMT(LL) = FIEMTILL) + EMOL(LL) * FIMTILL)
      FEIPTILL) = FIIPTILL) + EMOL(LL) * EIPTILL)
      FIMTILL) = 0.
  500 FIPTILL) = 0.
 6500 CONTINUE
      DO 303 LL=1,NIC
      DIPELL) = FIIPTELL) - FIPELL) * CFIL
      DIMELL) = FIEMTELL) - FIMELL) * CFIL
      FIIPTILL) = 0.
      FIEMTILL) = 0.
      TLCPELL)=TLCPELL)+DIPELL)
  303 TLCMELL)=TLCMELL)+DIMELL)
   50 CONTINUE
      RETURN
      END
C
      SUBROUTINE FREQ (K,NSHV,FMVS,CFIL)
C
C     ....DETERMINES THE FREQUENCY POINTS FOR THE LINE TRANSPORT
C
      COMMON/RAD/AMV(50),AMVL(259,C),C2,C3,C4,C5,DELTA,EPSI(90),FF(300),
     1FMV(25),FMVC(501,FMVN(25),FMVP(25),FIMI(11),FIPI(11),FL1,FL2,FLG,
     2FLG1,GAMP(300),GFFE(90),MI(6),MZI(6),NAFS,NBLP,NDI(300),NEC,NICH(11
     3),NIMVC,NMV,NUE(25),NY,PRES(11),TFEE(11),WOLE(11),XMOL,XQ(7,11),YDELT
     4,YY(11),CASE(15),TMSW(50),TMSWL(25) ,TM
      COMMON/LINE/HVL(300),KL,K2,FLCM(11),TLCPE(11),XNN(18,11),NXL,EA(9)
     1,NE,XMOL(300) ,GUP(300)
      COMMON/ENTCOM/R(20),M,N
      DIMENSION FMVS(11,XF(20),SK(20),OSK(20)
      DIMENSION AL(4)
      DATA AL(1),I=1,4)/1.5E-4,1.5E-3,1.5E-2,0.05/
      IRY=0
      M=7
      RR=NR
      CFIL=0.
      YMT=NY
C     CHECK BOUNDARIES OF LINE GROUPS
      IF(FMVL(K1)-FMVMEK)) 30,30,31
   31 IF(FMVL(K2)-FMVP(K)) 32,30,30
   30 WRITE(N,350)
  350 FORMAT(46H ****LINE CENTER OUT OF GROUP FREQUENCY RANGE*****)
      CALL EXIT
   32 CONTINUE
      EMUR=1.E-08/(C2*YYMY))
      EMIN=0.1*EMUM/YMY
      DO 50 J=81,K2
C
C     ESTABLISH LOCATION OF MOST REMOTE NODAL POINT ASSOCIATED WITH
C     EACH LINE
C
      INT=1
      JJ=MY
      IF(NDE(J1,GT.16) JJ=NI
      CALL MULE(HVL(J),SK)
      OSK(1)=1.E-04/C2
      DO 500 I=1,MY
      IF(SK(I)-EMUM) 501,500,500
  501 SK(I)=EMIN
  500 CONTINUE
      CALL ISLOVE(R,YY,SK,RF,YSK,1)
      TAUC=OSK(MY)*C2
C     SPECIAL CONSIDERATION FOR HYDROGEN LINES
      IF(GAMP(J)) 403,401,400
  401 INT=0
      GIL=HVL(J)**2/(4.*PI*C1*2*ENNES,NE)**.333
      IF(K-IAC3)      ) 403,402,403
  402 GAMP(J)=AL(1)*GIL
      GO TO 405
  403 IF(K-IAC4)      ) 405,406,405
  404 GAMP(J)=AL(2)*GIL
      GO TO 400
  405 IF(K-IAC5) )     407,406,407
  406 GAMP(J)=AL(3)*GIL
      GO TO 400
  407 IF(K-IAC2)      ) 403,408,400
  408 GAMP(J)=AL(4)*GIL
  400 CONTINUE
      IAR=ENNES,JBI*GAMP(J)*SORT(I),*TAUC)
      GOP=0.5*GAR
      TMAX=10.*GAR
      IF(INT.EQ.0) GAMP(J)=0.
      RF(I)=0.5
C
C     EACH FREQUENCY INCREMENT IS RELATED TO THE ADJACENT FREQUENCY
C     INCREMENTS BY A FACTOR OF 1+FR, WHERE THE INCREMENTS DECREASE
C     IN SIZE AS THE DIRECTION OF THE NEAREST LINE
C
      IPEJ-K1) 1,20,1
   20 SM=HVL(K1)-FMVMEK)
      IF(SM-GMAX) 81,81,82
   82 SM=GMAX
      GO TO 81
    1 SM=0.5*(HVL(J)-HVL(J-1))
      IF(SM-GMAX)81,81,86
   86 SM=GMAX
   81 IF(SM-GOP*2K) 80,40,2
   80 FMVS(IM)=HVL(J)-SM
      DO 11 L=2,MK
      LY=L+IRY
   11 FMVS(LY)=FMVS(LY-1)+SM/KK
      GO TO 151
C     CALCULATE FE FACTORS FOR FREQUENCIES LESS THAN THE LINE CENTER
    2 DO 9 J3=1,19
   41 SK(J3)=(FI.0+RF(J3))**MK-1.0)/RF(J3)
      OSK(J3)=RF(J3)*(1.0+RF(J3))**(KK*RF(J3))*(1.0+RF(J3))**(MK-1)-11.0+RF(J3))**
     1MK+1.0)
      IF(SK(J3)*GOR/SM-20.) 42,42,40
   40 IF(J3-1)44,44,43
   44 RF(J3)=RF(J3)/5.
      GO TO 42
   43 RF(J3)=RF(J-1)+(RF(J3)-RF(J-1))/5.
      GO TO 41
   42 XL=SM
      IF(ABS(SK(J3)*GOR/SM-1.0)-.0001) 6,6,45
   45 RF(J3)=RF(J3)*OSK(J3)*SM/GOR-SK(J3))
    9 CONTINUE
    6 WRITE(N,900)
  900 FORMAT(1H0,COX,10HERROR STOP// 4X,4HRMAT, 8X,8HBERAINDF8.15X,1HE,11
     1X,3HDMV,5X,3HMMEN-1MCREMENT,5X,2MSK,9X,3HDSK)
      DO 9 J2=1,20
      ERR=XL-SK(J2)*GOR
      WRITE(N,100) RF(J2),ERR,X,XL,GOR,SK(J2),OSK(J2)
  100 FORMAT(  2E13.6,11X,13.8X, 4E12.4)
    9 CONTINUE
      WRITE(N,200)
  200 FORMAT(46H FREQUENCY GRID ITERATION DID NOT CONVERGE)
      CALL EXIT
    8 FR=RF(J3)
      XF(1)=0.5
C     CALCULATE CORRESPONDING FREQUENCY POINTS
      DO 150 L=1,MK
      LY=L+IRY
      FMVS(LY)=HVL(J)-GOR*((1.+FR)**(MK+1-L)-1.)/FR)
  150 CONTINUE
  151 CONTINUE
      IF(J-K2) 7,21,7
   21 SP=FMVP(K)-HVL(J)
      IF(SP-GMAX) 12,12,90
   90 SP=GMAX
      GO TO 12
    7 SP=.5*(HVL(J+1)-HVL(J))
      IF(SP-GMAX) 12,12,91
   91 SP=GMAX
   12 IF(SP-GOR*XX) 92,92,8
   92 NI=NK+1
      NFK=2*NK+1
      MIK=NK+1
      IRI=NI*IRY
      FMVS(IRI)=HVL(J)
      DO 13 L=NTRP,NFK
      LY=L+IRY
   13 FMVS(LY)=FMVS(LY-1)+SP/XX
      GO TO 151
```

```
C     CALCULATE FX FACTORS FOR FREQUENCIES EQUAL TO OR GREATER THAN THE
C     LINE CENTER
      8 DO 9 JI=1,19
     61 SK(JI)=(FL-0.5*FX(JI))*ONK-1.03/FX(JI)
        OSK(JI)=(FX(JI)**2)/(XK*FX(JI)*(1.0+FX(JI)**2/(XK*(NK-1)-FL+0.5*FX(JI))**
        1NK+1.0))
        IF(SK(JI)*GOR/SP-20.) 62,62,60
     60 IF(JI-1) 64,64,63
     64 XF(JI)=XF(JI)/3.
        GO TO 61
     63 XF(JI)=XF(JI-1)+(XF(JI)-XF(JI-1))/3.
        GO TO 61
     62 KL=JP
        IF(ABS(SK(JI)*GOR/SP-1.0)-.00001) 10,10,65
     65 XF(JI+1)=XF(JI)*OSK(JI)**(SP/GOR-SK(JI))
        IF(ABS(SK(JI)*GOR/SP  -1.0)-.0001) 10,10,9
      9 CONTINUE
        XL=SP
        GO TO 6
     10 FK=XF(JI)
        NIK=NNK+1
        NFK=2*NK +1
C     CALCULATE CORRESPONDING FREQUENCY POINTS
        DO 250 L=1K,NFK
        LM=L*10V
        FHYS(LI)=HVL(J)+GOR*(1.-SX)**2*(1.-N(K)-1.5/FX)
    250 CONTINUE
    251 CONTINUE
        IS=NFK+10V
        CFSL = CFSL + (FHYS(IS)-FHYS(IS-1))*XNU(J)
        IRF=IRF+2*NFK+1
     50 CONTINUE
C     CALCULATE TOTAL NUMBER OF FREQUENCY POINTS IN KIN SUBGROUP
        NSHV=NU(K)*(2*NK+1)
        RETURN
        END
C
      SUBROUTINE MU (HV,XKT,AN,A1,A2,AM2,ACO,AH2,AC2,ACN,AC4,ACP,
     1AK,ANO,ANN,A3N,A+N,AN2P,EMOL,KAPNU)
      COMMON/CONTRY/NCRC(20)
      DIMENSION XKT(1),KAPNU(1,1)
      DIMENSION T(1)
      ALOG10(I)=ALOG(I)/2.3
      SOA=7.25E-16
      L=1
      I=1
      T(1)=XKT(1)/R.62E-05
      XLAM=1.24/HV
      ON=0.
      ONO=0.
      OM=0.
      KH=0.
      KNN=0.
      ON2P=0.
      XP=0.
      ONH=0.
      ONN=0.
      XIN=1.492E+05*(1.-EXP(-HV/.45))/(EXP(HV*0.4343)-1.0)
   13 XW=14.3/XKT(L)
      XO=13.4/XKT(L)
      XI=25.5/XKT(L)
      ONH=4.0*10.0*EXP(-2.38/XKT(L))+6.0*EXP(-3.57/XKT(L))
      OO=9.0*5.0*EXP(-1.98/XKT(L))+EXP(-6.18/XKT(L))
      OCN=9.0*5.0*EXP(-1.26/XKT(L))+EXP(-2.5*/XKT(L))+5.0*EXP(-6.18/
     1XKT(L))
      OCP=46.0*12.0*EXP(-5.33/XKT(L))
      OHPA = 7. *8.*EXP(-10.2/XKT(L))
      CALL FH(HV,Z0,Z1,Z2)
      XA=HV/XKT(L)
      EPC=1.0*EXP(-XA)
C.....NITROGEN HIGH LINE SERIES
      IF(NCRC(1)) 600,254,600
  600 BETA=19.6/XKT(L)
      REE1=5040.*HV**3*EXP(-XA)
      IF(HV-0.85) 2540,2540,2541
 2540 EQ3=2.73E-09*AN*EXP(-16.56/XKT(L))*10.**(EXP(BETA/10.)-1.)/BETA-
     10.0625)/(ONN**4*BETA)
      ONN5=EQ3/(REE1*1.42)
 2541 CONTINUE
C.....OXYGEN HIGH LINE SERIES
      IF(NCRC(2)) 601,2561,601
  601 IF(HV-0.85) 2562,2563,2563
 2562 EQ4=2.73E-09*AO*EXP(-BETA*4.)*((EXP(BETA/10.)-1.)/BETA-0.0625)/(00
     1**4.*BETA)
      ONH5=EQ4/(REE1*1.77)
 2563 CONTINUE
C.....N2+ CONTRIBUTION FROM BIBERMAN AND KN.
      IF(NCRC(3)) 602,3075,602
  602 IF(HV-2.23) 3075,3074,3074
 3074 IF(HV-4.46) 3073,3073,3075
 3073 IF(HV-1.45) 3084,3084,3083
 3084 ON2P=(AN2P*1.E-18)*10.**(-11.576*HV-.77*HV-0.91*HV**2)
      GO TO 3075
 3083 ON2P=(AN2P*1.E-19)*10.**(-40.0868*HV+.91823E-02*HV-3.23677E-06*HV*
     1*2+HV*130.616-0.98219E-02*HV)+0.13644F-06*HV*(EXP(-1.*HV**2)*(-4.9
     2684*HV-0.43903E-03*HV)-3.1954*F-07*HV**2)
 3075 CONTINUE
C     NEGATIVE ION CONTRIBUTIONS
      IF(NCRC(4)) 603,305,603
  603 IF(HV-1.22) 305,300,300
  300 XNN=XNN+AMM*AL*.6E-16
  305 CONTINUE
C.....C- CONTRIBUTION FROM SEMAN AND FRANSCOMB
      IF(NCRC(20)) 6600,6600,6601
 6601 IF(HV-1.25) 6600,6602,6602
 6602 XCH = XCH + 1.4E-17*AC*EXP(-(4.83E+19*TEL)**0.5*(HV*EXP(-1.25/XKT(L)
     1))/14.3)
 6600 CONTINUE
C.....H- CONTRIBUTION FROM CHANDRASEKHAR AND FLEART
      IF(NCRC(6)) 604,2502,604
  604 IF(HV-13.6) 2500,2500,2502
 2500 IF(HV-0.75) 2502,2501,2501
 2501 IF(HV-1.3) 6500,6500,6501
 6500 XHH = (AHH*1.E-17)*(-6.5)*7.15*HV*E
      GO TO 2502
 6501 IF(HV-6.) 6502,6502,6503
 6502 XHH = (AHH*1.E-17)*(6.765-1.7*HV+0.1258*HV**2.)
      GO TO 2502
 6503 XHH = (AHH*1.E-17)*(3.5-0.535*HV+0.0225*HV**2.)
 2502 CONTINUE
C.....O+ CONTRIBUTION FROM CHURCHILL,ARMSTRONG AND MUELLER
      IF(NCRC(610) 605,2510,605
  605 IF(HV-13.1 2503,2503,2510
 2503 IF(HV-1.5) 2510,2504,2504
 2504 IF(HV-3.5) 2505,2506,2506
 2505 XOH=AOH*6.2E-16
      GO TO 2510
 2506 IF(HV-6.7) 2507,2507,2508
 2507 XOH=AOH*1.E-18*(16.16-0.8*HV)
      GO TO 2510
 2508 XOH=AOH*1.E-18*(15.58-0.45*HV)
 2510 CONTINUE
C.....NO ULTRAVIOLET CONTRIBUTION FROM BIBERMAN AND KRATSANANYAN
      IF(NCRC(7)) 606,2525,606
  606 IF(HV-13.9) 2511,2511,2525
 2511 IF(HV-9.0) 2520,2520,2513
 2513 IF(HV-6.693)2514,2515,2515
 2514 ONO=(ANO*1.E-18)*10.0**(-4.2673*HV+0.08767)
      GO TO 2525
 2515 SP(HV-10.) 2517,2517,2516
 2517 ONO=ANO*1.9E-18
      GO TO 2525
 2516 ONO=(ANO*1.E-18)*(89.75-17.125*HV+1.033*HV**2)
      GO TO 2525
C.....NO VISIBLE CONTRIBUTION FROM BIBERMAN AND KRATSANANYN
 2520 IF(HV-2.7) 2525,2525,2521
 2521 ONO=(ANO*1.E-18)*(10.**(-3.4820-0.11509E-02*TEL)+0.15999E-06*TEL)**
     12+HV*(-2.37A6+0.10952E-02*TEL)-0.10099E-06*TEL**2)+(HV**2*(0.575
     2+9-0.17249E-03*TEL)+0.13878E-07*TEL)**2))
 2525 CONTINUE
C     NITROGEN ATOMIC CONTRIBUTION
      IF(NCRC(8)) 607, 15,607
  607 ON=SQA*AN*EXP(TEL)*(.5*EXP(-EX-XNU*ZN/HV**3)
      IF(HV-4.22) 15,206,206
  206 ON=ON*EXP(4.22/XKT(L)-EX)
      IF(HV-10.8) 15,201,201
  201 ON=ON+ANO*5.16E-17*EXP((10.8/XKT(L)-EX)/ONM
      IF(HV-12.0) 15,202,202
  202 ON=ON+ANO*4.46E-17*EXP((12.0/XKT(L)-EX)/ONM
      IF(HV-14.3) 15,203,203
  203 ON=ON+ANO*1.16E-17/ONM
C     OXYGEN ATOMIC CONTRIBUTION
   15 OT=0.
      IF(NCRC(9)) 608,609,608
  608 OT=SQA*AO*EXP(TEL)*(.079+.09*EXP(EX-EX)*2/HV**3
      IF(HV-4.22) 16,206,206
  206 OT=OT*EXP(4.22/XKT(L)-EX)
      IF(HV-10.81) 16,205,205
  205 OT=OT+ANO*5.16E-17*EXP((10.81/XKT(L)-EX)/ONM
      IF(HV-12.06) 16,207,207
  207 IF(HV-9.2) 204,208,18
  208 TO2=AO2*400.0*5251/(TANH(0.347*/XKT(L)))*EXP(-TANH(3.195/2.0*
     1XKT(L)))*(EHV-8.561/0.809)**2/2.687E+19
      GO TO 18
C.....SHUMAN-RUNGE BANDS FROM BIBERMAN AND KRATSAKYN
 1301 TO2=(AO2*1.E-18)*10.**(-23.413+0.60500*HV-07*T(L)-0.2444*F-06*T(L))**
     1EHV*10.2102-0.13958E-02*T(L)+3.6619E-07*T(L)**2)+(HV**2)*(-0.618
     2+.954*0.1)*(NOE-08*T(L)-0.4711E-04*T(L)**2))
C     NITROGEN MOLECULAR CONTRIBUTION
   18 ON2=0.0
      IF(NCRC(12)) 614,2010,614
  614 IF(HV-6.5) 2550,209,209
  209 IF(HV-10.5)211,211,2010
  211 IF(HV-10.5)211,211,212
C.....N2 BIRGE HOPFIELD DATA FROM APPLETON AND SETINSPEC FOR HV LARGER
C     THAN 10.5 EV - AND FROM ALLEN ET. AL. FOR HV LESS THAN 10.5 EV
  211 ON2=(AN2*2.52E+19)*EXP(2.302*HV*(-14.871-0.1054*F-03*T(L)+0.8691E-0
     1*T(L)**2+HV*(-0.90275+.01+0.6414*E-03*T(L)-0.4126E-05*T(L)**2)
     2+(HV**2*(0.12305-0.4843E-04*T(L))-2.2415*E-08*T(L)**2)))
      GO TO 2010
  212 ON2=(AN2*2.52E+19)*EXP(2.302*(-39.704+0.7376E-02*T(L)-0.4615E-0
     1*T(L)**2+HV*(4.1032-0.7691E-03*T(L)+0.5244E-07*T(L)**2)+(HV**2)
     2*(-3.7810E-01+0.1822E-04*T(L)-0.1276E-08*T(L)**2)))
      GO TO 2010
C.....N2 LOW FREQUENCY BANDS (1+ AND 2+) FROM BIBERMAN AND HV.
 2550 IF(HV-6.5) 2551,2551,2010
 2551 IF(HV-0.75) 2010,2552,2552
 2552 ON2=(AN2P*1.E-20)*10.**(-1.*(7.7*HV-0.410*HV**2-2.606/XKT(L)+2.E-1
     1*AN2P)10.,991-17.14+0.934*HV-1.(1.52*HV**2-5.28/XKT(L))
C     CO CONTRIBUTION
C.....CO FITS CHECKED AGAINST W.L.G.+ARDS DATA JAN-68
 2010 OCH=0.0
      IF(NCRC(13)) 619,118,619
  618 IF(HV-4.27) 118,220,220
  220 IF(HV-10.8) 221,221,118
  221 IF(HV-7.75) 2000,2000,200)
 2000 XIG=1.492E+05*(1.-EXP(-HV/XKT(L)))/((XLAM**5)*(EXP(HV/XKT(L))-1.))
      A1E-17.09*1.375E-05*T(L)-.051F-06*T(L)**2+HL*HV(-66.94+11.76F-03*
     1T(L)-0.767E-06*T(L)**2)
      OCO=AOO*REE1*2.*(2.59*ARG)/XIG
      GO TO 119
 2001 OCO=AOO*REE1*(-2.9259*(27.2-1630.*XLAM+4620.*(XLAM**2)*(1/818
C     HYDROGEN MOLECULAR CONTRIBUTION
C.....N2 LYMAN AND ARMER CONTRIBUTIONS FROM MEISNER
  119 OH2=0.0
      IF(NCRC(14)*619,119,619
  618 IF(HV-4.27) 118,220,220
  220 IF(HV-10.8) 221,221,118
  221 IF(HV-7.75) 2000,2000,200)
 2000 XIG=1.492E+05*(1.-EXP(-HV/XKT(L)))/((XLAM**5)*(EXP(HV/XKT(L))-1.))
      A1E-17.09*1.375E-05*T(L)-.051F-06*T(L)**2+HL*HV(-66.94+11.76F-03*
     1T(L)-0.767E-06*T(L)**2)
      OCO=AOO*REE1*2.*(2.59*ARG)/XIG
      GO TO 119
 2001 OCO=AOO*REE1*(-2.9259*(27.2-1630.*XLAM+4620.*(XLAM**2)*(1/818
C     HYDROGEN MOLECULAR CONTRIBUTION
C.....N2 LYMAN AND ARMER CONTRIBUTIONS FROM MEISNER
  119 OH2=0.0
      IF(NCRC(14)*619,119,619
  618 IF(HV-4.27) 118,220,220
  220 IF(HV-10.8) 221,221,118
  221 IF(HV-7.75) 2000,2000,200)
 2000 XIG=1.492E+05*(1.-EXP(-HV/XKT(L)))/((XLAM**5)*(EXP(HV/XKT(L))-1.))
      A1E-17.09*1.375E-05*T(L)-.051F-06*T(L)**2+HL*HV(-66.94+11.76F-03*
     1T(L)-0.767E-06*T(L)**2)
      OCO=AOO*REE1*2.*(2.59*ARG)/XIG
      GO TO 119
 2001 OCO=AOO*REE1*(-2.9259*(27.2-1630.*XLAM+4620.*(XLAM**2)*(1/818
C     HYDROGEN MOLECULAR CONTRIBUTION
C.....N2 LYMAN AND ARMER CONTRIBUTIONS FROM MEISNER
  119 OH2=0.0
      IF(NCRC(14)*619,119,619
  618 IF(HV-4.27) 118,220,220
  220 IF(HV-10.8) 221,221,118
  221 IF(HV-7.75) 2000,2000,200)
 2000 XIG=1.492E+05*(1.-EXP(-HV/XKT(L)))/((XLAM**5)*(EXP(HV/XKT(L))-1.))
      A1E-17.09*1.375E-05*T(L)-.051F-06*T(L)**2+HL*HV(-66.94+11.76F-03*
     1T(L)-0.767E-06*T(L)**2)
      OCO=AOO*REE1*2.*(2.59*ARG)/XIG
      GO TO 119
 2001 OCO=AOO*REE1*(-2.9259*(27.2-1630.*XLAM+4620.*(XLAM**2)*(1/818
C     HYDROGEN MOLECULAR CONTRIBUTION
C.....N2 LYMAN AND ARMER CONTRIBUTIONS FROM MEISNER
  119 OH2=0.0
      IF(NCRC(14)*619,119,619
  618 IF(HV-4.27) 118,220,220
  220 IF(HV-10.8) 221,221,118
  221 IF(HV-7.75) 2000,2000,200)
 2000 XIG=1.492E+05*(1.-EXP(-HV/XKT(L)))/((XLAM**5)*(EXP(HV/XKT(L))-1.))
      A1E-17.09*1.375E-05*T(L)-.051F-06*T(L)**2+HL*HV(-66.94+11.76F-03*
     1T(L)-0.767E-06*T(L)**2)
      OCO=AOO*REE1*2.*(2.59*ARG)/XIG
      GO TO 119
 2001 OCO=AOO*REE1*(-2.9259*(27.2-1630.*XLAM+4620.*(XLAM**2)*(1/818
C     HYDROGEN MOLECULAR CONTRIBUTION
C.....N2 LYMAN AND ARMER CONTRIBUTIONS FROM MEISNER
  119 OH2=0.0
      IF(NCRC(14)*619,119,619
  618 IF(HV-4.27) 118,220,220
  220 IF(HV-10.8) 221,221,118
  221 IF(HV-7.75) 2000,2000,200)
 2000 XIG=1.492E+05*(1.-EXP(-HV/XKT(L)))/((XLAM**5)*(EXP(HV/XKT(L))-1.))
      A1E-17.09*1.375E-05*T(L)-.051F-06*T(L)**2+HL*HV(-66.94+11.76F-03*
     1T(L)-0.767E-06*T(L)**2)
      OCO=AOO*REE1*2.*(2.59*ARG)/XIG
      GO TO 119
 2001 OCO=AOO*REE1*(-2.9259*(27.2-1630.*XLAM+4620.*(XLAM**2)*(1/818
```

```
C.....FOR HERTZBERG
  125 OC2=OC2+AC2*10.0**(-23.3444.7459*HV-0.48049*HV**2)
      IF(HV-1.) 1300,120,120
C.....SAHA
 1300 OC2=OC2*(1.E-18*AC2)*10.**(-51.16460.59289E-02*TEL)-0.43228-06*TEL
     1**2+HV*(140.864-0.47238E-02*TEL)+0.35379E-06*TEL**2)+(HV**2)*(-8.
     2089?*0.99369E-03*TEL)-0.73652E-07*TEL**2)
      GO TO 120
C.....MULLIKAN
  126 OC2=OC2+AC2*10.**(-16.7+2.*(5.35-HV))
C     CN CONTRIBUTION
  120 OCN=0.0
      IF(NRC(163) 618,121,618
  618 IF(HV-0.4) 121,226,226
  226 IF(HV-6.) 1227,1227,121
 1227 OCN=(ACN*(.E-19)*10.**(-1.1967+0.19902F-03*TEL)-0.10678E-07*TEL**
     2+HV*(6.6871-0.10164E-02*TEL)+D.607?1F-07*TEL**2)+(HV**2)*(-2.904
     2?+0.43612E-03*TEL)-0.26439F-07*TEL**2))
      IF(HV-7.) 121,1226,1226
 1228 OCN=OCN+ACN*10.**(-41.46+(1.?4*HV-1.946*HV**2)
C     CARBON ATOM CONTRIBUTION
  121 OC=0.
      IF(NRC(177) 619,122,619
  619 IF (HV-3.78) 122,120,120
  127 OC=50A*AC*1.33*EXTEL)*EXP(-(HV-12.26)/EXTEL)*EC/HV**5
      GO TO 122
  128 OC=50A*AC*1.33*EXTEL)*EXP(-(.5A/EXTEL))*EC/HV**5
      IF(HV-8.51) 122,228,228
  228 OC=OC+AC*2.2E-17*EXP(-2.15/EXTEL))/OCN
      IF(HV-10.0) 122,229,229
  229 OC=OC+AC*0.5E-17*EXP(-1.76/EXTEL))/OCN
      IF(HV-11.26) 122,230,230
  230 OC=OC+AC*9.0E-17/OCN
C     CARBON ION CONTRIBUTION
  122 OCP=0.
      IF(NCRE(181) 620,131,620
  620 IF (HV-15.08) 129,130,130
  129 OCP=8.3665E-20*ACP*EXTEL)*EXP(-(HV-24.4)/EXTEL))*EC/HV**5
      GO TO 131
  130 OCP=8.3665E-20*ACP*EXTEL)*EXP(-(-7.32/EXTEL))*EC/HV**5
      IF(HV-19.03) 131,231,231
  731 OCP=OCP+A.84E-17*EXP(-8.37*EXTEL))*EC*/OCP*
      IF(HV-24.49) 131,232,232
  232 OCP=OCP+1.32E-17*ACP/OCP*
  131 CONTINUE
      EAPHUI(,L)=EPC*(DN+DE*(D)*XNN*EF**(C     +XNN,*(OCO*OH2+OC2*OCN
     1*OO2+OH2*OHD+OH2P)+(XNN+XNN*OHD*OH*5)
C     HYDROGEN ATOM CONTRIBUTION
      IF(NCRE(191) 621,622,621
  621 IF(HV-0.601)?3,233,1405
  233 OH=6.26F-20*AH*T(L)*EXP(-(4V-13.6)/EXTEL))/HV**5
      GO TO 1450
 1405 OH=                                    6.268-20*AH*T(L)
     1*EXP(-12.8/EXTEL))/HV**5
      IF(HV-1.60) 1450,234,234
  234 OH = OH+1.47E-15*AH*EXP(-12.0/EXT(L))/(OH*AH*(**3)
      IF(HV-3.40) 1450,235,235
  235 OH = OH+4.47SE-15*AH*EXP(-10.2/EXT(L))/(OH*AH*(**3)
      IF(HV-13.56)1450,236,236
  236 OH=OH+9.98E-16*AH/(OH*AH**5)
 1450 EAPHUI(,L)=EAPHUI(,L)+EPC*OH
  422 CONTINUE
      RETURN
      END

      SUBROUTINE RULE(PHYS,SI)
      ?CALCULATES LINE ABSORPTION COEFFICIENTS
      COMMON/RAD/ANU(90),ANVL(29),C1,C2,C3,C4,C5,?OLTA,EPS(50),PP(300),
     1FNU(25),FNVE(90),FNUW(25),FNUP(25),FIN(1111),PIP(1111),FLB,FL2,FLG,
     2FLGL,GAM*300),GEEI(96),NU(24),N2(24),NAES,NBLA,NDE300),NIC,NICNEII
     3),NINVE,NNV,NUI?50,NY,PAES(111),YPF(111,NDL(119),PNDL,KQI?,BII,YDEL?
     4,YYE(1),CASE(195),TNSNE(90),TNSNL(2*) ,CN
      COMMON/LINE/NNL(300),KL(,K2,TLE*(111),TLEP(111),ENNE30,11),NEE,(14(91
     1,41,KNDL(300) ,GUPI300)
      DIMENSION SI(1) ,KR(?)
      ?IMENSION ALPHI8),BETA(8),DE(8),X1(4),SLA(4),SLBE80),SMA(8),SMB(8)
     1,SLAS(80),SLBS(8),SMAS(8),SMBS(4)
      DATA(ALPHI(J),J=1,8)/0.,2.F-6,2.F-6,4.F-6,6.E-6,1.2E-5,1.6E-5,2.4E-
     1?/
      DATA(BETA(J),J=1,8)/0.,5.F-6,1.E-5,2.F-5,3.E-5,5.F-5,7.E-5,1.F-2/
      DATA(DE(J),J=1,8)/0.,.07,.04,.08,.12,.16,.2,.24/
      DATA(X1(J),J=1,4)/0.,.02*,.04*,.1,.15,.2,.25,.3/
      DATA(SLA(J),J=1,4)/3.362,3.114,2.748,2.301,2.000,1.778,1.580,1.144
     1/
      DATA(SLB(J),J=1,4)/1.881,.886,?.147,2.748,?.000,1.786,1.278,0.909,0.491
     1/
      DATA(SMA(J) ,J=1,8)/1.231,.?96,.512,.079,-.244,-.522,-.782,-.921/
      DATA(SMB(J),J=1,8)/.492,.?,.621,.767,.06,-.337,-.537,-.721/
      DATA(SLAS(J),J=1,8)/-1.895E+03,-3.402E+03,-3.337E+03,-3.404E+03,
     1-4.141E+02,-5.08?E+02,-4.633F+02,-2.81%F+02/
      DATA(SLBS(J),J=1,8)/8.419E+02,3.016E+02,-6.786E+01,-5.509E+02,
     1-?.820E+02,-1.990E+02,-1.370F+02,-1.222F+02/
      DATA(SMAS(J),J=1,8)/-.245F-?,-.160E+2,-.?2BF+2,-.894E+1,-.738E+1,-
     1.6028+1,-.469E+1,-.446E+1/
      DATA(SMBS(J),J=1,8)/.140E+?,.643E+00,-.676E+1,-.762E+1,-.615F+1,-.
     1468E+1,-.353E+1,-.392E+1/
      DATA (X(J),J=1,?)/?3.291N*-24,?6.958E-24,19.937QE-24,1.873?8E-24
     1,29.291NF-24,26.548E-24,19.937QF-24/
      DO 50 I=1,NY
      S1(I)=0.
      T1=TEF#1**4.62F-9
      T2=TFE(I)*1.3809?F-16
      T3 = TEF(I)/10000.
      EX = 0.
C     START LOOP ON INDIVIDUAL LINES
      DO 250 J=K1,K2
C     ESTABLISH INDEXING ON SPECIES
      IK=NDL(J)
      IF(IK-6) 101,101,1
  101 ILK=4
      IRK=1
      ?R = 0.25
C     ...THE INDEX FOR NEUTRAL NITROGEN
      GO TO 10
    1 IF(IK-16) 102,102,2
  102 ILK=2
      IRK=2
      EX = 0.44
C     ....THE INDEX FOR NEUTRAL OXYGEN
      GO TO 10
    2 IF(IK-24) 103,103,3
  103 ILK=12
      IRK=3
      ER = .43
C     ...THE INDEX FOR NEUTRAL CARBON
      GO TO 10
    3 IF(IK-32) 104,104,4
  104 ILK=24
      IRK=4
      *ID = 1000.*(HVLI(J+.0001)
      GO TO 10
C     ...THE INDEX FOR NEUTRAL HYDROGEN
    4 IF(IK-40) 105,105,5
  105 ILK=3
      IRK=5
C     ....THE INDEX FOR THE NITROGEN ION
      GO TO 10
    5 IF(IK-48) 106,106,6
  106 ILK=1
      IRK=6
C     ....THE INDEX FOR THE OXYGEN ION
      GO TO 10
    6 ILK=13
      IRK=7
C     ....THE INDEX FOR THE CARBON ION
C
C     STATEMENT 6 COMPLETES THE INDEXING OPERATION.  CALCULATE THE
C     LEVEL POPULATIONS.
C
   10 KP=ANNI(LR,I)*GEE(IK)*(EXPE-EPS(IK)/T(I))/XQ(IRK,II)
C
C     CALCULATE LINE STRENGTHS USING INPUTTED F-VALUES
C
   14 SL=3.1416*2.8103E-13*FF(J)*XP
C     ....AND LINE WIDTHS USING ELECTRON NUMBER DENSITIES AND STARK
C     LINE WIDTHS / FREE ELECTRON
C.....SPECIAL TREATMENT FOR HYDROGEN LINES
      IF(ILK-14) 20,21,20
C     WDH IS ALPHA AS DEFINED BY EQ.48 OF AERODYNAMR REPORT 69-41
   21 CONTINUE
      VL = ANN(5,I)*.6667
      FD = V1?2.61*4.8E-10
      WDH=(9.898E+12/VL                 )*ABS(1./FHYS-1./HVLE(J))
      IF(NID-10?48) 23,22,23
C     LYMAN ALPHA LINE
   22 IF(WDH-0.0028) 122,129,129
  122 CALL DGLEE(1,WDH,0L,0,ALPH,SLA,SLAS)
      A=10.**AL
      GO TO 113
  123 A=?.692-5.128E-09*TEE(I)+2.365E-09*TEE(I)**2+ALOG10(ANN(5,I))**(-0.41
     127+2.907E-09*TEE(I)-?.65E-10*TEE(I)**2)
      A=3.1E-6*E.**WDH * FD                 1**0.5)/WDH**2.5
      GO TO 113
   23 IF(NID-12044) 33,90,33
C     LYMAN BETA LINE
   90 IF(WDH-0.021 32,33,33
   32 CALL DGLEE(1,WDH,0L,0,BETA,SLA,SLAS)
      A=10.**AL
      GO TO 113
   33 A=12.95-8.07E-09*TEE(I)+2.06E-09*TEE(I)**2+ALOG10(ANN(5,I))**(-0.775
     1+6.767?E-09*TEE(I)-1.23E-09*TEE(I)**2)
      A=3.78E-9?1.**WDH * FD                (**0.5)/WDH**2.5
      GO TO 113
   31 IF(NID-12?45) 43,85,45
C     LYMAN GAMMA LINE
   85 GAM=9.79E-21*XNN(5,I)*ALOG10(1.E+09*TEE(I)/116.*XNN(5,I)**0.5)*(*107
     19.7*TEE(I)**0.5
      GO TO 200
C     BALMER ALPHA LINE
   45 IF(NID-3888) 47,46,47
   46 IF(WDH-0.24) 340,141,341
  140 CALL DGLEE(1,WDH,0L,0,DEL,SHA,SHAS)
      A=10.**AL
      GO TO 113
  141 A=1.5702*(20090./TEE(I))**0.42-ALOG10(ANN(5,I))*0.1183*(10000./TEE
     1(I))**0.678
      A=1.3E-3*(1.+0*(  WDH * FD                1**.5)/WDH**2.5
      GO TO 113
C     BALMER BETA LINE
   47 IF(NID-2?49) 49,48,49
   48 IF(WDH-.3) 147,148,148
  147 CALL DGLEE(1,WDH,0L,0,BI,SMB,SMBS)
      A=10.**BL
      GO TO 113
  148 A=2.17*(10000./TEE(I))**0.330-ALOG10(ANN(5,I))*0.1139*(10000./TEE(I))
     1**0.333
      A=3.57E-10*(1.+0*( WDH * FD                1**.5)/WDH**2.5
      GO TO 113
   49 IF(NID-6401 20,140,20
C     PASCHEN ALPHA LINE
  140 GAM=9.79E-21*XNN(5,I)*ALOG10(1.E+09*TEE(I)/116.*XNN(5,I))**1267
     1.*TEE(I))**0.5
      GO TO 200
  113 A=(1.746*A/4067.898/(EHYS**2*(     FD                    1)
      GO TO 10
   20 CONTINUE
C.....LINES FOR SPECIES OTHER THAN H
      GAM=1.0*XNN(5,I)*T(I)**0.67
C     ADD IN THE CONTRIBUTION DUE TO RESONANCE BROADENING
      IF(GUP(J).LT.1) GO TO 200
      AIR = 0.175*GEE(IK)*FF(J)/HVLE(J)*SQRT(GEE(IK)/GUP(J))
      GAR = GAM+XP*AIR/2.687E+19
C     ....END OF LOOP TO SET THE LINE WIDTHS USING THE DOPPLER WIDTH EQUATION
  200 WD=HVLE(J)*SQRT(2.*0.693159*T2/ER(IRK))/2.997?6E+10
C
C     CALCULATE THE CONTRIBUTION OF EACH LINE TO THE ABSORPTION
C     COEFFICIENT AT FREQUENCY EHYS.  (LINE SHAPE FN WAS UNITS OF CM)
C     ....USING THE LORENTZ LINE SHAPE
C
      IF(2.0GAM-WD) 11,11,12
   12 B=GAM/3.1416*WD*5.D#((EHYS-HVLE(J))**2+GAM**2))
      GO TO 13
C
C     WHEN THE DOPPLER WIDTH IS LARGER ,THE DOPPLER SHAPE IS USED IN THE
C     CORE REGION.  IN THE WING REGION,HOWEVER, THE  LARGER OF THE TWO
C     SHAPES IS USED.EVEN WHEN THE DOPPLER EFFECT DOMINATES THE CORE
C     REGION!
C
   11 IF((EHYS-HVLE(J))**2-WD**2) 15,15,16
   15 B=SQRT(0.693159/3.1416)*EXP(-0.693159*(EHYS-HVLE(J))**2/WD**2)/(WD65.
     1*WD)
      GO TO 13
   16 B1=GAM/(3.1416*WD65.D*((EHYS-HVLE(J))**2+GAM**2))
      B2=SQRT(0.693159/3.1416)*EXP(-0.693159*(EHYS-HVLE(J))**2/WD**2)/(WD65
     1.*WD)
      IF(B2-B1) 17,17,18
   17 B=B1
      GO TO 13
   18 B=B2
C     ....THE ABSORPTION COEFFICIENT PER LINE IS THEN
   13 FAC=SL*B*E1.-EXP(-EHYS/T(I))
C     ....AND THE CORRECTION FOR INDUCED EMISSION HAS BEEN INCLUDED.
C     THE TOTAL ABSORPTION COEFFICIENT IS OBTAINED BY SUMMING OVER ALL
C     LINES
  250 S1(I)=S1(I)+FAC
   50 CONTINUE
      RETURN
      END
C
      SUBROUTINE METRANS2(NY,YY,NIC,NICN,C2 ,BEE,THU,EX,OH,DP,TAUT,FEN,FEP)
      DIMENSION ELNE(1), DY(1)
      ?IMENSION FE(1),DM(1),DP(1),?Y(1)
      DIMENSION       AGE(1),THM(1)                    ,TAUTE(1),NICNE(1),
     1  FINE(1),FIP(1)
      NYP = NY + 1
      NYM = NY - 1
      FINE(1) = 0.
      FIP(NY) = 0.
      ALF = 1.
      DO 40 I=1,NYM
```

```
      Z=YY(I+1)-YY(I)
   40 DY(I)=Z*C2
      EX(1) = 1.
      TAUT(1) = 0.
      DO 1 I=2,NY
      Y = TMU(I)/TMU(I-1)
      V1=V-1.
      DYAL=DY(I-1)*ALF
      IF(ABS(V1).GT.0.01) GO TO 2
      TAUT(I)=(1.+V1*(0.5+V1/24.*(1-7.*V)))*DYAL*TMU(I-1)
      DMU(I)=DYAL*(0.5-V1/8.*(1.-13.*V1/3.))*TMU(I-1)
      DP(I-1)=DYAL*(0.5+V1/24.*(4.-V))
      GO TO 1
    2 V3=ALOG(V)
      V32 = V3 * V3
      TAUT(I)=V1/V3*TMU(I-1)*DYAL
      DMU(I)=DYAL*(V3-V1/V3/V32
      DP(I-1)=DYAL*(V1-V32/V32
    1 CONTINUE
      I=NY
      DO 30 I=2,NY
      EXE(I)=EXP(-TAUT(I))
      ELN(I)=ALOG(EXE(I)/EXE(I-1))
      DEN=TAUT(I)-ELN(I)
      VUM=EXE(I-1)-EXE(I)*ELI
      PIP(I-1)=PIP(I)*EXE(I)+VUM/DEN*TAUT(I)
   31 I=I-1
      DO 32 I=2,NY
      DEN=ELN(I)+TAUT(I)
      VUM=EXE(I)-EXE(I-1)*EXE(I)
      PIM(I)=PIM(I-1)*EXE(I)+VUM/DEN*TAUT(I)
   30 CONTINUE
      DO 95 LL=1,NIC
      IF = NICNIL(L)
      DP(LL) = PIP(IF)
   95 DM(LL) = PIM(IF)
      DO 96 LL=1,NIC
      PI(LL) = DM(LL)
   96 PIP(LL) = DP(LL)
      DO 98 I=2,NY
   98 DP(I) = TAUT(I)
      TAUT(1) = 0.
      DO 99 I=2,NY
   99 TAUT(I) = TAUT(I-1) + DP(I)
      RETURN
      END
C
      SUBROUTINE ESLOV (N,X,Y,SP,R,NO)
      DIMENSION XI(3),YI(3),SR(3),RI(3)
      DIMENSION YY(5)
      DIMENSION XX(6),SLR(25),YL(25)
      DO 1 I=1,N
    1 YL(I)=ALOG(Y(I))
      CALL SLOPQ(N,X,YL,SLR,R)
      DO 2 I=1,N
    2 SR(I)=Y(I)*SLR(I)
      DO 3 I=2,N
      XI=1
      XD=X(I)-X(I-1)
      YS=Y(I)+Y(I-1)
      SD=SR(I)-SR(I-1)
      YD=Y(I)-Y(I-1)
      YDER=YD/XD
      YZDER=SD/XD
      YZ=ABS(XD*YDER)
      YS = ABS(Y(I)*SR(I)*XD/2.*XD)
      TS = ABS(Y(I-1)) + YZ
      IF(T3-0.15*T5) 4,4,5
    4 R(I) = R(I-1)+XD/2.*(YS-SD/6.*(5.
      GO TO 3
    5 YY(1)=ALOG(Y(I-1))
      RR=0.0
      XX(1)=X(I-1)
      DO 8 J=2,5
    8 XX(J)=XX(J-1)+XD/4.
      CALL OGLE(5,XX,YY,N,X,YL,.01,
      IF(NO-1) 9,9,10
   10 YMAX=YY(1)
      YMIN=YY(1)
      IF(YY(5)-YY(1)) 11,11,12
   11 YMAX=YY(5)
      YMIN=YY(1)
   12 DO 13 J=1,5
      IF(YY(J)-YMAX) 14,14,15
   14 IF(YY(J)-YMIN) 13,13,13
   15 CONTINUE
      GO TO 9
   13 SSR=4YY(5)-YY(1)*1/XD
      T4=ABS(2.*SSR*XD/(YY(5)+YY(1)))
      IF(T4-.00001) 19,18,17
   19 RR=0.5*XD*(EXP(YY(5))*EXP(YY(1)))
      GO TO 17
   18 RR=(EXP(YY(5))/SSR)*(1.-EXP(-SSR*XD/4.))
   17 R(I) = R(I-1)+RR
      GO TO 3
    9 DO 6 J=2,5
      SSR=(YY(J)-YY(J-1))/XD/4.1
    6 RR=RR+(EXP(YY(J))/SSR)*(1.-EXP(-SSR*XD/4.))
      R(I)=R(I-1)+RR
    3 CONTINUE
      RETURN
      END
C
      SUBROUTINE OGLE(N,XAR,PRR,NUMX,X,P,EM)
      DIMENSION XAR(1),XI(3),PI(3),EM(1),PRR(1)
      XOI=X(NUMX)-XI(1)
      I5=1
    2 DO 600 J=1,N
      XA=XAR(J)
      IP=1
      IT=2
   61 IF(XOI)P1 72,60,71
   62 IF(I5-1)67I,671,68
   71 IF(XA-X(I5)) 62,63,64
   72 IF(XA-X(I5)) 62,63,64
   60 I5=I5-1
      TT=2
      GO TO (61,661,10
  672 I5=NUMX
  671 I=I5
      M=0.
      DPDI=EM(1)
      GO TO 67
   63 PA=PI(5)
      DPDI=EM(5)
      GO TO 601
   64 I5=I5+1
      IF(I5-NUMX)69 ,672
   69 IP=2
      GO TO (61,65),IT
   65 I5=I5-1
   66 I=I5
      G=((EP(I+1)-P(I))/(XI(I+1)-XI(I))-EM(I))/(XI(I+1)-XI(I))
      H=((EM(I+1)-EM(I))/(XI(I+1)-XI(I)))-2.*G)/(XI(I+1)-XI(I))
      W=(P*(XA-XI(I+1))+G)*(XA-XI(I))
      DPDI=(W+H*W)*(XA-XI(I))+P*(XA-X(I))+PI(I)
   67 PP=(H*EM(I))*(XA-X(I))+PI(I)
  601 CONTINUE
      PRR(J)=PP
  600 CONTINUE
   60 CONTINUE
      RETURN
      END
C
      SUBROUTINE SLOPQ(N,X,Y,S,Z)
      DIMENSION X(1),Y(1),S(1),Z(1)
      IF(N-1) 9,9,1
    1 S(2)=(Y(2)-Y(1))/(X(2)-X(1))
      S(1)=S(2)
      DC=S(2)
      DO 7 I=3,N
      IP1=I-1
      IF(IP1-1)2,2,6
    2 XDT=X(I)-X(I-1)
      XTT=X(I-1)-X(I-2)
      XTD=X(I)-X(I-2)
      ADT=Y(I)-Y(I-1)
      ATT=Y(I-1)-Y(I-2)
      AC=Y(I)-Y(I-2)*XTT*XTD
      AAA=ADT*XTT
      ABB=ADT*XTD
      ACC=AC*DOT
      DA=DC
      DB=S(I)
      DC=S(I)*2
      S(I)=AA*(X(I)-XDT)+ABB-ACC
      S(I-1)=AA*(XDT-XTT)+ACC-AAA
      S(I-2)=AC*(XDT-XTD)+AAA-ABB
    3 IF(I-2)7,5,4
    4 S(I)=(S(I)+DA)/2.
    5 S(I)=(S(I)+DB)/2.
    6 XD=X(I)-X(I-1)
      YS=Y(I)+Y(I-1)
      SD=S(I)-S(I-1)
      YD=Y(I)-Y(I-1)
      SS=S(I)
      Z(I)=2(I-1)+XD/2.*(YS-XD/6.*SD)
      S(I)=SS
    7 CONTINUE
    9 RETURN
      END
C
      SUBROUTINE ZHYEHV,ZO,EM,ZI,ZC)
      E=HV
      IF (HV-0.62) 1,1,2
    1 ZO=0.99997956-0.31559480**2-0.62454798E-02*E**2 +0.67732838E-03*E**3
     1-9.6445854F-03*E**4 +0.05*0604AF-04*E**5 -7.70863746E-05*E**6 +2.
     2681332E-06*E**7
      GO TO 3
    2 ZO=(2./5.42)**3
    3 IF (HV-0.35) 4,4,5
    4 ZN=1.000148-0.41835346*X +0.16803591*E**2 -0.7794579E-02*E**3
     1+9.9544551E-02*E**4 -5.6095534F-03*E**5 +4.515535F-04*E**6 -1.4035
     2868E-05*E**7
      GO TO 6
    5 Z=(2./6.35)**3
    6 X=HV/4.0
      IF (X-4.6) 7,7,8
    7 ZI=1.0003794-0.2464766*X +7.5092616E-02*E**2 -1.702956E-02*E**3
     1+3.2795590E-03*E**4-2.126662F-04*E**5
      GO TO 9
    8 ZI=(2./7.37)**3
    9 E=HV
      IF (E-7.37) 25,25,26
   25 EC=0.99763674-0.6340182*E +6.5333163E-02*E**2 -1.5*91A8E-02*E**3
     1+6.0385449E-03*E**4-6.6764240E-04*E**5+2.9122261E-05*E**6-1.88352
     2*8E-07*E**7
      GO TO 28
   26 EC=(2./7.37)**3
   28 RETURN
      END
```

DESCRIPTION OF INPUT

CARD SET 1 - CONTROL CARD AND CASE IDENTIFICATION
CARD 1, FORMAT(5I1,15A5)
FIELD 1, (COLUMNS 1-5) KQS
COLUMN 1 DETERMINES IF CHANGES ARE TO BE MADE FOR PARAMETERS IN NAMELIST NAME2. SEE CARD SET 4.
0 NO CHANGES IN NAME2
1 CHANGES IN NAME2
COLUMN 2 DETERMINES IF MASS BALANCE OPTION TO BE USED. SEE ALSO THE PARAMETERS LSC AND CGS IN NAME2 OF CARD SET 4.
0 MASS BALANCE NOT USED
1 MASS BALANCE USED
COLUMN 3 DETERMINES IF RADIATIVE TRANSPORT IS CONSIDERED.
0 NO RADIATIVE TRANSPORT
1 RADIATIVE TRANSPORT
COLUMN 4 DETERMINES IF MOLECULES ARE TO BE INCLUDED IN RADIATIVE TRANSPORT.
0 MOLECULES INCLUDED (SEE CARD SET 7)
1 MOLECULES NOT INCLUDED
COLUMN 5 DETERMINES HOW THE LINE CONTRIBUTIONS ARE CALCULATED IN THE RADIATIVE TRANSPORT.
0 INCLUDE LINES, WEAK LINES TREATED APPROXIMATELY
1 INCLUDE LINES IN FULL DETAIL
2 EXCLUDE LINES
FIELD 2, (COLUMNS 6-80) CASE
CASE IDENTIFICATION (ALPHANUMERIC).

CARD SET 2 - FREESTREAM CONDITIONS, NUMBER OF NODES, NOSE RADIUS.
CARDS AS REQUIRED, NAMELIST FORMAT (NAME1)
VF FREESTREAM VELOCITY, METERS PER SECOND
RHOF FREESTREAM DENSITY, KILOGRAMS PER CUBIC METER
PF FREESTREAM PRESSURE, NEWTONS PER SQUARE METER
HF FREESTREAM ENTHALPY, JOULES PER KILOGRAM
RN BODY RADIUS AT STAGNATION POINT (NOSE RADIUS), METERS
KYS NUMBER OF NODES THROUGH LAYER INCLUDING WALL AND SHOCK LOCATIONS. MAXIMUM OF 11.
Y(I) ARRAY OF NONDIMENSIONAL LOCATION OF NODES THROUGH LAYER (I=1,KYS). Y(1)=0 AT WALL AND Y(KYS)=1 AT SHOCK.
KSE NUMBER OF NODES AROUND BODY. MAXIMUM OF 15.

CARD SET 3 - SPECIFICATION OF BODY SHAPE AT NODES AROUND BODY.
CARDS AS REQUIRED AND EQUAL TO KSE, FORMAT(5F15.7). ONE CARD FOR EACH BODY LOCATION. BEGIN AT S=0. LENGTHS TO BE NONDIMENSIONAL BY RN AND ANGLES IN RADIANS.
COLUMN 1-15 THETA, BODY ANGLE
COLUMN 16-30 S, DISTANCE ALONG BODY FROM STAGNATION POINT
COLUMN 31-45 YB, RADIUS OF BODY PERPENDICULAR TO AXIS.
COLUMN 46-60 XB, AXIAL DISTANCE FROM STAGNATION POINT
COLUMN 61-75 K, BODY CURVATURE TERM

CARD SET 4 - CONVERGENCE TERMS, OUTPUT, MASS BALANCE TERMS, ETC.
SKIP THIS SET IF KQS(1)=0.
CARDS AS REQUIRED, NAMELIST FORMAT(NAME2)
VALUES FOR THE PARAMETERS IN NAME2 ARE SET IN THE PROGRAM, BUT ARE NOT NECESSARILY GOOD VALUES FOR ALL PROBLEMS. TO CHANGE ANY OF THEM, SET KQS(1)=1 AND READ IN THE VALUES FOR THE PARAMETERS WHICH ARE TO BE CHANGED. FOR NO CHANGES, SET KQS(1)=0 AND SKIP THIS CARD SET.
DF1 MULTIPLY OF CORRELATION FOR INITIAL SHOCK STAND-OFF DISTANCE.
TIFRAC MULTIPLY OF VALUE FOR GETTING TIME STEP. MUST BE LESS THAN 1.0.
IKSC THE ITERATION TO BEGIN CHECKING FOR CONVERGENCE.
CC1 CONVERGENCE CRITERION. THE CHANGE IN ENTHALPY BETWEEN ITERATIONS, (H(N+1)-H(N))/H(N), MUST BE LESS THAN CC1 FOR CONVERGENCE.
CCF FRACTION OF NODES POINTS ALONG WALL, SHOCK, AND LAYER MIDPOINT FOR WHICH THE CONVERGENCE CRITERION MUST BE MET. VALUE FOR CCF MUST BE LESS THAN 1.0.
ICC CONSECUTIVE NUMBER OF ITERATIONS FOR WHICH THE ERROR CRITERION MUST BE MET.
IKSF MAXIMUM NUMBER OF ITERATIONS TO BE ALLOWED. CARDS ARE PUNCHED TO PICK UP CASE BY ANOTHER RUN, SEE CARD SET 5.
IOUTN PRINTED OUTPUT IS GIVEN FOR CONVERGED SOLUTION. FOR INTERMEDIATE OUTPUT, IOUTN IS THE NUMBER OF ITERATIONS BETWEEN OUTPUT.
IOUTF IF THE INITIAL VALUES (FIRST GUESS VALUES) ARE TO BE PRINTED, SET THE VALUE OF IOUTF TO IOUTN MINUS ONE. IF NOT, SET IOUTF EQUAL TO ZERO.
ITC NUMBER OF ITERATIONS BETWEEN CALCULATION OF THERMODYNAMIC PROPERTIES.
IRC NUMBER OF ITERATIONS BETWEEN CALCULATION OF RADIATIVE TRANSPORT.
IKSU(I) ARRAY FOR VALUES OF ITERATIONS AT WHICH THE VALUES FOR ITC AND IRC CAN BE CHANGED DURING SOLUTION. MAXIMUM OF 5.
ITCU(I) ARRAY OF VALUES FOR ITC WHICH CORRESPONDS TO IKSU(I).
IRCU(I) ARRAY OF VALUES FOR IRC WHICH CORRESPONDS TO IKSU(I).
NCTS IF NCTS EQUALS ZERO, THE TIME STEP CAN VARY AROUND BODY AND SOLUTION WILL GENERALLY CONVERGE FASTER. IF NCTS IS NOT EQUAL TO ZERO, THE MINIMUM TIME STEP IS USED AT ALL BODY LOCATIONS.
CGS CRITERION TO BE MET BEFORE MASS BALANCE OPTION CAN BE USED. THE SHOCK VELOCITY AT THE STAGNATION POINT (DELTAT(1)) MUST BE LESS THAN THE SET VALUE FOR CGS BEFORE THE MASS BALANCE OPTION CAN BE USED FOR CALCULATING THE SHOCK STAND-OFF DISTANCE AROUND BODY. THIS IS BECAUSE THE SHOCK STAND-OFF DISTANCE AT THE STAGNATION POINT MUST BE CONVERGED BEFORE USING THE MASS BALANCE OPTION.
LSC THE MINIMUM ITERATION AT WHICH THE MASS BALANCE OPTION CAN BE USED.

CARD SET 5 - INPUT FOR THE PICK UP OF A SOLUTION.
THE PROGRAM IS WRITTEN SO THAT A SOLUTION CAN BE PICKED UP FROM A SPECIFIED ITERATION.
FOR A NEW CASE, A BLANK CARD IS INSERTED FOR THIS CARD SET.
IF THE NUMBER OF ITERATIONS REACHES THE VALUE SET FOR IKSF (CARD SET 4) THEN A CONVERGED SOLUTION WAS NOT OBTAINED WITHIN THE SPECIFIED NUMBER OF ITERATIONS AND A SET OF CARDS ARE PUNCHED OUT. THIS SET OF PUNCHED OUTPUT CAN BE INSERTED FOR CARD SET 5 AND THE SOLUTION CAN BE PICKED UP BY ANOTHER RUN AT THAT ITERATION. FOR A PICK UP CASE, IKSF AND IKSC (CARD SET 4) MUST BE GREATER THAN THE VALUE OF IKSF FROM THE PRIOR RUN)

CARD SET 6, 7 AND 8.
THESE CARD SETS ARE THE CHEMISTRY INPUTS FOR THE CHEMICAL EQUILIBRIUM CALCULATIONS AND THE BASIC RADIATION AND SPECTROSCOPIC DATA FOR THE RADIATIVE TRANSPORT CALCULATIONS. THE INPUTS FOR THE CARD SETS ARE DESCRIBED IN THE REPORT - NICOLET, M.E. USER'S MANUAL FOR THE GENERALIZED RADIATION TRANSFER CODE (RAD/EQUIL). AEROTHERM REPORT NUMBER UM-69-9. AEROTHERM CORPORATION, MOUNTAIN VIEW, CALIFORNIA.
CARD SET 6 IS READ IN THE SUBROUTINE INPUT. CARD SETS 7 AND 8 ARE READ IN SUBROUTINE RADIN.

CARD SET 6 - CHEMISTRY INPUT.
THE INPUTS FOR THIS CARD SET ARE DESCRIBED IN GROUP 3 AND GROUP 4 OF DECK B IN THE REPORT BY NICOLET.
MODIFICATIONS
GROUP 3 IN COLUMNS 25-30 ON EACH ELEMENT CARD, EXCEPT ELECTRON, GIVE THE ELEMENTAL MASS FRACTION FOR THAT ELEMENT. (AS A NEGATIVE NUMBER) NOTE, MASS FRACTION OF ELEMENT.
GROUP 4 THE THERMODYNAMIC INPUT DATA (3 CARD SET) FOR THE ATOMIC SPECIES OF THE ELEMENTS MUST BE ARRANGED FIRST IN THE SAME ORDER AS GIVEN BY GROUP 3. THE DATA FOR THE ELECTRON AND IONIZED SPECIES ARE STILL AT THE END. CONDENSED SPECIES ARE NOT ALLOWED. MAXIMUM NUMBER OF SPECIES IS 40. A BLANK CARD MUST BE PLACED AT THE END OF GROUP 4 AS STATED BY NICOLET.

CARD SET 7 - CONTINUUM CONTRIBUTIONS TO RADIATIVE TRANSPORT. SKIP THIS CARD SET IF KQS(3)=0.
THE INPUTS FOR THIS CARD SET ARE DESCRIBED IN GROUP 6, CARD 3 OF DECK B IN THE REPORT BY NICOLET.
IDENTIFIES WHICH CONTINUUM CONTRIBUTIONS ARE TO BE INCLUDED IN THE CALCULATION OF RADIATIVE TRANSPORT.

CARD SET 8 - RADIATION AND SPECTROSCOPIC DATA. SKIP THIS CARD SET IF KQS(3)=0.
THE INPUTS FOR THIS CARD SET ARE DESCRIBED IN DECK A (ENTIRE DECK) IN THE REPORT BY NICOLET.

INPUT FOR SAMPLE CASE

```
$1101     .97 CO2 - .03 N2 (BY VOLUME), 60 DEG. CONICAL BODY, HIGH VEL.
 $NAME1   VF=11175.,  RHOF=.002285,  PF=117.3,  MF=-8860000.,  RM=.3048, KSE=10.
          KYS=9,  Y(1)=0.,.125,.250,.375,.500,.625,.750,.875,1.000,  $END
1.570796        0.              0.              0.              1.0
1.370796        .2              .198669         .019933         1.0
1.170796        .4              .389418         .078939         1.0
1.047198        .6              .566169         .172175         0.
1.047198        .8              .739171         .272175         0.
1.047198        1.2             1.085781        .472175         0.
1.047198        2.0             1.778601        .872175         0.
1.047198        3.0             2.644626        1.372175        0.
1.047198        4.0             3.510652        1.872175        0.
1.047196        5.0             4.376677        2.372175        0.
 $NAME2    LSC=600, IKSF=1200, ITC=100, IRCU(I)=200,200,200,200,100,
          IOUTV=200, IOUTF=199   $END
    0
 4
  6 CARBON        12.011     -.2676
  7NITROGEN       14.007     -.0193
  8 OXYGEN        16.000     -.7131
 99ELECTRON       .00055
  1006                                    JANAF 03/81                          C
 1708886+6 135500+5 444433+1 228125-3 40983046 492870+2  500. 3000.1  0.C
 1708886+6 135500+5 412212+1 261908-3 262886+7 492870+2 3000. 5000.1  0.C
  1007                                    JANAF 03/81                          N
 1129654+6 134370+5 486944+1 383516-4 958660+5 480900+2  500. 3000.1  0.N
 1129654+6 134370+5 428957+1 240844-3 417273+6 480900+2 3000. 5000.1  0.N
  1008                                    JANAF 06/62                          O
 5955904+5 135220+5 497228+1 390768-5 154749+5 500960+2  500. 3000.1  0.O
 5955904+5 135220+5 657489+1-224268-3-891782+7 500960+2 3000. 5000.1  0.O
  2  7                                   JANAF 9-30-65                        N2
      0+0 2216494+5 793097+1 319649-3-314295+6 637650+2   500  30001  -0N2
      0+0 2216494+5 878236+1 68 810-4-119262+7 637650+2  3000  60001  -0N2
  2  8                                   JANAF 9-30-65                        O2
      0+0 2344594+5 808690+1 497024-3-742932+6 679729+2   500  30001  -0O2
      0+0 2344594+5 1009246+2 636677-4-659192+7 679729+2  3000  60001  -0O2
  1  6  1  7                            JANAF 12-31-66                       CN
 1109994+6 232479+5 706816+1 994984-3-1072434+6 669760+2   500  30001  -0CN
 1109994+6 232479+5 126220+2-178667-3-1846804+8 669760+2  3000  60001  -0CN
  1  6  1  8                            JANAF 9-30-65                        CO
-2641694+5 2235694+5 808732+1 281527-3-3321244+6 653694+2   500  30001  -0CO
-2641694+5 2235694+5 885923+1 582009-4-1269514+7 653694+2  3000  60001  -0CO
  1  6  2  8                            JANAF 9-30-65                        CO2
-9405394+5 3653494+5 1352964+2 479823-3-8854704+6 798480+2   500  30001  -0CO2
-9405394+5 3653494+5 1448844+2 176547-3-1306224+7 798480+2  3000  60001  -0CO2
  2  6                                   JANAF 12/69      KS                  C2
 2002234+6 2467794+5 776930+1 671196-3 2088144+6 685590+2   300  30001  10C2
 2002234+6 2467794+5 843360+1 447514-3 2596366+6 685590+2  3000  60001  10C2
  2  6  1  7                            JANAF 3-31-67                        C2N
 1338004+6 3845994+5 1465534+2 722952-4-5421274+6 866270+2   500  30001  -0C2N
 1338004+6 3845994+5 1459504+2 590928-4 3565954+6 866270+2  3000  60001  -0C2N
  2  6  1  8                            JANAF 9-30-66                        C2O
 6849994+5 3860794+5 1420614+2 468192-3-780511+6 864460+2   500  30001  -0C2O
 6849994+5 3860794+5 1622974+2-141246-3-2537854+7 864460+2  3000  60001  -0C2O
  3  6                                   JANAF 12/69      KS                  C3
 1959994+6 3095794+5 996626+1 976478-3-168294+6 812354+2   300  30001  10C3
 1959994+6 3095794+5 1295054+2 166809-3-516560+7 812354+2  3000  60001  10C3
  4  6                                   JANAF 12/69      KS                  C4
 2319994+6 5109594+5 1835314+2 744725-3-6778144+6 948934+2   300  30001  10C4
 2319994+6 5109594+5 2084504+2 244726-5-3063504+7 948934+2  3000  60001  10C4
  5  6                                   JANAF 12/69      KS                  C5
 2339994+6 6533594+5 2347514+2 992624-3-9364914+6 1091284+3   300  30001  10C5
 2339994+6 6533594+5 2679434+2 382130-5-4128934+7 1091284+3  3000  60001  10C5
  1007 01 08                          JANAF 06/63                          NO
 2158004+5 2270004+5 877623+1 849031-4-7896564+6 884904+2   500. 3000.1  0.NO
 2158004+5 2270004+5 916264+1 697885-5-2125194+7 884904+2  3000. 5000.1  0.NO
  1  7  2  8                            JANAF 9-30-66                        NO2
 7909994+4 3448194+5 1315004+2 215749-5-8040864+6 8479504+2   500  30001  -0NO2
 7909994+4 3448194+5 1390444+2 720659-6-1697304+7 8479504+2  3000  60001  -0NO2
  2  7  1  8                            JANAF 12-31-66                       N2O
 1960994+5 3655294+5 1376184+2 322928-3-8249974+6 8159094+2   500  30001  -0N2O
 1960994+5 3655294+5 1488584+2 252427-5-2284724+7 8159094+2  3000  60001  -0N2O
  1 99                                JANAF 3-31-65                        O-
      0+0 1342294+5 4968004+1 000000-0-700991-3 1645894+2   500  30001  -0O-
      0+0 1342294+5 4967994+1 000000-0 216803-0 1645894+2  3000  60001  -0O-
  1  8  1 99                                JANAF 6-30-65                    O-
 2429994+5 1348194+5 497035A+1-566377-6 1986094+5 4928494+2   500  30001  -0O-
 2429994+5 1348194+5 4965464+1 402558-6 3499054+5 4928494+2  3000  60001  -0O-
  2  8  1 99                                JANAF 12-31-66                   O2-
-1138994+5 2358494+5 977974+1 127404-3-2696624+6 6930494+2   500  30001  -0O2-
-1138994+5 2358494+5 865324+1 136181-3 6317934+6 6930494+2  3000  60001  -0O2-
  1  6 -1 99                                CONVAIR ZPH-122 12/61            C+
+4289854+6+1501204+5+4896574+1+1807004-4+3480004+5+4842324+22000. 10000.1    C+
+4289854+6+1501204+5+4896574+1+1807004-4+3480004+5+4842324+22000. 10000.1    C+
  1  6  1  8 -1 99                          CONVAIR ZPH-122 12/61             CO+
+2942834+6+2438304+5+4936194+1+3780004-4-1509004+7+6665954+22000. 10000.1    CO+
+2942834+6+2438304+5+4936194+1+3780004-4-1509004+7+6665954+22000. 10000.1    CO+
  1  7 -1 99                                CONVAIR ZPH-122 12/61             N+
+4466414+6+1513104+5+5017514+1+6171004-4-1841004+7+4968474+22000. 10000.1    N+
+4466414+6+1513104+5+5017514+1+6171004-4-1841004+7+4968474+22000. 10000.1    N+
  1  7  1  8 -1 99                          JANAF 6-30-66                     NO+
 7366594+6 2214994+5 7922634+1 320385-3-3131634+6 6513204+2   500  30001  -0NO+
 7366594+6 2214994+5 8921634+1 385863-4-1469554+7 6513204+2  3000  60001  -0NO+
  2  7 -1 99                                CONVAIR ZPH-122 12/61             N2+
+3572584+6+2514704+5+1365084+2-327944-3-2256304+8+6566014+22000. 10000.1     N2+
+3572584+6+2514704+5+1365084+2-327944-3-2256304+8+6566014+22000. 10000.1     N2+
  1  8 -1 99                                CONVAIR ZPH-122 12/61             O+
+3719994+6+1492904+5+1336274+1+3067104-3+5902004+7+4848494+22000. 10000.1    O+
+3719994+6+1492904+5+1336274+1+3067104-3+5902004+7+4848494+22000. 10000.1    O+
  2  8 -1 99                                CONVAIR ZPH-122 12/61             O2+
+2796954+6+2487304+5+5947894+1+6264404-3+1035004+8+6777314+22000. 10000.1    O2+
+2796954+6+2487304+5+5947894+1+6264404-3+1035004+8+6777314+22000. 10000.1    O2+
  1  6  1  7 -1 99                          JANAF 6/69       KS                CN+
 4293994+6 2388594+5 811795+1 517816-3-1386434+6 702734+2   300  30001  -0CN+
 4293994+6 2388594+5 1024104+2-992339-5-4997524+7 702734+2  3000  60001  -0CN+
  1  6  1  7  1 99                          JANAF 6/69       KS                CN-
 1599994+5 2226294+5 7616494+1 420233-3-1007444+6 644934+2   300  30001  10CN-
 1599994+5 2226294+5 892374+1 373764-4-1428724+7 644934+2  3000  60001  10CN-

  1  1  1  1  1  1  1  1  1  1  1  1  1  0  1  1  1  1  0  1
2056 4
   0.40  +01   0.10  +02   0.60  +01   0.18  +02   0.54  +02   0.90  +02
   0.00  +00   0.00  +00   0.90  +01   0.50  +01   0.10  +01   0.50  +01
   0.30  +01   1.50  +01   0.90  +01   0.40  +02   0.90  +01   0.50  +01
   0.10  +01   0.40  +01   0.12  +02   0.15  +02   0.36  +02   0.00  +00
   0.20  +01   0.80  +01   0.18  +02   0.32  +02   0.00  +00   0.00  +00
   0.00  +00   0.00  +00   0.90  +01   0.00  +00   0.00  +00   0.00  +00   0
   0.00  +00   0.00  +00   0.00  +00   0.00  +00   0.40  +01   0.00  +00   0
   0.00  +00   0.00  +00   0.00  +00   0.00  +00   0.00  +00   0.00  +00   0
   0.60  +01   0.00  +00   0.00  +00   0.00  +00   0.00  +00   0.00  +00   0
   0.00  +00   0.00  +00   0.00  +00   0.00  +00   0.00  +00   0.00  +00   0
   0.00  +00   0.2984+01   0.3576+01   0.1045+02   0.1188+02   0.1300+02
   0.00  +00   0.00  +00   0.9A  -07   0.1967+01   0.4189+01   0.9144+01
   0.9519+01   0.1074+02   0.1099+02   0.1208+02   0.00  +00   1.2639+00
   2.6839+00   4.1825+00   7.5351+00   7.9461+00   8.6442+00   0.00  +00   0   125
   0.00  +00   0.1020+02   0.1208+02   0.1274+02   0.00  +00   0.00  +00   0
                                                                              0
                                                                              0
                                                                              0
                                                                              0
                                                                              0
                                                                              0
                                                                              0
                                                                              0
                                                                              0
                                                                              0
                                                                              0
   0.60  +00   0.81  +00   0.96  +00   0.12  +01   0.14  +01   0.162 +01
   0.24  +01   0.34  +01   0.40  +01   0.62  +01   0.80  +01   0.90  +01
   0.97  +01   0.1045+02   0.1080+02   0.1170+02   0.1210+02   0.1280+02
   0.1340+02   0.1380+02   0.00  +00   0.00  +00   0.00  +00   0.00  +00
   0.80  +00   0.95  +00   0.12  +01   0.14  +01   0.16  +01   0.24  +01
   0.3500+01   0.40  +01   0.60  +01   0.80  +01   0.90  +01   0.97  +01
   0.1045+02   0.1080+02   0.1170+02   0.1210+02   0.1280+02   0.1340+02
   0.1380+02   0.1490+02   0.00  +00   0.00  +00   0.00  +00   0.00  +00
   0.69  +00   0.89  +00   0.1050+01   0.1290+01   0.1460+01   0.1850+01
   0.2850+01   0.3700+01   0.5000+01   0.7110+01   0.8400+01   0.94  +01
   0.1007+02   0.1062+02   0.1120+02   0.1190+02   0.1241+02   0.1304+02
   0.1358+02   0.1470+02   .   +   .   +   .   +   .   +
 6 71316
 6 6 8 6 5 6 5 1 1 8101212 712 8 9 4 4 4
27          0.660       0.8421       5.67E  -20
16          0.685       0.198          110E-21 6.
27          0.6859      0.044          32LE-21 3.
 6          0.689       0.1597         187E-20 6.
23          0.710       0.208          639E-18 4.
```

5	0.7525	0.0149	446E-21	
22	0.844	0.0808	412F-21	3.
21	0.852	0.0687	108E-21	
5	0.875	0.0366	380E-21	4.
15	0.8840	0.1570	367E-21	
4	0.9158	0.00847	739E-22	
6	0.9304	0.0253	387E-20	2.
6	0.965	0.0262	387E-20	4.
16	0.991	0.0805	309F-20	2.
23	1.019	0.0329	205E-19	4.
5	1.0355	0.0735	331E-21	7.
22	1.079	0.1008	320E-21	8.
15	1.0980	0.7490	344F-21	
14	1.1320	0.2010	367E-21	
21	1.163	0.474	108E-21	
22	1.224	0.0245	262E-21	
5	1.2610	0.118	312E-21	3.
4	1.3190	0.1833	984E-22	
21	1.326	0.206	138E-21	3.
14	1.3380	0.9130	342E-21	
5	1.3677	0.0387	292E-21	
4	1.4380	0.256	824F-22	3.
13	1.4670	0.9500	865F-22	
21	1.487	0.0405	218E-21	
5	1.5527	0.0030	293E-20	
12	1.594	1.0300	709E-22	
4	1.6630	0.0923	998E-22	
15	1.767	0.0226	275E-20	3.
22	1.814	0.0039	350F-20	5.
5	1.8357	0.00566	293F-20	5.
26	1.888	0.6407		
14	2.015	0.0256	275E-20	3.
26	2.549	0.1193		
4	2.925	0.0070	1066-20	3.
13	3.0	0.010	810E-21	2.
12	3.167	0.00826	920F-21	
4	3.4724	0.00861	452E-20	3.
12	3.7110	0.0143	110E-20	
19	5.002	0.0676	113E-21	
18	6.424	0.07290	113E-21	
19	7.013	0.01410	500E-21	
19	7.078	0.0748	262E-21	
3	07.111	0.0634	912E-22	
13	7.481	0.105	673E-22	
19	7.717	0.00534	220E-20	
19	7.721	0.0367	109E-19	
17	7.947	0.283	208F-22	
19	8.030	0.70457	690E-19	
19	8.191	0.0116	130E-18	
19	8.203	0.00147	119E-19	
19	8.302	0.00831	538E-18	
2	08.3021	0.0740	912E-22	
18	8.368	0.011	214E-21	
19	8.377	0.00501	677E-18	
18	8.433	0.0142	500E-21	
18	8.474	0.0625	268E-21	
3	08.781	0.0435	661E-22	
18	9.137	0.00526	220E-20	
18	9.141	0.0362	109E-19	
3	09.301	0.0186	446E-21	
17	9.332	0.203	957E-23	
3	09.396	0.0119	229E-21	
18	9.450	0.0218	690E-19	
3	09.460	0.0360	338E-21	
09	9.5010	0.0471	548E-22	
18	9.611	0.0114	130E-18	
18	9.623	0.00143	119E-19	
17	9.697	0.01950	500F-21	
17	9.698	0.0038	235E-21	
17	9.709	0.0767	235E-21	
18	9.722	0.0081	538E-18	
18	9.797	0.00488	677E-18	
17	9.834	0.026	293E-21	
2	09.973	0.0890	661F-22	
3	10.102	0.0374	293E-20	

11	10.182	0.1510	653F-22	
25	10.196	0.4162		
1	10.332	0.1840	621F-22	
17	10.401	0.00719	220E-20	
17	10.405	0.0495	109E-19	
3	10.418	0.0225	532E-20	
2	10.493	0.0187	446F-20	
3	10.545	0.0131	796E-20	
2	10.619	0.0533	312E-21	
3	10.662	0.00819	268E-19	
17	10.714	0.0298	690E-19	
3	10.757	0.00518	437E-19	
10	10.761	0.1200	653E-22	
18	10.873	0.705	630E-21	
17	10.875	0.0155	130E-18	
17	10.887	0.00195	119E-19	
1	10.927	0.4540	161E-23	
17	10.986	0.011	253F-19	
11	11.007	0.0185	367E-21	
17	11.061	0.00659	677E-18	
3	11.200	0.0200	446E-21	
2	11.293	0.0418	293E-20	
3	11.310	0.0254	323E-21	
7	11.424	0.2760	143E-23	
2	11.609	0.0250	532E-20	
2	11.776	0.0220	796F-20	
11	11.806	0.0069	145E-20	
09	11.852	0.0199	367E-21	
2	11.874	0.0091	26AE-19	
2	11.948	0.00575	437E-19	
3	12.000	0.0269	299E-20	
09	12.067	0.0218	544E-21	
25	12.086	0.0791		
11	12.160	0.0019	128E-20	
10	12.181	1.05	159E-22	
3	12.316	0.0136	696F-20	
10	12.404	0.0461	653E-22	
2	12.414	0.0574	390E-21	
2	12.511	0.0279	337E-21	
09	12.521	0.0775	633E-22	
09	12.651	0.00524	145E-20	
25	12.745	0.02899	4.59E -20	
1	12.877	0.0233	446F-21	
1	13.004	0.1320	294E-21	
17	13.119	0.379	101E-21	
2	13.190	0.0489	299E-20	
2	13.508	0.0291	696E-19	
7	13.543	0.1610	950E-24	
18	13.601	0.295	159E-22	
1	13.677	0.0957	293E-20	
1	13.993	0.0584	532E-20	
1	14.160	0.0342	796F-20	
1	14.257	0.0212	268E-19	
1	14.332	0.0138	437E-19	
48				

0.02	0.1	0.2	0.5	0.6	0.8	
1.00	1.50	2.00	2.5	2.75	3.0	
3.25	3.50	3.75	4.0	4.5	5.0	
6.00	7.00	8.00	8.50	8.52	8.98	
9.00	9.19	9.21	9.99	10.01	10.79	
10.81	11.00	11.25	11.27	11.99	12.01	
12.18	12.20	12.99	13.00	13.39	13.41	
13.59	13.61	14.29	14.31	14.55	15.00	

OUTPUT FOR SAMPLE CASE

```
CASE -      .97 CO2 - .03 N2 (BY VOLUME), 60 DEG. CONICAL BODY, HIGH VEL.

FREESTREAM PARAMETERS     VELOCITY =  1.1175E+04 M/S
                          DENSITY =  2.8500E-03 KG/M3
                          PRESSURE =  1.1730E+02 N/M2
                          ENTHALPY = -8.6800E+06 J/KG
                          NOSE RADIUS =  9.0460E-01 M

BODY SHAPE, NONDIMENSIONAL BY NOSE RADIUS
      NS        S          XBOD          YBOD         THETA          R
       1     0.0000        0.0000        0.0000        1.5708        1.0000
       2     .2000         .0199         .1987         1.5708        1.0000
       3     .4000         .0789         .3896         1.5708        1.0000
       4     .6000         .1722         .5662         1.0472        0.0000
       5     .8000         .2722         .7596         1.0472        0.0000
       6     1.2000        .4722         1.0856        1.0472        0.0000
       7     2.0000        .8722         1.7186        1.0472        0.0000
       8     3.0000        1.3722        2.4446        1.0472        0.0000
       9     4.0000        1.8722        3.5107        1.0472        0.0000
      10     5.0000        2.3722        4.3767        1.0472        0.0000

PARAMETERS FOR NONDIMENSIONALIZATION
     VP =  1.1175E+04 M/S
     RHOP =  2.8500E-03 KG/M3
     VP**2 =  1.2489E+08 J/KG
     RHOP*VP*2 =  3.5591E+05 N/M2
     RHOP*VP*3 =  3.9772E+09 W/M2
     TS =  8.1816E+04 K
     VP*VP/TS =  1.4568E+04 J/(KG-K)
     RN =  9.0480E-01 M
     RN/VP =  2.7275E-05 S

NORMAL SHOCK PROPERTIES - NONDIMENSIONAL
     PRESSURE =  .9375
     DENSITY =  15.95
     ENTHALPY =  .4269
     TEMPERATURE =  1.000
     VELOCITY =  -.0627
     MOLECULAR WT. =  13.39
     ENTROPY =  1.592
     SONIC VELOCITY =  .2700


&NAMEZ
 TIFRAC  =  0.8E+00,
 IMSC    =  500,
 CGI     =  0.1E-03,
 CCF     =  0.95E+00,
 ICC     =  50,
 IMSP    =  1200,
 IOUTN   =  200,
 IOUTF   =  100,
 ITC     =  100,
 IRC     =  100,
 IMSU    =  100,  200,  400,  600,  800,  1000,
 ITCU    =  50,  50,  50,  50,  50,
 IRCU    =  200,  200,  200,  200,  100,
 MCTS    =  0,
 LSC     =  600,
 CCS     =  0.5E-03,
&END
```

```
CONVERGED OUTPUT          ITERATIONS =  1843          TIME =  1.5319E+01

BODY STATION  1          S =  0.0000      THETA =  1.5708      BETA =  0.0000      DELTA =  .0454      DELTAT =  0.
                         XBOD =  0.0000      YBOD =  0.0000      XSHOC =  -.0456      YSHOC =  .0000
                         QWT =  8.9166E-03      QNC =  4.7396E-03      QML =  4.1786E-03
                         VELZ =  6.2706E-02      SAZ =  0.

RY        1            2            3            4            5            6            7            8            9
Y         0.           1.250E-01    2.500E-01    3.750E-01    5.000E-01    6.250E-01    7.500E-01    8.750E-01    1.000E+00
P         9.779E-01    9.726E-01    9.764E-01    9.219E-01    9.693E-01    9.859E-01    9.002E-01    9.533E-01    9.375E-01
RHO       2.449E+01    1.900E+01    1.827E+01    1.779E+01    1.744E+01    1.714E+01    1.685E+01    1.652E+01    1.595E+01
M         3.100E-01    3.787E-01    3.912E-01    3.995E-01    4.054E-01    4.103E-01    4.146E-01    4.194E-01    4.269E-01
U         0.           0.           0.           0.           0.           0.           0.           0.           0.
V         0.           -4.413E-03   -1.048E-02   -1.703E-02   -2.422E-02   -3.210E-02   -4.075E-02   -5.015E-02   -6.270E-02
N         0.           1.735E-02    4.050E-02    6.514E-02    9.196E-02    1.212E-01    1.530E-01    1.873E-01    2.822E-01
T         7.632E-01    9.109E-01    9.373E-01    9.537E-01    9.664E-01    9.733E-01    9.807E-01    9.886E-01    1.000E+00
HN        1.502E+01    1.400E+01    1.384E+01    1.373E+01    1.366E+01    1.360E+01    1.354E+01    1.348E+01    1.339E+01
SX        1.487E+00    1.594E+00    1.553E+00    1.562E+00    1.568E+00    1.574E+00    1.578E+00    1.584E+00    1.592E+00
VX        2.201E-01    4.593E-01    <.588E-01    2.610E-01    2.635E-01    2.650E-01    2.664E-01    2.678E-01    2.700E-01
PX        -2.294E-02   -6.450E-02   -<.052E-02   -2.797E-02   -2.905E-02   -3.002E-02   -3.092E-02   -3.197E-01   -3.360E-01
WX        0.           1.787E-03    3.684E-03    5.393E-03    6.995E-03    8.511E-03    9.966E-03    1.142E-02    1.299E-02
WN        8.916E-03    9.931E-03    9.932E-03    9.598E-03    8.973E-03    8.084E-03    6.862E-03    5.029E-03    0.
QW        -8.916E-03   -8.169E-03   -8.248E-03   -4.202E-03   -1.978E-03   4.267E-04    3.107E-03    6.992E-03    1.299E-02
QD        1.179E-02    1.179E-01    3.355E-01    3.066E-01    4.024E-01    4.472E-01    5.497E-01    8.500E-01    1.474E+00
RHOF      4.016E-02    6.942E-03    2.954E-03    1.987E-03    1.597E-03    1.808E-03    1.188E-03    1.227E-03    0.
UI        0.           0.           0.           0.           0.           0.           0.           0.           0.
VI        0.           9.837E-07    2.410E-06    7.008E-06    1.031E-05    1.219E-05    1.280E-05    1.257E-05    0.
PI        4.546E-05    3.780E-05    4.442E-05    3.874E-05    4.024E-05    4.329E-05    4.720E-05    5.180E-05    0.
HI        -4.784E-04   8.104E-05    -2.940E-05   -4.408E-05   -1.549E-05   -1.977E-05   -9.917E-06   3.189E-06    0.
TAU       2.070E-02    1.823E-02    1.833E-02    1.863E-02    1.904E-02    1.956E-02    2.019E-02    2.093E-02    2.198E-02
SF        0.           0.           0.           0.           0.           0.           0.           0.           0.

          MASS BALANCE      FREESTREAM =  0.          SHOCK LAYER =  0.          DELTA MASS =  4.557E-02

BODY STATION  2          S =  .2000      THETA =  1.3708      BETA =  .0219      DELTA =  .0468      DELTAT =  0.
                         XBOD =  .0199      YBOD =  .1987      XSHOC =  -.0259      YSHOC =  .2080
                         QWT =  7.6793E-03      QNC =  4.1139E-03      QML =  3.5546E-03
                         VELZ =  1.9666E-01      SAZ =  1.2506E+00

RY        1            2            3            4            5            6            7            8            9
Y         0.           1.250E-01    2.500E-01    3.750E-01    5.000E-01    6.250E-01    7.500E-01    8.750E-01    1.000E+00
P         9.283E-01    9.249E-01    9.262E-01    9.259E-01    9.250E-01    9.233E-01    9.203E-01    9.142E-01    9.055E-01
RHO       2.349E+01    1.833E+01    1.786E+01    1.725E+01    1.699E+01    1.680E+01    1.664E+01    1.648E+01    1.615E+01
M         3.075E-01    3.752E-01    3.868E-01    3.964E-01    3.991E-01    4.023E-01    4.045E-01    4.064E-01    4.095E-01
U         8.627E-02    9.116E-02    1.062E-01    1.191E-01    1.322E-01    1.458E-01    1.596E-01    1.736E-01    1.877E-01
V         0.           -4.103E-03   -9.729E-03   -1.573E-02   -2.240E-02   -2.984E-02   -3.807E-02   -4.705E-02   -5.558E-02
N         1.928E-01    2.610E-02    4.155E-02    6.140E-02    8.633E-01    5.140E-01    6.245E-01    6.830E-01    7.440E-01
T         7.515E-01    9.014E-01    9.259E-01    9.410E-01    9.504E-01    9.565E-01    9.604E-01    9.636E-01    9.687E-01
HN        1.506E+01    1.404E+01    1.389E+01    1.380E+01    1.373E+01    1.369E+01    1.366E+01    1.364E+01    1.360E+01
SX        1.457E+00    1.539E+00    1.551E+00    1.559E+00    1.564E+00    1.568E+00    1.570E+00    1.573E+00    1.577E+00
VX        2.186E-01    4.547E-01    2.589E-01    2.594E-01    2.611E-01    2.621E-01    2.628E-01    2.634E-01    2.643E-01
PX        -2.700E-01   -2.531E-01   -2.717E-01   -2.699E-01   -2.849E-01   -3.003E-01   -3.053E-01   -3.101E-01   -3.199E-01
WX        0.           1.578E-03    3.262E-03    4.746E-03    6.111E-03    7.360E-03    8.499E-03    9.536E-03    1.060E-02
WN        7.693E-03    8.525E-03    8.480E-03    8.093E-03    7.471E-03    6.602E-03    5.450E-03    3.864E-03    0.
QW        -7.693E-03   -6.949E-03   -5.198E-03   -3.351E-03   -1.360E-03   7.588E-04    3.043E-03    5.690E-03    1.060E-02
QD        2.965E-02    2.003E-01    2.984E-01    3.225E-01    3.492E-01    3.776E-01    4.265E-01    6.541E-01    1.049E+00
RHOF      4.478E-02    2.766E-03    4.555E-03    5.859E-04    2.370E-03    1.944E-03    1.429E-04    -2.122E-04   0.
UI        1.219E-05    -8.057E-06   -5.720E-05   -5.364E-05   -3.543E-05   -1.092E-05   8.270E-06    1.629E-05    0.
VI        0.           -5.122E-06   -3.598E-06   9.103E-06    2.167E-06    3.632E-06    4.489E-06    5.037E-06    0.
PI        2.821E-05    3.704E-05    3.173E-05    2.607E-05    2.617E-05    2.623E-05    2.712E-05    2.884E-05    0.
HI        -1.716E-04   -9.549E-06   9.386E-05    -1.092E-06   -3.562E-05   -2.770E-05   8.295E-06    2.161E-05    0.
TAU       2.139E-02    1.883E-02    1.895E-02    1.926E-02    1.967E-02    2.023E-02    2.095E-02    2.180E-02    2.290E-02
SF        0.           4.017E-02    8.458E-02    1.341E-01    1.886E-01    2.484E-01    3.139E-01    3.850E-01    4.614E-01

          MASS BALANCE      FREESTREAM =  4.623E-01      SHOCK LAYER =  4.614E-01      DELTA MASS =  4.677E-02
```

BODY STATION 3 S = .4000 THETA = 1.1700 BETA = .0136 DELTA = .0505 DELTAT = 0.

XBOD = .0789 YBOD = .3894 XSHOC = .0324 YSHOC = .4093

QNI = 4.713E-03 QNC = 2.770E-03 QNL = 1.943E-03

VEL2 = 3.886E-01 SA2 = 1.429E+00

KY	1	2	3	4	5	6	7	8	9
T	0.	1.250E-01	2.500E-01	3.750E-01	5.000E-01	6.250E-01	7.500E-01	8.750E-01	1.000E+00
P	7.857E-01	7.859E-01	7.890E-01	7.917E-01	7.952E-01	7.994E-01	8.047E-01	8.097E-01	8.084E-01
RHO	2.060E+01	1.623E+01	1.569E+01	1.547E+01	1.534E+01	1.562E+01	1.625E+01	1.676E+01	1.720E+01
H	2.986E-01	3.049E-01	3.259E-01	3.611E-01	3.809E-01	3.770E-01	3.704E-01	3.636E-01	3.584E-01
U	1.233E-01	1.671E-01	1.899E-01	2.172E-01	2.503E-01	2.843E-01	3.176E-01	3.488E-01	3.778E-01
V	0.	-3.035E-03	-7.103E-03	-1.190E-02	-1.788E-02	-2.429E-02	-3.160E-02	-3.891E-02	-4.672E-02
M	5.755E-01	6.753E-01	7.543E-01	8.378E-01	9.893E-01	1.131E+00	1.278E+00	1.419E+00	1.560E+00
T	7.379E-01	8.713E-01	8.956E-01	9.073E-01	9.070E-01	8.989E-01	8.856E-01	8.696E-01	8.563E-01
MR	1.322E+01	1.415E+01	1.401E+01	1.395E+01	1.395E+01	1.400E+01	1.408E+01	1.418E+01	1.427E+01
SI	1.453E+00	1.536E+00	1.568E+00	1.594E+00	1.596E+00	1.569E+00	1.533E+00	1.494E+00	1.462E+00
VA	2.134E-01	2.476E-01	2.518E-01	2.528E-01	2.537E-01	2.523E-01	2.500E-01	2.472E-01	2.446E-01
PI	-3.374E-01	-2.820E-01	-2.998E-01	-3.093E-01	-3.074E-01	-2.981E-01	-2.849E-01	-2.713E-01	-2.628E-01
QP	0.	1.081E-03	2.263E-03	3.260E-03	4.064E-03	4.584E-03	4.922E-03	5.118E-03	5.227E-03
WR	4.712E-03	5.157E-03	5.004E-03	4.567E-03	3.888E-03	3.077E-03	2.241E-03	1.514E-03	0.
QR	-6.712E-04	-4.076E-03	-7.741E-03	-1.302E-02	1.545E-04	1.504E-03	2.707E-03	3.802E-03	5.227E-03
QD	3.616E-02	1.489E-01	2.162E-01	2.270E-01	2.230E-01	2.004E-01	1.658E-01	1.051E-01	2.593E-01
RHOT	9.646E-03	8.457E-03	9.267E-03	1.347E-02	1.967E-02	2.596E-02	3.362E-03	1.468E-03	0.
UT	4.732E-04	9.504E-05	-7.785E-05	-5.450E-05	-5.258E-05	-6.121E-05	-6.221E-05	-6.326E-05	0.
VT	0.	-7.990E-06	1.262E-05	1.963E-05	2.319E-05	3.078E-05	3.054E-05	4.280E-05	0.
PT	6.737E-05	1.777E-04	1.339E-04	1.379E-04	1.377E-04	1.319E-04	1.364E-04	1.835E-04	0.
MT	-1.221E-04	-8.157E-05	-2.864E-05	-2.044E-05	4.930E-05	1.960E-04	-1.207E-05	3.419E-05	0.
TAU	2.368E-02	2.070E-02	2.071E-02	2.100E-02	2.157E-02	2.230E-02	2.317E-02	2.417E-02	2.458E-02
SF	0.	1.283E-01	2.682E-01	4.247E-01	6.051E-01	8.151E-01	1.058E+00	1.337E+00	1.652E+00

MASS BALANCE FREESTREAM = 1.656E+00 SHOCK LAYER = 1.652E+00 DELTA MASS = 5.034E-02

BODY STATION 4 S = .6000 THETA = 1.0472 BETA = .0187 DELTA = .0525 DELTAT = 0.

XBOD = .1722 YBOD = .5662 XSHOC = .1267 YSHOC = .5924

QNI = 3.176E-03 QNC = 2.240E-03 QNL = 9.364E-04

VEL2 = 6.861E-01 SA2 = 1.472E+00

KY	1	2	3	4	5	6	7	8	9
T	0.	1.250E-01	2.500E-01	3.750E-01	5.000E-01	6.250E-01	7.500E-01	8.750E-01	1.000E+00
P	7.433E-01	7.442E-01	7.491E-01	7.410E-01	7.401E-01	7.379E-01	7.364E-01	7.329E-01	7.263E-01
RHO	1.987E+01	1.566E+01	1.523E+01	1.549E+01	1.617E+01	1.693E+01	1.758E+01	1.805E+01	1.832E+01
H	2.932E-01	3.159E-01	3.617E-01	3.622E-01	3.502E-01	3.379E-01	3.276E-01	3.217E-01	3.210E-01
U	1.379E-01	1.653E-01	2.067E-01	2.018E-01	1.902E-01	1.705E-01	1.455E-01	1.211E-01	9.845E-02
V	0.	-2.211E-03	-5.518E-03	-1.068E-02	-1.593E-02	-2.188E-02	-2.787E-02	-3.386E-02	-3.872E-02
M	6.508E-01	7.603E-01	9.567E-01	1.228E+00	1.495E+00	1.737E+00	1.964E+00	2.106E+00	2.221E+00
T	7.285E-01	8.562E-01	8.736E-01	8.862E-01	8.963E-01	8.969E-01	7.606E-01	7.634E-01	7.525E-01
MR	1.382E+01	1.422E+01	1.412E+01	1.419E+01	1.435E+01	1.453E+01	1.470E+01	1.486E+01	1.497E+01
SI	1.448E+00	1.553E+00	1.562E+00	1.594E+00	1.522E+00	1.507E+00	1.499E+00	1.482E+00	1.472E+00
VA	2.107E-01	2.449E-01	2.480E-01	2.480E-01	2.490E-01	2.339E-01	2.276E-01	2.223E-01	2.189E-01
PI	-3.677E-01	-2.906E-01	-3.030E-01	-2.955E-01	-2.819E-01	-2.832E-01	-2.993E-01	-3.198E-01	-3.375E-01
QP	0.	9.159E-04	1.823E-03	2.361E-03	2.591E-03	2.880E-03	2.720E-03	2.746E-03	2.707E-03
WR	3.176E-03	3.425E-03	3.076E-03	2.468E-03	1.657E-03	1.385E-03	9.533E-04	5.484E-04	0.
QR	-3.176E-03	-2.510E-03	-1.231E-03	-1.047E-04	7.341E-04	1.310E-03	1.766E-03	2.115E-03	2.707E-03
QD	5.360E-02	1.448E-01	1.825E-01	1.513E-01	1.087E-01	7.949E-02	6.650E-02	7.279E-02	9.163E-02
RHOT	-2.295E-02	-3.078E-04	-1.582E-03	-3.771E-03	-6.419E-03	-3.823E-03	1.358E-04	-9.338E-04	0.
UT	4.481E-04	-7.117E-04	-4.506E-04	-2.813E-04	-1.994E-04	-1.932E-04	-1.327E-04	-9.373E-05	0.
VT	0.	2.013E-06	2.439E-05	2.780E-05	2.801E-05	2.654E-05	2.431E-05	1.995E-05	0.
PT	-8.643E-05	1.220E-05	3.420E-05	1.787E-05	1.362E-05	-7.590E-06	-5.924E-06	-2.810E-06	0.
MT	3.384E-04	1.526E-03	2.639E-03	8.425E-05	1.006E-04	5.662E-05	-3.356E-06	1.418E-05	0.
TAU	2.492E-02	2.168E-02	2.176E-02	2.248E-02	2.378E-02	2.534E-02	2.717E-02	2.902E-02	3.069E-02
SF	0.	1.999E-01	4.322E-01	7.294E-01	1.108E+00	1.568E+00	2.102E+00	2.696E+00	3.335E+00

MASS BALANCE FREESTREAM = 3.342E+00 SHOCK LAYER = 3.335E+00 DELTA MASS = 5.256E-02

BODY STATION 5 S = .8000 THETA = 1.0472 BETA = .0338 DELTA = .0580 DELTAT = 0.

XBOD = .2722 YBOD = .7394 XSHOC = .2219 YSHOC = .7884

QNI = 2.083E-03 QNC = 2.117E-03 QNL = 7.097E-04

VEL2 = 4.774E-01 SA2 = 1.468E+00

KY	1	2	3	4	5	6	7	8	9
T	0.	1.250E-01	2.500E-01	3.750E-01	5.000E-01	6.250E-01	7.500E-01	8.750E-01	1.000E+00
P	7.496E-01	7.463E-01	7.460E-01	7.464E-01	7.465E-01	7.464E-01	7.462E-01	7.398E-01	7.353E-01
RHO	2.035E+01	1.606E+01	1.614E+01	1.649E+01	1.708E+01	1.813E+01	1.883E+01	1.883E+01	1.827E+01
H	2.880E-01	3.541E-01	3.548E-01	3.402E-01	3.284E-01	3.203E-01	3.167E-01	3.167E-01	3.197E-01
U	1.352E-01	2.202E-01	3.210E-01	3.814E-01	4.285E-01	4.565E-01	4.681E-01	4.681E-01	4.726E-01
V	0.	-2.069E-03	-6.003E-03	-1.102E-02	-1.616E-02	-2.108E-02	-2.570E-02	-3.006E-02	-3.255E-02
M	6.479E-01	9.103E-01	1.284E+00	1.687E+00	2.029E+00	2.211E+00	2.263E+00	2.263E+00	2.227E+00
T	7.231E-01	9.436E-01	8.907E-01	8.113E-01	7.458E-01	7.108E-01	7.063E-01	7.164E-01	7.238E-01
MR	1.364E+01	1.424E+01	1.431E+01	1.449E+01	1.469E+01	1.480E+01	1.487E+01	1.488E+01	1.488E+01
SI	1.441E+00	1.545E+00	1.515E+00	1.510E+00	1.495E+00	1.485E+00	1.480E+00	1.479E+00	1.481E+00
VA	2.108E-01	2.475E-01	2.455E-01	2.388E-01	2.326E-01	2.276E-01	2.221E-01	2.216E-01	2.223E-01
PI	-3.739E-01	-2.827E-01	-2.814E-01	-2.784E-01	-2.912E-01	-3.068E-01	-3.167E-01	-3.205E-01	-3.171E-01
QP	0.	9.132E-04	1.851E-03	1.974E-03	2.140E-03	2.247E-03	2.320E-03	2.412E-03	2.517E-03
WR	2.084E-03	3.019E-03	2.959E-03	2.804E-03	2.633E-03	1.838E-03	9.459E-04	4.026E-04	0.
QR	-7.884E-05	-2.864E-03	-6.839E-04	-5.399E-05	5.079E-04	9.187E-04	1.362E-03	1.809E-03	2.517E-03
QD	4.036E-02	1.354E-01	1.496E-01	9.658E-02	6.870E-02	5.800E-02	6.080E-02	8.178E-02	1.153E-01
RHOT	5.303E-03	-4.424E-03	-8.030E-03	-3.385E-03	-3.044E-03	-1.169E-04	2.654E-03	2.376E-03	0.
UT	3.115E-06	-6.089E-04	-2.483E-04	-1.362E-04	-6.848E-05	-2.956E-06	3.216E-05	6.565E-05	0.
VT	0.	5.130E-06	1.490E-05	-5.555E-06	-1.065E-05	-1.654E-05	-2.190E-05	-2.678E-05	0.
PT	-6.267E-05	-5.717E-05	-5.482E-05	-4.721E-05	-4.710E-05	-4.599E-05	-4.356E-05	-4.506E-05	0.
MT	-1.093E-04	6.136E-05	3.531E-05	1.814E-05	1.927E-05	-1.365E-05	-5.727E-05	-4.891E-05	0.
TAU	2.779E-02	2.443E-02	2.468E-02	2.643E-02	2.844E-02	2.998E-02	3.144E-02	3.268E-02	3.338E-02
SF	0.	2.914E-01	6.096E-01	1.028E+00	1.484E+00	2.036E+00	2.655E+00	3.335E+00	4.056E+00

MASS BALANCE FREESTREAM = 5.088E+00 SHOCK LAYER = 5.080E+00 DELTA MASS = 5.802E-02

BODY STATION 6 S = 1.2000 THETA = 1.0472 BETA = .0484 DELTA = .0765 DELTAT = 0.

XBOD = .4722 YBOD = 1.0858 XSHOC = .4059 YSHOC = 1.1241

QNI = 2.803E-03 QNC = 2.227E-03 QNL = 5.761E-04

VEL2 = 9.803E-01 SA2 = 1.466E+00

KY	1	2	3	4	5	6	7	8	9
T	0.	1.250E-01	2.500E-01	3.750E-01	5.000E-01	6.250E-01	7.500E-01	8.750E-01	1.000E+00
P	7.590E-01	7.613E-01	7.566E-01	7.532E-01	7.561E-01	7.490E-01	7.468E-01	7.428E-01	7.472E-01
RHO	2.130E+01	1.705E+01	1.765E+01	1.822E+01	1.840E+01	1.838E+01	1.826E+01	1.808E+01	1.808E+01
H	2.760E-01	3.442E-01	3.217E-01	3.243E-01	3.196E-01	3.190E-01	3.199E-01	3.216E-01	3.230E-01
U	1.321E-01	3.042E-01	4.020E-01	4.942E-01	4.973E-01	4.820E-01	4.621E-01	4.607E-01	4.593E-01
V	0.	-1.697E-03	-6.306E-03	-1.089E-02	-1.481E-02	-1.833E-02	-2.192E-02	-2.548E-02	-2.698E-02
M	6.459E-01	1.041E+00	1.476E+00	1.958E+00	2.044E+00	2.044E+00	2.066E+00	2.053E+00	2.039E+00
T	7.115E-01	8.167E-01	7.941E-01	7.756E-01	7.689E-01	7.678E-01	7.692E-01	7.719E-01	7.752E-01
MR	1.369E+01	1.449E+01	1.462E+01	1.476E+01	1.482E+01	1.483E+01	1.481E+01	1.478E+01	1.476E+01
SI	1.425E+00	1.509E+00	1.499E+00	1.480E+00	1.483E+00	1.483E+00	1.484E+00	1.486E+00	1.488E+00
VA	2.096E-01	2.355E-01	2.307E-01	2.258E-01	2.238E-01	2.234E-01	2.234E-01	2.247E-01	2.257E-01
PI	-3.858E-01	-2.768E-01	-2.822E-01	-2.977E-01	-3.055E-01	-3.078E-01	-3.071E-01	-3.053E-01	-3.001E-01
QP	0.	9.083E-04	1.556E-03	1.869E-03	2.084E-03	2.272E-03	2.440E-03	2.656E-03	2.860E-03
WR	2.803E-03	2.912E-03	2.495E-03	2.155E-03	1.876E-03	1.590E-03	1.295E-03	7.846E-04	0.
QR	-2.803E-03	-1.982E-03	-9.384E-04	-2.861E-04	2.078E-04	6.819E-04	1.215E-03	1.871E-03	2.860E-03
QD	8.409E-02	9.659E-02	8.542E-02	5.976E-02	5.065E-02	5.287E-02	6.295E-02	8.656E-02	1.237E-01
RHOT	2.229E-02	-5.463E-04	8.129E-04	2.035E-04	1.014E-03	1.619E-03	1.644E-03	0.	
UT	-4.117E-06	-4.798E-05	2.482E-05	2.582E-05	4.261E-05	4.258E-05	3.900E-05	0.	
VT	0.	2.787E-07	-8.762E-06	-1.069E-05	-1.272E-05	-1.310E-05	-1.326E-05	0.	
PT	1.412E-05	-2.984E-05	-9.290E-06	-1.369E-05	-1.641E-05	-1.612E-05	-2.084E-05	-2.378E-05	0.
MT	-3.521E-04	1.060E-05	-1.567E-05	-1.372E-05	-8.781E-06	-2.294E-05	-3.244E-05	-2.633E-05	0.
TAU	3.741E-02	3.303E-02	3.467E-02	3.647E-02	3.864E-02	4.005E-02	4.133E-02	4.259E-02	4.338E-02
SF	0.	5.445E-01	1.185E+00	2.426E+00	3.563E+00	4.731E+00	5.908E+00	7.078E+00	8.244E+00

MASS BALANCE FREESTREAM = 8.256E+00 SHOCK LAYER = 8.244E+00 DELTA MASS = 7.654E-02

BODY STATION 7 S = 2.0000 THETA = 1.0472 BETA = .0534 DELTA = .1186 DELTAT = 0.

XBOD = .8722 YBOD = 1.7786 XSHOC = .7693 YSHOC = 1.6880

QWI = 3.0996E-03 QWC = 2.5838E-03 QWL = 5.6812E-04

VEL2 = 4.5586E-01 SAZ = 1.4662E+00

KV	1	2	3	4	5	6	7	8	9
T	0.	1.4508E-01	2.4500E-01	3.7500E-01	5.0000E-01	6.2500E-01	7.5000E-01	8.7500E-01	1.0000E+00
P	7.6438E-01	7.5962E-01	7.5776E-01	7.5678E-01	7.5608E-01	7.5595E-01	7.5595E-01	7.4772E-01	7.5095E-01
RHO	2.2566E+01	1.8155E+01	1.6157E+01	1.4959E+01	1.4095E+01	1.4036E+01	1.4022E+01	1.4066E+01	1.4033E+01
H	2.5899E-01	3.4695E-01	3.9193E-01	3.1866E-01	3.1956E-01	3.2028E-01	3.2221E-01	3.2435E-01	3.2530E-01
U	1.1044E-01	3.8653E-01	4.5545E-01	4.5544E-01	4.5732E-01	4.5066E-01	4.5588E-01	4.5952E-01	4.5511E-01
V	0.	-1.9842E-03	-6.6149E-03	-9.8006E-03	-1.3131E-02	-1.6498E-02	-1.9844E-02	-2.3240E-02	-2.5819E-02
M	6.5858E-01	1.7095E+00	2.0146E+00	2.0461E+00	2.0452E+00	2.0436E+00	2.0206E+00	2.0161E+00	2.0136E+00
T	6.9560E-01	7.7644E-01	7.4688E-01	7.8476E-01	7.8496E-01	7.7412E-01	7.7336E-01	7.7860E-01	7.7921E-01
RR	1.4813E+01	1.4731E+01	1.4682E+01	1.4684E+01	1.4682E+01	1.4680E+01	1.4677E+01	1.4736E+01	1.4731E+01
SX	1.2995E+00	1.4689E+00	1.4682E+00	1.4681E+00	1.4683E+00	1.4684E+00	1.4684E+00	1.4688E+00	1.4690E+00
VA	1.9885E-01	2.2068E-01	2.2337E-01	2.2332E-01	2.2378E-01	2.2446E-01	2.2521E-01	2.2598E-01	2.2686E-01
PI	-4.0086E-01	-2.9466E-01	-2.3038E-01	-3.0538E-01	-3.8436E-01	-3.0246E-01	-3.0066E-01	-2.9966E-01	-2.9304E-01
QP	0.	1.1546E-03	3.7526E-03	2.6142E-03	2.4178E-03	2.7946E-03	3.0096E-03	3.3906E-03	3.8916E-03
QR	3.0944E-03	3.5156E-03	2.9860E-03	2.7122E-03	2.6432E-03	2.6146E-03	2.6456E-03	2.6836E-03	0.
QN	-3.0944E-03	-2.1560E-03	-1.1236E-03	-5.7026E-04	4.5804E-05	6.8495E-04	1.1418E-03	2.0306E-03	3.6932E-03
UD	8.2308E-02	9.2477E-02	9.3621E-02	9.4283E-02	9.4263E-02	9.4819E-02	9.4555E-02	9.7218E-02	1.1144E-01
RHOS	1.0796E-02	1.2366E-03	8.5086E-04	6.9698E-04	-2.1456E-04	-1.4887E-04	2.2644E-05	9.0534E-04	0.
UI	-1.0398E-04	5.9682E-05	1.5866E-05	7.4822E-06	1.8098E-06	-4.9136E-06	-7.4274E-06	-9.0446E-06	0.
VE	0.	3.8634E-06	-3.4138E-08	6.4611E-07	7.7226E-07	1.0238E-06	1.4746E-06	1.8901E-06	0.
PT	2.3902E-05	-7.3441E-06	4.9364E-06	1.5811E-06	9.4031E-07	1.6892E-07	-7.5331E-07	-1.6798E-06	0.
HT	-1.5677E-04	-1.4265E-05	-1.0884E-05	-3.7666E-06	3.8610E-06	2.9886E-06	-6.0842E-07	1.0833E-06	0.
TAU	5.9695E-02	5.6462E-02	5.6177E-02	5.8134E-02	5.9886E-02	6.1635E-02	6.3511E-02	6.5498E-02	6.6991E-02
SF	0.	1.1219E+00	2.2880E+00	4.7216E+00	6.6630E+00	8.5376E+00	1.0426E+01	1.2482E+01	1.4208E+01

MASS BALANCE FREESTREAM = 1.4226E+01 SHOCK LAYER = 1.4208E+01 DELTA MASS = 1.1888E-01

BODY STATION 8 S = 3.0000 THETA = 1.0472 BETA = .0543 DELTA = .1760 DELTAT = 0.

XBOD = 1.3722 YBOD = 2.4444 XSHOC = 1.2223 YSHOC = 2.7311

QWI = 3.0622E-03 QWC = 3.0940E-03 QWL = 5.8236E-04

VEL2 = 4.5508E-01 SAZ = 1.4662E+00

KV	1	2	3	4	5	6	7	8	9
T	0.	1.4506E-01	2.4500E-01	3.7508E-01	5.0006E-01	6.2504E-01	7.5008E-01	8.7506E-01	1.0008E+00
P	7.6644E-01	7.5968E-01	7.5808E-01	7.5734E-01	7.5597E-01	7.5175E-01	7.4962E-01	7.5916E-01	7.5160E-01
RHO	2.2608E+01	1.8796E+01	1.6884E+01	1.8866E+01	1.8852E+01	1.8838E+01	1.8825E+01	1.8810E+01	1.8802E+01
H	2.4208E-01	3.1557E-01	3.1966E-01	3.2178E-01	3.1942E-01	3.2008E-01	3.2220E-01	3.2435E-01	3.2541E-01
U	1.3208E-01	4.2633E-01	4.5531E-01	4.5456E-01	4.5550E-01	4.5038E-01	4.5562E-01	4.5941E-01	4.5438E-01
V	0.	-1.6648E-03	-6.0564E-03	-9.6199E-03	-1.2658E-02	-1.5993E-02	-1.9288E-02	-2.2658E-02	-2.6888E-02
M	4.9041E-01	1.9231E+00	2.0172E+00	2.0461E+00	2.0355E+00	2.0202E+00	2.0026E+00	2.0138E+00	2.0046E+00
T	6.8144E-01	7.8023E-01	7.4622E-01	7.8594E-01	7.8482E-01	7.7742E-01	7.7234E-01	7.7908E-01	7.7998E-01
RR	1.4560E+01	1.4689E+01	1.4689E+01	1.4685E+01	1.4682E+01	1.4680E+01	1.4678E+01	1.4735E+01	1.4729E+01
SX	1.2875E+00	1.4686E+00	1.4677E+00	1.4680E+00	1.4683E+00	1.4684E+00	1.4686E+00	1.4690E+00	1.4691E+00
VA	1.9931E-01	2.2117E-01	2.2368E-01	2.2328E-01	2.2378E-01	2.2446E-01	2.2516E-01	2.2596E-01	2.2670E-01
PI	-4.0766E-01	-3.1228E-01	-2.5116E-01	-3.0076E-01	-3.8065E-01	-3.0026E-01	-3.0005E-01	-2.9878E-01	-2.9416E-01
QP	0.	1.1356E-03	4.0468E-03	2.5578E-03	3.0182E-03	3.4344E-03	3.8682E-03	4.2178E-03	4.6066E-03
QR	3.0622E-03	3.9316E-03	3.4622E-03	3.3186E-03	2.9736E-03	2.8802E-03	2.8986E-03	3.0096E-03	0.
QN	-3.0622E-03	-2.5375E-03	-1.5746E-03	-7.5968E-04	3.9826E-05	8.5431E-04	1.7376E-03	2.8116E-03	4.6066E-03
UD	4.8806E-02	4.8851E-02	4.1711E-02	3.8258E-02	3.7346E-02	3.9401E-02	4.1555E-02	4.6038E-02	1.0056E-01
RHOI	9.3368E-03	9.0004E-04	9.0131E-05	-4.3858E-04	-6.8068E-04	-6.9201E-04	-4.9066E-04	-4.9368E-04	0.
UI	-3.4181E-04	1.9423E-05	-1.0995E-05	-1.1798E-05	-1.5991E-05	-1.8105E-05	-1.6938E-05	-1.8622E-05	0.
VE	0.	8.1982E-06	2.7801E-06	3.1698E-06	3.0146E-06	2.9788E-06	3.0246E-06	2.9991E-06	0.
PT	2.1856E-05	-1.5465E-05	-1.1751E-06	-2.9566E-06	-2.9101E-06	-3.1658E-06	-3.5955E-06	-5.9962E-06	0.
HT	-1.3038E-04	-7.6696E-06	1.4238E-06	9.0535E-06	9.0206E-06	8.2946E-06	8.1956E-06	7.2606E-06	0.
TAU	8.7931E-02	7.9681E-02	8.2695E-02	8.6786E-02	8.7096E-02	8.9638E-02	9.2356E-02	9.5216E-02	9.7488E-02
SF	0.	1.0842E+00	4.8096E+00	7.6696E+00	1.0306E+01	1.3138E+01	1.5946E+01	1.8784E+01	2.1546E+01

MASS BALANCE FREESTREAM = 2.1562E+01 SHOCK LAYER = 2.1546E+01 DELTA MASS = 1.3380E-01

BODY STATION 9 S = 4.0000 THETA = 1.0472 BETA = .0542 DELTA = .2275 DELTAT = 0.

XBOD = 1.8722 YBOD = 3.3107 XSHOC = 1.6752 YSHOC = 3.6244

QWI = 3.1064E-03 QWC = 3.5560E-03 QWL = 6.0715E-04

VEL2 = 4.5550E-01 SAZ = 1.4662E+00

KV	1	2	3	4	5	6	7	8	9
T	0.	1.4508E-01	2.4502E-01	3.7508E-01	5.0006E-01	6.2506E-01	7.5006E-01	8.7508E-01	1.0008E+00
P	7.6652E-01	7.5949E-01	7.5844E-01	7.5726E-01	7.5557E-01	7.5368E-01	7.5190E-01	7.4931E-01	7.5135E-01
RHO	2.2550E+01	1.9402E+01	1.6928E+01	1.8872E+01	1.8857E+01	1.8843E+01	1.8829E+01	1.8813E+01	1.8803E+01
H	2.4196E-01	3.1154E-01	3.1161E-01	3.1869E-01	3.1886E-01	3.2011E-01	3.2158E-01	3.2315E-01	3.2356E-01
U	1.3526E-01	4.2852E-01	4.5584E-01	4.5335E-01	4.5416E-01	4.5348E-01	4.5399E-01	4.5461E-01	4.5463E-01
V	0.	-1.6911E-03	-6.2496E-03	-9.3119E-03	-1.2596E-02	-1.5888E-02	-1.9191E-02	-2.2586E-02	-2.6888E-02
M	4.9242E-01	2.0012E+00	2.0781E+00	2.0431E+00	2.0388E+00	2.0277E+00	2.0221E+00	2.0156E+00	2.0059E+00
T	6.7222E-01	7.5534E-01	7.5390E-01	7.6431E-01	7.6378E-01	7.6099E-01	7.5726E-01	7.7552E-01	7.7998E-01
RR	1.4902E+01	1.4997E+01	1.4992E+01	1.4981E+01	1.4964E+01	1.4944E+01	1.4911E+01	1.4798E+01	1.4726E+01
SX	1.3357E+00	1.4726E+00	1.4736E+00	1.4729E+00	1.4682E+00	1.4686E+00	1.4686E+00	1.4686E+00	1.4691E+00
VA	1.9921E-01	2.2159E-01	2.2408E-01	2.2442E-01	2.2382E-01	2.2468E-01	2.2548E-01	2.2597E-01	2.2706E-01
PI	-4.0849E-01	-3.2227E-01	-3.1331E-01	-3.0396E-01	-3.1062E-01	-3.0136E-01	-3.0136E-01	-3.0106E-01	-2.9946E-01
QP	0.	1.3508E-03	3.2332E-03	2.9635E-03	3.4926E-03	3.9787E-03	4.4576E-03	4.9385E-03	5.4138E-03
QR	3.1041E-03	4.3394E-03	4.2659E-03	3.8452E-03	3.4427E-03	2.9644E-03	2.4186E-03	1.6625E-03	0.
QN	-3.1041E-03	-4.1999E-03	-3.1878E-03	-2.9651E-03	-2.9452E-03	-2.9852E-03	-3.0306E-03	-3.2778E-03	-5.4138E-03
UD	9.1161E-02	9.3934E-02	9.4259E-02	9.4842E-02	9.4427E-02	2.9644E-03	2.4186E-03	1.6625E-03	0.
RHOI	-4.1691E-03	-4.1999E-03	-1.8784E-03	-8.9651E-04	6.5222E-05	1.0338E-03	2.0596E-03	3.2778E-03	5.4138E-03
UI	1.1162E-02	3.9885E-04	8.6718E-04	8.4058E-04	3.3966E-04	3.5178E-02	3.9766E-02	5.9468E-02	9.1988E-02
VE	0.	-1.0218E-06	-9.4858E-06	-9.5996E-06	-7.2706E-06	-6.8385E-06	-8.1668E-06	-8.3691E-06	0.
PT	-4.4884E-04	-7.2268E-06	-1.6444E-05	-1.4466E-05	-1.7296E-05	-1.7378E-05	-1.5692E-05	-1.5552E-05	0.
HT	0.	6.4228E-06	2.6496E-06	2.6824E-06	2.4529E-06	2.8316E-06	2.1461E-06	1.8845E-06	0.
TAU	1.8408E-03	1.9691E-03	5.8467E-06	7.0624E-06	6.9428E-06	7.1428E-06	7.5028E-06	7.8296E-06	0.
SF	0.	1.1208E-04	1.9481E-04	1.9048E-04	1.9048E-04	1.9048E-04	1.9048E-04	1.9048E-04	0.
	1.1998E-01	1.1408E-01	1.1411E-01	1.1417E-01	1.1417E-01	1.1418E-01	1.1416E-01	1.1253E-01	1.1282E-01
	0.	2.3786E+00	4.2958E+00	6.0136E+01	1.3926E+01	1.5767E+01	1.7547E+01	2.5136E+01	2.2884E+01

MASS BALANCE FREESTREAM = 2.4687E+01 SHOCK LAYER = 2.2884E+01 DELTA MASS = 2.2756E-01

BODY STATION 10 S = 5.0000 THETA = 1.0472 BETA = .0538 DELTA = .2810 DELTAT = 0.

XBOD = 2.3722 YBOD = 4.3707 XSHOC = 2.1283 YSHOC = 4.5175

QWI = 4.0662E-03 QWC = 4.0251E-03 QWL = 6.3697E-04

VEL2 = 4.5546E-01 SAZ = 1.4662E+00

KV	1	2	3	4	5	6	7	8	9
T	0.	1.4508E-01	2.4508E-01	3.7508E-01	5.0006E-01	6.2508E-01	7.5008E-01	8.7508E-01	1.0008E+00
P	7.6644E-01	7.5491E-01	7.5385E-01	7.5716E-01	7.5576E-01	7.5396E-01	7.5196E-01	7.4944E-01	7.5122E-01
RHO	2.2517E+01	1.9422E+01	1.6911E+01	1.8788E+01	1.8763E+01	1.8748E+01	1.8734E+01	1.8718E+01	1.8708E+01
H	2.1955E-01	3.1503E-01	3.1268E-01	3.1538E-01	3.1737E-01	3.1885E-01	3.2038E-01	3.2226E-01	3.2252E-01
U	1.3676E-01	4.2992E-01	4.5722E-01	4.5388E-01	4.5338E-01	4.5348E-01	4.5408E-01	4.5436E-01	4.5467E-01
V	0.	-1.6722E-03	-6.2019E-03	-9.2866E-03	-1.2961E-02	-1.5878E-02	-1.9196E-02	-2.2572E-02	-2.5036E-02
M	4.9845E-01	2.0003E+00	2.0788E+00	2.0446E+00	2.0402E+00	2.0291E+00	2.0235E+00	2.0169E+00	2.0078E+00
T	6.6965E-01	7.5503E-01	7.5356E-01	7.6436E-01	7.6376E-01	7.6085E-01	7.5711E-01	7.7538E-01	7.7995E-01
RR	1.7188E+01	1.5003E+01	1.4994E+01	1.4984E+01	1.4965E+01	1.4942E+01	1.4908E+01	1.4777E+01	1.4722E+01
SX	1.3421E+00	1.4688E+00	1.4744E+00	1.4736E+00	1.4686E+00	1.4693E+00	1.4685E+00	1.4687E+00	1.4690E+00
VA	1.9847E-01	2.2178E-01	2.2401E-01	2.2417E-01	2.2377E-01	2.2436E-01	2.2546E-01	2.2546E-01	2.2669E-01
PI	-4.0781E-01	-3.2298E-01	-3.1179E-01	-3.2116E-01	-3.0411E-01	-3.0453E-01	-3.0336E-01	-3.0046E-01	-2.9966E-01
QP	0.	1.7096E-03	3.8911E-03	3.2742E-03	3.9878E-03	4.6978E-03	5.3932E-03	6.1138E-03	
QR	4.0662E-03	5.1056E-03	4.3168E-03	4.3168E-03	4.0858E-03	3.3611E-03	2.6980E-03	1.8784E-03	0.
QN	-4.0662E-03	-3.4947E-03	-1.1551E-03	-1.0268E-03	8.2048E-05	1.1496E-03	2.3587E-03	3.7088E-03	6.1388E-03
UD	1.1594E-02	1.3541E-02	1.3170E-02	1.3101E-02	1.2498E-02	1.2498E-02	3.5787E-02	5.6196E-02	8.5099E-02
RHOI	1.3268E-02	-4.4497E-04	-4.0098E-04	-7.2248E-04	-7.1496E-04	-6.8438E-04	-6.6848E-04	-7.0980E-04	0.
UI	-4.8778E-04	-1.5726E-05	-1.6088E-05	-2.4470E-05	-4.6196E-03	-1.5378E-05	-1.4190E-05	-1.4975E-05	0.
VE	0.	3.5868E-06	2.6081E-06	2.2968E-06	1.9238E-06	1.6422E-06	1.3846E-06	9.9788E-07	0.
PT	1.1958E-05	-2.6558E-06	-8.5968E-06	-9.6968E-06	-9.0238E-06	-9.8388E-06	-1.0228E-05	-1.0526E-05	0.
HT	-4.8268E-04	9.9936E-07	6.2248E-06	7.8096E-06	7.4698E-06	6.9838E-06	6.4558E-06	5.8468E-06	0.
TAU	1.9068E-03	1.3226E-01	1.4546E-01	1.3696E-01	1.4226E-01	1.4983E-01	1.5078E-01	1.5528E-01	1.5678E-01
SF	0.	3.3276E+00	6.0595E+00	1.2058E+01	1.7556E+01	2.2226E+01	2.6912E+01	3.1576E+01	3.6208E+01

MASS BALANCE FREESTREAM = 3.0246E+01 SHOCK LAYER = 3.6208E+01 DELTA MASS = 2.4836E-01